Modelling Flood Inundation in the Mlazi River under Uncertainty

by

Nokuphumula Mkwananzi

September 2003

In fulfillment of the requirements of a

Master of Science in Engineering

As set out by the University of Natal

Supervisor: Professor G Pegram

MODELLING FLOOD INUNDATION

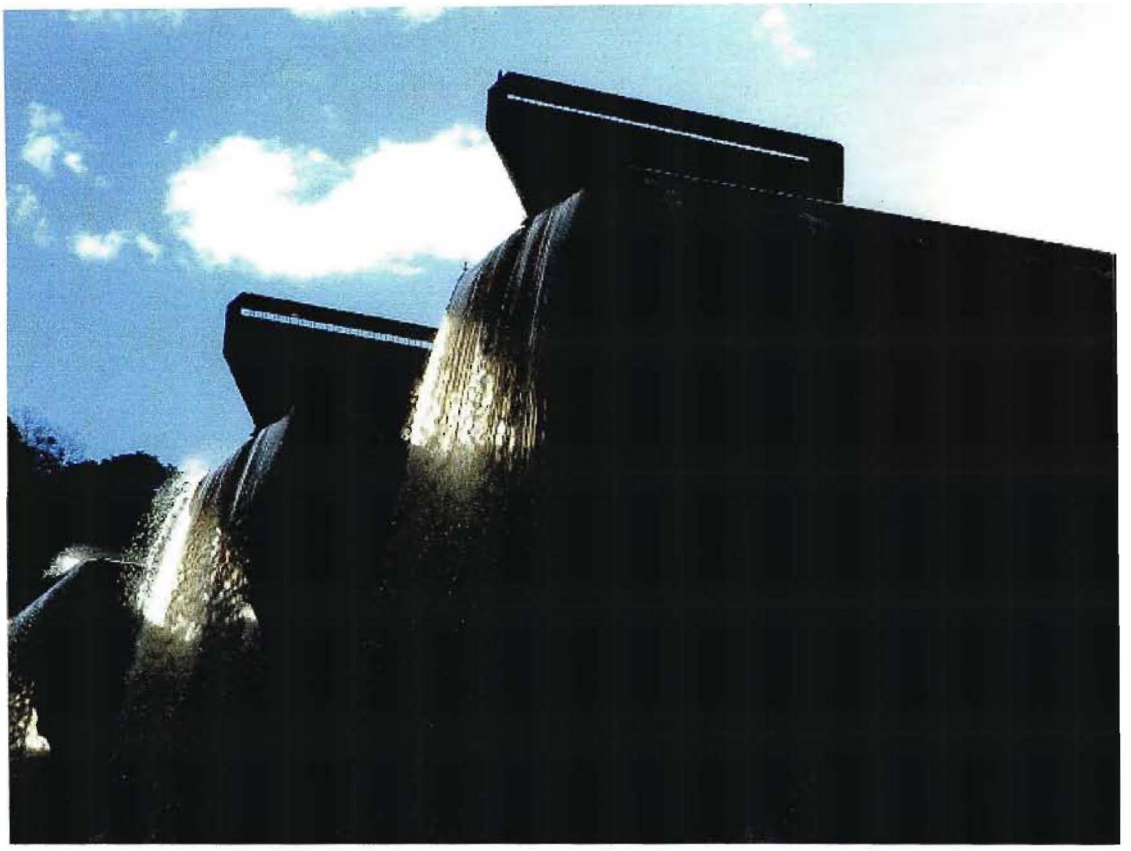

ABSTRACT

The research project described in this dissertation studies the modelling techniques employed for the Mlazi River in the context of flood analysis and flood forecasting in order to model flood inundation. These techniques are applicable to an environment where there is uncertainty due to a lack of historical input data for calibration and validation purposes. This uncertainty is best explained by understanding the process and data required to model flood inundation.

In order to model flood inundation in real time, forecasted flood flows would be required as input to a hydraulic river model used for simulating flood inundation levels. During this process, forecasted flood flows would be obtained from a flood-forecasting model that would need to be calibrated and validated. The calibration process would require historical rainfall data correlating with streamflow data and subsequently, the validation process would require real time streamflow data.

In the context of the Mlazi Catchment, there are only two stream gauges located in the upper subcatchments. Although these stream gauges have recorded data for 20 years, the streamflow data does not correlate with disaggregated daily rainfall data, of which there are records for at least 40 years. Therefore it would be difficult to develop the forecasting model based on the rainfall and streamflow data available. In this instance, a more realistic approach to modelling flood inundation involved the integration of GIS technology, a physically based hydrological model for flood analysis, a conceptual forecasting model for real time forecasting and a hydraulic model for computation of inundation levels. The integration of modelling techniques are better explained by categorising the process into three phases:

Phase 1 Desktop catchment modelling: A continuous, physically based simulation model (HEC-HMS Model) was set up using GIS technology. The model applied the SCS-UH method for the estimation of peak discharges. Synthetic hyetographs for various recurrence intervals were used as input to the model. A sensitivity analysis was implemented and subsequently the HEC-HMS model was calibrated against output SCS-UH method and peak discharges simulated. The synthetic hyetographs together with results from the HEC-HMS model were used for validation of the Mlazi Meta Model (MMM) used for real time flood forecasting.

Phase 2 Implementation of the Inundation Model: The hydraulic model (HEC-RAS) was created using a Digital Elevation Model (DEM). A field survey was conducted for the purpose of capturing the roughness coefficients and hydraulic structures, which were incorporated into the model and also for the confirmation of the terrain cross sections

from the DEM. Flow data for the computation of levels of inundation were obtained from the HEC-HMS model. The levels of inundation for the natural channel of Mlazi River were simulated using the one dimensional steady state analysis, whereas for the canal overbank areas, simulation was conducted for unsteady state conditions.

Phase 3 Creation of the Mlazi Meta Model (MMM): The MMM used for real time flood forecasting is a linear catchment model which consists of a semi-distributed three reservoir cell model (Pegram and Sinclair, 2002). The MMM parameters were initially adjusted using the HEC-HMS model so that it became representative of the Mlazi catchment. This approach sounds unreasonable because a model is being validated by another model but it gave the best initial estimate of the parameters rather than using trial and error. The MMM will be further updated using record radar data and streamflow data once all structures have been put in place. The confidence in the applicability of the HEC-HMS model is based on the intensive efforts applied in setting it up. Furthermore, the output results from the calibrated HEC-HMS model were compared with other reliable methods of computing design peak discharges and also validated with frequency analysis conducted on one of the subcatchments.

PREFACE

The study was carried out by the candidate to fulfill the requirements of a Masters of Science in Engineering as set out by the University of Natal. The study was conducted under the supervision of Professor GGS Pegram between January 2002 and July 2003.

The study was conducted at the offices of Arcus Gibb Consulting Engineers of Westville, Durban. The sole reasons for the choice of location was that the candidate was involved in the Mlazi floodplain delineation study conducted by Arcus Gibb for eThekwini Metro Council. Therefore, the environment provided a better workstation for the candidate due to the availability of relevant computer software necessary to conduct the desktop modelling.

It is therefore confirmed that all work described in this Dissertation was carried out by the candidate unless otherwise stated. The following work was not performed by the candidate although it should be noted that the candidate conducted verifications of some of the works and is fully aware of some of the processes involved:

- The use of Geographical Information Systems software for creation of the Digital Elevation Models (DEM) and also for data capture and processing including the display of inundation levels was conducted by ML Sultan College in conjunction with Arcus Gibb.
- The Mlazi Meta Model (MMM), which is a real time forecasting model for Mlazi, was designed and tested by Scott Sinclair under the Umgeni Water Project.
- The candidate also worked together with a team at Arcus Gibb to conduct fieldwork for the Mlazi River.
- The theoretical information and literature review is based on journals and textbooks as listed in the reference list.
- The Methodology, Decision Tools and Approaches as well as Statistical approaches was developed by Professor GGS Pegram, and the candidate. The candidate furthered and implemented the techniques, which eventually resulted in the documentation of this work.

The research was carried out as an extension of a pilot study sponsored by the Water Research Commission (WRC) for the Department of Civil Engineering, University of Natal, to deliver an operational flood forecasting system which will produce operational forecasts using Radar in real time to include levels of inundation for the Umgeni and Mlazi catchment for the eThekwini Disaster Management Center.

Signed at ..... on .....

ACKNOWLEDGEMENTS

The author would like to thank Professor GGS Pegram for his continued support and unlimited knowledge, which he graciously shared during the whole research study.

The author also extends his gratitude to the Arcus GIBB Management and Professional team in Durban for allowing him to pursue this research as a contribution to the flood studies they are conducting for eThekwini Metro Municipality. Their interest in the research showed a fulfillment of one of their policies of academic development of their staff member and also in addressing community based problems such as flooding in Durban. The author is indebted to two of the Arcus Gibb senior staff, Durban Branch Manager Director Wiero Vogelzang and Engineer Andy McDonald.

A word of 'Thank You' is extended to the Water Research Commission for funding the project. Through their funding, the structures required for this project were put in place, and the Author received travelling and subsistence allowances.

Furthermore the author is indebted to eThekwini Disaster Management Centre for their contribution to the funding of this project.

The contribution of other organisations such as DWAF, ML Sultan Technicon, and SAWS is most appreciated.

TABLE OF CONTENTS

LIST OF TABLES

LIST OF FIGURES

1. INTRODUCTION

1.1 Background

Natural watercourses have been modified for centuries for reason of human development or flood mitigation. However, there have been a lack of understanding of the natural phenomena in rivers and training works have often had negative impacts. Canalising of the natural stream channel, thereby changing the course of the river, was carried out for the Mlazi River in the mid 1950s by the Department of Transport, with the intention of deviating the river away from the proposed Durban Airport site. What was not properly considered were the hydrological implications, which have resulted in flooding problems. The 1987 floods, which caused widespread flooding in the Durban area, forced the closure of the Mondi Paper mill and the SAPREF oil refinery for ten days resulting in severe economic loss. Universities and other concerned organisations have involved themselves in flood studies. The studies include flood warnings, floodline delineation, forecasts of streamflow and display of levels of inundation in GIS so as to plan and react timeously to flood events and thus to reduce damage.

This dissertation presents the extension of previous research (funded by WRC) into a river flow nowcasting system using radar, to include levels of flood inundation, which are to be displayed on GIS in the eThekwini Metro Disaster Management Center.

This research study aims at applying the transfer function streamflow modelling approach developed by Pegram and Sinclair (2002) in the context of the Mlazi Catchment. The research study also aims to provide an inundation model (HEC-RAS), which would enable levels of inundation to be displayed through the GIS software as shown in Figure 1.1.1.

The objectives of the dissertation are addressed by introducing a real time flood forecasting model in the context of the Mlazi Catchment. The real time forecasting model is a linear catchment model (Pegram and Sinclair, 2002) hereinafter called the Mlazi Meta Model (MMM). This is a conceptual model, which requires parameter adjustments so that it becomes representative of the Mlazi catchment as discussed in Chapter 7. The validation of this model

requires a reliable record of rainfall and historical streamflow data so that an accurate forecast can be performed.

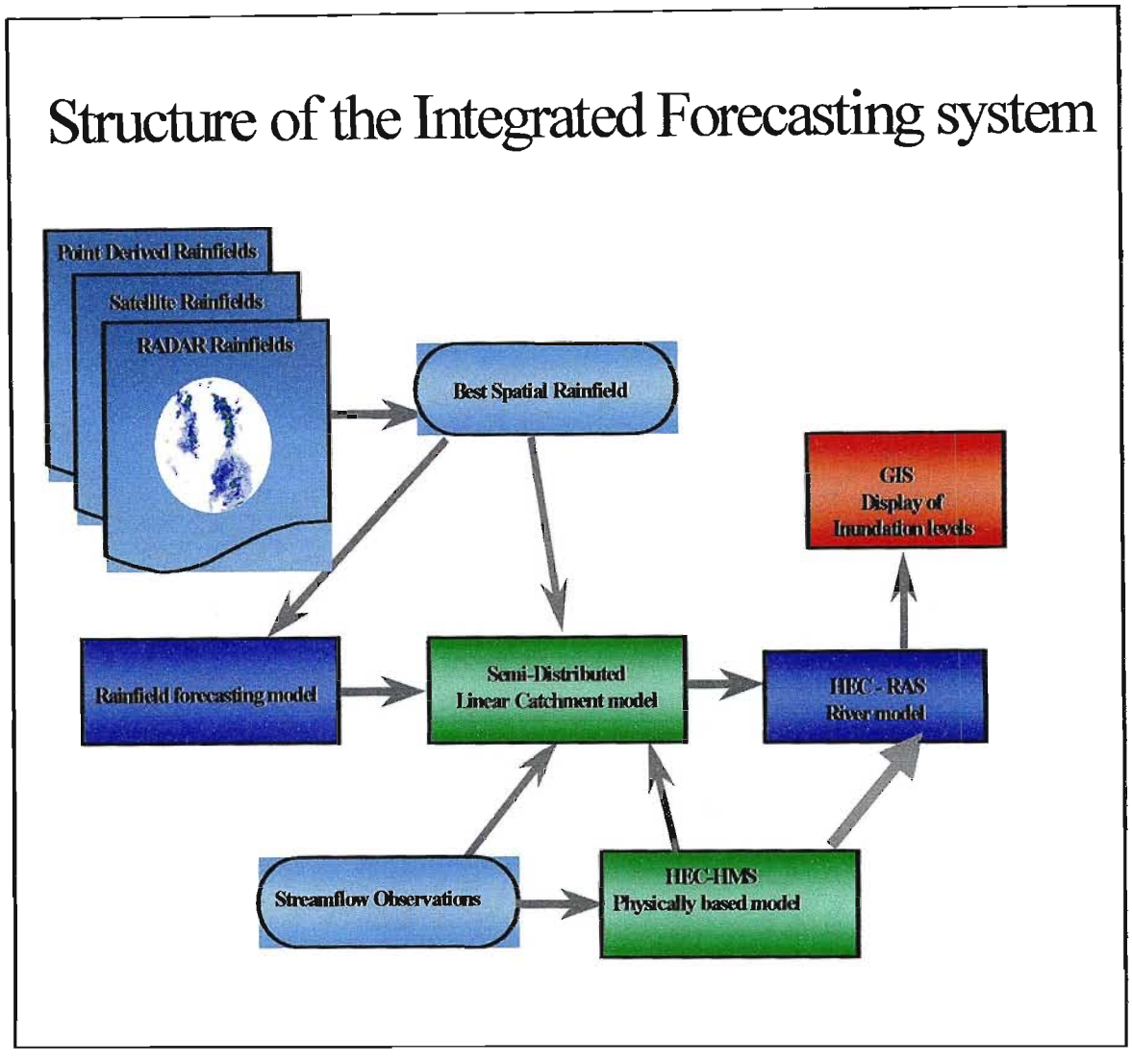

Figure (1.1.1): Structure of the Integrated forecasting System

The synthetic storms are input into the Mlazi Meta Model and the parameters are set so that the simulated stream flows from the model approximates the output from the calibrated physically based model (HEC-HMS). This approach might seem unreasonable because a model is being validated by another model, but it should be noted that this approach gives a better initial estimate of the parameters than trial and error. The MMM would further be updated using recorded radar data and streamflow data once sufficient real time radar data and streamflow data becomes available.

The confidence in the applicability of the HEC-HMS model is based on the intensive efforts applied in setting it up so that it is representative of the Mlazi catchment. Furthermore the output from the calibrated HEC-HMS model was compared with other reliable methods of computing peak discharges, discussed in Section 3.6.6.

1.2 Objectives

The aims of this study are:

- Application of the transfer function streamflow modelling approach developed by Pegram and Sinclair (2002) in the context of the Mlazi Catchment.
- To calibrate and set the initial parameters of the Mlazi Meta Model (MMM) by using input and output from the configured HEC-HMS model
- To provide an inundation model which would enable levels of inundation to be displayed through the GIS software
- To contribute to the flood warning system that is to be incorporated into the Durban Metro disaster management plans for the urban environment.

1.3 Study Area

Introduction

The study area is the Mlazi Catchment. The reason for the selection of this catchment is:

- The Mlazi Catchment forms part of the Durban urban area within which essential industries like the Mondi paper industry, Durban Airport and SAPREF refinery are located making the study very appropriate to prevent flood damage
- Sufficient data was available from previous studies to accomplish the analysis
- This study complements the Water Research Commission project entitled "Umgeni Nowcasting Using Radar".

The following two sections give a general description of the catchment and also the overview of flood characteristics.

1.3.1 General Description

The Mlazi River catchment is elongated in shape and covers 955 km^2. It is the second largest catchment in the eThekwini Metropolitan Area (EMA); it covers twenty-four percent of the TMA, extending from the coast into the regional council area as far as the South of Pietermartzburg. There are no other major tributaries flowing into the Mlazi besides the Mgoshongweni River. The locality map of the Mlazi is shown in Figure 1.3.1.

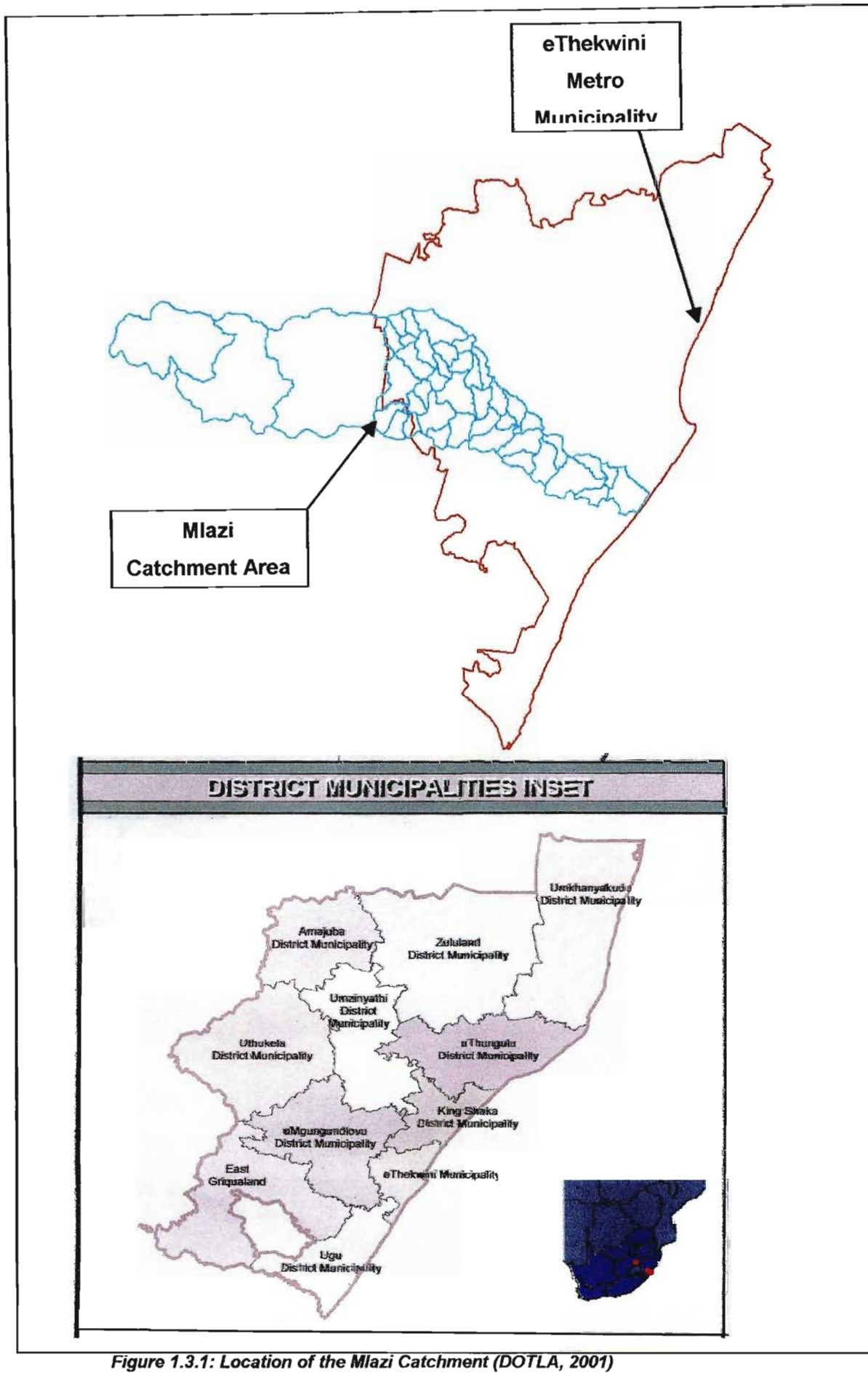

Figure 1.3.1: Location of the Mlazi Catchment (DOTLA, 2001)

The Mlazi Catchment is approximately 144 km in length with its width varying slightly from the upper catchment to the lower catchment. The upper catchment has a width of approximately twelve kilometers, the middle catchment is approximately fifteen kilometers wide and the lower catchment is approximately six kilometers wide. The following information describes some of the physical characteristics of the Mlazi Catchment in general:

- The catchment starts at Richmond, and its outlet is at Isipingo beach
- The key natural resources includes the Silverglen Nature Reserve, Shongweni Dam and Reserve, extensive forests, beach, rocky shores and marine habitats, wetlands, grasslands, floodplains and dams
- 60% of the population is formal and 40% population is informal and peri-urban. The majority of the settlements have a population density of below 50 people per hectare
- The catchment contains the largest concentration of formal residential areas in EMA after Umgeni. The Mlazi contains 19% of EMA's industries, 64% of EMA's mixed farming, 37% of DMA's informal residential , 36% of the catchment is undeveloped
- The mean annual precipitation varies from 600mm to 1000mm over the Mlazi Catchment.

In broad terms, the catchment consists of grasslands, extensive forest/woodlands and areas for terrestrial mammals in the upper catchment. Natural grasslands, forest/woodlands, wildlife habitats and recreation are evidenced in the middle catchment. In the lower catchment the area consists mainly of formal residential and commercial/industrial. The variation of land uses in each sub catchment was obtained by superimposing land use data obtained from the Durban Unicity Town Planning Department over the catchment using a Geographic Information System (GIS).

1.4 Literature Review

The literature review component of this study is split into three broad categories. The first section of this literature review focuses on GIS, an investigation into available literature regarding application of GIS and how they are integrated into hydrologic, hydraulic and forecasting model processes. This second section is a discussion on real time flood forecasting models. The third section firstly introduces early flood warning systems and then identifies flood forecasting as an advanced method of flood warning. This approach helps to give a better understanding of the purpose of introducing a flood forecasting system for this study. Various widely used real time forecasting models are discussed including the linear catchment model for real time flood forecasting (Pegram and Sinclair, 2002). This is the model used for conducting streamflow forecasts for the Mlazi Catchment. Lastly, a review of calibration procedures for models is presented.

1.4.1 GIS Technology

Geographic Information Systems (GIS) - are the processes of collecting, managing, analysing and displaying spatially distributed data using computer hardware and software.

GIS are a fast growing technology which has been applied in hydrology, water resources and data management. This section describes the application of GIS in hydrologic and hydraulic modelling. The significance of applications, which take advantage of spatially distributed data in GIS is also discussed.

Mancini and Rosso (1989) investigated the spatial variability of the Soil Conservation Service (SCS) curve number using a raster GIS and a distributed hydrologic model. The work conducted by Johnson (1989) demonstrated that compatible data sets on terrain and radar-rainfall data could be fully integrated into a catchment modelling system. Vieux (1991) used a GIS based Triangular Irregular Network (TIN) to process the terrain data from a small catchment for application of a finite element runoff model. Most of the results from the models developed show that GIS simplifies model setup. Maidment (1991) developed hydrological applications of GIS, which were limited to operations on steady state processes. The four distinct hydrologic applications of GIS identified by Maidment (1991) were:

- hydrologic assessment

- hydrologic parameter determination
- hydrologic model set up using GIS
- hydrologic modelling inside a GIS environment.

To date, a vast amount of research work has been conducted with regard to unsteady, distributed-parameter, hydrologic models within a GIS. Various GIS models have been developed for hydrologic data processing. These include:

- GRASS (1993); is a highly interactive and graphically oriented interface providing tools for developing, analysing and displaying spatial information. Ogden *et al* , (2001) states that the raster formulation of GRASS is very attractive for use in spatial distributed hydrologic modelling as spatial data can easily be translated from GIS to initialise the model and the model outputs can be transferred to the GIS for visualisation purposes
- GIS/HEC-1 Interface model (Prince William County Model) mentioned by Ogden et al, (2001); this model uses contoured elevation data that are converted to 6 m^2 grids for use in time of concentration calculations. The model realises the economics and efficiency of using a GIS in the process of fully automatic catchment hydrologic modelling and at the same time produces high quality graphics for reports and publications (Ogden *et al*, 2001)
- HEC-GeoHMS (2000). The HEC-GeoHMS was developed as a geospatial hydrology tool for preparing basin model files for the HEC-HMS hydrologic modelling program by way of a GIS. Its main function is to visualise spatial information, document catchment characteristics, perform spatial analysis, and delineate subbasins and streams and to construct inputs to the HEC-HMS model. This has been feasible due to the ability to perform spatial overlays of information to compute lumped or grid-based parameters. The HEC-GeoHMS interface was chosen for the creation of Mlazi Catchment information and data assemble as has been done for the other rivers within the eThekwini Municipality. The GIS application in flood line studies specifically for the rivers within the eThekwini area of KwaZulu-Natal is presented by Hansen *et al* (2001). The paper also describes the creation of the hydraulic model using the triangulated irregular networks (TIN), which are more accurate than raster based digital elevation models. The procedure employed is

discussed in Section 3.1. The pre-processing of GIS based data is discussed in Section 5.1.

- HEC-PrePro v.2.0 is an ArcView preprocessor for HEC's hydrologic modelling system and was the forerunner to the HEC-GeoHMS tool. Olivera and Maidment (1998b) explains how the system of Arcview scripts and associated controls have been developed to extract hydrologic and topologic information from digital spatial data of a hydrologic system. Furthermore the paper gives an explanation of the use of the Arcview scripts to prepare an input file for the hydrologic modelling system (HMS) developed by the Hydrologic Engineering Center (HEC) of the United States Army. Olivera (2001) also presented a study on extracting hydrologic information from spatial data for HMS modeling.

Ogden *et al* (2001) emphasises that GIS models and distributed hydrologic models would enable the progression of hydrology from a field dominated by techniques that require spatial averaging and empiricism to a more spatially descriptive science. The paper categorises the applications of GIS based models. The first category of applications involves the geospatial analysis of catchments and their hydrologic variables used for modelling, as in the case of Mlazi. The second category of applications involve use of models that take advantage of spatially derived catchment characteristic to make predictions or forecasts of hydrologic variables such as the runoff of water. Apart from these two categories, GIS is now also being integrated into meteorology.

Thomas (2001) recommends the use of GIS tools on meteorological data, which is also spatial in nature. The application of GIS on meteorological data could prove to be a very significant application especially for rainfall forecasting and also for streamflow forecasting since it helps in the interpretation of real-time data, enables fast computations and provides good estimates of rainfall characteristics. The advantage of this application includes the fact that meteorological data can be displayed more accurately spatially. However Shipley *et al* (1996) stated that most meteorologists consider data processing speed as being of greater importance than spatial accuracy. GIS has many applications to meteorology, this includes its ability to display multiple types of data over the same map area. GIS is able to combine information from various

sources in an efficient, understandable, spatially accurate manner, which supersedes any current meteorological software. The disaster management centre at eThekwini Municipality is currently applying ArcView GIS in the display of rainfall and stream flow forecast using radar data. There are intentions to have this facility nationwide.

With a good catchment and river model created, correct meteorological data captured and displayed in real time by the use of GIS technology, real time flood forecasting can be conducted with less uncertainty. The next section discusses real time flood forecasting models, which includes the linear reservoir-forecasting model of Pegram and Sinclair (2002), which is to be used for flood forecasting in the Mlazi study.

1.4.2 Real Time Flood Forecasting Models

One of the recent developments in flood management strategies worldwide involves the use of real time flood forecasting. Flood forecasting is a contribution to flood warning devices, which have been developed such as those stated by Gibb Africa (1996) for the SAPREF plant at the outlet of the Mlazi Catchment. The flood warning systems perform the same function and the difference between the types is mainly the communication medium, warning time and installation/maintenance costs. The communication systems typically used for early warning system are:

- manual systems,
- radio telemetry,
- satellite,
- telephone/modem, and
- cellphone/trunking radio.

Gibb Africa (1996) stated that the warnings do not relieve the floods but makes one aware of their occurrence. The early warning systems discussed predict the discharge of the river at the SAPREF refinery in flood plan of Mlazi based on stage information at some point upstream of the area of interest. However there are disadvantages associated with these warning systems such as the short warning time. The warning time for these systems is also affected by the magnitude of the floods. Harvey (1998) described the operation of flood warning systems, which are similar to those discussed by Gibb Africa (1996). The flood

routing method described by Harvey (1998), involves creating a model that describes flow at an upstream location as it propagates downstream to the site of interest. Harvey (1998) states that these have significant advantages over other methods because the predictions are based solely on measured river flow. The only significant disadvantage is that depending on the catchment response time, and also the magnitude of the flood and intensity of the rainfall, it becomes difficult to obtain a reasonable early warning time. The streamflow gauge would need to be far enough upstream to give a lead-time comparable with the time available to clear the affected area, but not too far that measured flow is unrepresentative. The problems cited in the use of the flood routing methods are partially solved by the introduction of flood forecasting.

Flood forecasting is becoming one of the most useful elements in disaster **management** and decision support systems. Flood forecasting systems have been implemented to allow early warnings to the population so as to minimize loss of life and property damage. Furthermore early warnings are also essential to the industries such as Mondi Paper industry and SAPREF refinery industries in the Mlazi river floodplain so as to reduce damage to property and machinery, which could result in massive economic losses due to disruption to production.

There are many forecasting models, which have been developed and further research is been carried out to integrate the forecasting models in a GIS. The linking of these models with a GIS is important to the disaster management centers that have to interpret the information in order to determine the risk of possible damage to property. GIS is useful to the disaster management team because they can see quickly which areas are likely to be inundated, and, for example which bridges will be impassable and therefore unsuitable for rescue services, etc. Most of the forecasting models are mathematical conceptual models and therefore there is a need to be confident that they represent the actual hydrologic processes by linking them with physically based models for validation of the forecasting models so as to reduce uncertainty. This approach is intended for the Mlazi study where there are few reliable rainfall and no streamflow historical records. The forecast models are intended to issue forecasts for the magnitude of the flood peak, the date and time when the river is expected to overflow its bank USGS (1999).

The following are some of the widely used real time forecasting models:

- Application of Combined Tank Model And AR Model In Flood Forecasting (Tingsanchali, 2001). This application involved the combining of deterministic and stochastic models such as the Tank model and the autoregressive (AR) model respectively. The rainfall forecast is assumed which means that the model actually relies on observed rainfall data as forecast rainfall. The spatial variation of rainfall together with limited rainfall stations results in the Tank model having errors in forecasting daily discharges. The remedy to these errors is done through use of forecast updating techniques and the AR model. The AR model is applied to model the time series of the error of forecast in the past, which is defined as the difference between the forecast results from the Tank model and the observed data in the past.

- Transfer Functions models (Harvey, 1998). These models are similar to unit hydrographs in the sense that they describe how unit rainfall for unit time at a given catchment appears to flow through the river. However, they are more parametrically efficient and are easier to adjust in real time than the unit hydrograph. There have been improvements of the transfer models resulting in the development of the physically realisable transfer function that enables a better representation of real rainfall-flow events.

- WAMM-Water Management Model (Pretner *et al*, 1999). WAMM uses a river-modelling tool called MIKE11 linked to a Digital Elevation Model (DEM) of the floodplain to predict flood extent. Flood forecasting is conducted by application of mathematical models, the forecasts are calculated as expected water levels at gauging stations. Hydraulic models are then applied and linked to GIS to create maps of the simulated inundation. There is, however, the difficulty of calibrating the models with respect to flow on the floodplains, as measurements are difficult to take during flood conditions and therefore calibration must rely on historical flood extent and aerial photographs of the hydrological and hydrodynamic.

  The calibration procedure for the WAMM is conducted by comparing

model predictions with flood maps obtained through Synthetic Aperture Radar (SAR) images and water levels measured by small portable sensor installed in floodplain. The SAR images are also used to obtain soil moisture data for input into WAMM. The innovation of the WAMM project is based on the integration of advanced technologies for flood analysis and forecasting, which have been modelling as separate processes in previous studies.

- Semi - Distributed Linear Reservoir Cell Model, Sinclair (2000). This forecasting model was initially developed under the WRC project "Umgeni Nowcasting using Radar" (Sinclair, 2000) to conduct rainfall and streamflow forecasts for the Mgeni River in Durban, South Africa. This forecasting model consists of semi-distributed cell models, which use a system of three reservoirs for describing hydrological systems to produce forecasts of streamflows. The model caters for rainfall losses by incorporating loss parameter computations. The model is formulated in Finite Difference form similar to an Auto Regressive Moving Average (ARMA) model. The response of the arrangement of linear reservoirs is governed by the use of ARMA that is derived from the State-Space equations. The response from each of the cells is linearly summed at the catchment outlets to produce the total catchment response. The response input to the model is the best-observed spatial rainfall field obtained by radar, which is followed by the short-term forecast rainfield. Transfer function models, which are conceptually similar to unit hydrographs, are used to convert the excess rainfall to runoff. Optimal (Kalman) filtering techniques are applied to update the state and parameters of the model based on the real flows (also input) available and the current state of the catchment. The forecast streamflows, which are similar to observed flows, are routed through the river hydraulic model (HEC-RAS).

Having discussed some of the early warning systems it therefore becomes apparent that a potential flood warning system should consist of three phases, as suggested by Alexander (2000). These criteria are modified as follows:

- Phase 1: Flood forecast based on meteorological forecast. Long warning but poorer forecast with length of lead-time.

- Phase 2: Flood forecast based on recorded rainfall. Moderate warning and increased accuracy.
- Phase 3: Flood forecast based on gauged upstream river flow. High accuracy but relatively shorter warning time.

This research study intends to integrate the Mlazi Meta Model with HEC-HMS hydrologic model and the HEC-RAS hydraulic model intended for hydraulic routing of the forecasted flows from the Shongweni Dam through the canal to the outlet. This would facilitate the production of forecast inundation levels to be displayed via GIS at the disaster management center of eThekwini Municipality. All these models are described in Chapter 3 and at this juncture it becomes necessary to discuss one important process in modelling, which is the model calibration. Without well-calibrated models, especially in an uncertainty environment like Mlazi then flood forecasts would fail to serve their purpose of enabling reliable early warning. The next section therefore discusses the model calibration process.

1.4.3 Model Calibration

Ponce (1989) defines model calibration as the process by which the values of model parameters are selected for a particular application. It is conducted in rainfall-runoff modelling to ensure that the simulated flows are as close as possible to the observed flows. The selection of the parameters can be done in various ways depending upon the availability of data, technology and expertise of the modeller. The parameters can be selected manually by trial and error, automatically by the model such as performed by the HEC-HMS model, or by use of mathematical optimisation techniques. Model calibration becomes extremely difficult when modelling catchments where uncertainty is high due to lack of historical data and also where a large number of model parameters have to be estimated.

The approach to model calibration depends on the type of modelling. For instance, deterministic models are highly predictable therefore are much easier to calibrate. However, conceptual modelling requires the implementation of a very reliable calibration procedure because the parameters have no direct link with the physical processes. Therefore calibration is required to determine the appropriate parameters.

The calibration of time-invariant processes and time-variant processes are quite different. During the calibration of time-invariant processes it is necessary to divide the calibration process into two stages, which are:

- Calibration: observed rainfall and runoff data is used for calibration
- Verification: rainfall and runoff data not used in the calibration is used to assess the accuracy of calibration.

In the case of time-variant processes and models, the difficulty lies in calibrating the parameters that change with time. The best approach would be to select a range for the variable such as low flow, average flow and high flow and then perform a calibration and verification for each flow level.

In this study calibration was carried out for all the models starting with the hydrologic HEC-HMS model used for the rainfall-runoff simulation to obtain peak-flows for input to the hydraulic HEC-RAS model. An effort was made to calibrate the river model so that the computed inundation levels would be close estimates of the historical levels. The forecasting Mlazi Meta Model was calibrated and verified with the use of a design hyetograph and output hydrograph from the physically based HEC-HMS model to determine the initial estimates of parameters. The forecasting model is validated by use of observed flow recorded at the stream-gauges. Therefore it is important to have reliable streamflow gauges at those points where streamflow forecast are being conducted. The calibration process is therefore approached in a more integrated manner where all the models become interlinked.

1.5 Structure of the Report

This report documents the methods used in hydrological modelling and hydraulic modelling of the Mlazi River with the objective of using the hydrologic model (HEC-HMS) to validate a real time forecasting model for the Mlazi Meta Model (MMM). Furthermore the peak discharges from the HEC-HMS model were input to the HEC-RAS model in order to produce levels of inundation. These inundation levels were later used to delineate floodplains using GIS technology to be displayed in the Disaster Management Center of the eThekwini Metro Municipality.

The report is divided into eight chapters and the content of these chapters is as follows. Chapter 2 is the theoretical background of the different modelling processes applied in the context of Mlazi. The chapter includes the following:

- hydrologic modelling,
- hydrologic routing,
- design storms,
- hydraulic modelling, and
- first Order Analysis of Uncertainty.

Data processing and hydrological modelling are discussed in Chapter 3. This chapter deals with data processing using GIS technology, including the creation of the digital elevation model for the HEC-HMS model. The hydrologic model, HEC-HMS, is described and applied to the Mlazi. The calibration process and sensitivity analysis of the hydrologic model is also discussed in Chapter 3.

The hydraulic modelling and inundation level determination presented in Chapter 4 contains the one-dimensional steady state hydraulic modelling of the Mlazi natural channel using the HEC-RAS model. The river model is configured, calibrated, analysed and applied to produce levels of inundation. Chapter 5 describes the canal hydrodynamic analysis using one-dimensional unsteady state hydraulic modelling processes. The delineated floodplains are used for the flood damage assessment in Chapter 6. Chapter 7 contains a discussion on the Mlazi Meta Model Development and Parameter fitting procedure. Chapter 8 contains a summary, conclusion and recommendation of the study. The report includes Appendix A, which contains the tabulated results of the capacity and overtopping of the Mlazi bridge structures. Attached is a compact disk

containing Appendix B and Appendix C, which include the HEC-RAS profile data in Excel spreadsheet, and cross-section reference photographs of the Mlazi River respectively.

2. THEORETICAL BACKGROUND

This chapter gives a background of the theory and assumptions of the different modelling processes applied in the context of the Mlazi catchment based on standard hydrologic and hydraulic textbooks, hydrologic and hydraulic journals and relevant papers published. The sections that are considered in this chapter cover the following:

- hydrologic Modelling,
- hydrologic Routing,
- design Storms,
- hydraulic Modelling, and
- first Order Analysis of Uncertainty.

The selection of the above listed sections was based on the technical approach to solving the problem of modelling in an environment where uncertainty is high due to lack of correlating streamflow and rainfall data. The procedure to addressing this problem was through an integration of various modelling techniques, which therefore required a good understanding of the theoretical background.

2.1 Hydrologic Modelling

Hydrologic models are employed to understand dynamic interactions between climate and land-surface hydrology (Singh and Woolhiser, 2002). Furthermore hydrologic models are fundamental to water resources assessment development and management. These models are utilized to quantify the impacts of catchment management strategies for environmental and water resource protection. Hydrologic models for Mlazi were employed for the delineation of inundation levels and flood forecasting using weather radar.

A vast amount of research on hydrologic (rainfall-runoff) models and their application has been conducted. These models require complex analysis of temporal or spatial variations of precipitation, hydrologic abstractions, runoff, and evapotranspiration. A hydrologic model is an application that simulates the hydrological cycle.

The simple standard steps in hydrologic modeling consist of the following:

- selection of the model,
- model formulation and construction,
- model testing, validation and calibration, and
- model application.

The important first step in model selection is entirely based on the following:

- its availability,
- knowledge of its structure,
- operation,
- limitations
- availability of input data.

2.1.1 Physically based Models

Physically based models are intended to simulate the hydrological process by reproducing the physical processes that convert rainfall into runoff and transform the runoff downstream after considering the losses in the catchment. These are complex models and they require very detailed information on the state and characteristics of the catchment. The use of GIS has been a great benefit in the capture and processing of the required catchment characteristics such as vegetation cover, soil type and properties, terrain information as well as climate variables. The advantage of these models is that they give results, which are approximate to the observed flows. The disadvantage to these models is that they are not reliable for real time flood forecasting, due to the many parameters which have to be considered and up dated when the state of the catchment changes.

Physical based modelling can be classified as event based and continuous modelling. The event based hydrologic models are short-term models designed to simulate individual rainfall-runoff events. Their major disadvantage is the lack of a process to estimate antecedent soil moisture conditions prior to storm events. The advantages of physically based continuous simulation models are discussed next.

2.1.2 Continuous Modelling

Continuous process models take into account all the runoff components including direct runoff and indirect runoff (interflow and ground water). The continuous models focus on evapotranspiration and other hydrological abstractions, and hence models the soil moisture balance explicitly. The modeling process is suited for long term simulations of daily, monthly and or seasonal streamflow. Continuous simulation hydrologic models such as the HEC-HMS model can simulate runoff using long, historical precipitation records. The models can handle precipitation from a number of gauges. Bradley *et al* (1996) state that soil moisture conditions are modelled throughout the catchment between storms. The paper also mentions that continuous simulation models can be coupled with dynamic flood routing hydraulic models to simulate backwater and flood plain storage such as what has been performed for the Mlazi Catchment.

Bradley *et al* (1996) introduced a new continuous hydrologic model applicable to urban watersheds. The new method introduced was the peak stage frequency analysis. This method was compared with other methods such as modified design storm approach and the peak to volume approach (flood frequency analysis) presented by Bradley and Potter (1992). The peak stage frequency differs from the flood frequency analysis in that for the peak stage frequency, a statistical approach is applied directly to the simulated peak stages to estimate peak stage exceedence probabilities. In the case of flood frequency analysis, the probability distribution is fitted to the flood volume and a statistical relationship is found between the flood peak and the associated flood volumes. The advantage associated with this approach is that the design storm and steady state assumptions are unnecessary and furthermore the frequency analysis is carried out on water levels rather than on storm rainfall.

A continuous hydrologic model for the Mlazi Catchment was set up using the HEC-HMS program and GIS software. HEC-HMS was developed by the Hydrologic Engineering Center (HEC) of the United States Army Corps of Engineers (USACE) (HEC-HMS, 2000). The calibrated HEC-HMS model was used for the creation of the Mlazi Meta Model to be used for real time flood forecasting. This is a very important concept whereby the physical processes of the Mlazi catchment are transferred to the conceptual model (MMM) through the use of input and output data from the HEC-HMS for validation.

2.1.3 Modern Hydrologic Models

Most modern hydrologic models are conceptual models, which use the concepts of physical models and apply mathematical techniques to reduce the complexity while retaining the characteristics of the catchment. The models vary in their configuration to suit different purposes. Singh and Woolhiser (2002) state the popularity of WATFLOOD models for hydrologic simulation in Canada. In their paper they mentioned a study sponsored by the World Meteorological Organisation (WMO) on inter-comparison of catchment hydrologic models. Singh and Woolhiser (2002) states that the first study dealt with conceptual models used in hydrologic forecasting. The conceptual model used in the hydrologic forecasting of Mlazi is a linear reservoir model (Pegram and Sinclair, 2002) and this model is comparable with other models applied in the USA as discussed in the literature review (Section 1.4.2).

2.1.4 Integration of the Models

The initial process in integration of models is the linking of the hydrologic models to Geographical Information Systems (GIS). The quality of hydrologic modeling has greatly improved through the integration of spatially distributed parameter models with practical data management scheme such as the GIS and database management systems mentioned in data analysis (Section 2.1). As mentioned in Section 1.4.1, GIS technology has enabled easier data collection and compilation for quantitative and qualitative modeling processes. Furthermore, modeling results can be displayed spatially in a more colourful and informative way especially to the disaster management centres (like the one in eThekwini Municipality) in order to help in decision-making. The integration of GIS with hydrological/hydraulic modeling is a feasible approach that mutually benefits both users of GIS and hydrologic modelers.

The current focus of the integration process is the integration of the continuous flood simulation models with the continuous flood forecasting models. The whole purpose of this approach is intended for the production of forecasts, which are more precise, and also to improve the modeling processes. The integration of models has been used in a wider spectrum of water resource planning and management.

Integration of models in the context of Mlazi involves a desk analysis of Mlazi and the forecasting application. During the desk top analysis, hydrologic and hydraulic spatially distributed data are captured through GIS technology as explained by Hensen *et al* (2001) in their paper on GIS application in flood line studies for specific rivers in the Durban area of KwaZulu-Natal South Africa. The other process linked with the GIS is the creation of the digital elevation models for both the hydrologic and hydraulic model as will be explained in the creation of Digital Elevation Model in Section 3.3. The general procedure involves the use of design storm hyetographs as input to the calibrated hydrologic model HEC-HMS. These design storms of various recurrence intervals are computed using appropriate synthetic storm distributions and the mean 24-hour and 72-hour design rainfall depth. These design storms are input to both the HEC-HMS model and the forecasting system developed by Sinclair (2000). The Mlazi Meta Model is calibrated so that the catchment response mimics the output from the HEC-HMS model, which is a physically based model. The fine tuned forecasting model is used together with telemetering gauges at the Shongweni Dam to conduct real time forecasts of floods.

The other aspect presented is the modelling of the Inundation process. This involves the use of the calibrated hydraulic model HEC-RAS to route the computed design flows to enable the simulation of levels of inundation. The levels of inundation are intended to be displayed online (based on forecast) and/or offline at the eThekwini Metro Disaster Management Center using GIS. The results from the HEC-RAS model consist of the levels of inundation, the depth grid and velocity grid, which are exported into GIS. The levels of inundation are displayed in the form of flood plains for the various recurrence intervals. The depth across the floodplain is displayed using colour coding. For instance a dark colour corresponds to a high water depth whereas a light yellow colour corresponds to a lesser water depth.

Having described the various hydrologic models applicable, the next section discusses the hydrological routing applicable to the selected hydrologic model. The choice of the hydrologic model is entirely based on the intended purpose, availability of the model and also the availability of input data.

2.2 Hydrological Routing

According to Chow *et al* (1988), the term hydrological routing is considered to imply an analysis to trace the flow through a hydrologic system. The analysis could be a lumped or distributed system routing. The lumped routing system is often referred to as hydrologic routing whereas the distributed system is referred to as the hydraulic routing. Both of these routing systems are applied to the Mlazi flood analysis. Hydrologic routing, which computes flow as a function of time, is applied in the HEC-HMS model discussed in Section 3.4. Hydraulic routing computes flows as a function of space and time and is discussed in Section 4.2. Hydraulic routing is used in the HEC-RAS model to trace flows in the Mlazi River and thereby compute the levels of inundation.

This section defines the hydrologic routing processes adapted for the channel reaches in catchment modelling process. It highlights the notion that the outflow hydrograph depends upon the channel geometry, bed slope, length of channel reach, roughness and initial and boundary conditions. The term flood routing refers to procedures, which involve determining the outflow hydrograph at the junction downstream as a function of the hydrograph at a junction upstream. The section addresses the use and selection of lumped hydrologic routing models to conduct hydrological routing for the Mlazi catchment.

2.2.1 Lumped Routing

The continuity equation and approximations of the momentum equation govern the formulation of lumped routing models. These models are said to be mathematically simple. They are therefore easy to compute and they possess an added advantage over other complex dynamic routing models in the sense that it is easier to obtain the parameters applicable to their application.

All the routing models require the following basic information, which can be difficult to obtain in a data sparse environment as in the case of the Mlazi. However, the alternative approaches together with the sensitivity and calibration of the models enables a good approximation of these parameters:

- Channel characteristics. The channel characteristics include the channel width, bed slope and cross-sectional shape. Faced with uncertainty it is difficult to determine the channel geometry precisely.
- Energy-loss model parameters. All routing models incorporate some type of energy-loss model. The physically based models such as the kinematic-wave model and the Muskingum-Cunge model use the Manning's equation and Manning's roughness coefficients (n values) (HEC-HMS, 2000).
- Boundary conditions. The boundary conditions to be considered depend on the modelling software being used. In the case of Mlazi catchment the HEC-HMS model provides the flow hydrograph inputs to the HEC-RAS river model as highlighted in Section 4.7.

Chow *et al* (1988) and Ponce (1989) states that for an ideal channel, storage is a function of inflow and outflow, whereas with ideal reservoirs, the storage is solely a function of outflow. These variables are related by the continuity equation as shown in Equation 2.2.1. S (t) is the storage within the system (channel reach or reservoir), I(t) is the inflow hydrograph at the upstream end of the reach, and Q(t) is the outflow hydrograph at the downstream end of the reach. The lumped routing models are therefore based on this differential equation of storage.

$$I(t) - Q(t) = \frac{dS(t)}{dt} \qquad \text{Eqn (2.2.1)}$$

The above equation cannot be solved directly so as to obtain the outflow hydrograph downstream of the river reaches. The reason being that although inflow hydrograph, I(t), is obtained from observed flows or the rainfall-runoff computations, S(t) and Q(t) are unknown. It therefore follows that a storage function relationship would need to be developed, relating S (t), I (t) and Q (t). The storage function required depends on the nature of the system being analysed.

Different methods have therefore been developed such as the Modified Puls (level pool) method used for computations for reservoir routing and the Muskingum method used for flow routing in channels.

The storage function relationship which takes into account the channel characteristics could have been obtained by using the Muskingum method. However, due to unavailability of channel characteristic data and flow data for the Mlazi River, the method was not applied. An investigation of the variation of the K and approximated X values for various channel reaches was conducted for Mhlatuzana River using the inflow and outflow results computed using the modified Puls routing. The other parameters necessary for the investigation were obtained from the hydraulic results from HEC-RAS. The aim was to determine whether the same K and X values could be used as an initial input to the Muskingum Cunge routing method for the Mlazi River. This approach was considered with the assumption that these rivers have the same channel reach characteristics. The attempt was not developed any further due to complications with regard to estimation of the other parameters required. A similar approach was later conducted as is discussed in Section 3.5.13. However, this comparison was done on the storage flow relationships obtained from the HEC-RAS model to be used in the modified Puls method discussed in Section 2.2.2. The Muskingum method is reliable for a situation where all the parameters required are available, it is therefore discussed in the following section.

2.2.2 Muskingum Routing

The storage in the reach is modeled as the sum of prism storage and wedge storage. Prism storage is the volume defined by a steady-flow water surface profile, whereas wedge storage is the additional volume under the profile of the flood wave, a diagrammatic presentation of these storages is found in the HEC-HMS manual (2000). The storage equation is discretised on an xt plane (Figure 2.2.1) to yield:

$$\frac{I_1 + I_2}{2} - \frac{Q_1 + Q_2}{2} = \frac{S_2 - S_1}{\Delta t} \qquad \text{Eqn (2.2.3)}$$

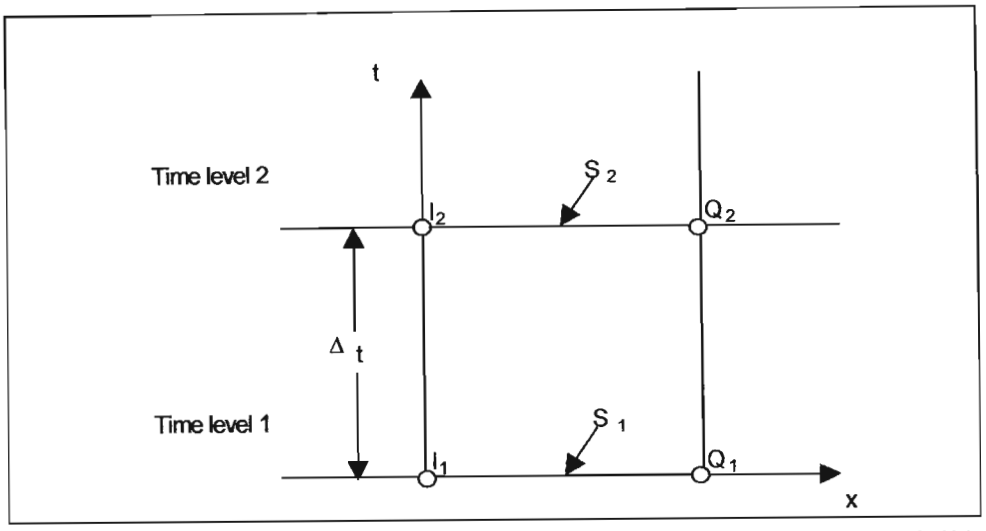

Figure 2.2.1: Discretization of storage equation in xt plane (Chow et al, 1988)

Equation 2.2.3 is then expressed at time levels 1 and 2:

$$S_1 = K\left[XI_1 + (1 - XQ_1)\right] \qquad \text{Eqn (2.2.4)}$$

$$S_2 = K\left[XI_2 + (1 - XQ_2)\right] \qquad \text{Eqn (2.2.5)}$$

where: S = storage volume, m^3

I = inflow, m^3/sec

Q = outflow, m^3/sec

K = a time constant or storage coefficient which accounts for the translation portion of the routing, and

X = dimensional weighting factor which accounts for the storage portion of the routing.

The range for X is:

$$(0 \le X \le 0.5)$$

Substituting the two Equations (2.2.4 and 2.2.5) into Equation 2.2.3 and solving for Q_2 gives:

$$Q_2 = C_0 I_2 + C_1 I_1 + C_2 Q_1 \qquad \text{Eqn (2.2.6)}$$

In which C_0, $C_1$and C_2 are routing coefficients expressed in terms of Δt, K, and X as follows:

$$C_1 = \frac{(\Delta t / K) + 2X}{2(1 - X) + (\Delta t / K)} \qquad \text{Eqn (2.2.7)}$$

$$C_0 = \frac{(\Delta t / K) - 2X}{2(1-X) + (\Delta t / K)} \qquad \text{Eqn (2.2.8)}$$

$$C_2 = \frac{2(1-X) - (\Delta t / K)}{2(1-X) + (\Delta t / K)} \qquad \text{Eqn (2.2.9)}$$

The routing coefficients are interpreted as weighting coefficients since $C_0+C_1+C_2 = 1$.

In the Muskingum method with K = Δt and X = 0.5,flow conditions are such that the outflow hydrograph retains the same shape as the inflow hydrograph, but is translated downstream a time equal to K. For X = 0, Muskingum reduces to linear reservoir routing. It is noted that the variation of the parameters X and K plays a major role in the translation and attenuation of the inflow hydrograph to result in an outflow hydrograph characterized by the channel characteristics, flow and time of travel.

2.2.3 Modified Puls

The storage function can either be invariable or variable. A variable storage-outflow relationship applies to long, narrow reservoirs and to open channels like in the case of Mlazi river reach channels. In this case the water surface profile may be significantly curved due to backwater effect. The backwater effect causes a retarding effect resulting in the peak outflow occurring later than when the inflow and outflow intersect. Peak outflow occurs when the outflow hydrograph intersects the inflow hydrograph. This is the case for reservoir systems with horizontal water surfaces, which have a pool that is wide and deep compared to its length in the direction of flow, and low flow velocities in the reservoir. A suitable method for such systems is the Modified Puls method.

The Modified Puls routing method, also known as storage routing or level-pool routing is based upon a finite difference approximation of the continuity equation, coupled with an empirical representation of the momentum equation. Chow *et al* (1988) explains the finite approximations in detail.

An Equation 2.2.10 similar to the Equation 2.2.3 but has unknown values at the LHS.

$$\left(\frac{S_2}{\Delta t}+\frac{Q_2}{2}\right)=\left(\frac{I_1+I_2}{2}\right)+\left(\frac{S_1}{\Delta t}-\frac{Q_1}{2}\right) \qquad \text{Eqn (2.2.10)}$$

A functional relationship between storage and outflow is required to solve Equation 2.2.10. For this study the water-surface profiles computed with the hydraulic model HEC-RAS define a relationship of storage to flow between two cross sections. The first estimate of the storage flow function for the reaches was obtained from the Mhlatuzana HEC-RAS model. These were later compared to the actual storage function of the Mlazi and it was observed that there is a close relationship between the two. The comparison of these relationships is shown in Section 4.5.

Summary

Various routing options for the HEC-HMS model as stated in HEC-HMS (2000) include Muskingum, Lag, Kinematic wave Muskingum Cunge and Modified Puls methods. The routing model chosen for the Mlazi is the Modified Puls because of the availability of the storage-flow relationships, which were obtained from HEC-RAS. It should be noted that the initial storage –flow relationships were derived from storage – flow rating curves for Mhlatuzana since the two rivers have similar catchment characteristics.

2.3 Design Storms

A design storm can be defined by the probability of a value for precipitation depth at a point, by a design hyetograph specifying the time distribution of precipitation during a storm, or by an isohyetal map specifying the spatial pattern of the precipitation depth (Chow *et al*, 1988). The design storm for the Mlazi Catchment is defined by a design hyetograph derived from the mean areal precipitation depth over the catchment, which is then distributed using a temporal distribution obtained either from SCS based synthetic rainfall distribution (Schmidt and Schulze, 1987) or the distribution developed by Adamson (1982). The two distributions could be applied together as was done for Mlazi (Section 3.5.3). Therefore, a revised synthetic rainfall distribution suitable for the Mlazi Catchment was used to distribute the design hyetograph. It will be noted in this discussion that short duration rainfall data is necessary for design flood estimations in the Mlazi context. Short duration, heavy rainfall in South Africa has typically a duration range of two to six hours (Alexander,

1993). The sections below discuss some of the parameters that are required in order to determine the design storm.

2.3.1 Precipitation Depth at a Point

Design precipitation depth can be classified as point precipitation or areal precipitation. Point precipitation occurs at a single point in space whereas areal precipitation is spatially distributed over a region. The frequency analysis process for the estimation of point precipitation involves the selection of the annual maximum precipitation for a given duration for each year of historical record. The process is repeated for each of series duration and subsequently the frequency analysis is carried out on the data to derive the design precipitation depths for various return periods. Smithers and Schulze (2000) conducted a frequency analysis, which resulted in the compilation of design rainfall depths at selected stations in SA.

The design precipitation depths are converted to intensities by dividing by the precipitation duration. Chow *et al* (1988) states that frequency analysis of areal precipitation still needs development. An average precipitation depth over an area is developed using point precipitation estimates in the absence of information on the probability distribution of areal precipitation. The averaging process results in location-fixed depth-area curves relating areal precipitation to point measurement.

2.3.2 Precipitation Intensity

Intensity can either be instantaneous intensity or the average intensity over the duration of the rainfall. Intensity is defined as the time rate of precipitation, that is the depth per unit time (mm/hr). The intensity is expressed as an equation or frequency curves. This section discusses intensity equations since they were the one considered to determine peak discharges. These equations depend on the location and site. Sherman (1905) observed that the maximum rain rate (i), in inches per hour, was related to duration (t), in minutes, as $i = 38.64/t^{0.687}$. For t<3hours he suggested an alternative form for the relation as i =420/(t+30).

Various other empirical intensity-duration-frequency relationships have been developed, such as the one by Bell (1969), $P = A/(t+b)^{n}$, where (P) is the average rainfall intensity in mm/min over (t) minutes for a particular return period. According to Bell (1969), (A) is a function of return period and location whereas (b) and (n) are functions of location only. Menabde *et al* (1999) describe a simple scaling hypothesis applied to the intensity-duration-frequency (IDF) description of rainfall. The paper develops a formula that enables the calculation of rainfall amounts of a chosen return period and duration shorter than a day, directly from data obtained from the analysis of daily data.

The Hydrological Research Unit (HRU) undertook studies on large and small area storm precipitation in South Africa. The HRU published DDF relationships in HRU 2/78 (Midgley and Pitman 1978). These relationships were based on the mean annual precipitation (MAP), locality (coastal or inland), and the published Weather Bureau (South African Weather Service) recording rain gauge data (Le Roux, 1974). The log extreme value (EV) distribution was fitted to the annual maximum series. Chi-square tests were conducted to confirm the goodness of fit. The relationship applied for several duration were:

$$I = \frac{I_0}{(I + BD)^{\eta}} \qquad \text{Eqn (2.3.1)}$$

Where (I) is the intensity (mm/h) associated with a duration of (D) hours, (I_0), (B) and (η) are parameters associated with a given region, MAP and the return period.

Another (IDF) relation was proposed by Koutsoyiannis *et al.* (1982) in the form:

$$i = \frac{a(T)}{b(d)} \qquad \text{Eqn (2.3.2)}$$

Where (i) is the rainfall intensity, (T) is the return period, and (d) is the duration of the extreme event. The function, b (d), is obtained from b (d) = $(d+\theta)^{\eta}$, where (θ) and (η) are phenomenological parameters to be estimated. The function, a (T), is determined from the probability distribution function of the maximum rainfall intensity.

Wenzel (1982) provided coefficients from a number of cities in the United States for an equation of the form:

$$i = \frac{a}{T_d^b + c} \qquad \text{Eqn (2.3.3)}$$

where

i = intensity (mm/hr)
a, c = constants
T = Return Period

The intensity equation used for the computation of intensity for Mlazi catchment was:

$$i = \frac{P_{d=t_c}}{t_c} \qquad \text{Eqn (2.3.4)}$$

where: $P_{d=tc}$ = the rainfall depth for a duration equal to the time of concentration (mm)
t_c = the catchment (hr)
I = intensity (mm/hr)

Having discussed the background on the intensity-duration frequency relationships, the next section features the design hyetographs, which are input to the HEC-HMS model for the Mlazi Catchment.

2.3.3 Design Hyetographs at a Point

The U.S. Department of Agriculture, Soil Conservation Service (SCS, 1986) has developed synthetic storm hyetographs for use in USA. These hyetographs have been for storms of 6 and 24-hour duration. The hyetographs were derived from data presented by Herschfield (1961) and Miller *et al* (1973). Four 24-hour duration storms called Type I, IA, II, and III were developed. These are applicable to various locations in the USA (Chow *et al*, 1988). A similar approach based on a digital rainfall data was adopted for Natal (Schulze and Schmidt, 1987). Ratios of D-hour to 24-hour rainfall were computed (from digitised rainfall database for Natal) for selected storm duration using a number of extreme value distributions. The ratios were plotted against the 24-hour duration symmetrically about a central point for a duration range of 5 minutes to 20-hours. The original SCS and Adamson (1982) distributions were plotted. The range of plots made enabled the identification of four distributions, which are presented in Section 2.3.4.

Chow *et al* (1988) describes various methods, such as the Alternating Block Method, and the Instantaneous Intensity Method to design hyetographs. A simple method for estimating the design hyetograph is the Triangular Hyetograph Method (see Figure 2.3.2). The method uses the design precipitation depth (P) and the duration (T_d) to compute the height of the triangle based on the given expression:

$$P = \frac{1}{2} T_d h \qquad \text{Eqn (2.3.4)}$$

Making h the subject of the formula gives:

$$h = \frac{2P}{T_d} \qquad \text{Eqn (2.3.5)}$$

The storm advancement coefficient (r) defined as the ratio of the time before the peak (t_a) to the total duration is computed as

$$r = \frac{t_a}{T_d} \qquad \text{Eqn (2.3.6)}$$

This enables the expression of the recession time (t_b) in terms of (T_d) and the storm advancement coefficient:

$$t_b = T_d - t_a \qquad \text{Eqn (2.3.7)}$$

$$t_b = T_d(1-r) \qquad \text{Eqn (2.3.8)}$$

A value of (r) determines the occurrence of the peak intensity relative to the storm duration. For instance r =0.5 corresponds to the peak intensity occurring in the midpoint of the storm duration, r<0.5 and r> 0.5 corresponds to the peak intensity occurring earlier and later than the midpoint of the storm duration (Chow *et al*, 1988) respectively.

Triangular Hyetograph

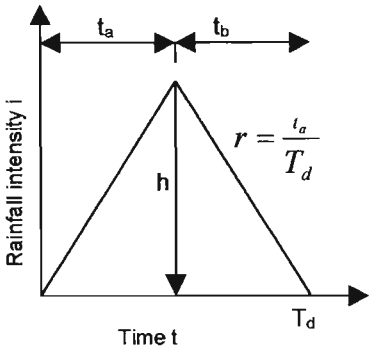

Figure 2.3.2: Triangular Hyetograph

The method applied in the design of synthetic hyetographs for the Mlazi catchment was the alternating block method. The triangular method was used as a rough quick check and therefore its application is not discussed in this dissertation. The next sections describe the distributions that were considered for the time distribution of the precipitation depths developed for various return periods for the design of synthetic hyetographs.

2.3.4 Dimensionless Distributions

As already mentioned the time distributions used for the Mlazi catchment study are based on the work carried out by Schulze and Schmidt (1987) and Adamson (1981). Schulze and Schmidt (1987) identified four distributions, which were termed:

- SA Type 1: SCS Type I distribution,
- SA Type 2: Durban's 10-year return period and SCS Type II distribution,
- SA Type 3: Adamson's summer rainfall region distribution, and

- SA Type 4: Estcourt's 50-year return period distribution.

The design hyetographs used as input into the HEC-HMS model were based on these types of distributions although some minor alterations were done to suit the Mlazi. The SA Type 2 distribution was selected for the Mlazi based on the regionalisation of synthetic rainfall distributions in South Africa (Schmidt and Schulze, 1987). The 24-hour storm duration and three-day storm duration were developed in 1-hour increments and applied to the Mlazi.

2.3.5 Storm Duration

In South Africa most high intensity rainfall is the consequence of heavy convective storms over a period of two to six hours (Alexander, 2000). Hypothetical storm options included in HEC-HMS permit storm design that can last from a few minutes to several days (HEC-HMS manual, 2000). The chosen duration should be such that it exceeds the time of concentration of the catchment. It is argued that the storm duration should be 3 or 4 times the time of concentration (County, 1990). The approximate time of concentration for Mlazi catchment is 15 hours, when the time of concentration is multiplied by four it gives 60 hours. Studies conducted by Levy and McCuen (1999) showed that a 24-hour hypothetical storm is a reasonable selection if the storm duration exceeds the time of concentration of the watershed. The storm durations for Mlazi considered are for the 24-hour duration and the 72-hour duration. The use of three-day storm duration (72-hours) for Mlazi was therefore justified.

The alternating block method (Chow et al, 1988) was used to develop the three-day synthetic hyetograph from the three day rainfall depths obtained from Smithers and Schulze (2000). The daily rainfall depth for each of the three-day rainfall depths had to be distributed using the temporal distribution to produce a hyetograph with a 1-hour computation interval. The three 24- hour hyetograph were arranged randomly to give the 72 hour hypothetical storm.

The three-day design storm had six random combinations, which are equi-probable temporal distributions because there is negligible correlation between daily amounts of rain in a sequence of wet days. Zucchini and Adamson, (1984). The scenarios based on the six random combinations were developed. The daily rainfall depth with the lowest depth was labelled L, then the depth of a medium magnitude was labelled, M and the depth of the highest magnitude was

labelled, H. Figure 2.3.3. represented the LMH scenario in which the lowest depth L was considered to contribute to the first day of the 3 days followed by the medium M and then the highest H. The worst scenario could have been the most favourable to be used for analysis. However it was deduced from the historical flooding of the canal that such a scenario has not really occurred as yet and since the delineation of the flood plain was calibrated based on historical flood events, the scenario used was the MHL. The synthetic hyetograph was used as input to the HEC-HMS model and also as input to the MMM.

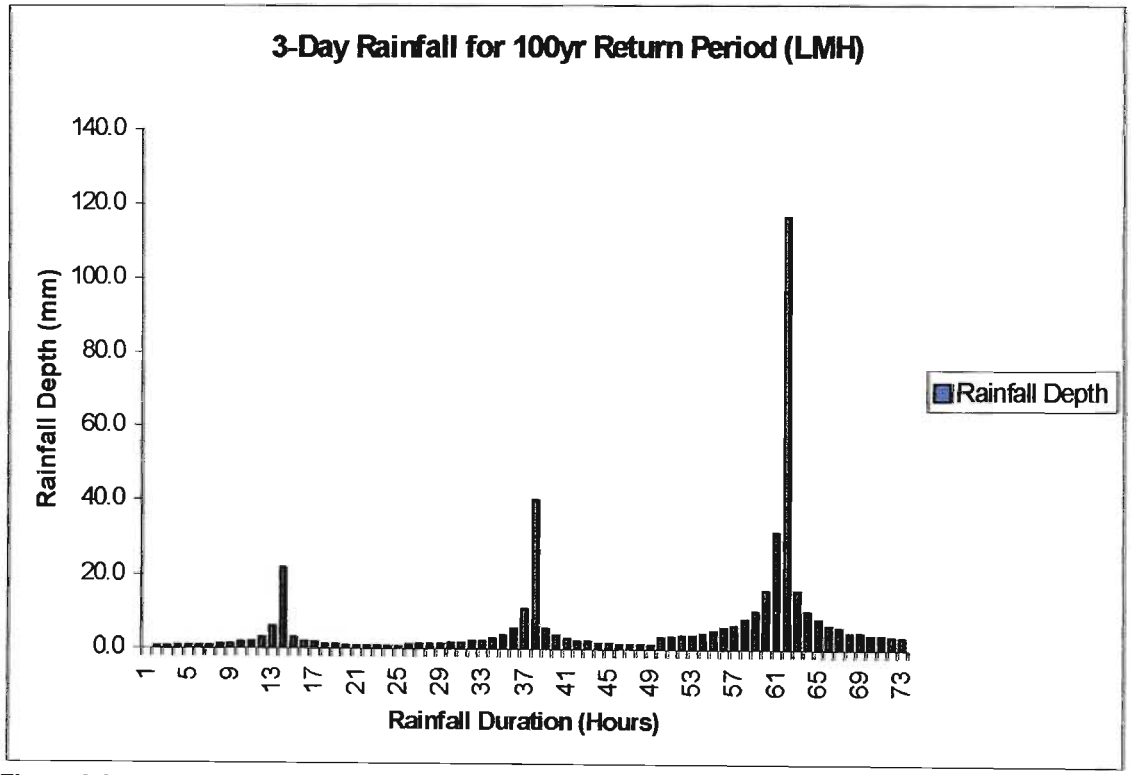

Figure 2.3.3: 3-Day Rainfall Temporal Distribution for the worst scenario (LMH)

The method discussed in this section were applied to the Mlazi during the computation of flows which would have to be routed through a hydraulic model using the hydraulic modelling techniques discussed in the next section.

2.4 Hydraulic Modelling

This section presents the flow hydraulic theory and concepts for open channel flow, which are needed in the understanding of the hydraulic routing of peak flows and computation of inundation levels in the Mlazi River. The hydraulic river analysis is performed using one-dimensional flow. The hydraulic routing model to be applied is the HEC-RAS model, which is discussed in detail in Section 4.3. It should be noted that there are various flow hydraulic models that can be used for the solution of full, dynamic equations of motion for one-dimensional unsteady flow in open channels.

A good river model requires a substantial knowledge of the basic fluid flow concepts and these can be obtained from hydraulic textbooks such as Open-Channel Hydraulics (Chow, 1959), and Open Channel Flow (Henderson, 1966).

2.4.1 Flow Classification

Chow (1959) classifies open channel flow into two main categories and sub-categories as follows:

- Steady flow
    - i) Uniform flow
    - ii) Varied flow
        - a) Gradually varied flow
        - b) Rapid varied flow
- Unsteady flow
    - iii) Unsteady Uniform flow (not common)
    - iv) Unsteady flow (unsteady varied flow)
        - c) Gradually varied unsteady flow
        - d) Rapid varied unsteady flow

Steady Flow and Unsteady Flow; Time as the Criterion

The steady flow and unsteady flow classification is a time based criterion as stated by their definitions. For instance flow in an open channel is said to be steady if the depth of flow does not change or it can remain constant during a selected time interval. The flow is unsteady if the depth changes with time. During this study, the steady state condition was considered for natural open channels of the Mlazi River where the riverbed is generally steep and there is not much lateral flow. The unsteady state was condition was considered for the Mlazi canal where there exist flood plains, which inundates due to surplus flows

from the canal. This implies that the main channel flow in the canal changes with respect to time. This a major concern for the area around the canal because in order to be able to install a streamflow forecasting system, the stage of flow as the flood wave passes and the time variant should be closely monitored to enable precise predictions for developing a flood warming system.

In steady on unsteady state analysis the velocity at a point across the section is dependent on its location relative to the x-dimension and the y-dimension. Three types of dimensional flow have been identified based on how the velocity was assumed to be affected by its location.

One-dimensional, two-dimensional and three-dimensional flows

A three – dimensional flow is one in which the velocity at a point on the cross section is dependent on the streamwise location (the x-dimension) as well as on the distances of the point in the cross section from the bed and the sidewall. If the channel were very wide in relation to the depth, the time -averaged velocity at any given elevation in a section would be constant, in such a case the velocity would be independent of the distance from the sidewall. This kind of flow is two-dimensional flow. A simplified analysis of the flow features can be conducted by using an average velocity over the cross-section. When only the variations of the average velocity with x are considered then such a flow is one-dimensional, which can either be analysed under steady or unsteady. In the Mlazi study the one-dimensional steady state analysis is carried out for the natural channel. Two-dimensional unsteady state analysis was intended to be used for the Mlazi canal area as flood flows through flat and wide flood plains have flow across the floodplain, which are of the same order of magnitude as that of flow down the channel. However one-dimensional unsteady state analysis coupled with off-channel storage proved to be reliable for the Mlazi canal analysis as will be discussed in Chapter 5.

Uniform Flow and Varied Flow; Space Criterion

Uniform flow in a channel exists when the depth, discharge and mean velocity do not change along the length of the channel. Under these conditions, the streamlines are straight and the convective acceleration is zero. In a channel, uniform flow must also be steady, i.e. not changing with time, else the surface would distort and destroy uniformity. The constant velocity results in a constant specific energy, which therefore implies that the energy grade line and water

surface will have the same slope as the channel bottom. For a given distance x along the length of the channel derivatives such as these apply

$$\frac{dy}{dx} = 0 \qquad \text{Eqn (2.4.1)}$$

$$\frac{dV}{dx} = 0 \qquad \text{Eqn (2.4.2)}$$

$$\frac{dQ}{dx} = 0 \qquad \text{Eqn (2.4.3)}$$

$$\frac{dH}{dx} = \frac{dz}{dx} = S_o \qquad \text{Eqn (2.4.4)}$$

where: y = the flow depth
V = the velocity at a cross section
Q = the volumetric flow at a cross section
Z = the bed elevation
H = the total head at a section
S_o = the constant bed slope.

Flow is varied if the depth of flow changes along the length of the channel (also described as nonuniform flow), the above-mentioned variables change along the length of the channel as shown in Figure 2.4.1.

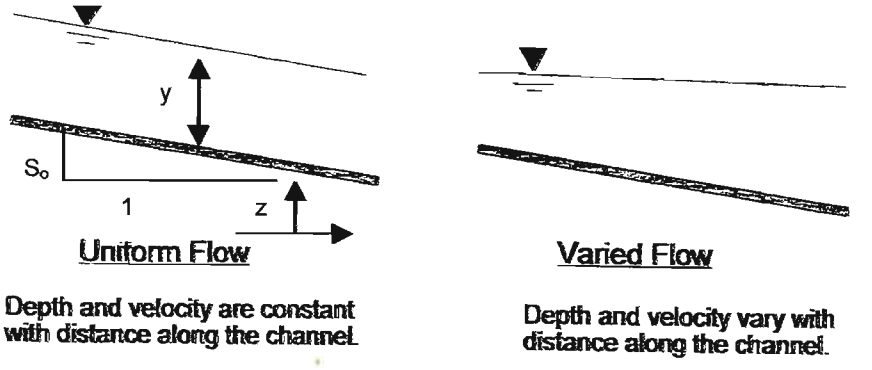

Figure 2.4.1: Uniform versus Varied Flow (Chow, 1959)

Varied flow may further be subdivided into gradually varied and rapidly varied flow depending on whether these flow variations are gradual or rapid. The flow for the Mlazi River was generally identified as gradually varied flow although there is evidence of rapidly varied flow at certain places as will be evidenced by the output flow profile results from the HEC-RAS model in Appendix A

2.4.2 Open Channel Equations for Gradually Varied Flow

The open channel equations for gradually varied flow are based on the three energy conservation principles such as these; conservation of water mass, conservation of the mechanical energy content of the water, and conservation of the momentum content of the water that are available for the analysis of 1-D steady flow. Conservation of thermal energy is not considered because temperature-change and heat-transfer effects do not affect depth and discharge. These conservation principles have lead to the development of the dynamic or energy equation, which is described and derived in hydraulic texts such as; Chow (1959) and Henderson (1966). It is apparent from the standard textbooks that a choice of which conservation principle, which should be considered for a model, can be based on how well the various flow parameters and variables can be approximated. Furthermore on how well each particular principle works when approximations to physical reality are possible. The models are good when precise input parameters are available but this is not so in the case of Mlazi because of the uncertainly of the parameters.

The passage of overland flow into a channel can be viewed as lateral flow. These flows generally enter approximately at right angles to the main channel flow, and when these flows interact then considerable turbulence occurs. The application of the energy-conservation principle would require that the kinetic and potential energy of lateral flows is estimated, and such estimates are nearly impossible to make accurately. Therefore the energy principle is only applicable to gradually varied flow situations. The transition from subcritical to supercritical is a rapidly varying flow situation as in the case of stream junctions and bridge constrictions. For such instances then it is advisable to apply the principle of momentum. This is the approach adopted for the HEC-RAS model applied for Mlazi river hydraulics (see Chapter 4).

In order to understand how these principles are applied it is necessary to describe the open channel equations; their assumptions and in certain cases their derivations. The equations are:

1) Energy Equation
2) St. Venant Equation
3) Chezy Equation
4) Manning's Equation

Energy Equation

The open channel flow energy equation is:

$$z_1 + y_1 + \alpha_1 \frac{V_1^2}{2g} = z_2 + y_2 + \alpha_2 \frac{V_2^2}{2g} + h_L \qquad \text{Eqn (2.4.7)}$$

Where z is the bed elevation, y is the depth of flow, $V_1^2/2g$ is the velocity head, α is the kinetic energy correction factor and h_L is the headlosses.

If the following assumptions are valid:

- The head loss due to friction is equal to zero. This implies that the channel is a perfectly frictionless surface.
- The α_1 and α_2 are coefficients that account for a non-uniform velocity distribution are set to 1 then the velocity distribution is assumed to be uniform and Equation 2.4.7 becomes:

$$z_1 + y_1 + \frac{V_1^2}{2g} = z_2 + y_2 + \frac{V_2^2}{2g} = C \qquad \text{Eqn (2.4.8)}$$

which is the Bernoulli equation written in open channel flow form.

The energy equation is applied in HEC-RAS for the computation of the mean energy at each cross section. The HEC-RAS software is a one-dimensional steady flow water surface model, therefore it can only compute a single water surface at each cross section. This is the reason why the mean energy has to be computed. A flow-weighted energy from the subsections of the cross section needs to be computed. In order to compute the mean kinetic energy, it is necessary to obtain the velocity head weighting coefficients α = k.e correction factor:

$$\alpha \frac{\overline{V^2}}{2g} = \frac{Q_1\left(\frac{V_1^2}{2g}\right) + Q_2\left(\frac{V_2^2}{2g}\right)}{Q_1 + Q_2} \qquad \text{Eqn (2.4.9)}$$

2.4.3 St Venant's Equations

The Saint Venant equation, developed by Barre de Saint-Venant in 1871, describe unsteady, gradually varying one dimensional open channel flow, which are applied to the canalised section of the Mlazi.

Assumptions

The major assumptions used in the derivation of the Saint-Venant equation (Chow *et al*, 1988) are as follows:

- The flow is one-dimensional, meaning that depth and velocity vary only in the longitudinal direction of the channel. This implies that the velocity is constant and the water surface is horizontal across any section perpendicular to the longitudinal axis.
- Flow is assumed to vary gradually along the channel so that hydrostatic pressure prevails and vertical accelerations can be neglected (Chow, 1959).
- Channel alignment with respect to the effect of directional changes on the conservation of momentum principles is assumed to be rectilinear even though the channel is curvilinear. Thus, the water surface in any cross section of the stream is assumed to be horizontal. Super-elevation effects on the water surface in channel bends are not considered in the analysis and are assumed to have a small effect on the results
- The bed of the channel has shallow slope so that:
  (a) The tangent and sine of the angle that the bottom makes with the horizontal have nearly the same value as the angle
  (b) The cosine of the slope angle is approximately 1
  The channel geometry is fixed so that the effect of deposition or scour of sediments is negligible.
- Resistance coefficients for steady uniform turbulent flow are applicable so that relationships such as Manning's equation can be used to describe resistance effects. The fluxes of momentum and energy along the cross section resulting from non-uniform velocity distribution may be estimated by means of average velocities and flux-correction coefficients

that are functions of location along the stream and water-surface elevation.

- The flowing fluid is incompressible and homogeneous throughout the flow (constant density).

The two equations used in modelling are the continuity equation and the momentum equation. These equations are based on Reynolds Transport theorem (Chow *et al*, 1988).

Continuity Equation

The conservative form of the continuity equation, which is applicable at channel cross section, is as follows:

$$\frac{dQ}{dx} + \frac{dA}{dt} = q \qquad \text{Eqn (2.4.10)}$$

The equation is valid for prismatic or non-prismatic channel. Chow *et al* (1988) defines the prismatic channel as one, which has a cross sectional shape that does not change along the channel and has a constant bed slope. There are cases when some methods for solving the Saint-Venant equations require a non-conservation form of the continuity equation. This non-conservation form of continuity equation is as follows:

$$V\frac{dy}{dx} + y\frac{dV}{dx} + \frac{dy}{dt} = 0 \qquad \text{Eqn (2.4.11)}$$

Momentum Equation

The momentum equation is derived from Newton's second law that has been written in the form of the Reynolds transport theorem for control volume V:

$$\sum F = \frac{d}{dt}\int\int_{c.v} \int V\rho V \cdot dA \qquad \text{Eqn (2.4.12)}$$

The full derivations of these formulae as described in hydraulic textbooks such as Chow *et al* (1988) and will not be dealt with in this section. The momentum equation can also be derived from energy principles. The non-conservation form (per unit width element) and the conservation form of the momentum equation are given below as Equation 2.4.13 and Equation 2.4.14 respectively:

$$\frac{dV}{dt} + V\frac{dV}{dx} + g\frac{dy}{dx} - g(S_0 - S_f) = 0 \qquad \text{Eqn (2.4.13)}$$

$$\frac{1}{A}\frac{dQ}{dt} + \frac{1}{A}\frac{d}{dx}\left(\frac{Q^2}{A}\right) + g\frac{dy}{dx} - g(S_0 - S_f) = 0 \qquad \text{Eqn (2.4.14)}$$

It should be noted that the terms in Equation 2.4.14 could be classified as:

$$\frac{1}{A}\frac{dQ}{dt} = \quad \text{Local acceleration term}$$

$$\frac{1}{A}\frac{d}{dx}\left(\frac{Q^2}{A}\right) = \quad \text{Convective acceleration term}$$

$$g\frac{dy}{dx} = \quad \text{Pressure force term}$$

$$g(S_0 - S_f) = \quad \text{Gravity and Friction force term}$$

Chezy Equation and Manning's Equations

Open channel flow is evaluated by using empirical formulas such as Manning's and Chezy equations. These equations are derived on the basis of the Darcy-Weisbach equation for head losses due to wall friction (Chow *et al*, 1988).

The Chezy equation according to Chow *et al* (1988) was developed by French engineer Antoine Chezy (1769) as the first uniform formula. The formula was derived based on two assumptions:

- It was assumed that the force resisting the flow per unit area of the streambed is proportional to the square of the velocity (KV^2), with (K) being a proportional constant.
- It was also assumed that the channel was undergoing uniform flow.

The difficulty with the Chezy formula is the determination of the value of (C). There are various formulas which are applied in order to compute (C) such as the G.K.formula, the Bazin formula, the Powell formula and the Darcy-Weisbach formula.

The Darcy –Weishbach equation for pipe flow is:

$$h_f = f\frac{L}{D}\frac{V^2}{2g} \qquad \text{Eqn (2.4.15)}$$

Where h_f is the head loss over a length (L) of the pipe diameter (D) for a flow with velocity (V), where (f) is the Darcy-Weisbach friction factor and (g) is the acceleration due to gravity (Chow *et al*, 1988). The formula is manipulated by defining the frictional slope $S_f = h_f/L$ and introducing the hydraulic radius (R) for a circular pipe = D/4 and making (V) the subject of the formula for uniform channel flow when $S_o = S_f$ to give:

$$V = \sqrt{\frac{8g}{f}RS_f} \qquad \text{Eqn (2.4.16)}$$

The chezy (C) is identified as:

$$C = \sqrt{\frac{8g}{f}} \qquad \text{Eqn (2.4.17)}$$

The Equation 2.4.16 is then written as:

$$V = C\sqrt{RS_f} \qquad \text{Eqn (2.4.18)}$$

The Manning's equation was late developed in 1889 by deriving a relationship between Manning's "n" and Chezy's "C" in imperial unit

$$C = \frac{1.49}{n}R^{1/6} \qquad \text{Eqn (2.4.19)}$$

The equation was finally modified to SI units by dropping the factor to give the widely used Manning's formula:

$$V = \frac{1}{n}R^{2/3}S_f^{1/2} \qquad \text{Eqn (2.4.20)}$$

The Manning's formula is valid for fully turbulent flow and is used in the computations by the HEC-RAS model. The section discusses rapid varied flow experienced when flow passes through structures such as bridges and culverts.

2.4.4 Flow Types Past Hydraulic Structures-Rapid Varied Flow

Chow (1959) explains that the sudden transitions with the change of cross sectional dimensions occurring in relatively short distances induce rapid varied flow. The transitions observed are in the form of contractions and expansions

vertical as well as horizontal. Chow (1959) states that experiments and test have been conducted to analytically investigate the contractions in supercritical flow by applying the mechanics of supercritical flow and also for contractions in subcritical flow.

The South African Committee of State Road Authorities has produced a guideline for the hydraulic design and maintenance of river crossings (CSRA, 1994), which gives five types of flow through a constriction in a channel. HEC-RAS assumes that a constriction occurs whenever the velocity head downstream is greater than the velocity head upstream. Likewise, when the velocity head upstream is greater than the velocity head downstream, the program assumes that a flow expansion is occurring. Typical constriction values for subcritical flow contraction and expansion coefficients used for Mlazi are given in section 4.6. The methods adopted by the HEC-RAS model in computation of losses through the bridge are:

- Energy Equation (standard step method)
- Momentum Balance
- Yarnell Equation
- FHWA WSPRO method.

Summary

In this section the flows likely to be observed in the output results from HEC-RAS have been discussed. It has also been observed that flows through constrictions can be categorised based on whether they are high flows or low flows. The flow classification for the bridges determines the bridge modelling approach. For instance the bridge modelling approach used for low flows for the Mlazi was the energy and momentum methods, which uses the energy and momentum principles, discussed under the open channel flow equations. Since most of the bridge piers observed during fieldwork were square nose piers, a C_d = 2.0 was used for the momentum method. The high flows through the constrictions were computed using the Pressure flow and weir flow. In this case the pressure flow option used was one whereby the bridge constriction was assumed flowing completely full. The submerged inlet and outlet coefficient chosen is 0.8.

The open channel flow equations such as the energy equation and the Manning's equation have been stated and a brief account of their application

has been discussed. The St Venant's equations have been introduced together with their assumptions. Their applications on the model will be further discussed in the model descriptions in Section 4.3.

The following section discusses the analysis of uncertainty on some of the parameters that are used for computations of inundation levels based on the open channel equations already discussed in this section.

2.5 First Order Analysis of Uncertainty

A first order analysis of uncertainty is a procedure for quantifying the expected variability of a dependent variable calculated as a function of one or more dependent variables (Chow *et al*, 1988). The work presented by Christiaens and Feyen (1999) highlights an approach whereby both a Sensitivity Analysis (determining crucial inputs) and an Uncertainty Analysis (studying uncertainty of model outputs) are simulated. A sensitivity analysis of different models is first conducted and based on this analysis the most certain output is determined. Christiaens and Feyen (1999) states the replacement of mathematical simulation models in a deterministic way by the joint-stochastic deterministic approach can be used to quantify sensitivity and uncertainty. Stedinger (1997) demonstrates the use of expected probability (EP) flood-risk proposed by Beard (1960), for project evaluation that incorporates into economic calculations uncertainties in hydrologic, hydraulic and economic parameters.

Uncertainty assessments have become a vital procedure in hydrological and hydraulic modelling. They have been conducted for regionalised flood frequency estimates. The methods for representing sampling uncertainty involved constructing intervals to express uncertainty in terms of interval estimators that in repeated sampling would contain the true value of a parameter with a desired frequency (Al-Futaisi *et al.*1999).

A simplified method was developed by De Michele and Rosso (2001) for the uncertainty assessment of regionalised flood frequency estimation by the use of the Generalised Extreme Value distribution. They stated that an approximation of the variance of quartile estimators is introduced to evaluate the confidence limits of the estimated growth curve of regionalised flood flows. The result is combined with the variance of the index flood estimators to obtain an

uncertainty model for evaluation of the variance of flood estimators by the index flood method.

There has always been a tendency to assume that the input variables and parameters represent reality in an accurate way. This has not been the case with Mlazi, the difficulties of collecting and sorting out input hydrological, catchment and hydraulic data has been problematic resulting in possible errors. As is observed in Section 3.6.2 dealing with calibration of the HEC-HMS model, there is no substantial correlation between the observed hourly rainfall time series and the stream flow hourly time series for the Mlazi. The sensitivity analysis therefore addresses this predicament. The sensitivity of both the HEC-HMS (hydrological) model and HEC-RAS (hydraulic) river model for Mlazi is addressed by conducting various simulations by use of different input variables and therefore checking how the model responds to those inputs. Ponce (1989) states that in large catchments, such as the Mlazi, the model's sensitivity focuses on the spatial distribution of the storm, this phenomenon is taken into consideration by the distribution of the design storm across the catchment whereby each subcatchment is given its own meteorological data input.

The approach to dealing with uncertainty focuses on the sensitivity of a given parameter, small changes in a value of the parameter may cause large changes in the model output. This phenomenon is ascertained qualitatively in the case of the sensitivity of the hydraulic and hydrologic model to the Manning's "n" and also the SCS Curve Number "CN" respectively. The uncertainty and sensitivity analysis is a substantial justification for the reason why significant effort was applied in the data analysis and also fieldwork conducted for Mlazi.

Hydrologic uncertainty according to Chow *et al* (1988) can be grouped into three categories namely:

- Natural, or inherent uncertainty: These arise from the random variability of hydrologic phenomena.
- Model uncertainty: which arise from approximations made when representing phenomena by equations.
- Parameter uncertainty: which is a result of the unknown nature of the coefficients in the equations such as the bed roughness in Manning's equations.

Suppose a variable y is expressed as a function of x, then:

$$y = f(x) \qquad \text{Eqn (2.5.1)}$$

Two sources of error are noticeable in (y). Firstly the function (f), or model could be incorrect and secondly the measurement of x may be inaccurate. In this illustration, it is assumed that the model has no error or bias.

Based on the assumption that the model is correct, a nominal value of x, denoted $(\bar{x})$ is selected as design input and the corresponding value of y calculated:

$$\bar{y} = f(\bar{x}) \qquad \text{Eqn (2.5.2)}$$

A Taylor series can be used to expand f (x) around $x = \bar{x}$ so as to estimate the effect of the discrepancy caused by (x) differing from $(\bar{x})$

$$y = f(x) = f(\bar{x}) + \frac{df}{dx}(x - \bar{x}) + \frac{1}{2!}\frac{d^2f}{dx^2}(x - \bar{x})^2 + \ldots\ldots \qquad \text{Eqn (2.5.3)}$$

Where the derivative df/dx, d^2f/dx^2 ... are evaluated at $x = \bar{x}$. When the second and higher order terms are neglected, the resulting first order expression for the error in (y) is:

$$y - \bar{y} = \frac{df}{dx}(x - \bar{x}) \qquad \text{Eqn (2.5.4)}$$

The variance of this error is:

$$s_y^2 = E\left[(y - \bar{y})^2\right] \qquad \text{Eqn (2.5.5)}$$

Where (E) is the expectation operator, that is:

$$s_y^2 = E\left\{\left[\frac{df}{dx}(x - \bar{x})\right]^2\right\} \qquad \text{Eqn (2.5.6)}$$

or

$$s_y^2 = \left(\frac{df}{dx}\right)^2 s_x^2 \qquad \text{Eqn (2.5.7)}$$

The value of s_y is the standard error of estimate of y. Equation 2.5.7 gives the first order estimation of the variance of a dependent variable y as a function of the variance of an independent variable x when assuming that the relationship y= f (x) is correct. Chow *et al* (1988) states that for a variable y depending on several mutually independent variables x_1, x_2,..x_n :

$$s_y^2 = \left(\frac{df}{dx_1}\right)^2 s_{x_1}^2 + \left(\frac{df}{dx_2}\right)^2 s_{x_2}^2 + ... + \left(\frac{df}{dx_n}\right)^2 s_{x_n}^2 \qquad \text{Eqn (2.5.8)}$$

Which applies if the covariance between x_i and x_j is negligible for i.j = 1,2, ...n.

2.5.1 First Order Analysis of Manning's Equations

Depth as the dependent variable

The Manning's equation is used by the HEC-RAS model to determine depths of flow and levels of inundation for the Mlazi. The formula takes into account the resistance to flow in channels caused by the bed roughness. The procedure discussed in Section 4.5 involves using various flow rates from HEC-HMS, roughness coefficients obtained during field work and the shape and slope of the channel from the Digital Elevation Model (DEM) (discussed in Section 3.8), calculate the levels of inundation (water surface elevation). The determined levels of inundation can be used to delineate the flood plain. This section is used to estimate the effect of uncertainty in (Q), (n), and (S_f) on (y).

The first analysis considered is the effect on flow depth of variation in the flow rate Q (Chow *et al*, 1988):

$$Q = \frac{1}{n} S_f^{1/2} A R^{2/3} \qquad \text{Eqn (2.5.9)}$$

Where A is the cross-sectional area and R the hydraulic radius, both depending on the flow depth y. Assuming that variations in y are dependent only on variations in Q, using Equation 2.5.7 then:

$$s_y^2 = \left(\frac{dy}{dQ}\right)^2 s_Q^2 \qquad \text{Eqn (2.6.10)}$$

Where dy/dQ is the rate at which the depth changes with changes in Q, its inverse dQ/dy is given for Manning's equations by:

$$\frac{dQ}{dy} = Q\left[\frac{2}{3R}\frac{dR}{dy} + \frac{1}{A}\frac{dA}{dy}\right] \qquad \text{Eqn (2.6.11)}$$

The derivative is substituted in Equation 2.6.10 to give:

$$s_y^2 = \frac{s_Q^2}{Q^2\left(\frac{2}{3R}\frac{dR}{dy} + \frac{1}{A}\frac{dA}{dy}\right)^2} \qquad \text{Eqn (2.6.12)}$$

Since the coefficient of variation of the flow rate $CV_Q = s_Q/Q$, Equation 2.6.12 becomes:

$$s_y^2 = \frac{CV_Q^2 + CV_n^2 + (1/4)CV_{S_f}^2}{\left(\frac{2}{3R}\frac{dR}{dy} + \frac{1}{A}\frac{dA}{dy}\right)} \qquad \text{Eqn (2.6.13)}$$

In flood-risk management, methodologies that explicitly quantify and integrate uncertainty in flood-risk analysis have been developed such as the HEC-FDA program (HEC-FDA, 1998). A damage function explained and derived in a paper on hydrologic and economic uncertainties and flood-risk project design (Ahmed AL-Futaisi *et al*, 1999) is an example of a function where the uncertainty based on the depth (y) and flow (Q) parameters can be integrated into the flood-risk analyses. The damage function was derived from the Manning's equation and depends upon the relationship between the flow (Q) and the water depth (y). A paper on expected annual damages and uncertainties in flood frequency estimation (Arnell, 1989) states that the estimates of expected annual damages are very uncertain. The uncertainty is as a result of uncertainties in both the estimation of flood frequency relationship from the limited data and the relationship between magnitude and damage.

2.5.2 Discharge as the Dependent Variable

Manning's equation is also applied in the determination of the Mlazi canal capacity Q_C for a given depth, roughness coefficient n, bottom slope, and cross sectional geometry.

The Manning's equation in Equation 2.5.9 can be expressed as:

$$Q_C = \frac{1}{n} S_f^{1/2} A^{5/3} P^{-2/3} \qquad \text{Eqn (2.5.14)}$$

Where, (P) is the wetted perimeter. The first order analysis is performed on Equation 2.6.14, to give the coefficient of variation of the capacity expressed as:

$$CV_Q^2 = CV_n^2 + \frac{1}{4} CV_{S_f}^2 \qquad \text{Eqn (2.5.15)}$$

Assuming that $CV_A = 0$ and $CV_P = 0$

where, CV_A is the coefficient of variation of the area (A)

CV_n is the coefficient of variation of the roughness (n)

CV_{sf} is the coefficient of variation of the friction slope (s_f)

CV_P is the coefficient of variation of the wet perimeter (p)

The Manning's equation for a channel and flood plain can be further expressed as:

$$Q = \left(\frac{1}{n} A_c^{5/3} P_c^{-2/3} + \frac{2}{n_b} A_b^{5/3} P_b^{-2/3} \right) S_f^{1/2} \qquad \text{Eqn (2.5.16)}$$

Where n_c and n_b are the roughness coefficients for the channel and the floodplain, respectively A_c, P_c, A_b and P_b are the cross sectional areas and the wetted perimeters of the channel and the overbank Chow *et al* (1988)

2.5.3 Relative Sensitivity Analysis

The relative sensitivity (S_R) of parameters is defined as the percentage change in model results divided by the percentage change in parameter value. This method gives a consistent measure for the comparison between parameters. The method was applied in the context of irrigation system by Guttien *et al* (1999).

In the context of Mlazi, the application of the relative sensitivity will be discussed in Section 3. 7. The analysis was carried out for the sensitivity of the HEC-HMS model (hydrological) input parameters such as:

- SCS parameter inputs i.e. I_a, CN, T_c
- Channel Routing, i.e. storage/flow relationship.

The relative sensitivity was furthermore carried out for the HEC-RAS river model in prediction of the levels of inundation for the Mlazi canal. The parameters and model procedures investigated were:

- Manning's "n"
- Off-channel storage
- Steady and unsteady state analysis
- Channel geometry

The relative analysis included in Section 5.6 is related to Manning's n.

Summary

This section has given a theoretical background to uncertainty and sensitivity analysis. It has highlighted the importance of these analyses to various hydraulic and hydrologic modelling procedures. It should be noted that there is still much ground that needs to be covered in this field. Some of the techniques discussed in this section are applied to the models used for the Mlazi as highlighted in Chapter 4.

With a good feel of the response of the model to variations in input parameters it becomes possible to conduct accurate calibration of the models. In order to be able to assess the sensitivity of a model it is necessary to understand the theory and applicability of the model. The next chapter gives a detailed description of the application of the models.

3. DATA PROCESSING AND HYDROLOGICAL MODELLING

Data processing and hydrological modelling of the Mlazi Catchment are discussed in this chapter. The data processing is divided into stages such as Pre-processing and Hydrologic Processing. The Pre-processing phase was mainly conducted by the ML Sultan Technikon Town Planning Resource Unit in conjunction with the candidate. The Hydrologic Processing in the context of this study involved hydrological modelling whereby a physically based model was created and applied to simulate runoff from rainfall. The application of the HEC-HMS model, its calibration and a sensitivity analysis are presented. The HEC-HMS results were compared with other methods for computing peak discharges. The results from the calibrated HEC-HMS model were further validated by flood frequency analysis of the 20-year peak discharges from the Baynesfield and Mlaas Road stream gauges as presented in Section 3.6.1. The input synthetic hyetograph and the output HEC-HMS results were used for the validation of the MMM. The linear MMM as discussed in Chapter 7 has advantages over the non-linear HEC-HMS model when conducting real time forecasting because it is quicker and less tedious to update its internal state parameters. The flows computed by the HEC-HMS model are input to the HEC-RAS model for the computation of levels of inundation.

3.1 Data Processing

Data collection and processing was categorised into two sets namely; Meteorological, Hydrological and Physical-GIS.

3.1.1 Meteorological and Hydrological

Precipitation data were obtained from the South African Weather Service's (SAWS), Meteorological Systems and Technology (METSYS). There has been a growing interest worldwide to make the meterological data compatible with the GIS software, which will enable powerful temporal analysis capabilities within the GIS (Thomas, 2001). The streamflow data for two upstream streamflow gauges were obtained from the Department of Water Affairs and Forestry (DWAF). Historical streamflow data and rainfall data were selected and used for calibration of the HEC-HMS model.

The precipitation-input data for the Mlazi catchment model was in the form of user defined design hyetograph. The user-defined hyetograph were synthetic hyetographs inferred from the one and three-day design rainfall depths at gauges within and around Mlazi catchment

obtained from Smithers and Schulze (2000). The procedures conducted in sorting out the data for each model is described in the relevant models.

3.1.2 Physical-GIS

Most of the data required for this study were already in GIS format and available from the Durban City Engineer's department. The data collected for the Mlazi study included the following:

- Cadastral data containing information on land value, ownership etc
- Land use
- Contours- 2 m and 5 m resolution
- Most recent digital aerial photography
- Soils and Geology

Some of the data had to be captured or derived from the base, or raw information. These included the following:

- Contours: Although there were 2 m contours available in GIS format for some areas these did not cover the entire catchment. It was therefore proposed that the use of the 5m contours, which already exist in the Durban Metro database, be used for the hydrological modelling. However the hydraulic model required a better quality of 2m contours which meant that further capturing of the contours had to be done by the ML Sultan students through the following process:
  a) Scanning: Contours were traced from 1:2000 orthophotos onto overlays, then scanned, vectorised, georeferenced and edge matched.
  b) Contours were digitised from a few maps
  c) Some areas had no 2m contours on the orthophotos and these areas had to be flown, mapped and contours derived from the resulting Digital Elevation Model (DEM)
- Initial estimates of the Manning's roughness coefficient had to be derived from the land use layer according to the prescribed tables however these had to be further confirmed by values obtained during field work.

Since the majority of the data was available from the eThekwini Metro Council, it was all in the same format and co-ordinate system. As a result of use of the same format, the overlaying and processing of the data became much more convenient. The data output for the display of the floodplain was also of the same format and coordinate system.

3.2 Pre-processing GIS Data

Pre-processing involves the collection of information and the derivation of new information from and within that database. This includes sub-catchments, drainage lines, average slope, runoff lengths etc. The most crucial pre-processing phase however is the creation of the Digital Elevation Model (DEM) for the hydrological model and for the hydraulic model. The hydraulic model was split at the Shongweni dam into two parts namely; the Mlazi upper and the Mlazi lower for easier computations.

The software used during the GIS process includes the following:

- Arcview GIS
- Arcview Spatial Analyst
- Arcview 3D Analyst
- MS Excel Spreadsheet
- MS Access Database
- MS Word
- MS Project.

The candidate's input to the pre-processing phase involved confirmation and validation of the processes carried out together with the creation of ArcView themes. The themes created are as follows:

- Centreline (line themes of the Mlazi river channel invert-thalweg): The lines were digitised starting from upstream working downstream. Each polyline defined a reach. The centerline is used for the determination of stationing and stream and reach naming.
- Cross-section: digitising was performed consistently from left to right facing downstream at intervals of about 100m. In the case of river bends and existence of hydraulic structures a smaller interval is used in order to capture all the relevant details.
- Flowpath lines: these were used to calculate the downstream reach length for HEC-RAS input. The lines were digitised starting from upstream working its way downstream as was done for the centerline. Three sets of flowpaths were produced namely; left, right and the main flow path.

3.3 Creation of Digital Elevation Model

Digital elevation models (DEM) are arrays of elevation values at equally spaced points of the terrain. Since they are in the matrix form, they can be stored in raster or grid format, which is a data structure composed of square cells or pixels of equal size arranged in rows and columns (Oliver, 2001). The other form of the digital elevation model is the Triangulated Irregular Network (TIN's), which is more accurate than the raster based DEM's. Although the TIN's demand more processing power, they are the preferred method for the creation of the DEM for the hydraulic model (HEC-RAS). The creation of the DEM was conducted through the use of GIS software. The process of creating the DEM for Mlazi was carried out in two phases namely; the DEM for the HEC-HMS model and the DEM for the HEC-RAS model.

3.3.1 DEM for the Hydrologic Model (HEC-HMS)

This phase involved the following steps:

- Data Assembly
- Raster Based Terrain analysis
- Hydrological Processing.

Data Assembly

The data collected was analysed and processed as mentioned in Section 3.1. The data assembled could be of different formats, coordinate systems and projections, but in the case of Mlazi all data was in the same geographic system and format. A confirmation was however conducted to ensure that the data captured covered the entire catchment. This was achieved by buffering the catchment boundaries, as delineated on a 1:50 000 map, by an arbitrary distance that ensured those small variances in the boundaries as a result of differences in boundaries. The quality of the 5m contour, was also tested, by using the buffer, the contours for the DEM creation were clipped using the 5m and 2m contour dataset for the same area and comparing the results. The use of the 5m contours was therefore justified since the Mlazi catchment is of reasonable size such that use of 5m contours would not cause significant loss in accuracy.

Raster Based Terrain Analysis

This analysis uses the Jensen and Domingue's (1988) algorithms. The algorithms are used to determine flow directions, drainage areas and catchments from the DEM. Values are assigned to each terrain cell depending on which of its 8 neighbouring cells is the lowest.

The first step was the creation of the flow direction grid, which stores a value that refers to its downstream cell out of the eight neighbouring cells. The downstream cell was selected such that the descent slope from the cell was the steepest.

The second step involved the use of the flow direction grid in creation of a flow accumulation grid, which determines the number of uphill cells draining into a given cell. The drainage area of any cell was calculated by multiplying the cell value with the cell-area. A threshold was defined either in terms of area or number of cells (of the drainage area) which happened to be the determining factor in whether a stream is created or not. If the cell in the flow accumulation grid had a value higher than that specified in the threshold then it would be assumed that the cell is part of a stream.

A downstream path was therefore determined by connecting the cell to its downstream cell and so forth resulting in a stream network. The stream network has the shape of a spanning tree that represented the paths of the catchment.

The next process involved the delineation of the catchment. The process uses the flow direction grid and the stream links grid. On the stream network, stream segments are defined as the flow-paths that connect two consecutive junctions. The stream segments are elementary modelling units in which the hydrologic parameters such as slope, cross section and roughness are uniform. Catchment outlets are identified at the downstream cell of each segment. The catchment outlets are either the cells located just upstream of junctions or the cells at which the segments were subdivided. The system outlet is identified as the catchment outlet. The outlet grid stores the outlet identification number, which is equal to the number of its corresponding segment. Based on the flow direction grid, catchments are delineated for each outlet. The process of delineating catchment consists of assigning to the outlet the terrain cell whose downstream flow-path passes through the outlet (Francisco, 2001). It should be noted that the candidate conducted a manual delineation of the Mlazi Catchment using the 1:50 000 map as a verification of the computed catchment.

Hydrologic Processing

The HEC-HMS model applies lumped models to each hydrologic element, which implies that hydrologic parameters have to be calculated for the catchments and stream segments. Using scripts, the catchment grid and the stream grids are converted from raster to vector. The vectorisation process consists of creating a polygon dataset of the catchment and a line data set of stream segments. The catchment and segment identification numbers are transferred to the catchment table and segment table of the vector datasets, so as to preserve the link between the catchment and the segments. Further vector analysis was carried out (i.e merging of dangling catchment polygons) to ensure that each catchment is represented by a single polygon.

The next process involves the population of the converted catchment and segment databases with information relevant to the hydrology of the catchment. The population process is conducted in two steps, namely the input to the stream database and the input to the catchment database.

Input to the stream database includes the following:

- Upstream elevation, which is the elevation of the point where the stream crosses the upper most boundary of the sub-catchment in which it is located in
- Downstream elevation, which is the elevation of the point where the stream crosses the lower most boundary of the sub-catchment in which it is located in
- Length refers to the length of all rivers in the sub-catchment
- Slope, is calculated using the vertical difference between the upstream and downstream elevations and the horizontal length of the stream
- A stream profile can be created if so desired.

Input to the catchment database includes the following:

- Area
- Elevation of centroid derived using the centroid layer, which is created using one of four methods, i.e. bounding box, ellipse, flow path or user specified
- Longest flow path length derived using the 'longest flowpath' layer
- Upstream elevation obtained from the stream layer
- Downstream elevation, obtained from the stream layer
- Slope between end points obtained from the stream layer
- Slope between 10% and 85%

- Centroidal length derived using the 'centroid flowpath' method and measuring length from the centroid to the oulet.

The above mentioned data needed to be prepared before being exported to the Hydrological Modelling System (HEC-HMS) software. The stream segments are automatically named, as are the basins. The map units are converted to HEC-HMS units if they differ. A data check was conducted and the candidate created a schematic HEC-HMS layout to confirm the number of sub basin to be finally created. The data was exported to the HEC-HMS where the candidate proceeded to add hydrological input parameters and rainfall data to the model.

3.4 Hydrologic Modelling Using HEC-HMS

The process of determining the catchment runoff was carried out by using a deterministic modelling approach. The model used for the runoff determination was the US Army Corps of Engineers Hydrologic Modelling System (HEC-HMS) computer program.

HEC-HMS is a precipitation – runoff simulation program. The program comprises a number of models (components), which together provide a presentation of the catchment behaviour. This physically based model mimics physical processes on the Mlazi catchment to determine flows occurring in the channel. This is the model which was used for initial parameter optimisation of the Mlazi Meta Model (MMM) for use in real time forecasting at the Mlazi River.

The HEC-HMS model required hydrologic input data. The hydrologic data input were captured from a spreadsheet containing some of the SCS information captured from the GIS. The SCS spreadsheets assisted in the computation of the curve number (CN) and lag time (T_{lag}) needed as input to the HEC-HMS model described below. The hydrologic database created depended on the choice of the methods to be used in the HEC-HMS program for runoff-volume, direct-runoff computations and channel routing and visa versa.

3.4.1 Description

This section describes the HEC-HMS model based on the description found in the HEC-HMS (2000) user manual.

The HEC-HMS hydrologic model requires three data components:

- basin Model,
- meteorologic Model, and
- control Specifications.

Figure 3.4.1 below shows the display windows for the Basin Model, Meteorologic Model and the Control Specification

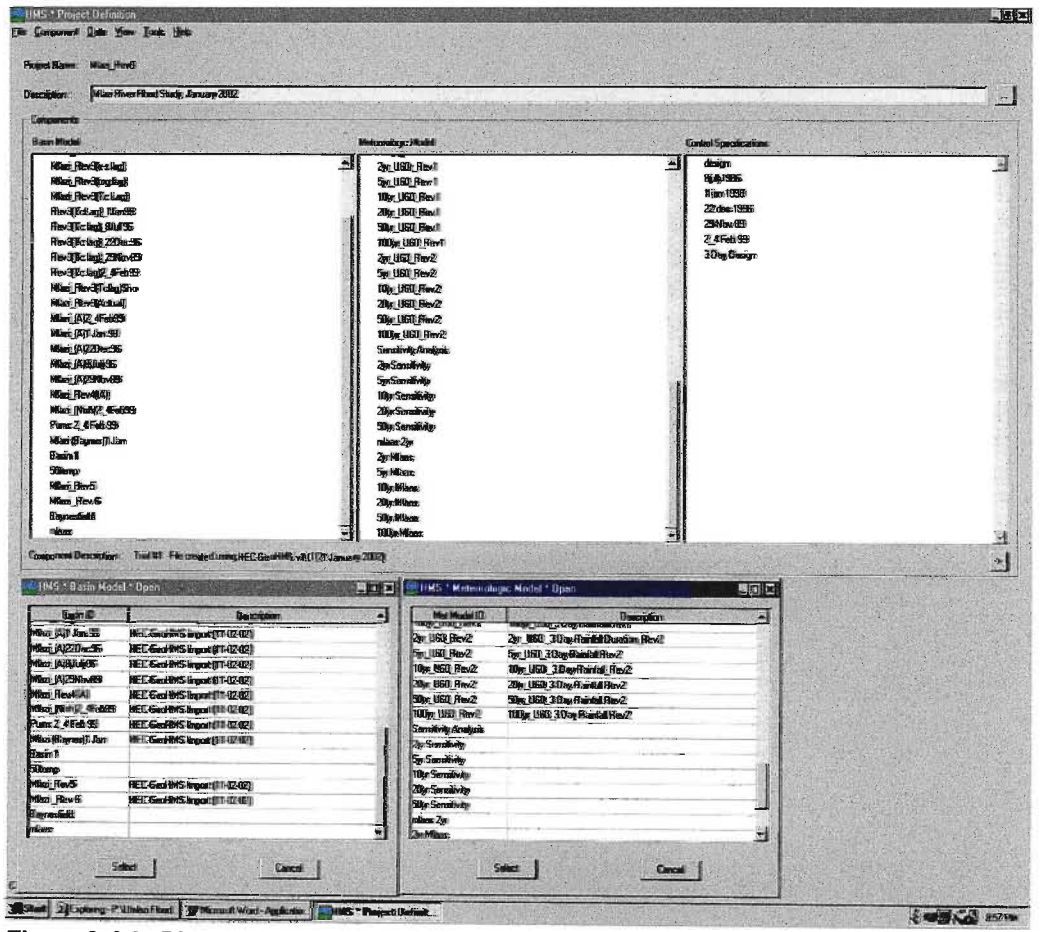

Figure 3.4.1: Display windows for the Basin Model, Meteorological Model and the Control Specification

Basin Model

The Basin Model screen is used for managing basin models, creating the element network, entering and editing element data, and viewing run results. The screen is presented to the user automatically after opening a basin model.

A global summary table displays output results for the last computed run. Detailed results for each element are obtained by clicking on the element in the display area with the right mouse button and selecting the "View Results" prompt.

Meteorological Model

The Meteorological Model screen is used for managing and editing meteorologic models. A meteorologic model contains a precipitation method and optionally an evapotranspiration method. Only one method of each type can be contained in the model. The screen can be accessed by opening a meteorologic model.

The data required for computing precipitation for each subbasin is stored in the precipitation tab. Several different methods are available for computing precipitation: user hyetograph, inverse-distance gauge weighting, gridded precipitation, frequency storm, and standard project storm. The method chosen for computing precipitation for the Mlazi study was the user hyetograph.

Control Specifications

The Control Specifications screen is used for editing and managing control specifications. The screen can be accessed by double-clicking a control specifications name shown on the Project Definition screen. In the control specification component, storm duration is specified.

3.5 Applications

The overall catchment was subdivided into smaller sub-catchments and these were represented in the catchment model by 'basin elements'. The 'basin elements' were interconnected by reaches and junctions, thus creating a mathematical approximation of the river catchment system.

The schematic presentation of the HEC-HMS model for Mlazi is shown in Figure 3.5.1 and this forms the catchment model, which contains parameters and connectivity data for hydrologic elements such as subcatchments, routing reach, and junctions. The model

produced was compared to the quaternary catchments identified as U60a, U60b, U60c and U60d based on the outlets where streamgauges are located (Midgley *et al*, 1994).

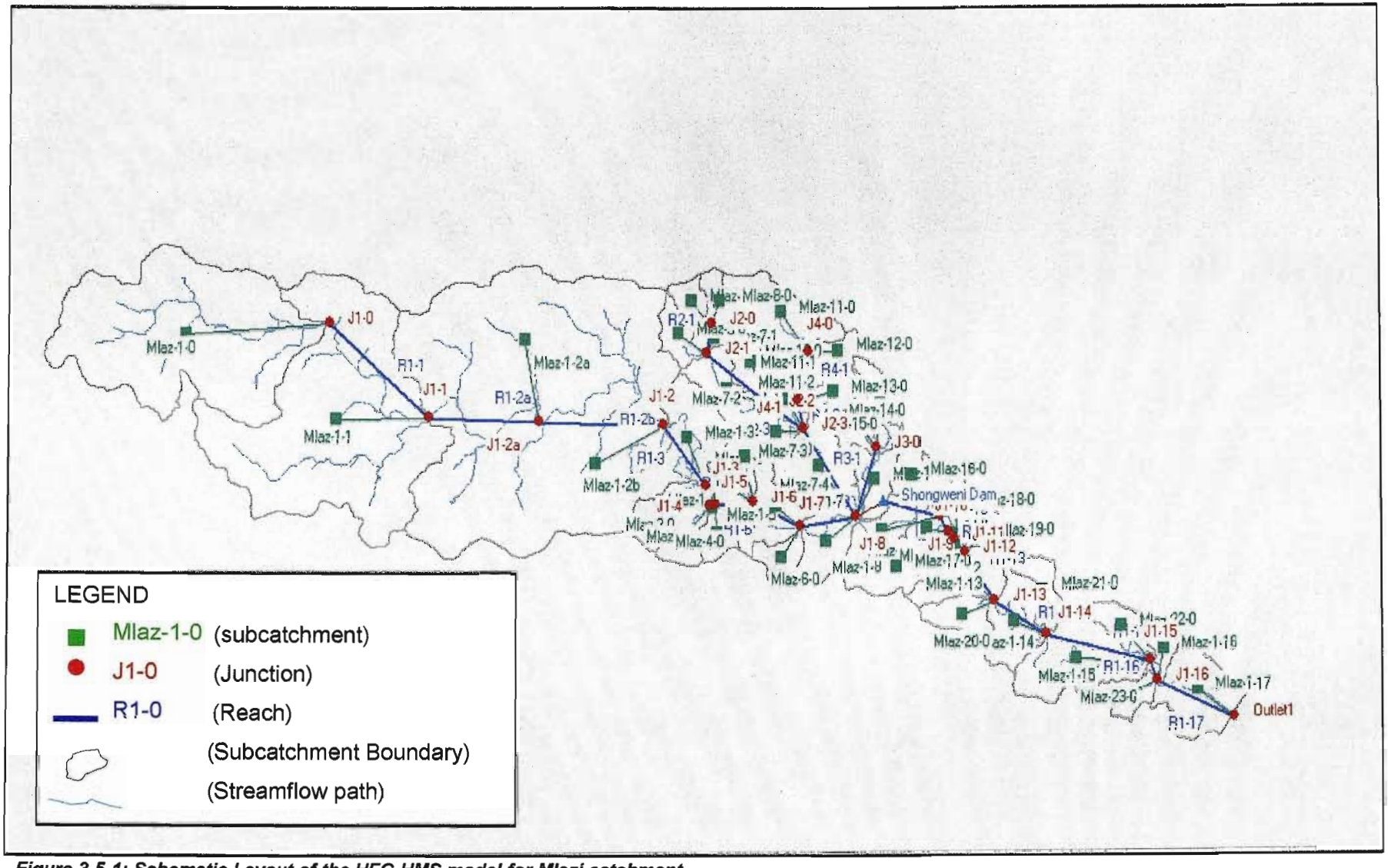

Figure 3.5.1: Schematic Layout of the HEC-HMS model for Mlazi catchment

For each of the HEC-HMS models there are a number of alternative analysis methods available. The applicability of the various methods for any particular sub-catchment depends on the assumptions that are inherent in the model and the nature of the sub-catchment itself.

The input to the HEC-HMS program is:

- Rainfall data.

The models in the program are:

- Catchment Loss Model,
- Direct Runoff Mode,l
- Baseflow Model, and
- Routing Model.

These individual modules comprise the overall catchment model. The following sections describe the modelling procedures that were adopted for the Mlazi study.

3.5.1 Rainfall

The precipitation input into the Mlazi catchment model was in the form of synthetic user-defined hyetograph described in Section 2.3. The design 1-day mean rainfall depth and 3-day rainfall depth for various recurrence intervals were obtained from Smithers and Schulze (2000). An areal reduction factor (ARF) of 0.88 used to cater for the variability in space was applied as stated by Alexander (1993) for the 1-Day mean rainfall depth for the whole catchment. However the variability in space for the 3-Day rainfall depth was obtained through using different mean rainfall depths for each quaternary catchment. The temporal distributions used for the hourly distribution of the mean rainfall depths are discussed in Section 2.3.4 and are based on the works carried out by Schulze and Schmidt (1987) and Adamson (1982).

Data required to define the hyetograph is:

- P_{MAP} = total storm mean-areal precipitation (P_{MAP}) depth over the catchment
- Temporal Distribution = Variation of P_{MAP} with time.

3.5.2 Mean-areal Precipitation Depth

The first attempt in obtaining the mean-areal precipitation depth was inferred from design 1-day rainfall depths (precipitation depth at a point) at gauges within and around the Mlazi catchment. Radar images (for the 2-4 Feb 99-storm event) and the 1- day rainfall depths at selected gauges indicate that the rainfall for Mlazi is temporally and spatially distributed over the quaternary catchments and that there is existence of orographic influences on rainfall. The arithmetic mean method was used to determine the areal average rainfall depth for various return periods. Furthermore the areal average 1-day rainfall depths were factored using a suitable area reduction factor (ARF) and then distributed using the temporal distribution described in the following section. The 3-day rainfall depths, which represented a 72-hour duration (approximately 4 times the Mlazi time of concentration), were also captured and rearranged to investigate the response of the model to various rainfall inputs.

3.5.3 Temporal Distribution

The initial Temporal distribution applied was derived for different return periods by multiplying the factored 24-hr rainfall depths given in Table (3.5.1) by the dimensionless SCS Type 2 synthetic storm distribution developed by Schmidt & Schulze (1987) as shown Figure 3.5.1. The temporal distribution resulted in a double peak being developed at the twelfth and thirteenth hour and was therefore later revised by applying Adamson (1982) distribution which resulted in a more realistic distribution as shown in Figure 3.5.2. The theory on the dimensionless distributions is discussed in Section 2.3.4.

Weather Bureau Station Ref	Elevation (m MSL)	Mean Annual Rainfall (mm)	1-day rainfall (mm) for different return periods			Years of Record
			20yr	50yr	100yr	
Hilly Prospect,	1340	1035	131	163	191	37
Richard-Natal	847	1022	135	177	215	83
Little Harmony, R	853	912	142	186	226	55
Pietermaritzburg	819	949	116	152	184	49
Baynesfield Est.	841	917	118	154	187	71
Thornville	853	845	112	146	177	28
Cliffside	792	815	137	179	218	33
Cosmoore, Cato Ridge	777	769	137	179	218	33
Mid- Illovo	777	942	172	225	273	28
Umlazi Road	790	753	113	147	179	46
Eston	803	766	122	159	194	75
Camperdown	600	600	124	162	197	85
Meyer Camper	598	738	112	147	178	36
Killarney Isles	614	648	109	142	173	49
Powerscourt	658	964	183	239	290	30
Inchanga	700	787	138	181	219	70
Shongweni (A)	315	705	125	163	198	66
Shongweni (B)	315	705	127	162	192	75
Bothas Hill	640	833	172	225	273	48
Intake	693	926	187	245	298	69
Kloof (pur)	551	1035	178	232	282	67
Municipal Kloof	488	1037	203	265	322	31
Pinetown (Mag)	346	947	208	265	314	71
Northdene (mun)	95	1018	197	252	299	59
Umlaas W.Work	47	917	184	235	278	78
Coedmore	126	1031	191	243	288	61
Louis Botha	16	986	187	239	283	40
Durban – Point	5	1051	206	262	311	54
Average	-	**879**	**150**	**195**	**235**	**55**

Table 3.5.1:1-day design rainfall at gauges in close to the Mlazi Catchment (Smithers & Schulze, 2000)

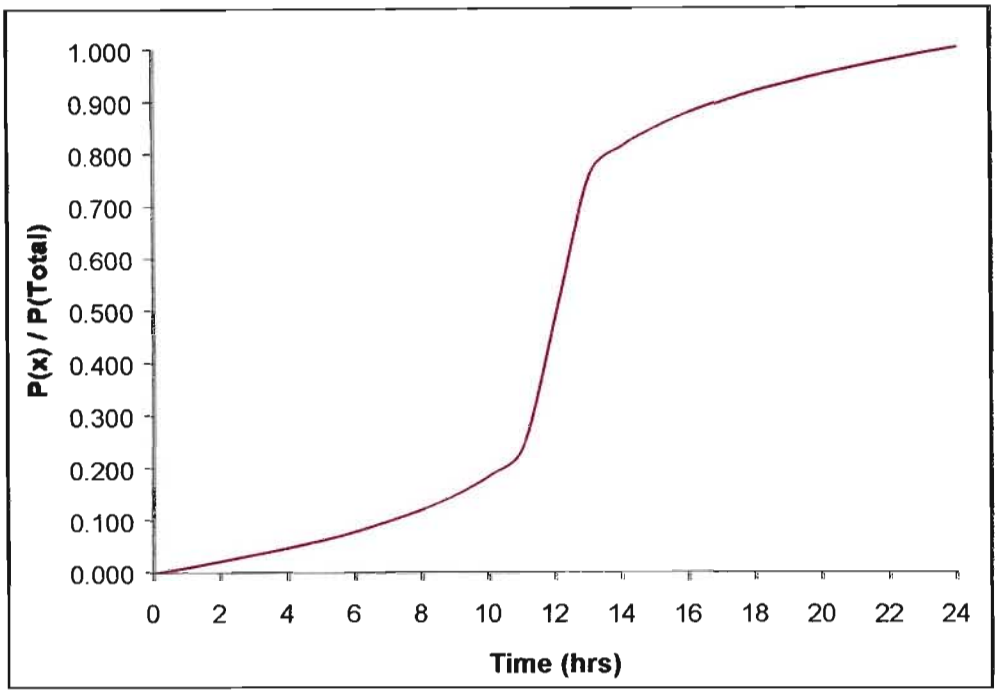

Figure 3.5.2a: SCS Type II 24 hr rainfall distribution (Schulze &Schmidt, 1987)

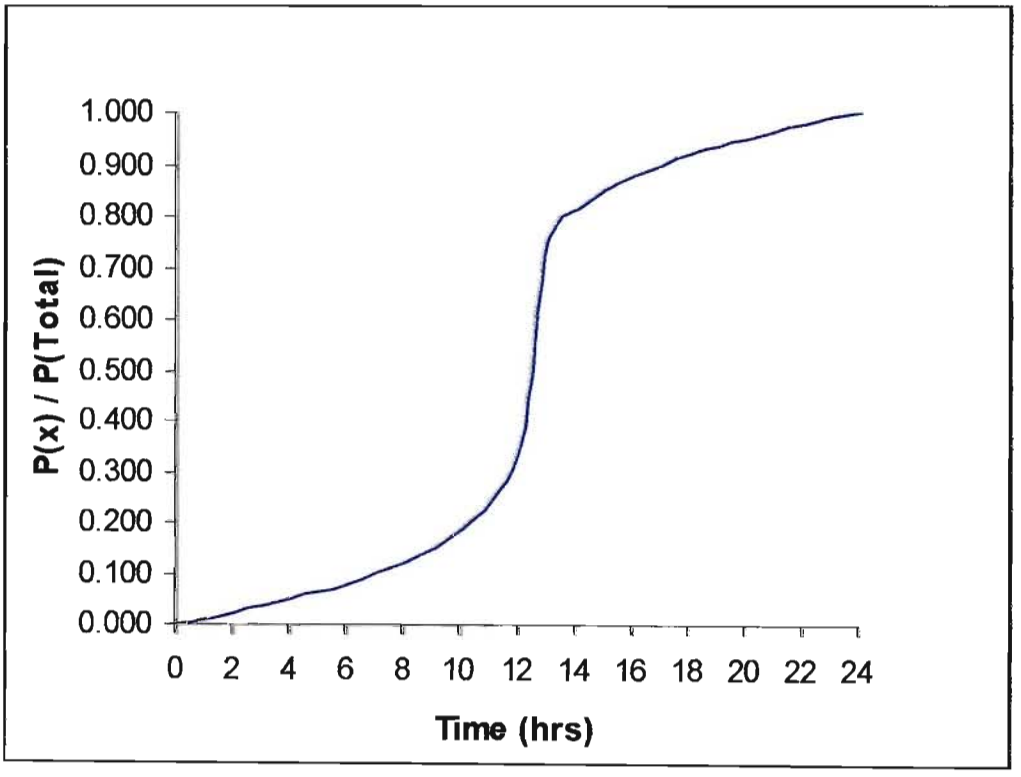

Figure 3.5.2b: SCS Type II 24 hr rainfall distribution (Adamson, 1982)

Incremental Synthetic Hyetograph Inputs

The synthetic hyetographs created from the above mentioned distributions and rainfall depth were entered incrementally as precipitation gauges at a time series of 1-hour. Figure 3.5.3a and 3.5.3b shows the 1-Day hyetograph produced from the use of the above distributions.

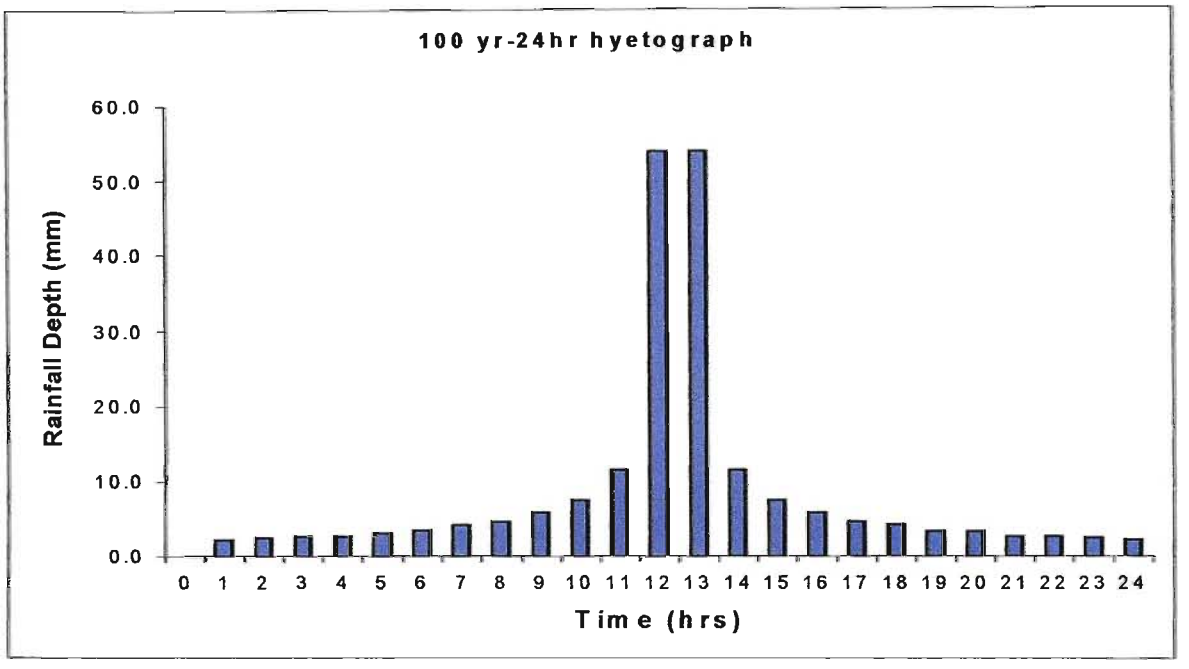

Figure 3.5.3a: 1-Day Hyetograph based on Schulze and Schmidt's Distribution

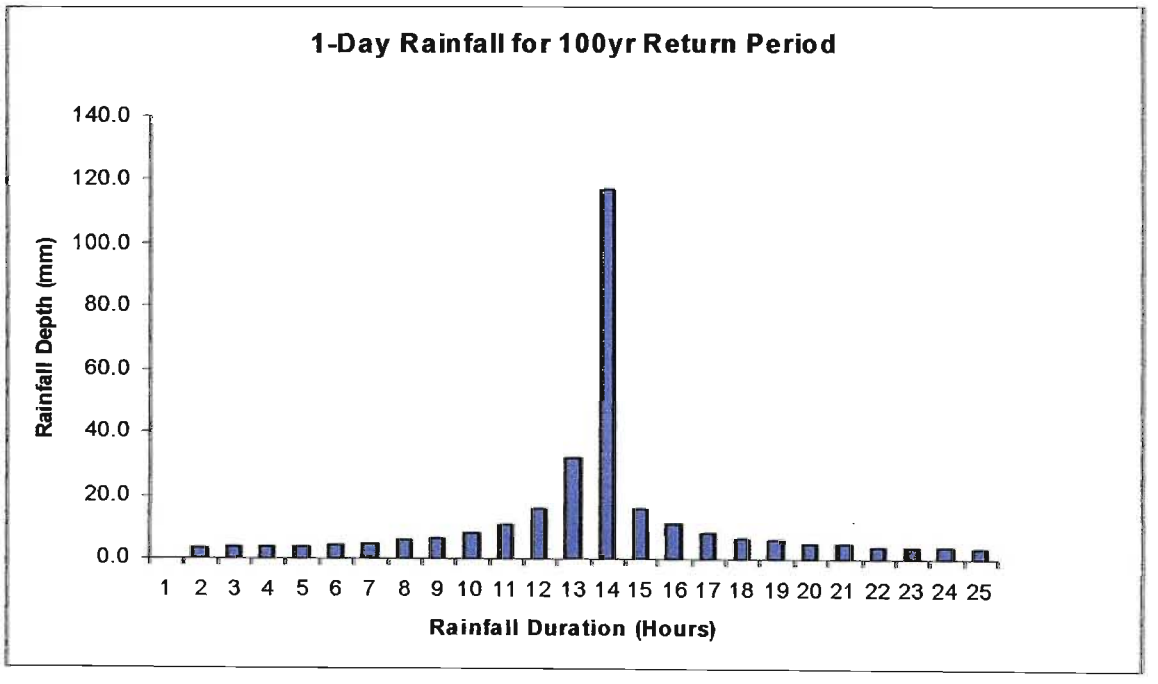

Figure 3.5.3b: 1-Day Hyetograph based on Adamson's distribution

Figures 3.5.4a, 3.5.4b and 3.5.4c show the three of the six permutations for the 3-Day hyetographs for the 100yr return period. As stated in Section 2.3.5 these are equi-probable temporal distributions because there is negligible correlation between daily amounts of rain in a sequence of wet days (Zucchini and Adamson, 1984). The scenarios are based on the order in which the magnitude of rainfall depth is selected. LMH represents the order in which the lowest depth (L) was considered to contribute to the first day of the 3 days followed by the medium (M) and then the highest (H). The worst scenario (LMH) could have been the most favourable to be used for analysis. However, it was deduced from the historical flooding of the canal that such a scenario has not really occurred as yet and since the delineation of flood plains was calibrated based on historical flood events the scenario used was the MHL.

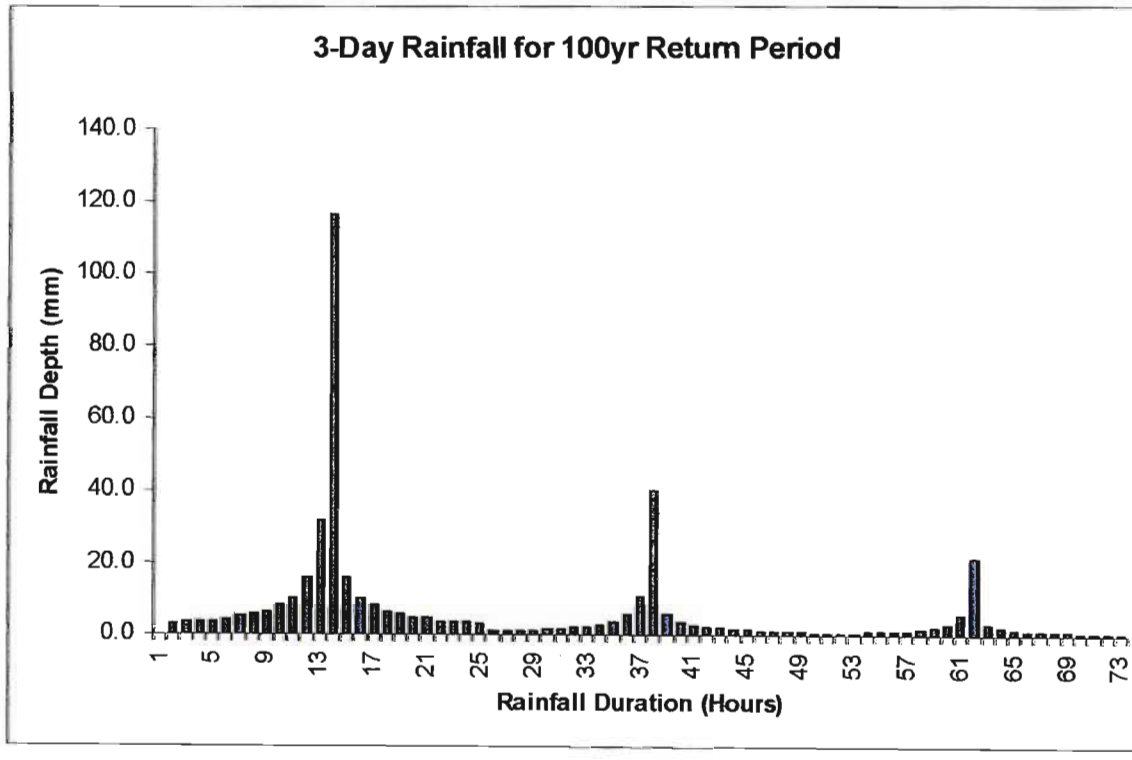

Figure 3.5.4a: 3-Day design Hyetographs for 100yr return period based on the HML Scenario

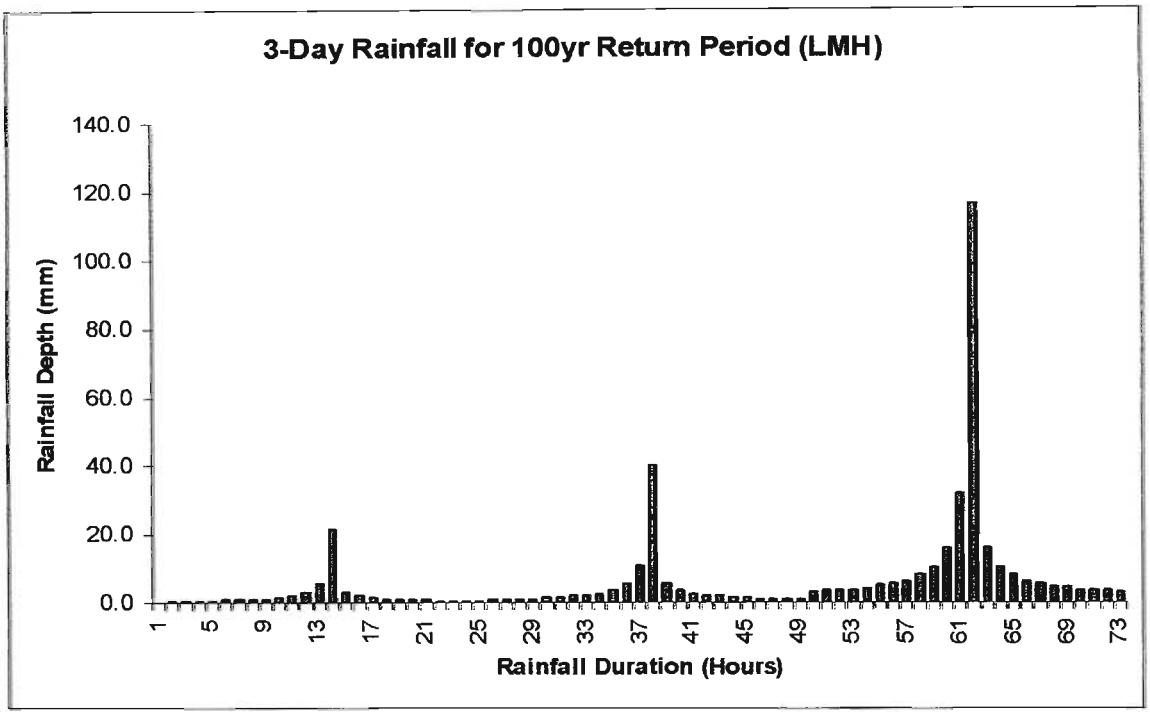

Figure 3.5.4b: 3-Day design Hyetographs for 100yr return period based on the LMH Scenario

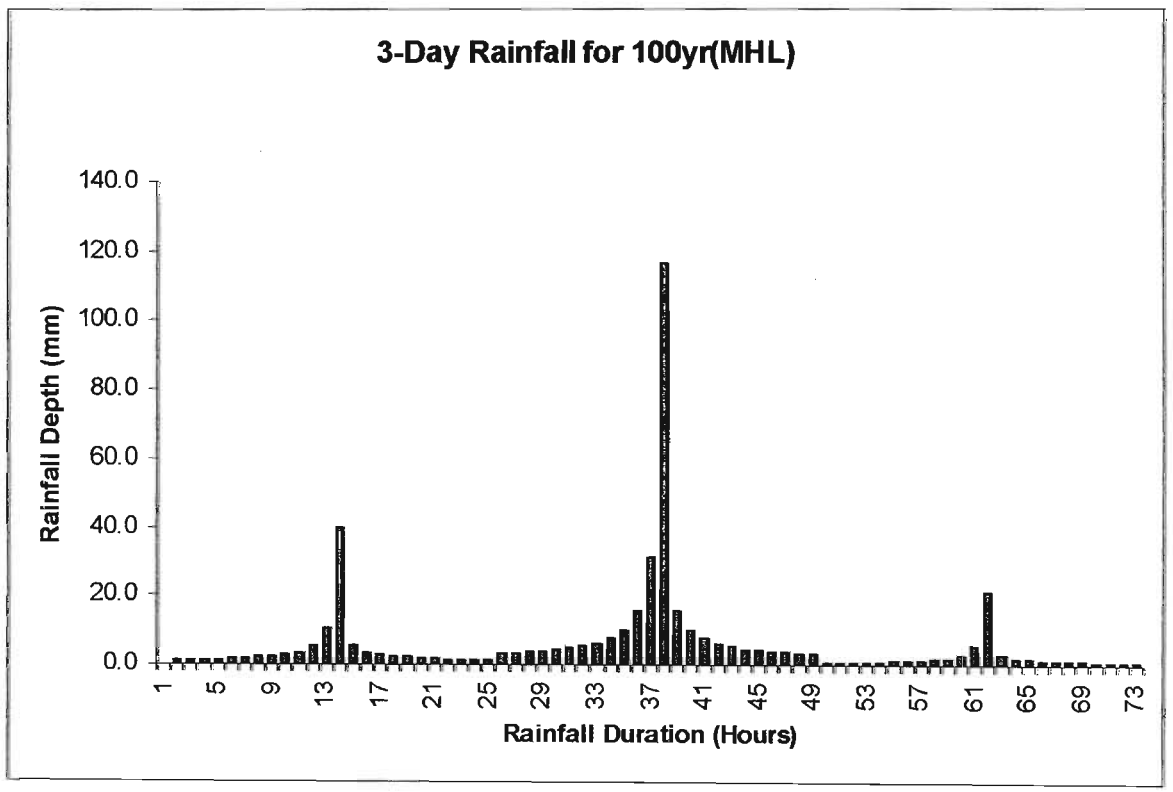

Figure 3.5.4c: 3-Day design Hyetographs for 100yr return period based on the MHL Scenario

3.5.4 Distribution of the Design Hyetograph at a Point

The hyetographs were treated as precipitation gauges by the HEC-HMS model. In this case each precipitation gauge was used as input to a subcatchment. The precipitation gauge corresponding to a particular hyetograph for a particular return period was selected and distributed over the subcatchment. A selected network of these precipitation gauges became the meteorological model. Various meteorological models were created based on the different scenarios of precipitation input. In the case of Mlazi the 1-Day hyetographs for each return period were distributed throughout the whole catchment for each subcatchment. Subsequently the precipitation gauges for the 3-Day hyetographs were identified based on the quaternary catchments. Therefore four sets of precipitation gauges identified for Mlazi were 60a, u60b, u60c and u60d each representing catchment areas with their outlet at these stations; Baynesfield, Mlaas, Shongweni, and Durban. The distribution of these across the whole catchments is shown in Figure 3.5.5.

New GIBB Ref	Rainfall Gauge
Mlaz - 1 - 0	U60A
Mlaz - 1 - 1	U60B
Mlaz - 1 - 2a	U60C
Mlaz - 1 - 2b	U60C
Mlaz - 1 - 3	U60C
Mlaz - 1 - 4	U60C
Mlaz - 1 - 5	U60C
Mlaz - 1 - 6	U60C
Mlaz - 1 - 7	U60C
Mlaz - 1 - 8	U60C
Mlaz - 1 - 9	U60D
Mlaz - 1 - 10	U60D
Mlaz - 1 - 11	U60D
Mlaz - 1 - 12	U60D
Mlaz - 1 - 13	U60D
Mlaz - 1 - 14	U60D
Mlaz - 1 - 15	U60D
Mlaz - 1 - 16	U60D
Mlaz - 1 - 17	U60D
Mlaz - 2 - 0	U60C
Mlaz - 3 - 0	U60C
Mlaz - 4 - 0	U60C
Mlaz - 5 - 0	U60C
Mlaz - 6 - 0	U60C
Mlaz - 7 - 0	U60C
Mlaz - 7 - 1	U60C
Mlaz - 7 - 2	U60C
Mlaz - 7 - 3	U60C
Mlaz - 7 - 4	U60C
Mlaz - 8 - 0	U60C
Mlaz - 9 - 0	U60C
Mlaz - 10 - 0	U60C
Mlaz - 11 - 0	U60C
Mlaz - 11 - 1	U60C
Mlaz - 11 - 2	U60C
Mlaz - 12 - 0	U60C
Mlaz - 13 - 0	U60C
Mlaz - 14 - 0	U60C
Mlaz - 14 - 1	U60C
Mlaz - 15 - 0	U60C
Mlaz - 16 - 0	U60D
Mlaz - 17 - 0	U60D
Mlaz - 18 - 0	U60D
Mlaz - 19 - 0	U60D
Mlaz - 20 - 0	U60D
Mlaz - 21 - 0	U60D
Mlaz - 22 - 0	U60D
Mlaz - 23 - 0	U60D

Figure 3.5.5: Meteorological Model for 3-Day Synthetic Storm for Mlazi.

Physical Data Input

The physical database created for data input to the basin model was captured through GIS, manipulated in excel spreadsheets and then input to the HEC-HMS model. As already stated, the data input is dependent on the methods selected for each model.

3.5.5 Catchment Loss Model

HEC-HMS has a catchment loss model which computes excess rainfall, also referred to as runoff volume. The excess rainfall is obtained by computing the volume of water intercepted, infiltrated, stored, evaporated and transpired and by subtracting all from the precipitation, interception, infiltration, storage, evaporation and transpiration collectively are referred to in the HEC-HMS program as **losses**.

The excess rainfall can be defined as:

$$P_e = P_T - (I_a + F_a)$$

where P_e (mm) is the rainfall excess,
P_T (mm) is the total rainfall,
F_a (mm) is the continuing abstraction (losses), and
I_a (mm) is the initial abstraction.

The runoff model adopted for the Mlazi study was the SCS Curve Number Model. The model estimates precipitation excess as a function of precipitation, soil cover, land use and catchment wetness, by using a Curve Number (CN). The CN is a function of **soil type** and **land use** in a given sub-catchment.

The data input required for the SCS Curve number method is listed in Table 3.5.2.

Sub-catchment		HEC-HMS Basin Junction	Stream Gauge Staion	SCS INITIAL PARAMETERS			
Quaternary Catchment Name	HEC-HMS Ref. No.			CURVE NUMBER	INITIAL ABSTRACTION Ia = 0.1 S	AREA (km ^{2})	L = 0.6 Tc Lag Time (mins)
U60a	Mlaz 1-0	J1-0	Baynesfield	72	10	105	114
U60b	Mlaz 1-1	J1-1		66	13	175	109
	Mlaz 1-2a	J1-2a	mlaas	68	12	117	145
U60c	Mlaz 1-2b	J1-2		81	6	117	132
	Mlaz 1-3	J1-3		81	12	25	89
	Mlaz 2-0			84	5	10	44
	Mlaz 1-4	J1-4		73	9	1	10
	Mlaz 3-0			75	8	9	29
	Mlaz 1-5	J1-5		72	10	6	35
	Mlaz 4-0			74	9	6	21
	Mlaz 1-6	J1-6		72	10	6	35
	Mlaz 5-0			80	6	6	27
	Mlaz 1-7	J1-7		76	8	18	49
	Mlaz 6-0			74	9	7	24
	Mlaz 7-0	J2-0		84	5	6	38
	Mlaz 8-0			82	6	6	34
	Mlaz 9-0	J2-1		85	5	7	52
	Mlaz 7-1			82	5	3	19
	Mlaz 7-2	J2-2		85	4	14	63
	Mlaz 10-0			82	5	10	37
	Mlaz 7-3	J2-3		85	5	6	49
	Mlaz 11-2			83	5	5	30
	Mlaz 14-0	J3-0		57	19	7	49
	Mlaz 15-0			63	15	7	34
	Mlaz 11-0	J4-0		79	7	22	57
	Mlaz 12-0			73	9	5	24
	Mlaz 11-1	J4-1		85	4	8	45
	Mlaz 13-0			79	7	8	29
	Mlaz 1-8	J1-8	Shongweni	76	8	14	49
	Mlaz 14-1			65	14	10	32
	Mlaz 7-4			74	9	21	73
U60d	Mlaz 1-9	J1-9		82	6	10	35
	Mlaz 16-0			72	10	9	31
	Mlaz 1-10	J1-10		79	7	5	35
	Mlaz 17-0			83	5	15	49
	Mlaz 1-11	J1-11		83	5	0	6
	Mlaz 18-0			78	7	8	37
	Mlaz 1-12	J1-12		81	6	1	11
	Mlaz 19-0			79	7	6	30
	Mlaz 1-13	J1-13		80	6	16	56
	Mlaz 20-0			77	7	9	30
	Mlaz 1-14	J1-14		78	7	17	99
	Mlaz 21-0			74	9	8	46
	Mlaz 1-15	J1-15		79	7	28	108
	Mlaz 22-0			80	7	8	55
	Mlaz 1-16	J1-16		75	8	5	29
	Mlaz 23-0			84	5	8	42
	Mlaz 1-17	Outlet	Outlet	65	14	22	77

Table 3.5.2: Mlazi Catchment HEC-HMS Model Data

As suggested by Schmidt and Schulze (1987), the equation applied by the model for the estimation of excess precipitation is as follows:

$$P_e = \frac{(P - 0.1S)^2}{(P + 0.9S)} \qquad \text{Eqn (3.5.1)}$$

where: P_e = accumulated precipitation excess at time t

P = accumulated rainfall depth at time and

S = potential maximum retention, a measure of the ability of a catchment to abstract and retain storm precipitation.

An empirical relationship of I_a and S has been developed by the SCS through the analysis of various small catchments. The relationship recommended by Schmidt and Schulze (1987) for catchments in South Africa, which was used for most of the Mlazi subcatchment:

$$I_a = 0.1S \qquad \text{Eqn (3.5.2)}$$

The cumulative excess at time t shown in Equation 3.5.1 then becomes:

$$P_e = \frac{(P - 0.1S)^2}{(P + 0.9S)} \qquad \text{Eqn (3.5.3)}$$

The incremental excess for a time interval is computed as the difference between the accumulated excess at the end of and beginning of the period.

The maximum retention, S, and catchment characteristics are related through an intermediate parameter, the Curve Number (commonly abbreviated CN) as:

$$S = \frac{25400 - 254CN}{CN} \qquad \text{Eqn (3.5.4)}$$

The SCS reflect that there are wide sets of CN values, which range from 100 (for water bodies) to approximately 30 for permeable soils with high infiltration rates.

The methodology of obtaining the input data (CN and I_a) to the catchment loss model is discussed in the following section.

3.5.6 Estimating SCS CN

The procedure applied to determine a single weighted CN value for each sub-catchment involved the overlaying of physical catchment characteristics using techniques in GIS. The CN for each sub-catchment for Mlazi was determined as a function of land use and soil type. The SCS land category was obtained from Schmidt and Schulze (1987). The initial estimates of CN values were input into the model and trial runs were conducted which resulted in the adjustment of the CN values - this is discussed further in the Section (3.6) when dealing with calibration.

3.5.7 Estimation of the Lag time (*L*)

The procedure applied to determine the catchment lag, which is used to determine peak discharge in the HEC-HMS model was obtained from Schmidt and Schulze (1987). The three methods suggested by Schmidt and Schulze (1987) are the following;

- lag by the original SCS lag equation,
- lag by the Schmidt-Schulze lag equation, and
- lag by the equation given by Kent (1973).

The lag equation chosen was the one given by Kent (1973), which relates the catchment lag to the catchment's time of concentration as;

$$L = 0.6T_c$$

where L is the lag (hr)

T_c is the time of concentration in (hr)

The time of concentration is computed using the following formula

$$T_C = \left[0.87 \frac{\left(\frac{L_f}{1000} \right)^2}{1000 S_{1085}} \right]^{0.385}$$

where L_f is the longest flow length (m)

S_{1085} is the bed slope (m)

T_c is the time of concentration (hr)

3.5.8 Hydrological Soil Groups

The soil cover within each of the Mlazi sub-catchments was assessed based upon soil maps and seven hydrological soil groups. The five soil groups are made up of four main groupings (A, B, C and D) and two intermediate groupings (A/B and B/C). The main groups represent:

- Soil Group A: Low stormflow potential,
- Soil Group B: Moderately low stormflow potential,
- Soil Group C: Moderately high stormflow potential, and
- Soil Group D: High stormflow potential.

The SCS method assigns a particular soil classification (e.g. Clovelly, Hutton, etc) to one of the five categories above based on its overall diagnostic properties. Figures 3.5.7a, Figure 3.5.7b and Figure 3.5.7c show some of the maps highlighting the general trend of the physical characteristics of the Mlazi Catchment (Arcus Gibb, 2002).

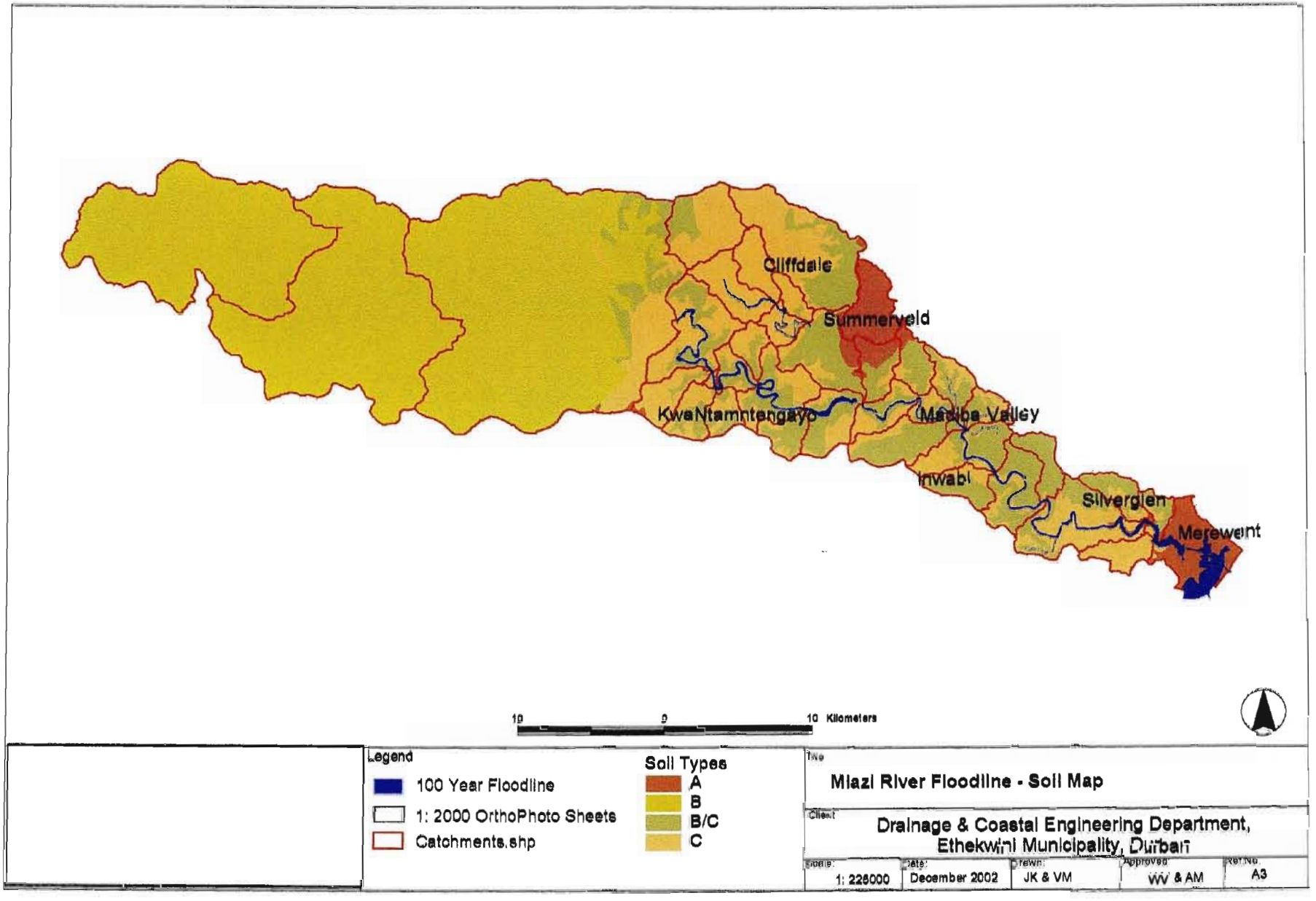

Figure 3.5.7a: Mlazi Soil Type (ARCUS GIBB, 2002)

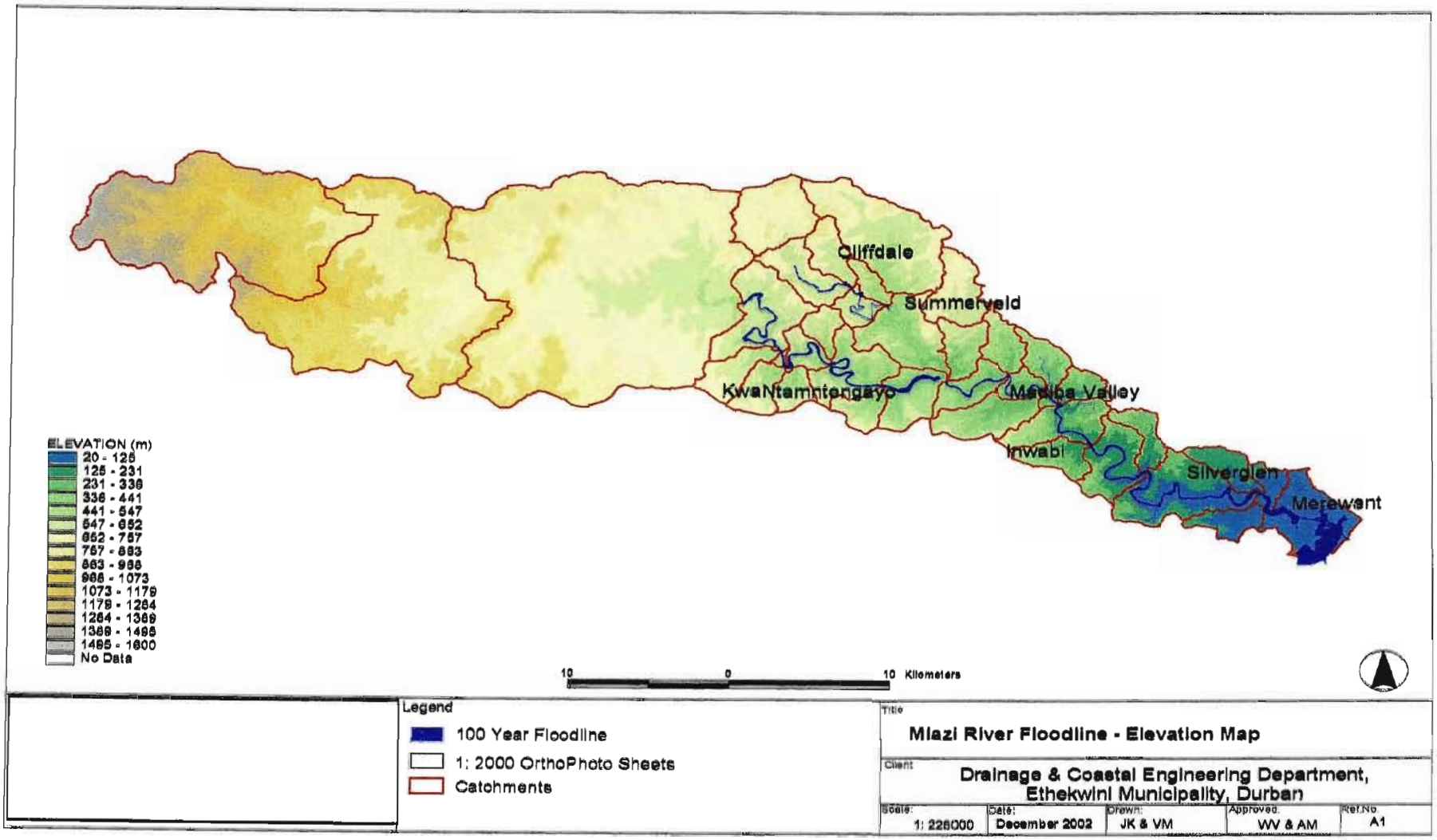

Figure 3.5.7b: Mlazi Topograph (ARCUS GIBB, 2002)

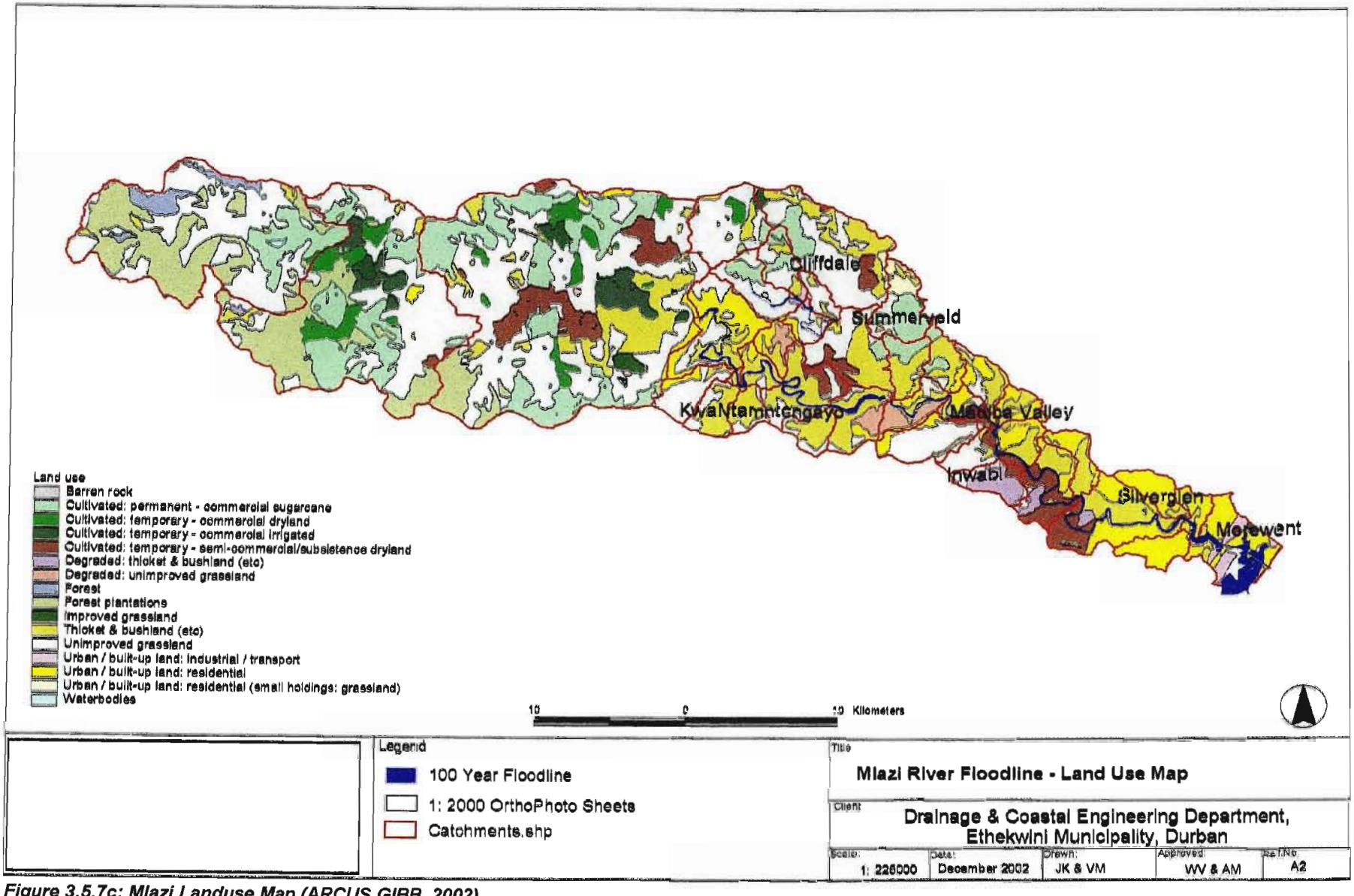

Figure 3.5.7c: Mlazi Landuse Map (ARCUS GIBB, 2002)

3.5.9 Land Use Classes

The existing land use within each of the Mlazi sub-catchments was abstracted from Landsat information (see Figure 3.5.7c). These land use descriptions were consolidated into generalised land uses corresponding to those defined in the SCS methodology (see Table 3.5.8).

LANDSAT Land Use		Corresponding SCS Land Use
Code	Description	
1	Barren Rock	N/A
2	Cultivated; permanent-commercial-sugarcane	Sugarcane, planted on contour <50% cover
3	Cultivated; temporary-commercial-dryland	Veld/pasture (Medium)
5	Cultivated –semi-commercial/subsistance dryland	Open Space (<50% grass cover)[peri-urban settlement
6	Degraded Thicket and Bushland	Natural Forest (High)
7	Degraded unimproved Grassland	Veld/pasture (High)
8	Forest (Natural)	Natural Forest (Medium)
9	Forest Plantations	Forest/plantations (Medium)
10	Improved Grassland	Open Spaces (50 - 75% grass cover)
11	Thicket and Bushland	Natural Forest (Medium)
12	Unimproved Grassland	Veld/ pasture (High)
13	Urban/Developed;Industrial/Transport	Commercial/Industrial
14	Urban/Developed; Residential	Residential (38% impervious)
15	Urban/Developed; Res.(Small holdings & grassland	Residential (38% impervious)

Table 3.5.8: Catchment land-use classification

Typically a flood producing rainfall event in the Durban area is preceded by a several days of persistent rain (Arcus Gibb, 2001). In the SCS methodology, an adjustment can be made to the initial CN to account for the typical soil moisture conditions prevailing at any given location prior to the design storm. No adjustment was, however, made for the Mlazi Study. Instead, it was assumed that the initial abstraction (i.e. the amount of rainfall initially required to saturate the soil and to fill up storage) was 0.1S. This has a similar effect of assuming 'wet' antecedent soil moisture conditions.

Direct Runoff Model

The Direct Runoff Model was used to transform the excess precipitation (ie precipitation minus losses) into point runoff at the sub-catchment outlet.

The method chosen to model the transformation of precipitation excess into point runoff for the Mlazi study was the Unit Hydrograph (UH) method, or more specifically the SCS UH Model, adapted for use in Southern Africa (Schmidt and Schulze, 1987).

3.5.10 The Unit Hydrograph

The unit hydrograph was developed by Sherman in 1932 and is mostly used for large catchments. It is defined by Chow *et al* (1988) as the unit response function of a linear hydrologic system. The direct runoff hydrograph results from 1cm of excess rainfall generated uniformly over the catchment at a constant rate for an effective duration. The unit hydrograph can be combined with a design storm by numerical convolution to produce a flood hydrograph. In South Africa the synthetic unitgraphs were compiled by Pullen (1969) and these are modelled using linear storage model by Bauer and Midgley (1974). These unit graphs should be applied with caution to ungauged locations. A unit hydrograph model does exist in the HEC-HMS model but was not applied in this study due to unavailability of data and the fact that it is based on assumptions not applicable to the Mlazi catchment such as the assumption of linearity and assumption of time invariance. Therefore an SCS-based method was selected for the computation of the rainfall-runoff conversion. The next sections describe the SCS method but for completeness a summary of the UH method used by HEC-HMS is given here.

During the computation of direct runoff hydrograph with UH, HEC-HMS uses a discrete representation of excess precipitation, in which a "pulse" of excess precipitation is known for each time interval. It then solves the discrete convolution equation for a linear system:

$$Q_n = \sum_{m=1}^{n<M} P_m U_{n-m+1} \qquad \text{Eqn (3.5.5)}$$

where: Q_n = storm hydrograph ordinate at time $n\Delta t$;

P_m = rainfall excess depth in time interval $m\Delta t$ to $(m+1)\Delta t$;

M = total number of discrete rainfall pulses; and

U_{n-m+1} = UH ordinate at time $(n-m+1)\Delta t$.

Q_n and P_m are expressed as flow rate and depth respectively, and U_{n-m+1} has dimensions of flow rate per unit depth.

The following basic assumptions are inherent in this model:

- The excess precipitation is distributed uniformly spatially and is of constant intensity throughout a time interval Δt
- The ordinates of a direct-runoff hydrograph corresponding to excess precipitation of a given duration are directly proportional to the volume of excess. Thus, twice the excess produces a doubling of runoff hydrograph ordinates and half the excess produces a halving. This is called the assumption of linearity
- The direct runoff hydrograph resulting from a given increment of excess independent of the time of excess and of the antecedent precipitation. This is the assumption of time – invariance
- Precipitation excesses of equal duration are assumed to produce hydrographs with equivalent time bases regardless of the intensity of the precipitation (HEC-HMS, 2000).

3.5.11 SCS UH Model

The UH model was adopted for the computation of direct runoff for Umlazi catchment. The SCS UH model is a **Synthetic** UH that relates the parameters of a parametric UH model to the catchment characteristics. By using the relationships, it is possible to develop a UH for catchments or conditions other than the catchment conditions originally used as the source of data to derive the UH. The model is based upon averages of UH derived from gauged rainfall and runoff for a large number of small agricultural catchments throughout the US. The model was subsequently adapted for use in South Africa by Schmidt and Schulze (1987). The advantage to the use of this method

is that the modeller has to concentrate most of the estimation effort into a single parameter, the Curve Number (CN) which is based on the soil type, and landuse.

The SCS UH model comprises a dimensionless, single-peaked UH. The dimensionless UH, expresses the UH discharge, U_t, as a ratio to the UH peak discharge, U_p, for any time t, a fraction of T_p, the time to UH peak.

Research by the SCS suggests that the UH peak and time of UH peak are related by:

$$U_p = C\frac{A}{T_p} \qquad \text{Eqn (3.5.6)}$$

where:

A = catchment area (km^2),

Tp = time to peak (hr)

C = conversion constant (0.208 in SI system),

and

U_p = the peak discharge (m^3/sec).

The time of peak (also known as the time of rise) T_p is related to the unit excess precipitation duration as:

$$T_p = \frac{\Delta t}{2} + t_{lag} \qquad \text{Eqn (3.5.7)}$$

where:

Δt = the excess precipitation duration (which is also the computational interval in HEC-HMS); and

t_{lag} = the basin lag, defined as the time difference between the centre of mass of rainfall excess and the peak of the UH.

It is recommended in the HEC-HMS manual (2001), that for an adequate definition of the ordinates on the rising limb of the SCS UH, a computational interval $\Delta t < 29\%$ should be applied.

When the lag time is specified, HEC-HMS solves Equation 3.5.7 to find the time of UH peak, and Equation 3.5.6 to find the UH peak. With U_p and T_p known, the UH can be found from the dimensionless form, which is included in HEC-HMS, by multiplication. The lag time is determined by using empirical equations. The option chosen for this study was the one, which states that lag time is equal to $0.6T_c$.

The lag time and CN are then used with the synthetic SCS unit hydrograph to determine peak discharge in the HEC-HMS model. The lag time and CN values for the Mlazi subcatchments are contained in Table 3.5.2.

It should be noted that there are other methods, which have been applied for the estimation of flood peaks prior to this study, which have been used for the validation of the magnitude of peak discharges obtained by this approach. These methods are tabulated and briefly discussed in Section 3.6.6.

3.5.12 Baseflow Model

Baseflow was assumed to be zero in the Mlazi catchment model because it is very small compared with the flood discharges and therefore has negligible effect on the peak flood discharges.

3.5.13 Routing Model

The purpose of this model is to compute a downstream hydrograph, using the upstream hydrograph as the upstream boundary condition (produced by the transformation process) as input. The model computes the downstream hydrograph by use of the continuity and momentum equations, also known as St. Venant equations. The simplest derivative of the St. Venant equations was discussed in Section 2.4.4.

The most appropriate routing method applied for the computation of the downstream hydrographs in the Mlazi sub-catchments was the Modified Puls (or storage routing) method. The Modified Puls technique has the advantage over the other routing methods available

as discussed in Section 2.2 (e.g. Kinematic Wave, Muskingum-Cunge) in that it can incorporate the backwater effects caused by downstream conditions such as bridges and culverts. These backwater effects cause attenuation of the flood wave. Furthermore it requires parameters (storage – flow relationship) for each routing reach, which are relatively easy to obtain. The storage – flow relationship required by the modified Puls method was obtained from the HEC-RAS model that defines the storage – flow relationship between two cross sections. Storage for a given flow is computed from the volume stored in the reach calculated by numerical integration.

The initial estimate of the storage-flow relationship was obtained by the use of the storage-flow relationship of the Mhlatuzana River since the HEC-RAS model was not yet ready to be used for capturing the storage-flow relationship for various reaches within the Mlazi River. This approach is acceptable as in general, the storage – flow relationship of the Mhlatuzana River is similar to that of the Mlazi Catchment as the two rivers have close similarity with regard to their catchment characteristics (steep rivers, elongated shape, soil type and landuse). The procedure conducted to obtain the storage-flow relationships was as follows:

- Various storage-flow values for reaches along the Mhlatuzana River were captured from the HEC-RAS model of Mhlatuzana. The storage-flow relationship for Mlazi river were developed based on plotting the storage flow values from Mhlatuzana and developing the k relationship related to the reach length (L) as shown by Equation 3.5.8:

$$k = 0.556L^{0.8034} \qquad \text{Eqn (3.5.8)}$$

The graphical depiction of the *k: L* relationship developed is shown in Figure 3.5.13a below.

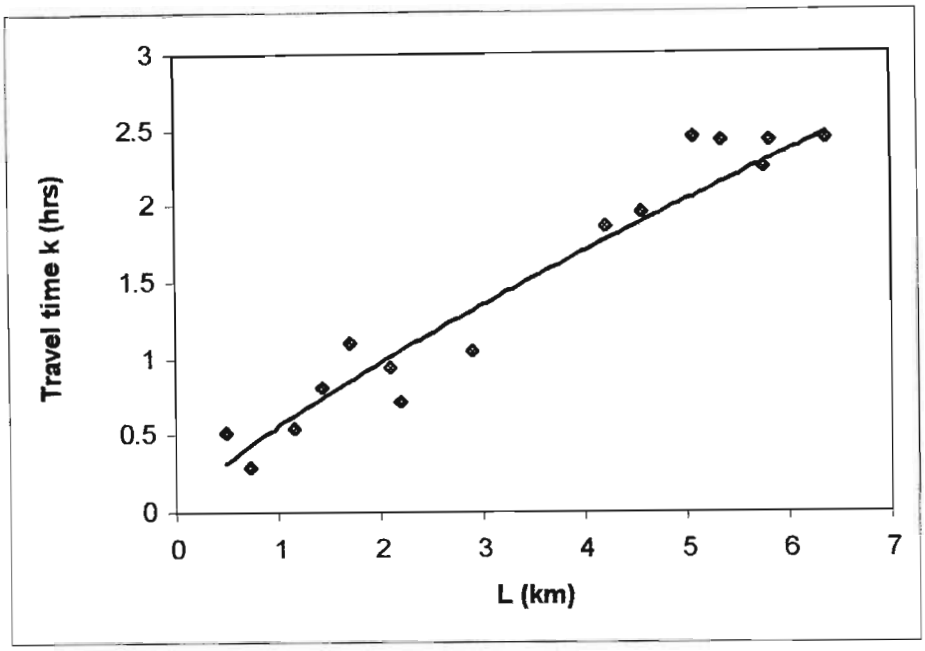

Figure 3.5.13a: Travel time k (h) versus Reach length L (km) for storage-flow relationship for the Mhlatuzana River Reaches, used initially on Mlazi.

The computation of the Mlazi storage (S) m^3 for given flows (Q) m^3/sec in this case was computed using the following formula:

$$S = 0.556QL^{0.8034} \qquad \text{Eqn (3.5.9)}$$

Another relationship was developed based on plotting the storage per meter reach length (S/m) against flow (Q) on a spreadsheet resulting in a relationship; S/m = cQ in which the (c) values were captured and the mean value of the constant c obtained was 2.24. An expression relating the reach length (*L*) to the (*k*) value was developed based on the constant (c) as shown in Equation 3.5.10:

$$k = \frac{L}{c} \qquad \text{Eqn (3.5.10)}$$

The graphical depiction of the *k: L* relation ship is shown in Figure 3.5.13b

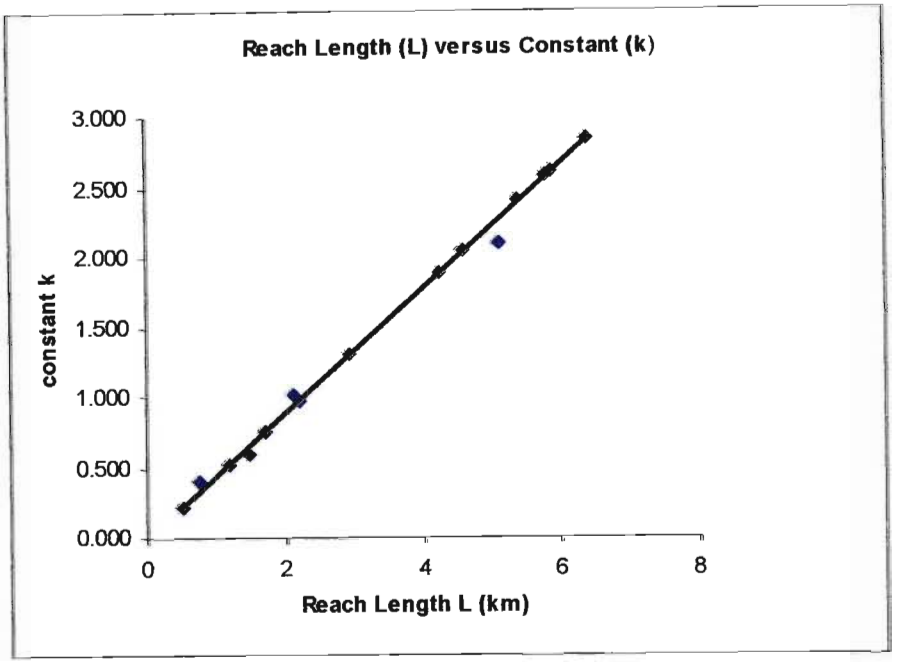

Figure 3.5.13b: Reach length versus constant k value for storage/m-flow relationship for the Mlazi River Reaches

The relationship in Equation 3.5.10 resulted in the development of the storage-flow relationship shown by Equation 3.5.11:

$$S = Q\frac{L}{2.24} \qquad \text{Eqn (3.5.11)}$$

- The Mlazi storage formulae from Equation 3.5.9 and Equation 3.5.11 were used to compute the storage for various selected flows. The storage-flow relationships obtained by using Equation 3.5.11 were entered into the Modified routing model as the initial estimates of the storage–flow relationship required by the Modified puls method.

- When the HEC-RAS model became available for the Mlazi, a wide range of flow data was input into the river model for the computation of the actual storage-flow relationships which were then captured and subsequently compared with the empirically computed storage-flow relationships. The plotted curves in Figure 3.5.4 indicate that the Mhlatuzana initial estimates (obtained from Equation 3.5.9) and second Mhlatuzana second estimates (obtained from Equation 3.5.11) were quite close to

the actual. Therefore this confirmed that the assumption made prior to the computation of the storage-flow relationships for the Mlazi Catchment based on the Mhlatuzana was valid.

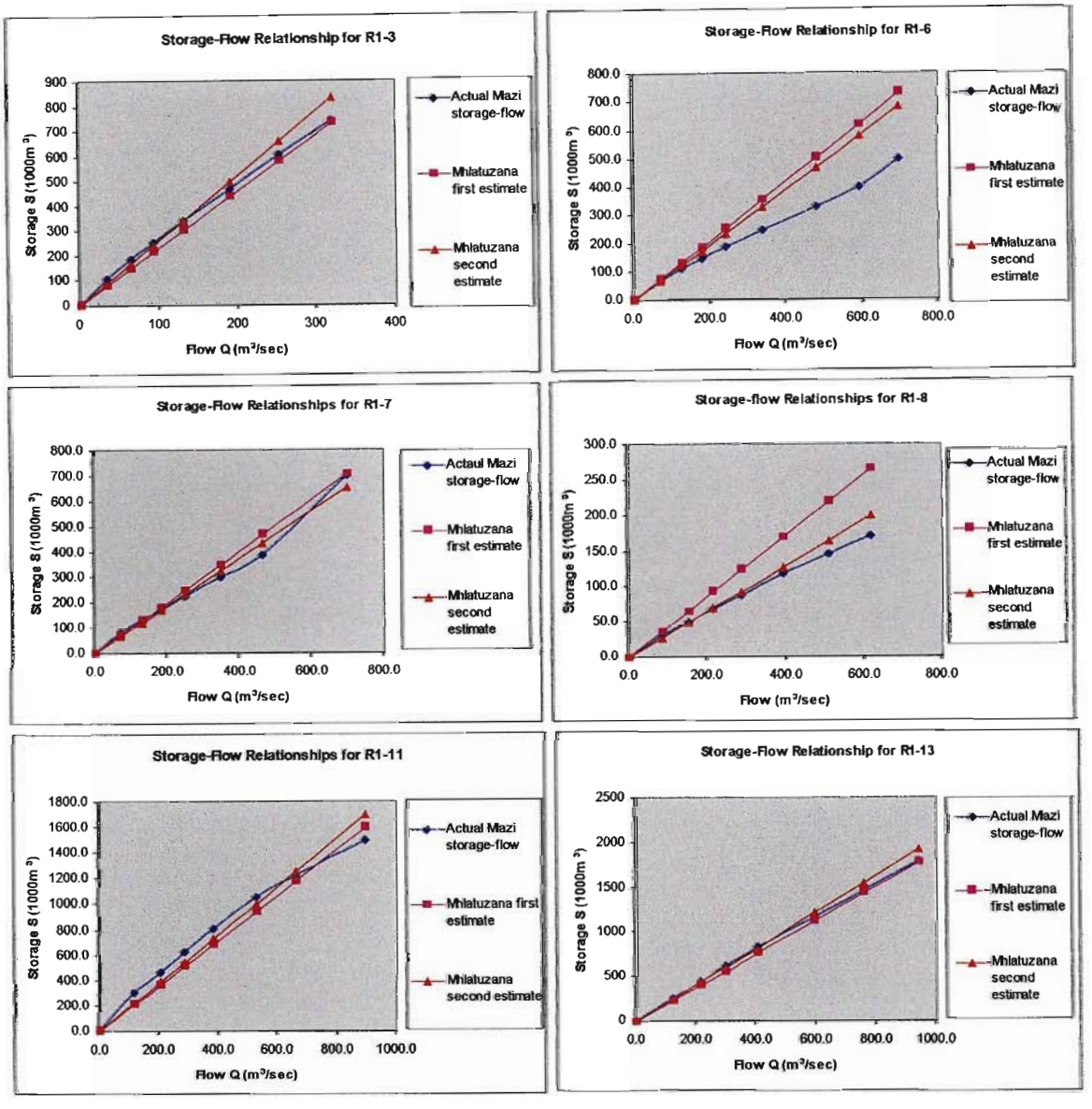

Figure 3.5.14: Comparison of the Storage –flow relationships for the Mlazi River Reaches

Runoff from upstream sub-catchments are routed through the current sub-catchment (using the channel geometry to quantify the flow volumes), and the runoff from the current sub-catchment then added to the routed flow at the downstream outlet point to give the outflow hydrograph.

3.6 Calibration of HEC-HMS Model

The SCS – UH method used for estimating design flood values uses a number of parameters in the process. Initial estimates of the values of the parameters are based on the physical catchment characteristics as measured from topographical and other maps and from field observations. It is usually the case that adjustments are required to the various parameters to obtain more realistic results from the design flood models.

Model calibration is the process of adjusting model parameter values until model results match historical data. Since this study was carried out in an environment where there is uncertainty due to a lack of historical data for calibration purposes, a different approach in calibration was applied.

The calibration process was first applied to two selected subcatchments of Mlazi, which have reasonable historical streamflow and rainfall data. The two subcatchments are namely the Baynesfield and Mlaas Road sub-catchments located at the up stream part of the Mlazi Catchment as shown in Figure 3.6.1a.

The approach to calibration of the subcatchments was conducted in two phases. The first phase of the approach involved the use of a particular storm event chosen among a range of storm events based on the correlation of the streamflow and rainfall data.

The second phase of the approach, which was more of a validation process, involved the use of flood frequency analysis of the 20-year peak discharges from the two stream gauge stations namely; Baynesfield and Mlaas Road streamgauges referred by DWAF as UH6002 and UH6003 respectively. Once the calibration had been carried out for the two subcatchments, the whole catchment was calibrated by applying a constant parameter correction factor across the catchment as discussed in this section. It should be noted that in such an environment the most important factor is to get the best initial

parameter estimates so as to reduce the error significantly before calibration is conducted.

The figure below shows the distribution of the rain gauge in and around Mlazi catchment. The various point rain gauge are represented by the black dots. The red dots highlights the position of the stream gauge UH6002 , UH6003 and the Shongweni

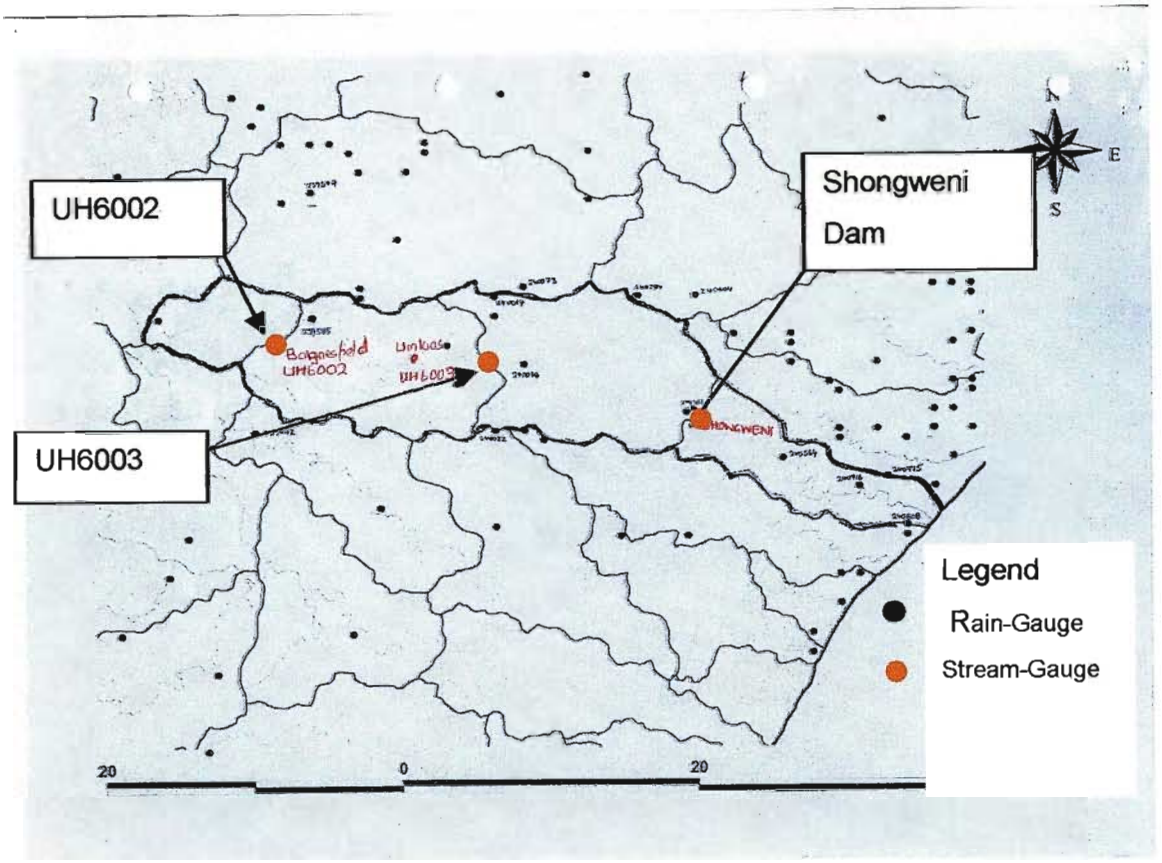

Figure 3.6.1a: Rain and Stream gauge location

The process of comparing model-produced results with actual observed data was carried out using the SCS-UH method within the HEC-HMS catchment-modelling program. The general procedure for the first phase of the calibration is shown below in Figure 3.6.1b, and the results achieved at different gauges on the Mlazi catchment for different historical storm events are covered in the following sections.

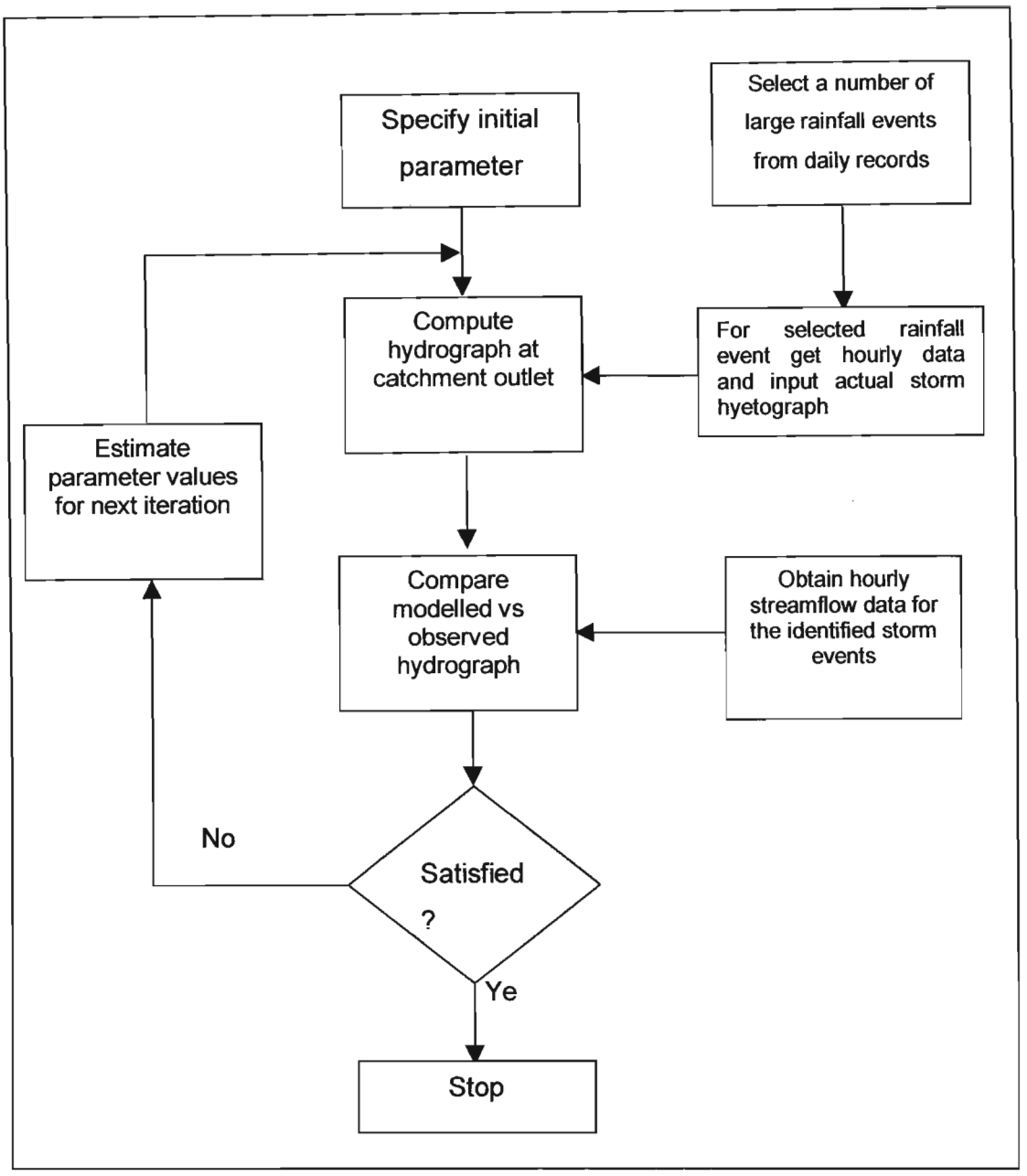

Figure 3.6.1b: First Phase Calibration Procedure

3.6.1 Calibration Locations

The location of stream gauges along the Mlazi River are shown in Table 3.6.1. Figure 3.6.2 shows the stream gauges at the Baynesfield and Mlaas road stations.

The calibration process was initially carried out for two upper sub catchments on the Mlazi River, each corresponding to a flow gauge station from which hourly streamflow data correlating with rainfall data was available.

Station	Location	Position on 1:50000 hardcopy map
U6H002; Baynesfield	Latitude; 29° 44′ 55″ Longitude; 30°19′08″	2930CD
U6H003; Mlaas Road	Latitude; 29° 48′ 13″ Longitude; 30°30′58″	2930DC
U6R001; Shongweni Dam	Latitude; 29° 44′ 55″ Longitude; 30°19′08″	2930DC

Table 3.6.1: Stream gauge locations in the Mlazi Catchment

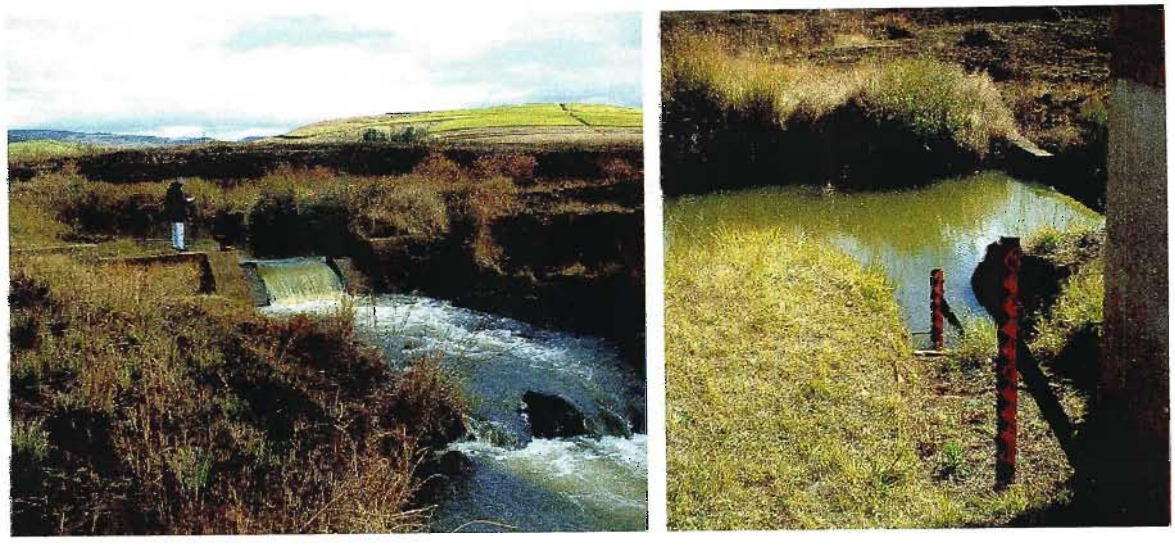

BAYNESFIELD WEIR STREAM GAUGE

MLAAS ROAD WEIR STREAM GUAGE

Figure 3.6.2: Baynesfield and Mlaas Road Weir Stream Guages

The stream gauge system used for recording stream flow at the weirs shown in Figure 3.6.2 uses a pressure probe submerged into the stilling pool on the upstream side of the weirs. The cables from the probe are connected to a housing that contains an OTT data logger. The data logger record heights at time intervals of approximately 12 minutes. These heights are then converted into flows using rating curves. These gauges are not ideal for flood forecasting since they not very reliable in recording high flows associated with flooding.

It should be noted that although there is a stream gauge station at the Shongweni dam, this was not used for calibration because the streamflow data were not reliable. However it is of vital importance that a reliable streamflow gauge be located at Shongweni in the future. The reason being that it is a strategic point for locating a flood warning device and also for monitoring flow, especially for the radar stream flow forecasting. As part of an integrated flood warning system this will contribute towards damage cost control in the lower reaches of Mlazi River.

3.6.2 Streamflow Data

The hourly streamflow data for the selected storm events were obtained from DWAF. The raw streamflow data came in the form of pdf and txt files. The raw data had to be processed. The processing procedure involved determining some of the high peak flows not recorded by the stream gauges using a rating curve obtained from DWAF. The other reason for applying the rating curve was because those gauge were designed to measure low flows and in this instance high flood peak discharges were the values required. The time series for the recorded stream flow data had to be converted to hourly since it was breakpoint recorded with an average interval time of about 12 minutes between each recorded flow. The streamflow data obtained was for the storm event identified in Table 3.6.2. However, there were cases where good streamflow data was obtained but it did not have the corresponding rainfall data, and vice versa.

Storm event	Station with stream flow data
29 Nov 1989	Baynesfield and Mlaas
8 July 1996	Baynesfield and Mlaas
22 Dec 1996	Baynesfield and Mlaas
1 Jan 1998	Baynesfield and Mlaas
2-4 Feb 1999	Baynesfield and Mlaas

Table 3.6.2: Selected Storm events

The above mentioned storm events had to have corresponding continuously recorded rainfall, but the use of autographic rainfall from the Durban Airport and Pietermaritzburg was discarded for reason discussed in Section 3.6.3, hence the streamflow data for those events also became invalid. The streamflow data for the 2-4 Feb 1999 storm event was the only data used. The data was analysed, and it was apparent that high flows were not recorded during this period due to a gauge error. The good data was therefore input to the HEC-HMS model to be compared with the simulated hydrograph obtained from the 2-4 Feb 1999 rainfall, whilst acknowledging that only peaks up to a certain value could be compared.

Rainfall Data

The HEC-HMS model requires rainfall hyetographs from the actual storm events which occurred at the Mlazi catchment. The daily rainfall totals at a number of gauges within the catchment were obtained from the South African Weather Service (SAWS) at the Durban Weather Office. The hourly-distributed autographic rainfall data is then obtained for the Durban Airport and Pietermaritzburg stations from SAWS.

Rainfall Selection Procedure

The task of rainfall selection was conducted as follows:

(a) Daily rainfall records were obtained from 1989 to 1999.

(b) From the above records, 20 highest rainfall records were selected.

(c) A request was made to the Durban weather station for the hourly autographic rainfall for the selected 20 highest rainfall records. A number of storm events which had hourly distributed rainfall for either the Pietermariztburg and Durban Airport stations were identified.

(d) Using the events identified in (c), the hourly stormflow data corresponding to the identified event had to be sorted.

(e) It became apparent at this point that due to a lack of good records, there was really only one event that had reliable rainfall and streamflow data. Table (3.6.3a) shows the chosen

2-4 Feb 1999 storm event daily rainfall total for selected rain gauge.

Rain gauge	2-Feb 99	3-Feb 99	4-Feb 99	Total
Richmond	10.9 mm	-	-	10.9 mm
Baynesfield	64 mm	17 mm	7 mm	88 mm
Eston	-			
Camperdown	83.4 mm	5.2 mm	7.1 mm	95.7 mm
Camperdown in				
Shongweni	34.2 mm	11.2 mm	60.4 mm	105.8 mm
Intake weir	-	-	-	-
Umlaas w/w	-	-	-	-
Pietermaritzburg	84.4 mm	4.6 mm	7 mm	105.8 mm
Durban Airport	6.5 mm	29.4 mm	128 mm	163.9 mm

Table 3.6.3a: 2.4 Feb 99 Rainfall Depth For Mlazi Rain gauge.

(f) Besides the lack of good records it was also not possible to use the Pietermaritzburg and the Durban Airport autographic rainfall data for the rainfall inputs for UH6002 and UH6003 respectively. The problem was related to the autographic distribution not being a true representation of the rainfall distribution due to the following factors:

- the autographic rainfall gauges are located outside the UH6002 and UH6003 subcatchments which have the stream gauge data

- wind speed, with a speed of about 20 km/hr, the lag between the rainfall at Pietermaritzburg and the rainfall at Baynesfield is approximately one hour

- there were errors in time for which the rainfall was recorded at the rain gauge stations.

(g) The radar rainfall distribution for the 2-4 Feb 1999 storm event obtained from Scott Sinclair (Umgeni Water) was used for "stitching" the 3-Day total rainfall depths for gauge stations within the Mlazi catchment. The radar distributed data proved to be very useful since it gave a spatial distribution over the quaternary catchment as compared to the point distribution from the rain gauge. The radar timing was also accurate in terms of lag time since this was also compared with the expected response time of the catchment and the time at which observed peak flows occurs.

(h) The radar-distributed rainfall was input into HEC-HMS precipitation model and distributed according to the rainfall distribution within the catchment as shown by Table (3.6.3b).

Quaternary Catchment	Raingauge Station	Radar Distribution	Total 3-Day Rainfall
U60a	Baynesfield	U60a	88 mm
U60b	Camperdown	U60b	95.7 mm
U60c	Shongweni	U60c	105.8 mm
U60d	Durban Airport	U60d	163.9 mm

Table 3.6.3b: 2.4 Feb 99 Rainfall Distribution For Mlazi

Figure 3.6.3a below shows the graph of the hyetograph (from radar depth) for the 2-4 Feb 99 event taken at the quarternary cacthment U60a together with the streamflow recorded at the UH6002 stream gauge. The graph shows a lag between the hyetograph (blue) and stream flow (red).

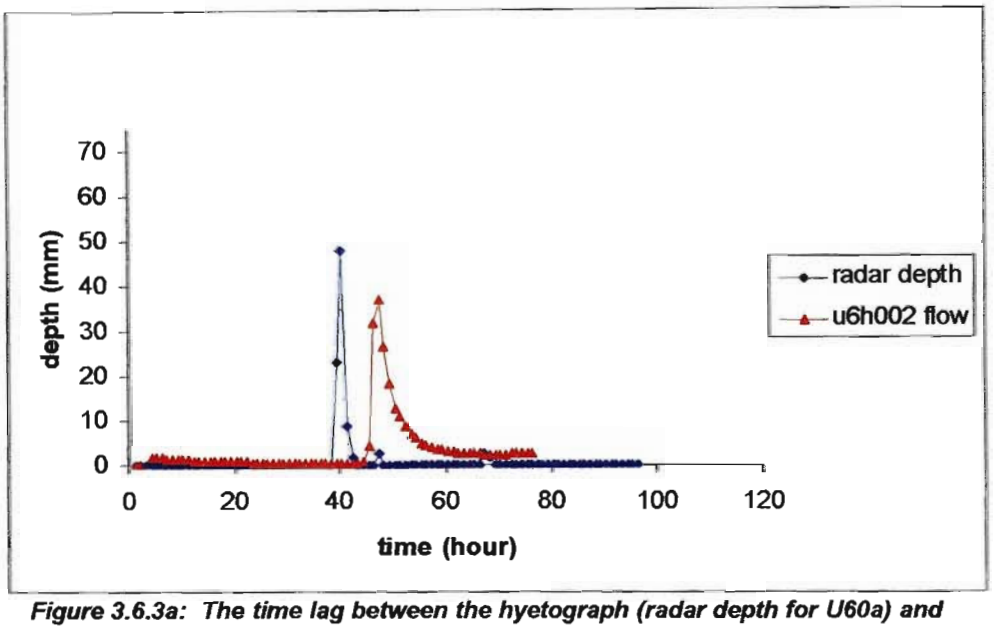

Figure 3.6.3a: The time lag between the hyetograph (radar depth for U60a) and the streamflow at UH6002

3.6.3 Comparison of Modelled vs Observed Streamflow Hydrographs

The HEC-HMS program was run with the initial parameters shown in Table 3.6.4a together with the radar-distributed rainfall and corresponding output hydrographs were then obtained. The subsequent hydrographs were compared with the observed flows at the outlets of the modelled subcatchments.

The initial parameter values for the Baynesfield and Mlaas catchments are as follows:

Station	Area	Initial Input Parameters		
	km^2	CN	Lag Time (mins)	Ia (mm)
U6H002	105	72	114	10
U6H003	312	68	145	12

Table 3.6.4a: Initial Parameters for calibration gauges during the first phase

Initial Calibration Results

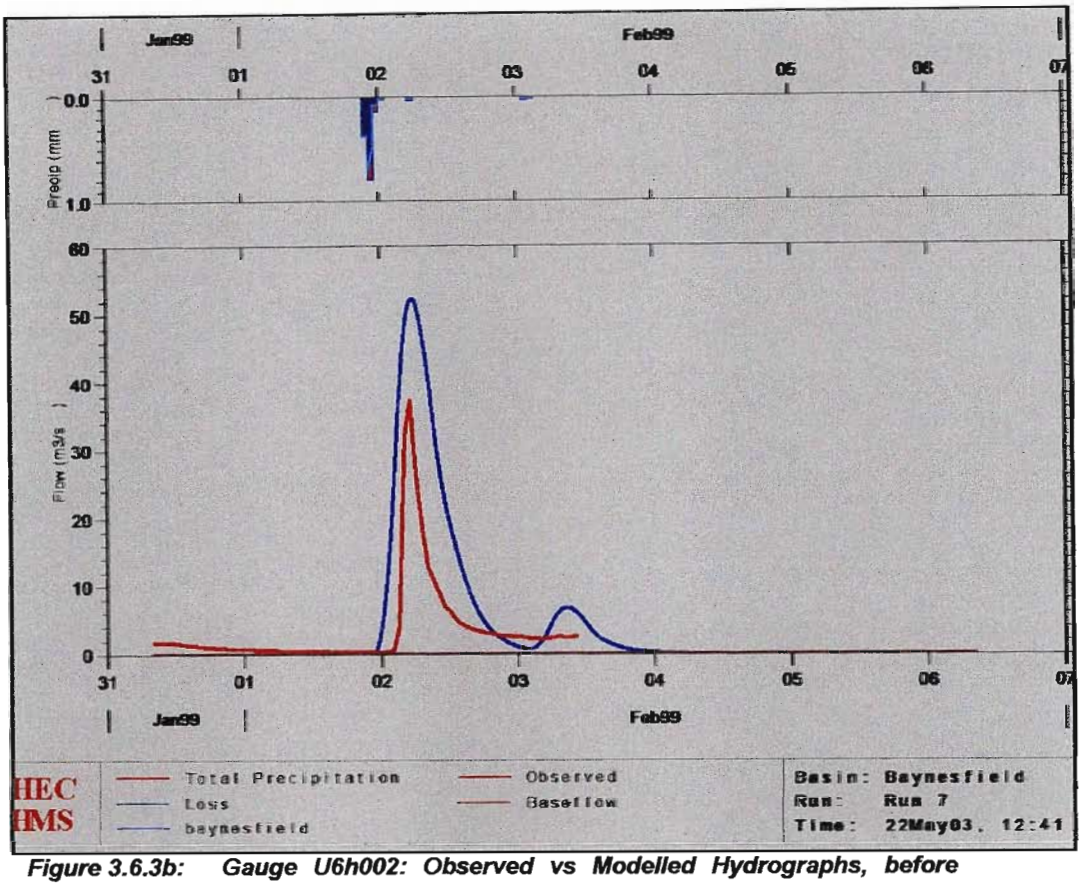

Figure 3.6.3b: Gauge U6h002: Observed vs Modelled Hydrographs, before parameter adjustment

Figure 3.6.3b shows the model hydrograph based on the ***initial*** parameter estimates and the observed hydrograph at U6H002. In general the computed peaks are not occurring at the same time as the observed and their peak discharge is higher than the observed, therefore the initial parameters need to be adjusted as explained in the next section.

3.6.4 Adjustment of the initial parameter (at UH6002 and UH6003)

The parameters to be adjusted from the initial input values were the following:

- Initial abstraction I_a
- SCS Curve number, CN

A manual adjustment process was conducted on these parameter with the intention of making the computed values match the observed in terms of the peak discharge. The trial and error method was applied to the initial input parameters until the computed peaks matched the observed. The changes made to the initial parameter values are shown in Table 3.6.4b.

The table shows a decrease in CN values of about 10%. The adjusted values were input to the HEC-HMS model, and the computation conducted resulted in the modelled hydrograph matching the observed as shown in Figure 3.6.4.

Station	**Initial Input Parameters**			**Final Input Parameters**		
	CN	Lag Time (minutes)	I_a (mm)	CN	Lag Time (minutes)	I_a (mm)
U6H002	72	114	10	66	114	14
U6H003	68	145	12	62	145	16

Table 3.6.4b: Parameter adjustments for calibration gauges during the first phase

Figure 3.6.4 shows the modelled hydrograph ***after*** the catchment parameters have been adjusted - the fit is now much closer. The simulated peak discharge occurs at the same time as the observed and the two are approximately of equal magnitude approximately 37 m^3/sec.

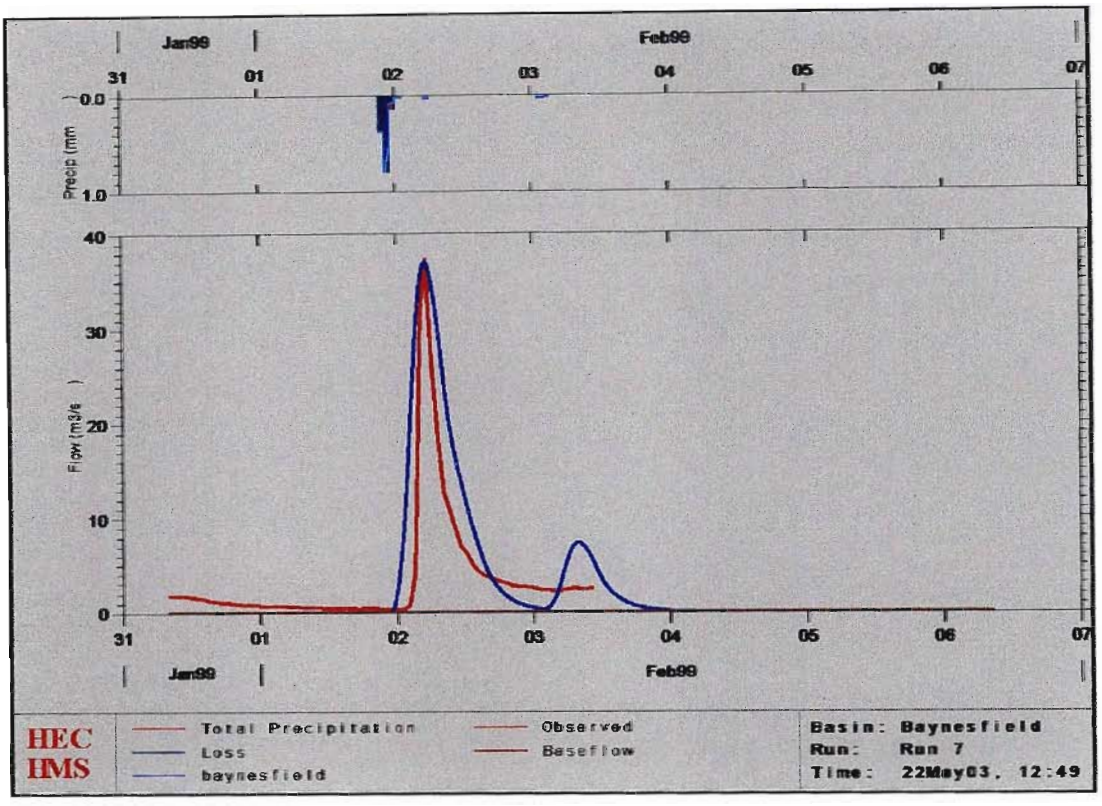

Figure 3.6.4: Gauge U6h002: Observed vs Modelled Hydrographs, after parameter adjustment

It was necessary to relate the changes made to the initial parameters to the physical catchment assumptions, ie to determine what adjustments were required to the initial physical catchment data in order for them to re-produce the optimised model parameters.

The changes made on the CN values were effected by altering CN values for the landuse and soil type that carry a greater weighting factor for the two upper catchments (UH6002 and UH6003). The adjustment of the CN values was conducted by either shifting the soil classifications up or down by one or so categories or altering the land use CN value.

The initial range of CN values based on various SCS land use and corresponding soil type are also adjusted by shifting the soil classifications of the equivalent SCS land uses carrying a greater weighting factor for the two upper catchments (UH6002 and UH6003). Table 3.6.5 shows various CN values initially assigned to the landuse

and hydrological soil types. Based on the optimised CN numbers obtained by manual adjustment and the weighted landuse composition of the sub-catchments, the various initial CN ascribed to the landuse were changed. Table 3.6.6 shows the new CN values after the alterations.

Landuse		Hydrological Soil Group				
LANDSAT	**Equivalent SCS Land Use**	**A**	**A/B**	**B**	**B/C**	**C**
2 – Cultivated: permanent-commercial - sugarcane	Sugarcane, planted on contour <50% cover	65	70	75	79	82
3 – Cultivated: temporary-commercial - dryland	Veld/pasture (Medium)	49	61	69	75	79
5 – Cultivated: semi-commercial / subsistence dryland	Open Spaces (<50% grass cover) [peri-urban settlements]	69	73	78	82	85
6 – Degraded Thicket and Bushland	Natural Forest (High)	45	56	66	72	77
7 – Degraded unimproved Grassland	Veld/pasture (High)	68	74	83	86	88
8 – Forest (Natural)	Natural Forest (Medium)	36	49	60	68	73
9 – Forest Plantations	Forest/plantations (Medium)	41	53	64	69	74
10 – Improved Grassland	Open Spaces (50-75% grass cover)	49	61	69	75	79
11 - Thicket and Bushland	Natural Forest (Medium)	36	49	60	68	73
12 – Unimproved Grassland	Veld/pasture (High)	68	74	83	86	88
13 – Urban / Developed: Industrial / Transport	Commercial/Industrial	84	86	88	89	90
14 – Urban / Developed: Residential	Residential (38% impervious)	61	69	76	81	84
15 - Urban / Developed: Res. (Small holdings & grassland)	Residential (20% impervious)	51	61	68	75	78
16 - Water-bodies		98	98	98	98	98

Table 3.6.5: Generalised SCS Runoff Curve Numbers (Initial estimates)

Landuse		Hydrological Soil Group				
LANDSAT	**Equivalent SCS Land Use**	**A**	**A/B**	**B**	**B/C**	**C**
2 – Cultivated: permanent-commercial - sugarcane	Sugarcane, planted on contour 50-75% cover	**25**	**46**	**59**	**67**	**75**
3 – Cultivated: temporary-commercial - dryland	Veld/pasture (Low)	**39**	**51**	**61**	**68**	**74**
5 – Cultivated: semi-commercial / subsistence dryland	Open Spaces (50-75% grass cover) [peri-urban settlements]	**49**	**61**	**69**	**75**	**79**
6 – Degraded Thicket and Bushland	Natural Forest (High)	45	56	66	72	77
7 – Degraded unimproved Grassland	Veld/pasture (Medium)	**49**	**61**	**69**	**75**	**79**
8 - Forest (Natural)	Natural Forest (Low)	**25**	**47**	**55**	**64**	**70**
9 - Forest Plantations	Forest/plantations (Low)	**30**	**43**	**56**	**61**	**66**
10 – Improved Grassland	Open Spaces (75%+ grass cover)	**39**	**51**	**61**	**68**	**74**
11 – Thicket and Bushland	Natural Forest (Medium)	36	49	60	68	73
12 – Unimproved Grassland	Veld/pasture (Low)	**39**	**51**	**61**	**68**	**74**
13 – Urban / Developed: Industrial / Transport	Commercial/Industrial	84	86	88	89	90
14 – Urban / Developed: Residential	Residential (38% impervious)	61	69	76	81	84
15 - Urban / Developed: Res. (Small holdings & grassland)	Residential (20% impervious)	51	61	68	75	78
16 - Water-bodies		98	98	98	98	98

Table 3.6.6: Generalised SCS Runoff Curve Numbers (final estimates) Note that the CN values in bold are those that have been changed from the previous estimates

3.6.5 Estimation of Peak Discharge *(for Validating HEC-HMS model output)*

The purpose of this section is to give an overview of the flood estimation, which was conducted for the Mlazi river so as to compare the HEC-HMS peak discharges with those computed using other accepted methodologies. The methods that have been applied are described by Chow et al. (1988) and also by Ponce (1989). The methods in general compute peak floods for a particular return period.

The section is divided into three components:

- collection and selection of methods,
- empirical formula suggested for rivers within the eThekwini Municipality, and
- comparison of computed results flood peaks for Mlazi River.

A substantial amount of work has been done with regards to estimation of flood peaks. The flood literature references quoted by Alexander in the Standard Design Flood User Manual (2002) are evidence of the work that has been carried out.

3.6.6 Selection and Collection of Methods for Design Flood Estimation

- Deterministic Methods

These methods are derived from the statistical properties of point rainfall. Deterministic methods are therefore based on an understanding of the rainfall-runoff processes producing flood storms. The rainfall-runoff process is influenced by catchment characteristics such as:

- catchment size,
- catchment slope,
- catchment shape,
- catchment land use, and
- climate as characterised by storm type, intensity duration, and spatial distributions.

The ancient but mostly used reliable deterministic method is the rational method developed in 1850. Alexander (2002) developed a Standard Design Flood (SDF) method, which is a numerically calibrated version of the rational method. A detailed approach to the development of this method is stated in Alexander's reports entitled "Statistical analysis of extreme floods" and "The standard design flood-theory and practice" and the "User Manual" (Alexander, 2002). The other relevant contribution to the rational method is the Modified Rational Formula (MRF). This method applies flood-scaling properties of rainfall depth/intensity in South Africa together with the relationship between T_c and area, which all result in the modified rational formula (Menabde *et al*, 1999). The rational formula is useful for small catchments and was therefore applied for computation of flood peaks for the subcatchment identified for calibration purpose. Other methods such as the unit hydrograph developed by Sherman in 1932 are mostly used for large catchments. It is defined by Chow et.al. (1988) as the unit response function of a linear hydrologic system. In South Africa the unitgraphs are obtained from the synthetic unitgraphs compiled by Pullen (1969) and these are modelled using linear storage model by Bauer and Midgley (1974).

3.6.7 Statistical Methods

The direct statistical methods are applicable only when there is availability of historical data such as flood peak and volume for the catchment under study. Chow *et al* (1988) and Ponce (1989) mention various statistical frequency analysis methods together with distributions associated with the methods. Chow *et al* (1988) mentions that fitting distributions can be accomplished by the method of moments developed by Pearson (1902). Hazen (1914) observed that the logarithms of the annual flood maxima were approximately normally distributed. The most common distributions applied are as follows:

- Log normal (2 or 3 parameter)
- Exponential
- Gamma

- Pearson Type III (or 3 Parameter Gamma)
- Log Pearson Type III
- Extreme Value Distribution.

In South Africa, the widely used distribution is the log Pearson Type III distribution. However, it has to be used with caution for return periods longer than 30 to 50 years (Alexander, 2002). There have been computer programs developed for the prediction of flood frequency using the above mentioned distributions such as the REGFLOOD model stated in Alexander (1993).

Due to unavailability of historical data for Mlazi, design floods were estimated using historical flow data from two subcatchments. The flood frequency analysis included plotting the AMS data using Cunnane's plotting position. A plot of the computed HEC-HMS peak discharges for various recurrence intervals was then conducted. The curves produced were compared and the HEC-HMS parameters manipulated until the HEC-HMS curve was approximate to the observed. The process and results of this validation is discussed in detail in Section 3.6.7.

3.6.8 Empirical Methods

The most essential contribution to flood peak estimation came from the works of Kovacs (1988). Kovacs of the Department of Water Affairs developed the Regional Maximum Flood (RMF). The RMF is recommended for determining the upper limit design flood in South Africa. It was therefore used as a tool for comparison of the SCS flood peaks obtained through the HEC-HMS model. An empirical formula like the Durban Corporation formula (DCF) based on the HEC-HMS results has also been developed during this study (HEC-HMS Formula) and its results compared with the RMF.

(a) Durban Corporation Flood Formulae (Scott *et al*, 1986). The City Engineer derived two empirical formulae based on analysis of local floods. An estimation of the peak discharge of specified return periods using the following formulae was carried out:

$$Q_N = 1090(0.1 + 1.45\log_{10} N)A^{0.552} \qquad \text{Eqn (3.6.1)}$$

This is the original formula in METRIC units and is applicable for area greater than 8km^2, the formula has however been converted into the SI units to become:

$$Q_N = 18.253 D_N A^{0.552} \qquad \text{Eqn (3.6.2)}$$

where:

$$D_N = 0.1 + 1.45\log_{10} N \qquad \text{Eqn (3.6.3)}$$

N = return period
A = catchment area (km^2)
Q_N = discharge (m^3/sec)

The above formula gives good initial estimates of the peak discharges although it tends to give over estimates of the peak discharges at higher recurrence intervals (Scott *et al*, 1986). The other problem with the use of this formula was the fact that during its derivation the eThekwini Municipality boundary was smaller than the present situation such that it did not take into consideration some of the rivers and catchments which fall inside the new boundary. Furthermore it was derived specifically for elongated catchments. These problems have been therefore, the driving force to the development of the Empirical formula.

(b) Empirical Formula based on HEC-HMS results

The Empirical formula (EF) is based on an analysis of HEC-HMS peak discharges, which have been computed for rivers within the eThekwini Municipality. In this case, flood discharges derived from the physically based hydrologic model were plotted against the catchment areas. It should be noted that most of these catchments are elongated and are almost homogenous in nature, however the effect of the shape of the catchments is still being investigated

using some of the techniques described by Ponce (1989). The formula so far derived depends on two parameters, which are the catchment area and the return period. The advantage of using the formula is that it is based on the physical parameters of the catchment and furthermore it also relates to the RMF. It can therefore be used, as an early and quick estimation of the peak discharges especially when that information is required immediately by the decision-makers at the disaster management department. The derived formula is:

$$Q = C(T)A^{0.42} \qquad \text{Eqn (3.6.4)}$$

The formula is applied to compute Q (m^3/sec) for various return periods T. The term C (T) varying for each return period caters for the physical parameters of the catchment of an area A (km^2). Tables 3.6.7 and 3.6.8 contain the tabulated peak discharges computed using the EF and the HEC-HMS results respectively. The graphical plots of the peak discharges at various return periods from the above mentioned tables are presented for comparison in Figures 3.6.5 and 3.6.6. The comparison of the peak discharges between the HEC-HMS results and the Empirical Formula is represented as a percentage difference, which is seen in Table 3.6.9 to be approximately plus or minus 10%.

Table 3.6.7: Peak Discharges based on Empirical Formula

	Return Period (T)	2yr	5yr	10yr	20yr	50yr	100yr
	Constant (C)	12.75	27.89	43.98	62.33	91.83	120.1
Peak Discharge	$Q = C(T)\ A^{0.42}$						
River	Area (km^2)	2yr	5yr	10yr	20yr	50yr	100yr
Umbilo	80	80	176	277	393	578	757
Mhlatuzana	118	95	207	326	462	681	891
Mlazi	956	228	498	785	1113	1640	2145
Mbokodweni	248	129	283	446	631	930	1217

Table 3.6.7: Peak Discharges based on Empirical Formula

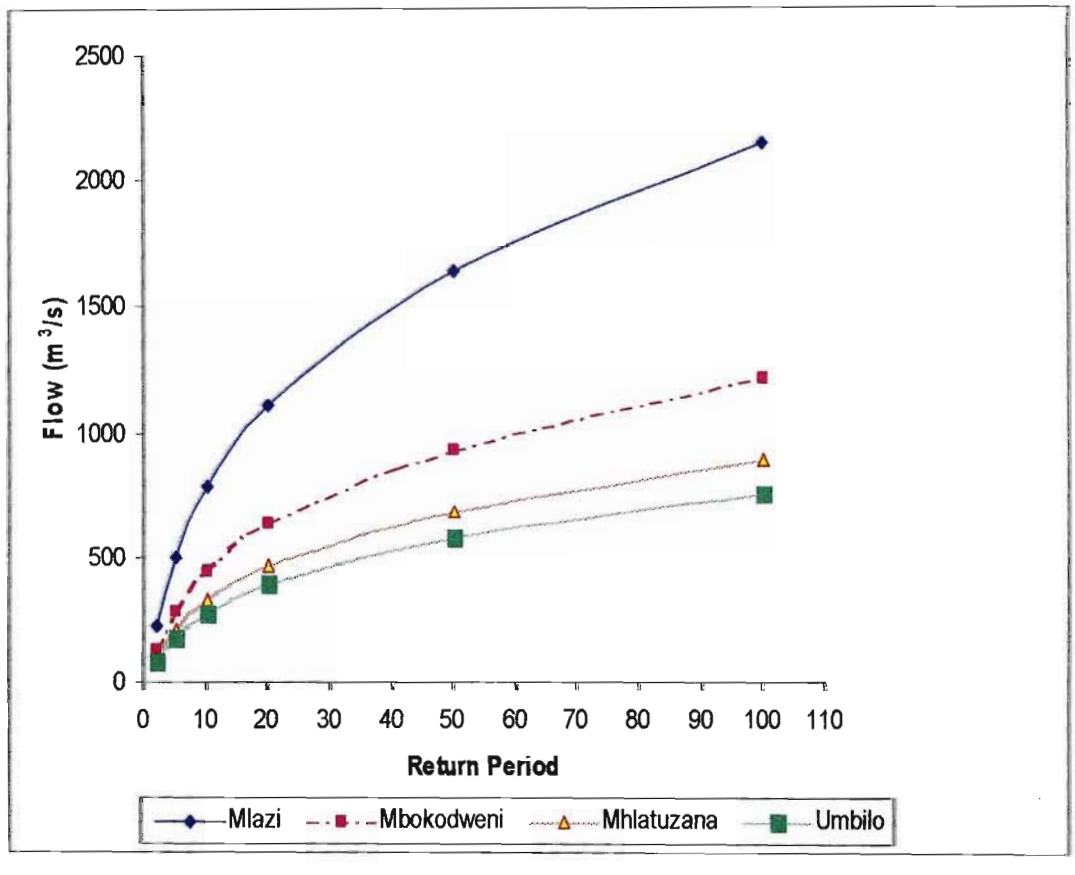

Figure 3.6.5: Peak Flow Discharge for Durban Rivers using Empirical Formula

Peak Discharge	HEC-HMS RESULTS						
River	Area (km^2)	2yr	5yr	10yr	20yr	50yr	100yr
Umbilo	80	79	198	316	451	626	816
Mhlatuzana	118	127	244	334	457	649	809
Mlazi	956	248	490	737	1028	1589	2200
Mbokodweni	248	125	289	449	671	994	1319

Table 3.6.8: Peak Discharges based on HEC-HMS

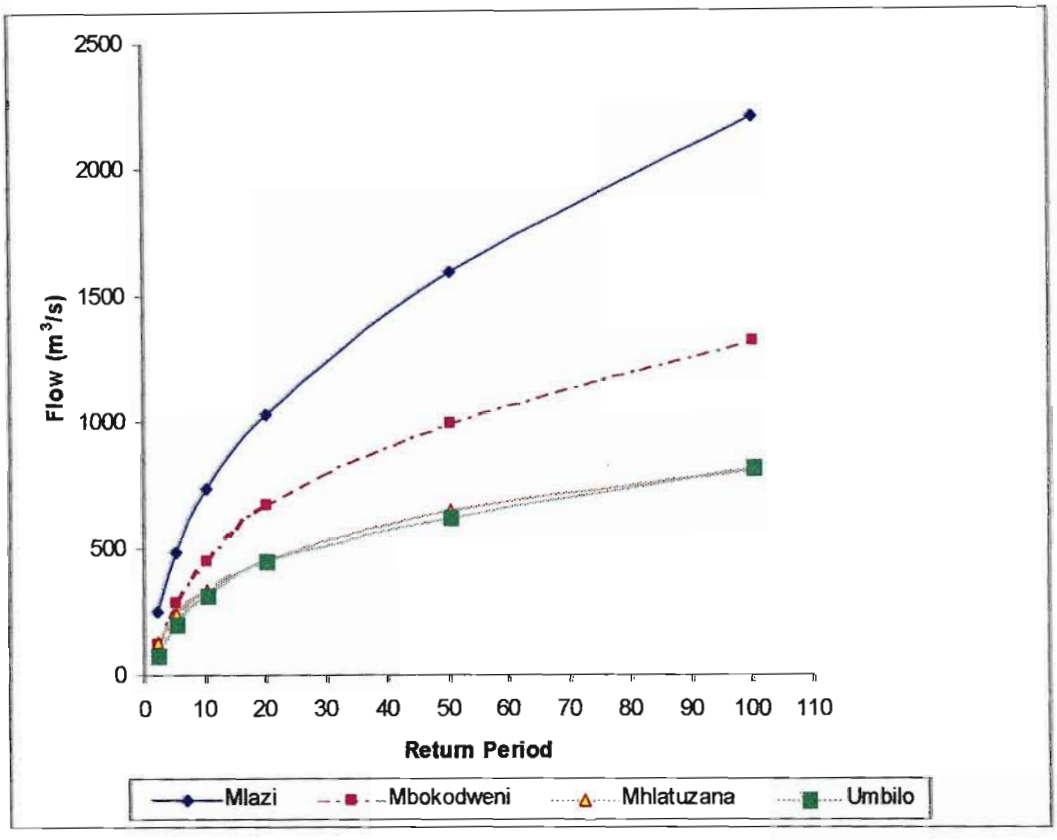

Figure 3.6.6: Peak Flow Discharge for Durban Rivers using HEC-HMS.

The flow curves in Figure 3.6.5 are similar to those shown in Figure 3.6.6. Although they are minor variations in flows for Mhlatuzana it is evidence that the empirical formula can be used as an initial estimation of the peak discharges computed using HEC-HMS model. A plot of peak discharge from EF against catchment size is shown in Figure 3.6.7. This curve gives the initial estimate of peak discharges for catchments within the eThekwini municipality boundary.

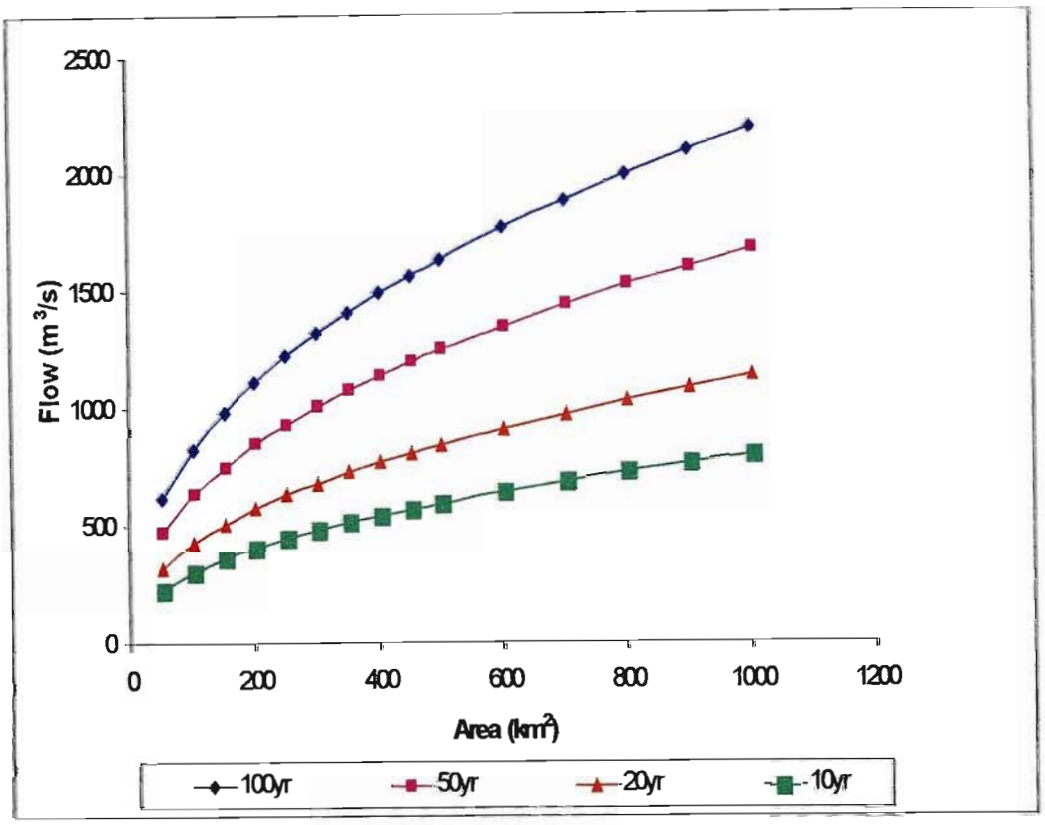

Figure 3.6.7: Peak Flow Discharge based on catchment area using Empirical Formula.

3.6.9 Comparison of the HEC-HMS peak discharges to those computed by use of other Methods

Computation of peak discharges based on other methods were carried out and then compared with the HEC-HMS peak discharge results obtained in the study. Figure 3.6.8 shows a plot of peak discharges (for catchments within eThekwini municipal boundary) at various return periods computed using the methods discussed in Section 3.6.6 and the HEC-HMS method. It is evident from the plot that the HEC-HMS results based on the SCS method are within the envelope created by the RMF and the rational methods. The Durban Corparation Formula (DCF) peak discharge values are closer to the RMF peak discharge values whereas the Standard Design Formula (SDF) peak discharge values are smaller in magnitude than those computed using the rational method. The HEC-HMS results tends to be closer and above the rational method by approximately 10%. Table 3.6.9 shows a summary of the Mlazi peak discharges that have been computed using various methods. The peak discharges in the

summary table were extracted from various studies that have been carried out for the Mlazi catchment. It is evident from the table that the variation in values of the peak discharges are attributed by the different catchment areas assumed for Mlazi especially when analysing the values obtained in the previous studies. During the current study it was however ensured that the methods were compared based on the same catchment area computed by GIS technology and verified manually using 1:50 000 scale maps.

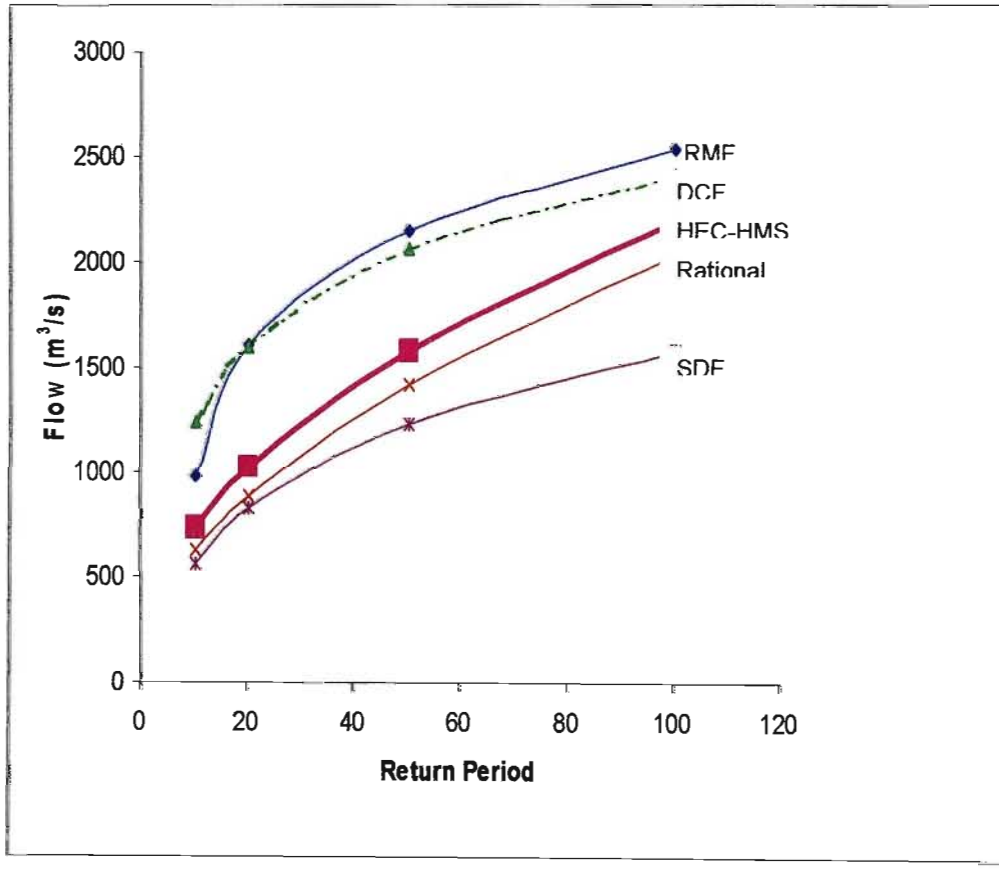

Figure 3.6.8; Comparison of HEC-HMS Peak Flow Discharge with other methods.

Having compared the computed HEC-HMS results with other methods it became apparent that these would need to be compared with observed streamflow data. A good model is one whose results compare favourable to the observed. The process could have involved capturing HEC-HMS results for the whole catcment and comparing it with a collection of streamflow data for the whole catchment. This was however not possible due to lack of historical data. Therefore the validation process discussed in

Section 3.6.7 was implemented, which is based on the stream flow data from two upper sub-catchments of the Mlazi.

Report	Method	Area km^2	Estimate Peak Flow for Various Return Periods					
			Q_{10yr} m^3/s	Q_{20yr} m^3/s	Q_{50yr} m^3/s	Q_{100yr} m^3/s	Q_{200yr} m^3/s	Q_{RMF} m^3/s
Scott *et al*,1996	Durban Corp-Formula	1000	-	1653	2130	-	-	-
	Unit Hydrograph	1000	-	790	1100	-	-	-
	Rational Method (c=0.4)	1000	-	1010	1375	-	-	-
	Roberts method	1000	-	830	1120	-	-	-
	Pitman & Midgley	1000	-	500	780	-	-	-
DWAF ,1988		1000	455	680	1940	2200	2790	4120
GIBB Africa,1996			1050	1450	2060	2560	3130	-
Shongweni Dam Rehabilitation (Stewart Scott, 1993)			450	630	920	1200	-	4500
Arcus Gibb,2002	Rational Method	955	636	886	1423	2042	2450	-
	Durban Corporation	955	1249	1601	2066	2418	2770	
	RMF	955	977	1610	2149	2540	-	3907
	SDF	955	563	833	1240	1583	-	-
	SCS (02/10/02) (HMS.Ia=0.1S & new CN, V/Q)	955	737	1028	1589	2200	4126	

Table 3.6.9: Mlazi Peak Discharges Computations based on various methodologies

3.6.10 Validation of the first Calibration Phase Using Flood Frequency Analysis

The validation processes uses the concept discussed by Chow *et al* (1988), which includes a graphical check that the selection probability distribution fits the set of hydrologic data. The data are plotted using suitable plotting position formulae such these:

- California's formula,
- Chegodayev's formula,
- Weilbull formula, and
- Cunnane's formula.

During this process observed peak flows for the 20 highest annual maximum series for the two stream gauge stations were ranked as shown by Figure 3.6.10 and Figure 3.6.11. The standard hydrological year for South Africa (October-September) was used for selecting the 20 highest peak flows. Each of the ranked flow data was assigned a probability value computed by use of the Cunnane (1978) plotting position formula expressed as:

$$T = \frac{n + 0.2}{r - 0.4} \qquad \text{Eqn (3.6.5)}$$

where: T is the return period assigned to the ranked flow data
n is the number of ranked annual maximum series
r is the rank number of the particular flow data.

Year	Record Number	Peak Flow (m^3/sec)
1981/1982	1	36.23
1982/1983	2	28.19
1983/1984	3	19.25
1984/1985	4	18.29
1985/1986	5	17.88
1986/1987	6	13.63
1987/1988	7	13.01
1988/1989	8	9.99
1989/1990	9	9.55
1990/1991	10	9.10
1991/1992	11	8.53
19921/1993	12	8.40
1993/1994	13	7.87
1994/1995	14	7.59
1995/1996	15	7.55
1996/1997	16	7.35
1997/1998	17	7.18
1998/1999	18	6.60
1999/2000	19	6.55
2000/2001	20	6.26

Figure 3.6.10: 20 Highest annual maximum series for U6H002(Baynesfield)

Year	Record Number	Peak Flow (m^3/sec)
1981/1982	1	651.15
1982/1983	2	435.85
1983/1984	3	253.14
1984/1985	4	194.99
1985/1986	5	133.60
1986/1987	6	105.63
1987/1988	7	104.92
1988/1989	8	59.07
1989/1990	9	45.28
1990/1991	10	42.10
1991/1992	11	42.00
19921/1993	12	42.00
1993/1994	13	39.16
1994/1995	14	36.29
1995/1996	15	35.87
1996/1997	16	31.56
1997/1998	17	30.31
1998/1999	18	28.99
1999/2000	19	22.81
2000/2001	20	20.23

Figure 3.6.11: 20 Highest annual maximum series for U6H003 (Mlaas)

Once the return period had been determined for each of the ranked flow data, the reduced variate y_T was computed using the following formula:

$$y_T = \left[\ln\left(\frac{T}{T-1}\right)\right]^{-1} \qquad \text{Eqn (3.6.6)}$$

The observed flows were plotted against y_T .The same procedure was carried out on the peak discharges for various selected return periods computed by the HEC-HMS. The initial discharge values were based on the initial parameter estimates and they were subsequently adjusted

to align them with the observed. The reduced variate y_T for the computed peak discharges were computed using the Equation 3.6.6 but the value of T was the selected return period based on the assumption that the peak discharges have the same recurrence interval as the input design rainfall depths used for their computations. Having been satisfied with the adjusted HEC-HMS results these were also compared with peak discharges (for various return periods) computed using the Regional Maximum Flood (RMF) and the rational method. The data were then fitted with straight lines for better comparison.

Table 3.6.10 shows the adjusted parameters after conducting the second phase. The CN number was the one manipulated because the discharge volume computed is highly sensitive to the CN as was confirmed by the relative sensitivity computed (see Section 3.7). It was observed that the CN values obtained in the first phase were about 2% higher than the ones obtained in the second phase. Table 3.6.11 shows the data used for plotting the graphs in Figure 3.6.12, which shows the comparison of, computed peak discharges with observed peak flows for the Baynesfield station. A similar approach was conducted for the Mlaas stream gauge station.

Station	**Input Parameters From First Calibration Phase**			**Adjusted Input Parameters From Second Phase**		
	CN	Lag Time (minutes)	I_a (mm)	CN	Lag Time (minutes)	I_a (mm)
U6H002	66	114	14	65	114	14
U6H003	62	127	16	60	127	16

Table 3.6.10: Parameter adjustments for calibration gauges during the second phase

Rank	Peak Flow	T	y_T
1	362.3	33.67	3.501
2	203.3	12.63	2.495
3	84.4	7.77	1.982
4	75.0	5.61	1.628
5	71.3	4.39	1.353
6	38.4	3.61	1.125
7	29.1	3.06	0.927
8	19.5	2.66	0.751
9	17.8	2.35	0.589
10	16.1	2.10	0.439
11	14.1	1.91	0.296
12	13.7	1.74	0.158
13	12.1	1.60	0.023
14	11.3	1.49	-0.112
15	11.1	1.38	-0.249
16	10.6	1.29	-0.392
17	10.1	1.22	-0.545
18	8.7	1.15	-0.718
19	8.6	1.09	-0.930
20	7.9	1.03	-1.257

Plotting Observed flows using Cunnane Plotting Position

Selected T	Variate y_T	HEC-HMS CN = 66	HEC-HMS CN = 72	RMF	Rational
2	0.4	40.5	50.62	95	19
5	1.5	105.9	128.96	244	54
10	2.3	183.1	218.69	338	106
20	3.0	275.6	313.13	558	185
50	3.9	441.9	506.02	745	445
100	4.6	604.3	680.36	880	796

Plotting Positions for Various Return Period using Reduced Variate

Table 3.6.11: Observed and Computed Peak Flows data for various return period for U6H002 (Baynesfield)

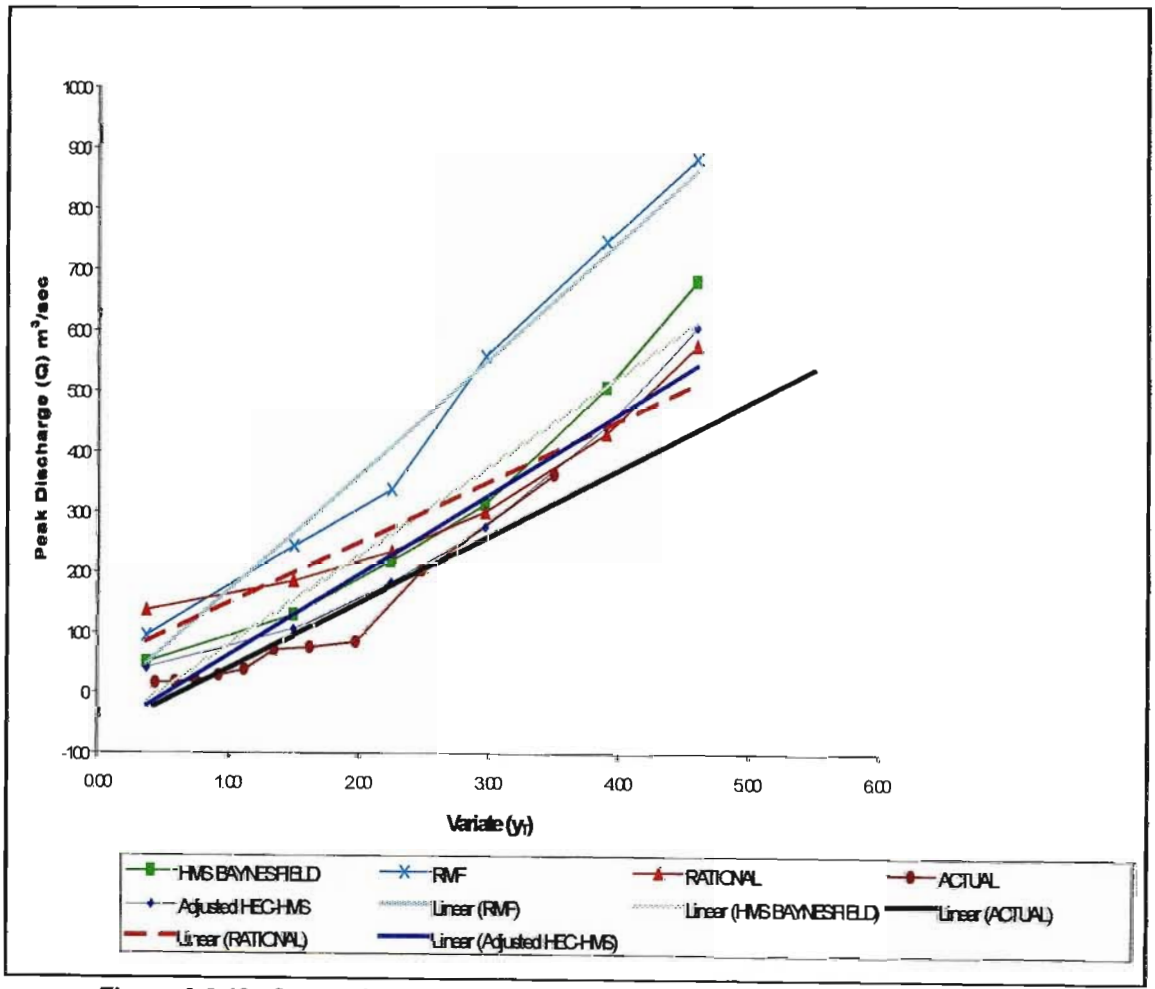

Figure 3.6.12: Comparison of Computed Peak Discharges with observed peak flows

3.6.11 Summary of calibration procedure

Based on the limited amount of historical data available for calibration purposes, the model is generally correctly predicting the peak discharge. However the model calculates high peak flows which were not recorded by the stream gauges.

The calculated peak flows are deemed justified because the radar rainfall images (not included in the dissertation) reflected that at those times there were heavy storms that occurred. Furthermore, the statistical validation using 20 historical monthly flow peaks provides confidence that peak flows of such magnitude are likely for those catchments. Although the peak discharges from HEC-HMS computed with an adjusted CN value of 65 were approximate to the observed the peak discharges, eventually used were those obtained from a CN value of 72 which is a 10% increment to cater for errors. The whole catchment was then calibrated by a constant shift of the land use category to evenly increase the CN value across the catchment. The next section discusses the sensitivity analysis of the HEC-HMS model.

3.7 Model Sensitivity Analysis

The simulated results require verification to determine that they agree reasonably with related analyses and expected results. The general procedure to sensitivity analysis involves the input of various parameter variables to the model and subsequently carrying out runs and recording computed results. The relative sensitivity (S_R) of parameters is defined as the percentage change in model results divided by the percentage change in parameter value. This is applied in the context of the Mlazi Catchment as a consistent measure for the comparison between parameters.

The sensitive analysis was carried out to the HEC-HMS (hydrological) model using a representative subcatchment (U60a) located at the upstream part of the Mlazi catchment. The procedure involved variation of one input parameter whilst keeping other variables and parameters constant. The varied input parameters are:

- Rainfall distribution (*special case*)
- Physical parameter such as the initial abstraction (I_a), SCS curve number (CN) and Time of concentration
- Variation of the storage/flow relationship in Channel Routing using the Modified puls method.

The SCS curve number CN 's sensitivity analysis is the one discussed in this section because the variation of the curve numbers has a great impact on the computed peak discharges. Table 3.7.1 contains the range of the selected SCS curve numbers (CN) (based on soil type and land use) and the computed peak discharges (Q_{peak}) together with the relative sensitivity (S_R). The relative sensitivity indicates some consistency in the changes of the peak discharge relative to the change in the curve number. Figure 3.7.1 show plots of the curve number versus the peak discharge for the U60a quaternary catchment. Based on the plot it is evident that there is near linearity between the curve number and the computed peak discharges.

CN	Q_{peak} (m^3/sec)	%ΔCN	%ΔCN	SR = $\%\Delta Q_{peak}/\%\Delta CN$
72	680.36	2.78	3.79	1.37
70	654.55	2.86	3.87	1.36
68	629.19	2.94	3.96	1.35
66	604.28	3.03	4.05	1.34
64	579.83	3.13	4.14	1.32
62	555.84	3.23	4.24	1.31
60	532.30	3.33	4.34	1.30
58	509.22	3.45	4.45	1.29
56	486.57	3.57	4.56	1.28
54	464.37	3.70	4.69	1.27
52	442.60	3.85	4.82	1.25

Table 3.7.1: Relative Sensitivity Analysis for Curve Number (CN) and Peak Discharge

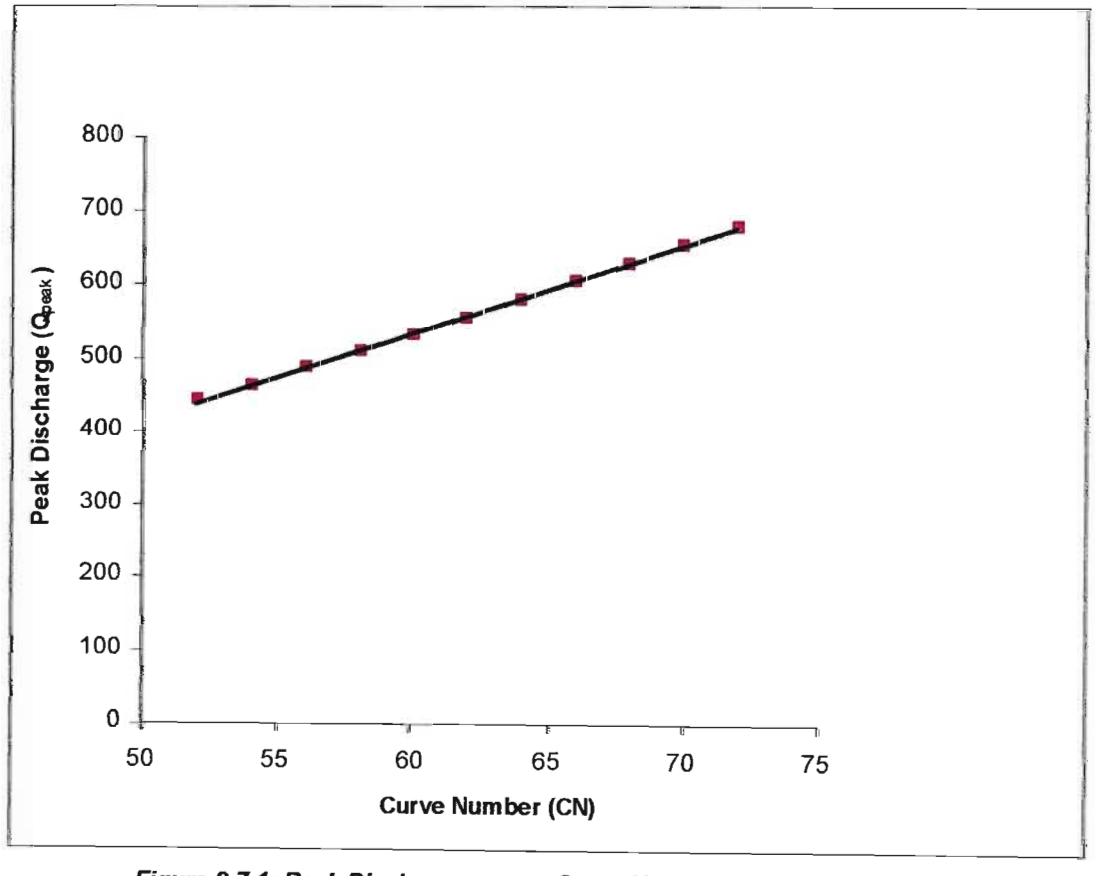

Figure 3.7.1: Peak Discharge versus Curve Number

3.8 HEC-HMS RESULTS

The HEC-HMS output result shown in Figure 3.7.2 represents the hydrographs at the entrance to the canal. The hydrograph in red represents the outflow from the Shongweni Dam whereas the small grey peak represents the hydrograph due to the cumulative subcatchments (Mlaz-1-17) downstream of Shongweni Dam. The hydrograph in blue is the sum of the red and grey hydrographs. The sum is approximately equal to the red hydrograph indicating that there is insignificant contribution of runoff by the subcatchments downstream of shongweni. This observation implies that the outflow hydrograph at the outlet of shongweni is a good estimate of the magnitude of the hydrograph at the entrance to the canal. This observation is a justification for the proposed location of the streamgauge and forecasting system at the outlet of Shongweni dam for the flood warning of the industries such as SAPREF and Mondi located at the flood plain around the canal.

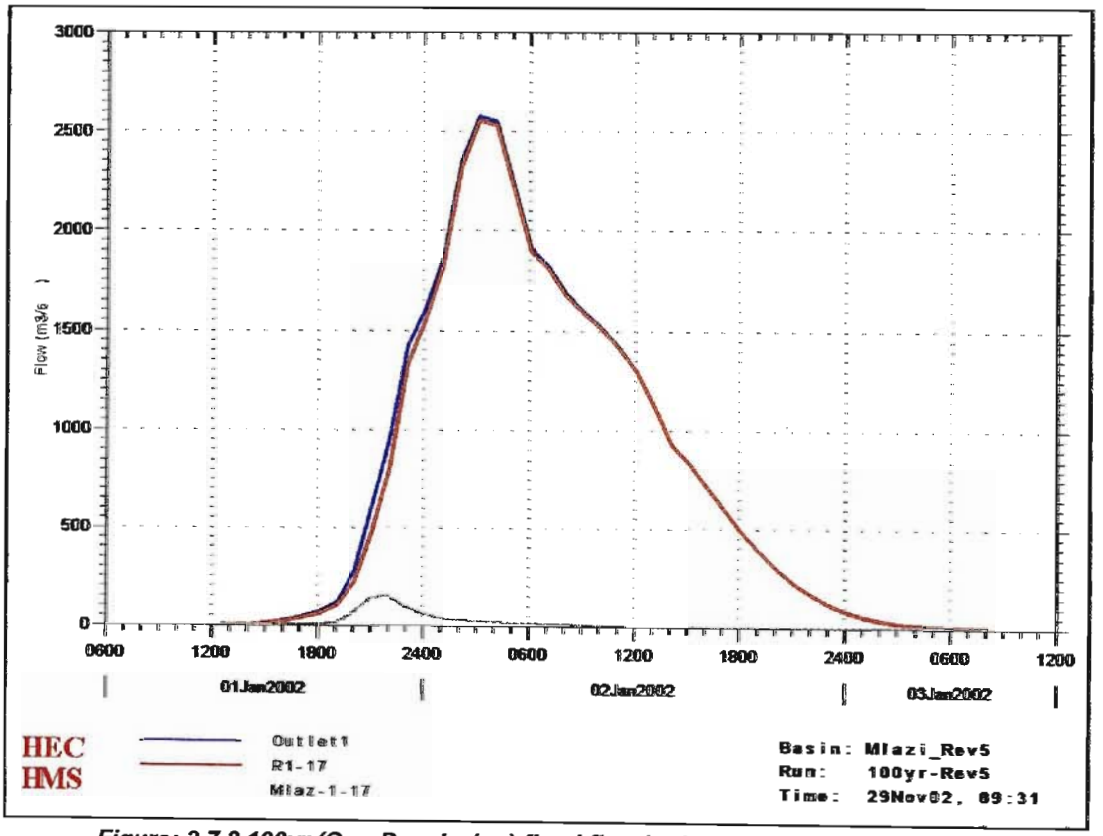

Figure: 3.7.2 100yr (One-Day design) flood flow hydrograph at outlet

The results shown in Figures 3.7.3a-c show hydrographs at the entrance to the canal for various arrangement of the three-day design rainfall. The LMH combination gives a peak value of approximately 3800 m^3/sec, the MHL gives a value of 3200 m^3/sec and the HML gives a peak discharge value of approximately 2200 m^3/sec.

Figure 3.7.4 shows the inflow to the shongweni dam and the shongweni storage capacity above a datum level of 298 m. The figure indicates that the peak discharge was initially attenuated at a flow of 1700 m^3/sec. When the dam reached a capacity of 5100 m^3 above the datum level of 298m the attenuation effect ceased. Shongweni Dam has a less peak flow attenuating effect for flows of a magnitude greater than 1700 m^3/sec.

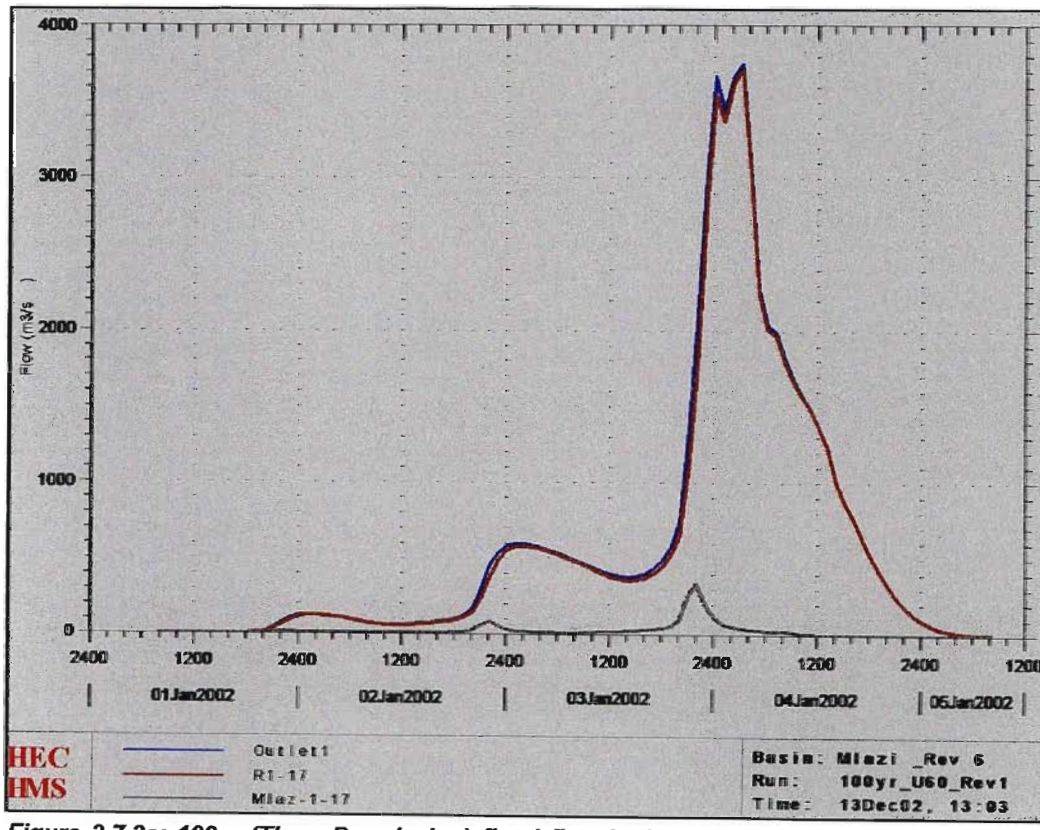

Figure 3.7.3a: 100yr (Three-Day design) flood flow hydrograph at inlet to canal (LMH)

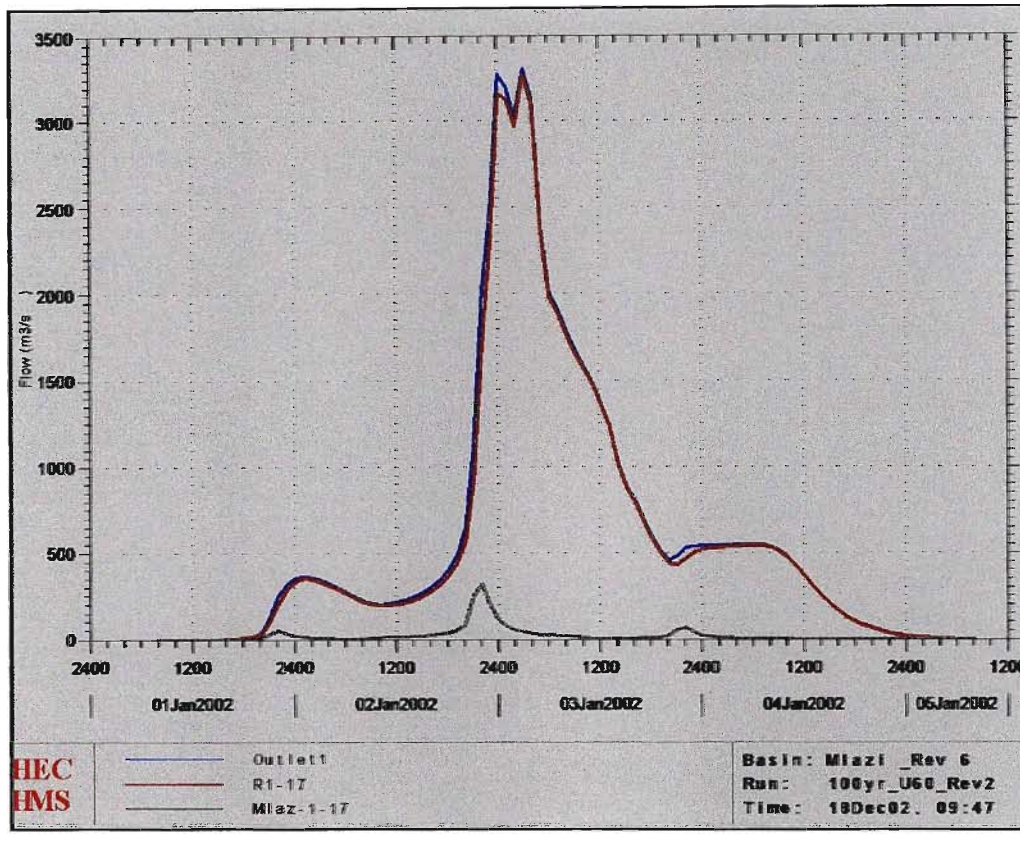

Figure 3.7.3b: 100yr (Three-Day design) flood flow hydrograph at inlet to canal (MHL) HEC-HMS Output Note difference in scale.

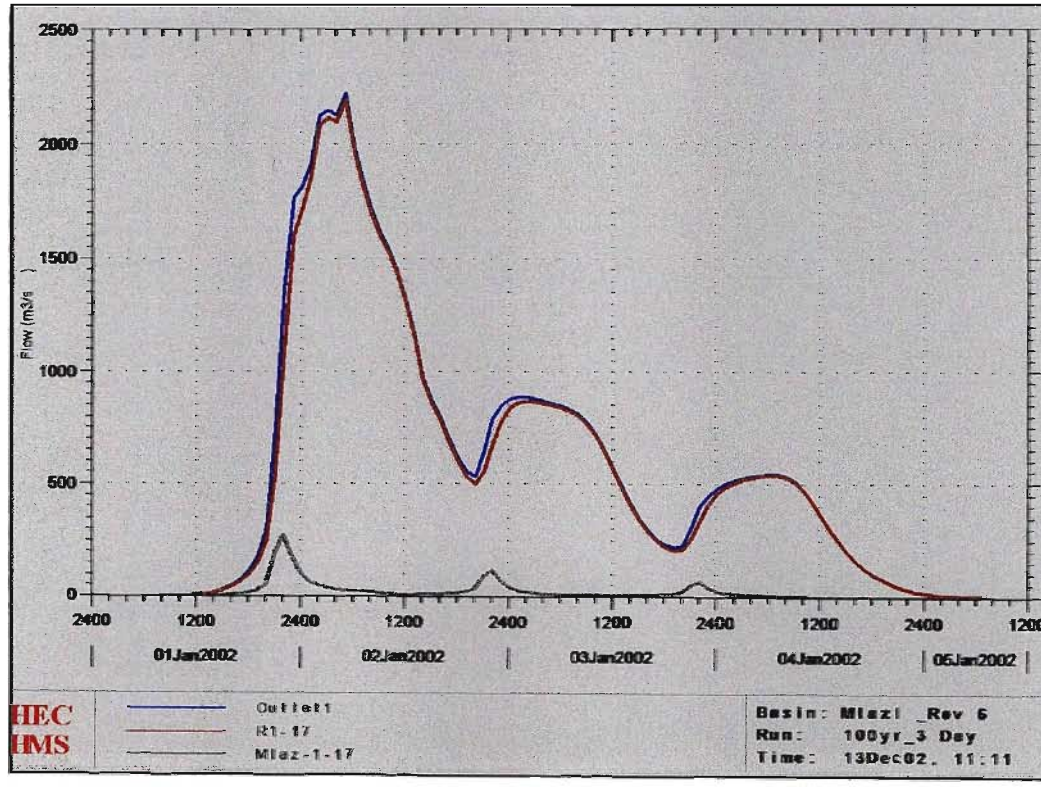

Figure 3.7.3c: 100yr (Three-Day design) flood flow hydrograph at inlet to canal (HML)

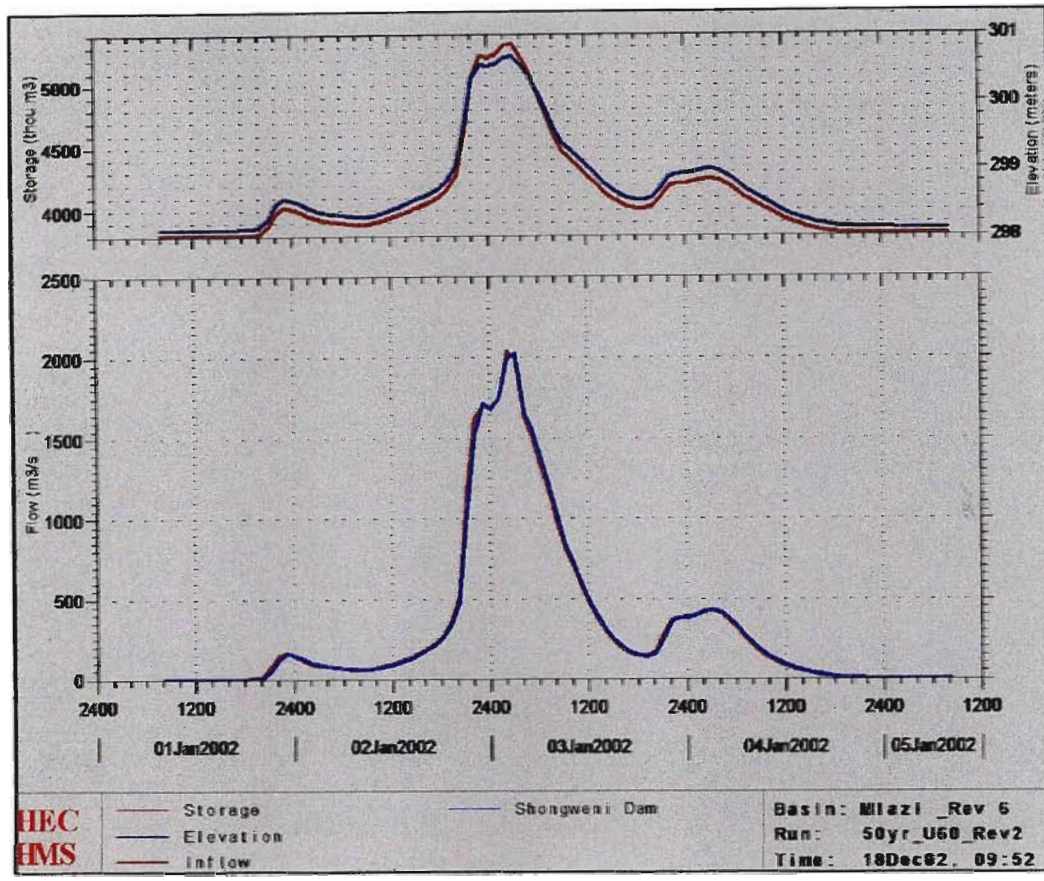

Figure 3.7.4: 50yr (three-day design) flood flow hydrograph at Shongweni (MHL)

Summary

The calculated peak flows are deemed justified because the radar rainfall images (not included in the dissertation) reflected that at those times there were heavy storms that occurred. Furthermore the statistical validation using 20 historical monthly flow peaks provides confidence that peak flows of such magnitude are likely for those catchments. Although the peak discharges from HEC-HMS computed with and adjusted CN value of 66 were approximate to the observed the peak discharges, those eventually used were those obtained from a CN value of 72 which is a 10% increment to cater for errors. The whole catchment was then calibrated by a constant shift of the land use category to evenly increase the CN value across the catchment.

The above results indicate that using the final adjusted parameters and based on the limited amount of calibration data, the model can, on average, predict the magnitude of the peak discharge with reasonable

accuracy. Therefore the parameters obtained are to be set as default until more reliable historical data becomes available. The output and input data for the HEC-HMS model was the applied for the parameter fitting of the Mlazi Meta Model and subsequently the output peak discharges were used as input to the HEC-RAS river model for the computation of levels of inundation.

4. HYDRAULIC MODELLING AND INUNDATION LEVEL DETERMINATION

This chapter discusses the approach to determine the inundation levels for the Mlazi. The first section discusses the data processing for the HEC-RAS Model followed by the creation of the digital elevation model to be used for the set up of the river model using HEC-RAS software. In addition, the HEC-RAS model is described including the assumptions and algorithms applied in the context of modeling the Mlazi River. Furthermore, the river modelling procedure is divided into two sections since the hydraulic modelling was conducted in two stages based on the type of the channel and the selected simulation procedures. The first stage of the hydraulic modelling of Mlazi River was the modelling of the natural channel of the river. A steady state simulation was carried out for this portion of the Mlazi River. However, in order to prevent the HEC-RAS model from 'crashing' due to supercritical flow on steep reaches, the natural channel was divided into two sections at the Shongweni Dam resulting in the establishment of the Upper Mlazi and Lower Mlazi. The second stage of river modelling involved the unsteady simulation of the Mlazi canal. Although the intention of this study was to determine the levels of inundation of the Mlazi River, additional work was conducted in the canal hydrodynamics and also a flood damage assessment was carried out based on inundation in the simulated floodplains.

4.1 Data Processing for the HEC-RAS Model

The procedure for collection and processing of data used to set up the HEC-RAS model and input data was carried out similar to the procedure done for the HEC-HMS as described in Section 3.1.2. However the DEM and input data such as the Manning's n required verification. This was ascertained by fieldwork conducted, which provided the opportunity to capture measurement of hydraulic structures such as the bridge and culverts required as input data.

4.1.1 The Creation of DEM for the Hydraulic Model

The DEM for the hydraulic model (HEC-RAS) needed to be more accurate in terms of the topographic data than the raster based DEM created for the HEC-HMS model. The reason being that this was the model where the floodplain and levels of inundation were delineated. During this study the portion of the Mlazi river modelled was the one within the eThekwini Unicity boundary. The first step

in this process involved the assembly of data of appropriate resolution (5 m resolutions for the Mlazi river) to create the TIN (Triangular Irregular Networks). The 2m contours proved to be adequate for this exercise. Various options for the capture of the terrain for the DEM were considered such as these listed below:

a) Collection of all available electronic 2m contour data. For areas where there was no electronic data, contours were captured from the 1:2000 orthophotos by means of scanning and digitizing carried out by the students at MLST.

b) Use of Airborne Laser Solutions (ALS) to survey the full river corridor (within the eThekwini Unicity boundary).

The relative costs of each option and benefits were evaluated and presented to the client for approval. The option chosen was (a), therefore students from MLST had to scan and digitise the contours for the section of river channel not covered by electronic data.

Triangular Irregular Networks "TIN's" were created using the Hard Breakline Input method. The TIN created covered the areas around the centerline of the river as far as the cross-sections were planned to extend. The centerline, cross sections and flowpath lines themes were produced using ArcView, which were used for the creation of the TIN's. These themes were digitized, attributed and created into the 3D DEM using AVR as functions. The land use layer was also included, which contained strings referring to specific land uses and were converted to Manning's 'n' values to represent resistance to flow. It should be noted that these were just initial estimates of the Manning's 'n' values, since field work had to be conducted to capture more realistic values as well as to conduct some ground 'truthing' for the HEC-RAS model produced. All themes created were overlaid onto the TIN and exported to the HEC-RAS in the form of ASCII files. Figure 4.1.1 shows part of the HEC-RAS model created from the DEM.

4.2 Hydraulic Modelling Using HEC-RAS

Having defined the peak flows at various points along the river channel for different flood events (see Chapter 3), the calculation of corresponding peak water levels in the river was performed using standard hydraulic computation methods through the creation and calibration of a river model. The hydraulic analyses also provide information on the flow regime in the river, including depths, velocities, erosion potential and bridge/culvert capacities. As well as delineating the floodplain area for planning and hazard warning purposes, this information therefore also provides an indication of critical areas in the river drainage system, which can lead to the identification of flood mitigation and damage reduction measures.

This section describes the hydraulic modelling methodology, whilst the results are included in tabular form in Appendix B. A qualitative discussion on the results generally, as well as in more detail for the critical areas, is provided in Chapter 6.

4.3 Description

The USACE's Hydrologic Engineering Centre River Analysis System (HEC-RAS v3.0) computer program was used to perform the hydraulic analyses.

The input to the program is:

- Steady/or unsteady Flow data (e.g. Flood Peak discharge values at strategic locations along the river channel)
- Geometric data (i.e. a geometric representation of the river system, including, Manning's coeffients, bridge and culvert structures).

The hydraulics and assumptions applicable to the Mlazi HEC-RAS model were obtained from hydraulic textbooks such as Chow (1959), Henderson (1966) and also the HEC-RAS (1997).

4.3.1 Assumptions

- The assumption of steady flow was valid for the Upper Mlazi and Lower Mlazi because it is characterised by steep, well-defined channels and the flow is frequently supercritical.
- The exception was in the lower canalised reach, where overtopping of the canal causes extensive inundation of the adjacent low-lying land. In

this instance, unsteady flow modelling was used to determine flood volumes; this process is described further in Section 5.4.

- Flow is gradually varied (this flow is non-uniform flow in which the depth, discharge and mean velocity along the length of the channel gradually varies along the length of the channel).
- Flow is one–dimensional (velocity is in direction of flow only).

4.4 Equations for Basic Profile Calculations

Water surfaces for steady state were computed from one cross section to the next by solving the Energy equation with an iterative procedure called the standard step method. The Energy equation is written in head form as:

$$Y_2 + Z_2 + \alpha_2 \frac{V_2^2}{2g} = Y_1 + Z_1 + \alpha_1 \frac{V_1^2}{2g} + h_e \qquad \text{Eqn (4.4.1)}$$

where: Y_1, Y_2 = depth of water at cross sections 2 and 1 (1 downstream of 2)
Z_1, Z_2 = elevation of the main channel inverts
V_1, V_2 = average velocity
α_1, α_2 = velocity weighting coefficients
g = gravitational acceleration
h_e = head loss between sections 2 and 1.

This formulation (computation in upstream direction) requires the flow to be subcritical.

The Saint Venant equations stated in Section 2.4.4 were applicable to the one-dimensional unsteady canal flow down stream of Mlazi as discussed in Section 5.4.

The energy head loss (h_e) between two cross sections is comprised of friction losses and contraction or expansion losses. The equation for the energy head loss is as follows:

$$h_e = L\overline{S_f} + C\left[\frac{\alpha_2 V_2^2}{2g} - \frac{\alpha_1 V_1^2}{2g}\right] \qquad \text{Eqn (4.4.2)}$$

where: L = discharge weighted reach length

$\overline{S_f}$ = Average friction slope between two sections

C = expansion or contraction loss coefficient.

4.4.1 Computation Procedure

The unknown water surface elevation at the upstream cross section was determined by an iterative solution of Equations 4.4.1 and 4.4.2. The computation procedure is as follows:

- Assume a water surface elevation Ws at the downstream cross section for computation of a subcritical profile (or upstream cross-section if a supercritical profile is being calculated).
- Based on the assumed water surface elevation, determine the corresponding total conveyance and velocity head.
- With values from the second step, compute Sf and solve Equation 4.4.2 for h_e.
- With values from the second step and third step, solve Equation 4.4.1 for WS2 = Y2 + Z2.
- Compare the computed value WS2 with the value assumed in previous step; repeat the first step through the last until the values agree to within (0.003 m), or the user defined tolerance.

4.5 Conveyance Calculations

The determination of total conveyance and the velocity coefficient for a cross section required that the flow be subdivided into units for which the velocity is uniformly distributed. The approach used in HEC-RAS was to subdivide flow in the overbanks areas using the input cross-section n-value break points (locations where n-value change) as the basis for subdivision. Conveyance was calculated within each subdivision from the following form of Manning equation (based on SI units):

$$Q = KS_f^{0.5}$$

$$K = \frac{AR^{2/3}}{n}$$

where: K = conveyance for subdivision

n = Manning's roughness coefficient for subdivision

A = flow area for subdivision (m^2)

R = hydraulic radius for subdivision (area/wetted perimeter,m).

The program summed up all the incremental conveyances in the overbanks to obtain a conveyance for left overbank and right overbank.

Friction loss evaluation: The friction slope (slope of the energy gradeline) at each cross section was computed from Manning equation as follows:

$$S_f = \frac{Q^2}{K}$$

Alternative expressions for the representative reach friction slope (S_f) in HEC-RAS are as follows:

- Average Conveyance Equation
- Average Friction Slope Equation
- Geometric Mean Friction Slope Equation
- Harmonic Mean Friction Slope Equation.

The Average conveyance slope equation was the one used for Mlazi and it is the default equation used by the program. The program also contains an option to select equations, depending on flow regime and profile type (e.g. SI, MI, etc). The Average conveyance slope equation is express as follows:

$$S_f = \frac{1}{2}\left[\frac{Q_1^2}{K_1} + \frac{Q_2^2}{K_2}\right]$$

4.6 Contraction and Expansion Loss Evaluation

Contraction and expansion losses in HEC-RAS are evaluated by the following equation:

$$h_c = C\left[\frac{\alpha_1 V_1^2}{2g} - \frac{\alpha_2 V_2^2}{2g}\right] \qquad \text{Eqn (4.6.1)}$$

where: h_c = Contraction and expansion losses

C = The contraction or expansion coefficient.

The program assumes that a contraction is occurring whenever the velocity head downstream is greater than the velocity head upstream. Likewise, when the velocity head upstream is greater than the velocity head downstream, the

program assumes that a flow expansion is occurring. Table 4.6.1 below shows typical 'C' values for subcritical flow contraction and expansion coefficient.

	Contraction	Expansion
No transition loss computed	0.0	0.0
Gradual transition	0.1	0.3
Typical Bridge sections	0.3	0.5
Abrupt transitions	0.6	0.8

Table 4.6.1a: Subcritical Flow Contraction and Expansion Coefficients (HEC-RAS, 1997)

Where the change in river cross section is small, and the flow is subcritical, coefficients of contraction and expansion are typically on the order of 0.1 and 0.3, respectively. The maximum value for the contraction and expansion coefficient is one (1.0). In general, the empirical contraction and expansion coefficient should be lower for supercritical flow. In supercritical flow the velocity heads are much greater, and small changes in depth can cause large changes in velocity head. Using contraction and expansion coefficients that would be typical for critical flow can result in over estimation of the energy losses and oscillation in the computed water surface profile.

4.6.1 Geometric data

The basic geometric data for the river channel was created by defining cross-sections and river station values. This information was abstracted from a digital elevation model (DEM) of the river catchment (see Section 4.1.1).

Additional pertinent information to complete the geometric data includes:

- Structure data (i.e. dimensions of bridges, culverts, weirs)
- Channel roughness (defined by the manning's 'n' coefficient)
- Loss coefficients (eg expansion and contraction).

This information was gathered during a field survey of the river undertaken in June 2002 as discussed in Section 4.6.2. Figure 4.6.1 shows the geometry plan modelled for the downstream part of Mlazi River (redline) starting from the Shongweni dam to the entrance to the canal. The cross sections (greenlines) drawn are numbered starting from down stream going upstream.

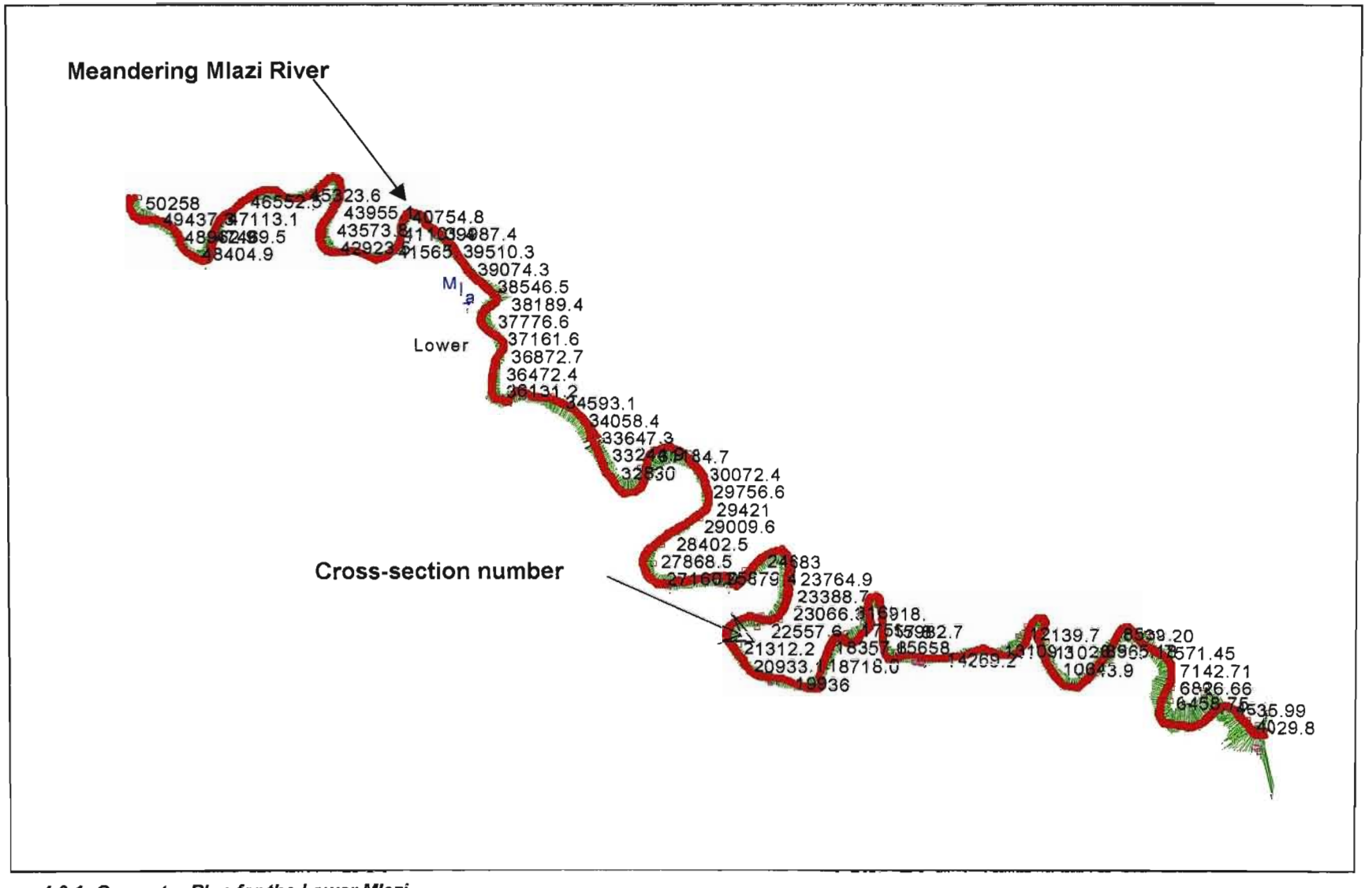

Figure 4.6.1: Geometry Plan for the Lower Mlazi

Figure 4.6.2 shows a typical cross section for a selected river station just close to the canal entrance, the cross sectional data which includes, the Manning 'n' station and elevations were entered using the cross section editor. The figure also shows the corresponding photo of the vegetation cover for the river station.

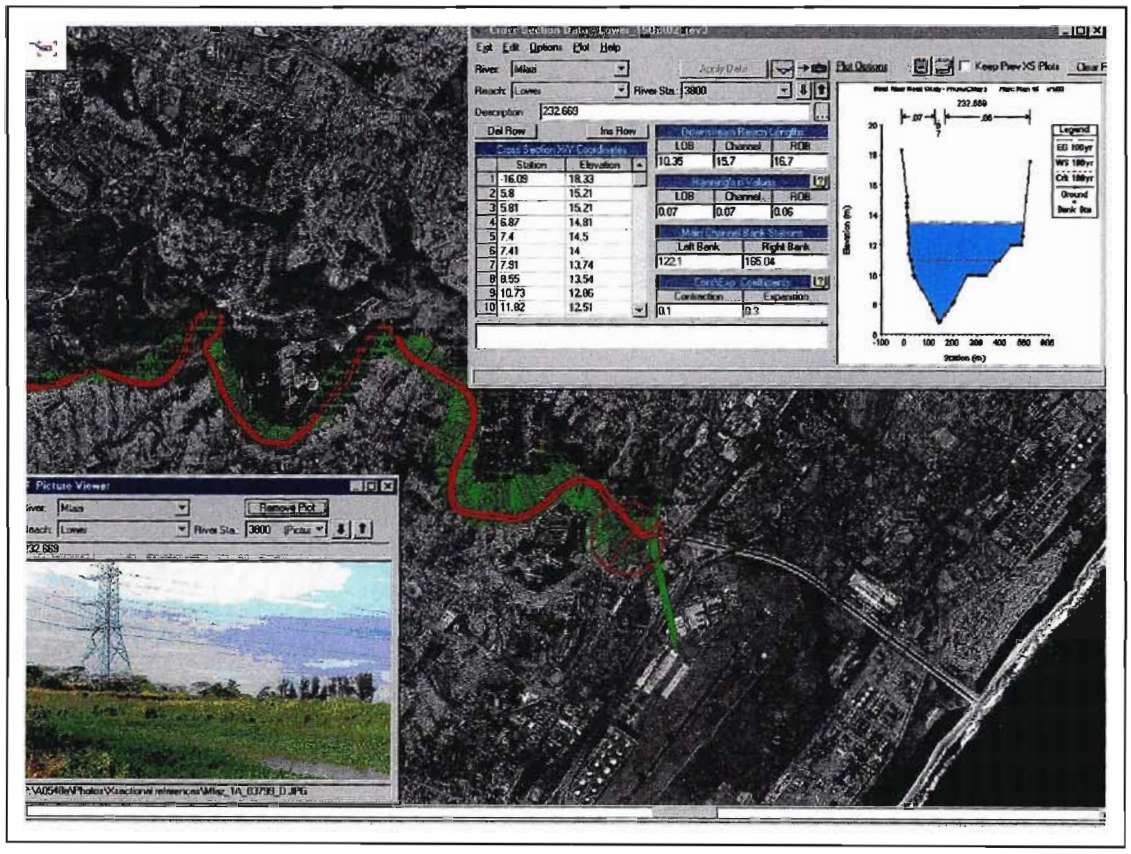

Figure 4.6.2: Typical Cross-sectional data for Mlazi River

Figure 4.6.3 below shows the longitudinal plot of the Mlazi River downstream of Shongweni. The Mlazi River is generally steep with an average slope of 0.01. and it experiences supercritical flows. However there exist minor drop in the surface bed at certain river stations, which cause rapids and critical flows as will be displayed by the results in Appendix B.

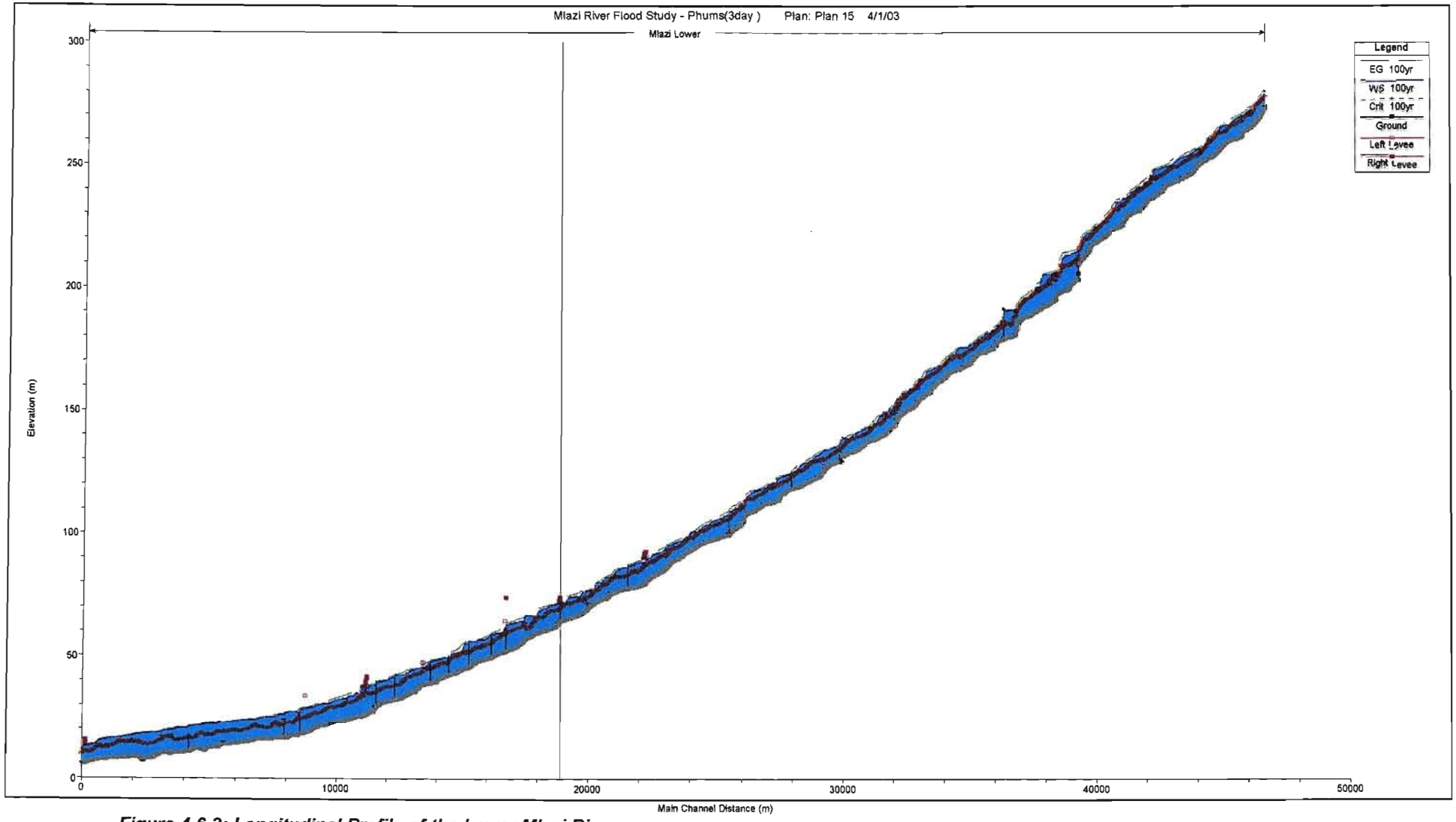

Figure 4.6.3: Longitudinal Profile of the Lower Mlazi River

4.6.2 Field Survey

The field survey of the Umlazi was essential for data acquisition for instance the capturing of Manning's roughness coefficients, hydraulic structural data such as dimension and location of bridges and culverts, channel cross-sections, vegetation cover and water flow depth.

It should be noted that there are also empirical methods, which have been developed for the estimation of channel roughness coefficients. These methods are based on factors such as the following:

- The type and size of the materials that compose the bed and banks of the channel
- The shape of the channel.

Cowan (1956) used these factors to develop a procedure for estimating Manning's 'n' suggesting:

$$n = (n_b + n_1 + n_2 + n_3 + n_4)m \qquad \text{Eqn (4.6.1)}$$

where: n_b = base value of n for a straight, uniform, smooth channel in natural materials

n_1 = a correction factor for the effect of surface irregularities

n_2 = a value for variations in shape and size for the channel cross section

n_3 = a value for obstructions

n_4 = a value for vegetation and flow conditions

m = a correction factor for meandering of the channel.

Another approach to determine the Manning's 'n' values as was developed by Limerinos (1970). Limerinos related 'n' values to hydraulic radius and bed particle size bed on samples from 11 stream channels having bed materials ranging from small gravel to medium size boulders. The Limerinos equation is expressed as follows:

$$n = \frac{(0.8204)R^{1/6}}{1.16 + 2.0\log\left(\frac{R}{d_{84}}\right)} \qquad \text{Eqn (4.6.2)}$$

where: R = hydraulic radius, in meters

d_{84} = the particle diameter in meters that equals or exceeds the diameter of 84 percent of the particles (passing a chosen sieve size).

The survey was furthermore conducted as a way of 'ground truthing' i.e. confirmation that the models produced by the digital elevation model (DEM) are a good approximation and representation of the Mlazi Catchment. Photographs of the river cross-sections, hydraulic structures together with the riverbanks were also captured as validation of the state of the river and for incorporation into a database at the office of the City of Engineer in Durban. The procedure for the fieldwork conducted for Mlazi was similar to the one conducted for the Blue river study (Limerinos, 1970).

4.6.3 Capturing of Manning's Roughness Coefficient

The capturing of the Manning's roughness coefficient during field survey was conducted based on a consensus of a consortium of four field researchers. The procedure required visual observation, judgement and experience. The process involved assessment of the vegetation cover on the left and right overbanks, streambed condition in terms of the bedding (sandy or rocky streambed) and water depth. Table 4.6.1 contains Manning's values ascribed to various main channels and flood plain characteristics.

Item	Channel Description	Normal Value
1	**Main Channel : man-made**	
	a. Concrete canal	0.018
	b. Concrete canal with sand/gravel on bottom	0.020
	c. Mattress lining canal sides	0.022
	d. Mattress lining on canal sides, with grass/shot bush	0.030
	e. Earth bank canal with thick vegetation growth	0.035
2	**Main Channel : natural**	
	a. Clean, straight, full, no deep pools, few weeds ,sand bottom	0.030
	b. As above, but more stones and weeds	0.035
	c. Clean, winding, some pools and shoals	0.040
	d. As above, but with some stones and weeds	0.045
	e. As above, but with more stones	0.050
	f. Sluggish reaches, deep pools, weedy	0.070
3	**Flood Plains (i.e. Overbank Areas)**	
	a. Short grass, no bush	0.035
	b. Long grass, no bush	0.040
	c. Scattered bush, thick weeds	0.050
	d. Thick reeds	0.060
	e. Medium bush, no trees	0.070
	f. Dense bush, a few trees	0.100
	g. Trees with dense bush between	0.150

Table 4.6.1.b: Roughness Coefficients (Chow, 1959)

These were used during the field survey to identify the Manning's coefficients associated to various riverbed characteristics. The ascribed values for the Mlazi river model (HEC-RAS) were compared with the U.S.G.S photo produced by Arcement and Schneider (2001) as reference for selection of appropriate Manning's coefficients. This process is essential especially because the Manning's equation is most sensitive to uncertainty of the Manning's 'n' as proven by first order analysis of the Manning's equation explained in Section 2.5. A great effort was therefore applied to the selection of the Manning's roughness coefficients because it reduces the uncertainty significantly. A

demonstration of the identification of various Manning's coefficient based on the survey photographs is shown in Figure 4.6.5a-d. *Note that the photographs on the right are the ones representing Mlazi where the ones on the left are standard photographs from USGS (Arcement and Schneider,2001).*

As a matter of interest, the field investigators became so skillful at estimating the 'n' value in the field that they could look at picture of a calibrated section of the river and estimate with considerable accuracy the hidden 'n' value.

The published guides for selecting Manning's roughness coefficients for natural channels and floodplains are such as the one produced by Arcement, and Schneider (2001) for the United States Geological Survey Water-supply (U.S.G.S) papers (2339) and paper (1849). The U.S.G.S (paper 2339), which presents two methods applied to determine the roughness coefficients of floodplains. The first method involves the evaluation of the effects of certain roughness factors in the flood plain. The second method involves the evaluation of the vegetation density of the floodplain to determine the 'n' value. This second method is particularly suited to handle roughness for densely wooded floodplains. In this paper reference is made to other authors who have suggested values for Manning's 'n' such as Chow (1959), and Henderson (1966). In addition to contribution by these authors, the HEC-RAS (1997) also contains a table of Manning's 'n' values for various channels. This guide emphasises the significance of selecting the Manning's 'n' with values with reference to the accuracy of the computed water surface profiles.

n=0.03	Description		
Site	**Vegetation Cover**	**Stone Size and Sand**	**Channel Description**
Main Channel	Few Weeds	Sand bottom	Clean straight pool,no deep pools
Flood Plain	Short grass, no bush		

n=0.035	Description		
Site	**Vegetation Cover**	**Stone Size and Sand**	**Channel Description**
Main Channel	More Weeds	Sand bottom with more stones, gravel bed with boulders. d_{50}=175mm	straight pool, no deep pools
Flood Plain	Short grass, no bush		

Figure 4.6.5(a): Manning's Roughness Coefficients Estimated from Photos (Photos on Left are USGS, on Right are from Mlazi)

n=0.04	Description		
Site	**Vegetation Cover**	**Stone Size and Sand**	**Channel Description**
Main Channel	Clean	Gravel bed with boulders. d_{50}=265mm	Winding with some pools
Flood Plain	Long grass, no bush		

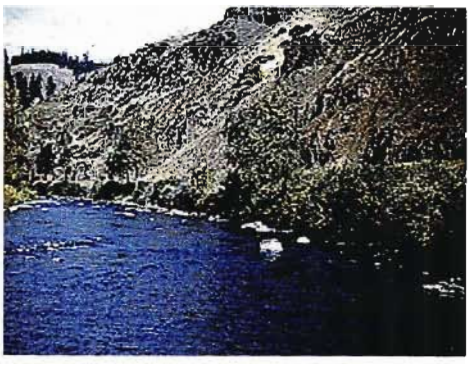

n=0.045	Description		
Site	**Vegetation Cover**	**Stone Size and Sand**	**Channel Description**
Main Channel	weedy	Gravel bed with some stone and boulders. d_{84}=285mm	Winding with some pools
Flood Plain	weedy		

Figure 4.6.5(b): Manning's Roughness Coefficients Estimated from Photos (Photos on Left are USGS, on Right are from Mlazi)

n=0.05	Description		
Site	**Vegetation Cover**	**Stone Size and Sand**	**Channel Description**
Main Channel	More weed	Gravel bed with more stones, gravel bed with boulders. d_{50}=175mm and d_{84}=375mm	Winding with some pools
Flood Plain	Thick weed, scattered bush		

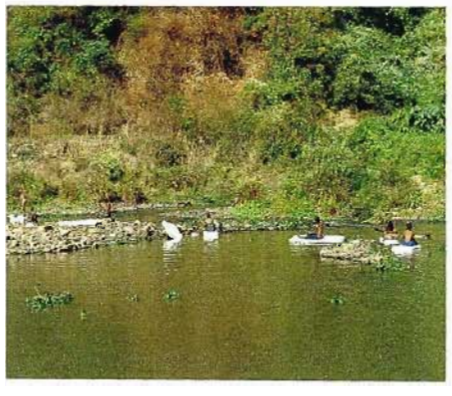

n=0.06	Description		
Site	**Vegetation Cover**	**Stone Size and Sand**	**Channel Description**
Main Channel	More weed	Gravel bed with more stones, gravel bed with boulders. d_{84}=375mm	Winding with 1.5m deep pools
Flood Plain	Thick reeds		

Figure 4.6.5(c): Manning's Roughness Coefficients Estimated from Photos (Photos on Left are USGS, on Right are from Mlazi)

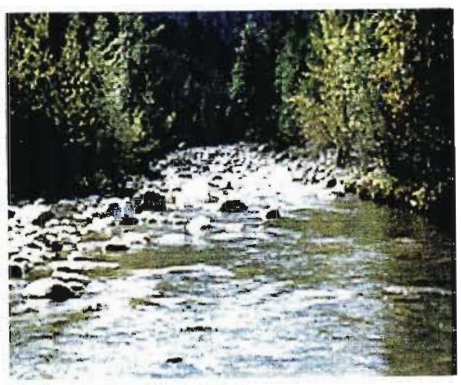

n=0.07	Description		
Site	**Vegetation Cover**	**Stone Size and Sand**	**Channel Description**
Main Channel	very weedy	Gravel bed with more stones, gravel bed with boulders. d_{84}=415mm	Sluggish reaches, 2m deep pools
Flood Plain	Medium bush with no trees	Banks with boulders	

Figure 4.6.5(d): Manning's Roughness Coefficients Estimated from Photos (Photos on Left are USGS, on Right are from Mlazi)

Note that the above picture for the Mlazi differs from the one from the USGS yet it conforms to the description given by Chow (1959) since it shows weedy deep pools. The USGS photo however shows boulders of with size of the magnitude stated in the description probable the lack of weeds might have been due to the season during which the photo was taken.

Hydraulic Structures Survey

Hydraulic structures such as the bridges and culverts, which cross the Mlazi River, were surveyed and the survey data was captured using field survey forms. The data was input into HEC-RAS and was also stored in a database form consistent with the GIS. The structural data captured during fieldwork was verified where possible by the record drawings obtained from the eThekwini Municipality City Engineers. Appendix A shows photographs of some of the bridge structures captured during the fieldwork. It is evident from the photographs that most of these structures have decks that are quite high in elevation in comparison to the likely flood elevations. The piers (and debris caught on them) are therefore the most likely obstruction to flow and cause of any backwater effect.

4.6.4 Steady flow modelling

The peak discharges for different design flood events were routed through the geometry model of the river using HEC-RASv3.0. The flows were input at various HEC-RAS river stations corresponding to the HEC-HMS junction points. Table 4.6.2 shows the flow-input data. The program checks for both subcritical and supercritical profiles and accounts for backwater effects at bridges and structures. A maximum water surface level envelope is thus produced for each design event, and these are exported to Arcview for plotting as floodlines. Further evaluation of the results is carried out to assess the capacity of bridge structures and tendency for flooding at particular locations. This is discussed further in Chapter 6.

Sub-catchment		HEC-HMS Basin Junction	Stream gauge Station	Peak Discharge For Various Return Periods							HEC-RAS River Station No.
Quaternary Catchment Name	HEC-HMS Ref. No.			Q_{2yr} (m^3/s)	Q_{5yr} (m^3/s)	Q_{10yr} (m^3/s)	Q_{20yr} (m^3/s)	Q_{50yr} (m^3/s)	Q_{100yr} (m^3/s)	Q_{200yr} (m^3/s)	
U60a	Maz 1-0	J1-0	Baynesfield	60	157	259	377	583	778	1009	-
U60b	Maz 1-1	J1-1		107	315	547	781	1186	1588	2332	-
	Maz 1-2a	J1-2a	mlaas	142	394	637	929	1477	2025	1046	-
U60c	Maz 1-2b	J1-2		139	399	645	981	1704	2398	950	84062 (u)
	Maz 1-3 Maz 2-0	J1-3		137	384	618	907	1600	2348	4155	72053 (u)
	Maz 1-4 Maz 3-0	J1-4		139	386	621	913	1609	2361	4028	70711 (u)
	Maz 1-6 Maz 4-0	J1-5		140	388	624	914	1614	2368	3989	69964 (u)
	Maz 1-6 Maz 5-0	J1-6		139	383	616	894	1595	2363	4009	64160 (u)
	Maz 1-7 Maz 6-0	J1-7		140	383	615	888	1506	2302	4024	55658 (u)
	Maz 1-8 Maz 14-1 Maz 7-4	J1-8	Shongweni	254	495	729	992	1620	2653	4729	50258 (L)
U60d	Maz 1-9 Maz 16-0	J1-9		247	481	710	991	1632	2653	4402	44744 (L)
	Maz 1-10 Maz 17-0	J1-10		249	484	715	996	1647	2656	4263	39862 (L)
	Maz 1-11 Maz 18-0	J1-11		252	490	723	1000	1653	2666	4273	39355 (L)
	Maz 1-12 Maz 19-0	J1-12		254	494	728	1003	1656	2669	4269	38221 (L)
	Maz 1-13 Maz 20-0	J1-13		256	498	735	1008	1654	2685	4299	33227 (L)
	Maz 1-14 Maz 21-0	J1-14		254	494	730	1010	1661	2670	4329	24254 (L)
	Maz 1-15 Maz 22-0	J1-15		247	484	728	1016	1573	2680	4405	7867 (L)
	Maz 1-16 Maz 23-0	J1-16		249	488	732	1021	1580	2732	4184	6226 (L)
	Maz 1-17	Outlet	Outlet	248	490	737	1028	1589	2751	4126	3567 (L)

Table 4.6.2: HEC-RAS Input Flow data for Steady State Analysis

4.6.5 Hydraulic Computations Through the Bridge

Though it has being noted that they were very few bridges crossing the Umlazi River, these bridges were analysed using HEC-RAS by application of various methods without changing the bridge geometry. The bridge information was obtained during fieldwork as already mentioned above. The bridge routines have the ability to model low flow and weir flow (with adjustment for submergence on the weir), pressure flow (orifice and sluice gate equations), pressure and weir flow.

4.6.6 Hydrodynamic modelling

The steady flow analysis approach described above cannot be used to determine flood volumes associated with a design flow hydrograph. This limitation is not of concern for the majority of the Mlazi River, where there are no significant off-channel storage areas. The exception is at the Mlazi Canal, where under high flow conditions, overtopping occurs, causing inundation of the adjacent large flat area. In this instance, the unsteady flow facility in HEC-RASv3.0 was used to determine the volume of water that is likely to be spilled during a design flood event. From this volume it was thus possible to estimate the depth of the ponding in the adjacent low-lying area. The hydrodynamic modelling procedure is described in detail in Chapter 5.

Generally, a further important requirement for unsteady modelling is the incorporation of tidal effects at the outlet of a river to the sea. In the case of the Mlazi River, however, the base of the channel invert at the outlet is higher than the spring tide, therefore no effect on upstream water levels.

Calibration

Calibration of the hydraulic model could not be carried out to any detailed degree due to the limited availability of observed data from historical flood events. The sensitivity analysis was conducted for the Manning's coefficient as discussed in Section 5.6.

Summary

The hydraulic model (HEC-RAS) was created using the Digital Elevation Model (DEM) to define the terrain cross-section along the streams, and hydraulic structures such as culverts and brides were incorporated into the model. The roughness coefficients and boundary conditions were added to the program manually after having conducted field survey to determine the appropriate values to be used. Flow data for the computation of levels of inundation were obtained from the HEC-HMS model. The levels of inundation for the natural channel of Mlazi river were simulated under the one dimensional steady state analysis whereas the levels of inundation for the canal were simulated under unsteady flow analysis.

The inundated levels will be displayed online (based on forecasts) and/or offline at the eThekwini Metro Disaster Management Center using GIS software.

5. MLAZI CANAL HYDRODYNAMIC ANALYSIS

5.1 Introduction

This chapter provides a brief description of the modelling procedures adopted for the Mlazi canal. It furthermore gives an overview of flood conditions in the lower canalised section of the Mlazi River.

This canalised portion of the river was analysed separately due to the nature of overtopping of the canal and the sensitive nature of the surrounding land use. The analysis of the canal was conducted under unsteady state conditions using the HEC-RAS program. Off channel storages were introduced to monitor the lateral flow spilling over the canal during over topping.

5.2 Background

5.2.1 Historical Background

The canal was constructed in the mid-1950s by the Department of Transport. Its purpose was to deviate the Mlazi River away from the site of the new Louis Botha Airport (Durban Airport). Details of the deviation canal are provided below:

- Total length = 3769m
- Bottom width = 65m
- Top Width = 73m
- Depth = 4.6m
- Parapet Wall Height = 0.9m
- Longitudinal slope = 1 in 879.

Along much of its length the floor of the canal is elevated slightly above the natural ground level.

The canal was originally designed for a maximum discharge of 1806m^3/, (subsequently the capacity has been re-estimated at more like 1200m^3/s) which was almost double the previous highest flood peak recorded in 1917. Despite this, the canal has been subject to overtopping on two occasions, in May 1959 and September 1987 (Campbell *et al*, 1988). Embankment failure as a result of

localised stormwater erosion has also caused flooding of the adjacent low-lying areas on two further occasions (DWAF, 1988).

In addition to creating land for the new airport, the draining of the Mlazi lagoon attracted industries. The SAPREF oil refinery (in the early 1960s) and the Mondi paper factory (in the early 1970s) were constructed on the south and north banks of the canal respectively. Both are below the level of the canal and were subsequently inundated during the 1987 floods.

5.2.2 Previous Reports

Due to the sensitive nature of the adjacent land use, the Mlazi Canal has been the subject of numerous studies since the damaging floods of 1987:

- Campbell *et al* (1988) - report prepared for SAPREF
- DWAF (1988) - report prepared for Department of Transport
- GIBB Africa (1996) - report prepared for SAPREF.

The Campbell *et al* (1988) and DWAF (1988) reports both address the specific case of the September 1987 flooding and provide recommendations as to remedial works for the prevention of future flood damage. The DWAF report also provides information on the likely extent of flooding for various return period events. This took the form of flood inundation maps.

The purpose of the report by GIBB Africa was to review available literature, assess the flood risk that SAPREF is exposed to and identify protection schemes, ranging from flood protection bunds to flood warning telemetry systems.

5.3 Purpose of the Hydrodynamic Analysis

This investigation into flooding of the Mlazi Canal forms part of the floodline study for the entire Mlazi River. In this regard, therefore, the objective is to delineate the inundation levels for the 20-, 50- and 100 year return period events. It also affords an opportunity to review the recommendations from the earlier reports (listed in Section 5.2.2 above) in terms of inundation maps and flood protection measures in the light of the more recent estimates for design peak discharges. These new values were derived from a detailed catchment

modelling process that has been completed as part of the Mlazi River Flood Study.

The hydraulic modelling of the canalised section of the Mlazi River has been carried out separately from the rest of the river as it requires a different approach to be taken.

5.4 Methodology - one-dimensional unsteady flow modelling

A well-defined channel without extensive overbank areas can be modelled to determine floodlines using simple hydraulic analysis methods that assume flow is steady and one-dimensional. The natural sections of the Mlazi River can be modelled in this way, as can the canal up to its nominal capacity level. The assumption of one-dimensional steady flow is no longer valid, however, once the canal walls start overtopping.

Figure 5.4.1 below shows the HEC-RAS model of the Mlazi canal. The outlet to the sea of the canal cuts through the coastal dunes. The model is made up of cross sections, which are numbered starting from the sea to the entrance of the canal. The canal is about 3km long as shown by the cross section number at the entrance to the canal.

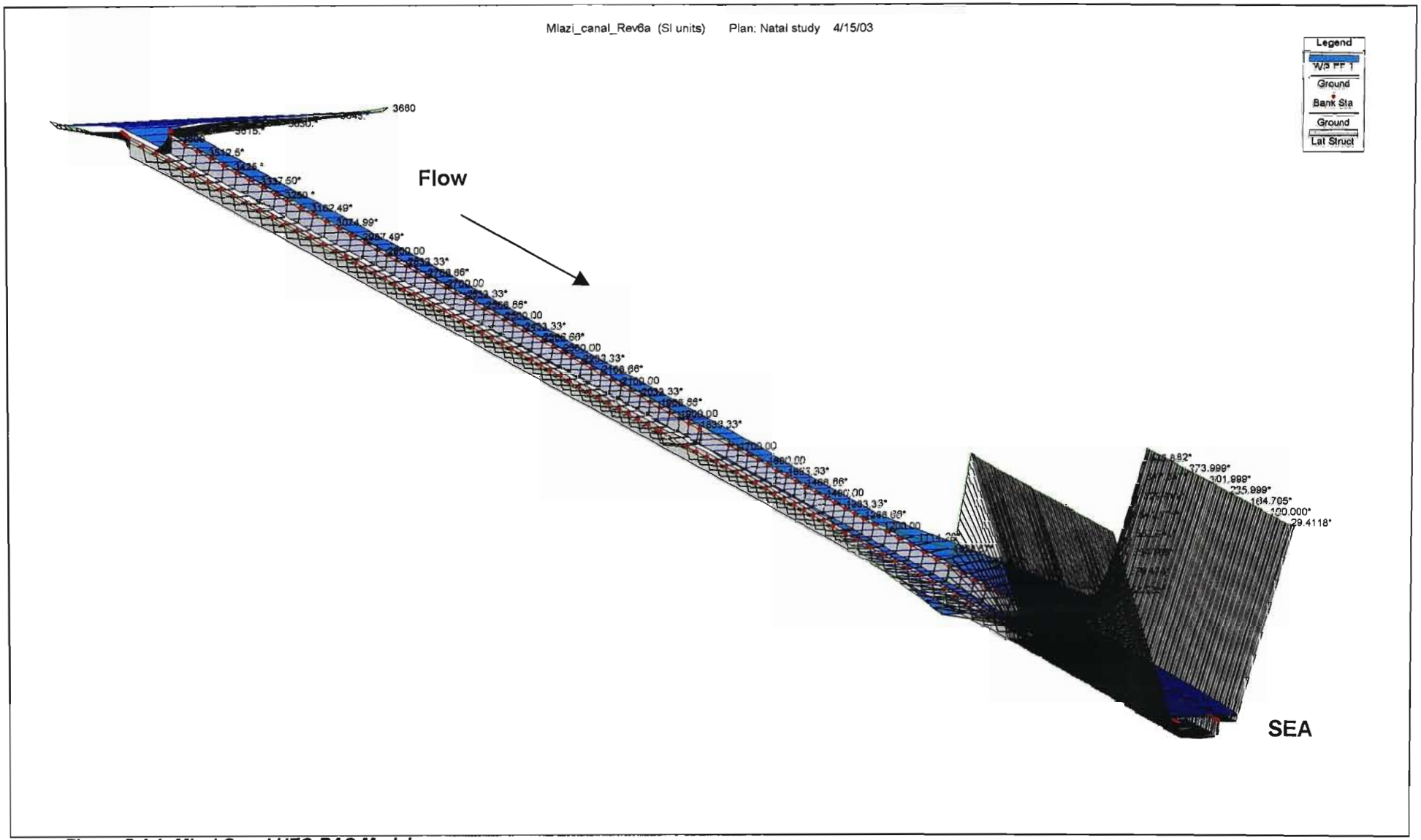

Figure 5.4.1: Mlazi Canal HEC-RAS Model

A typical cross-section through the canal is shown in Figure 5.4.2 to highlight the problem. Up until the water level reaches the top of the canal walls, flow can be considered as being perpendicular to the cross-section, i.e. into the page. This is the one-dimensional flow scenario. When water starts overtopping the canal walls, it does so in a lateral direction, i.e. perpendicular to the flow in the canal.

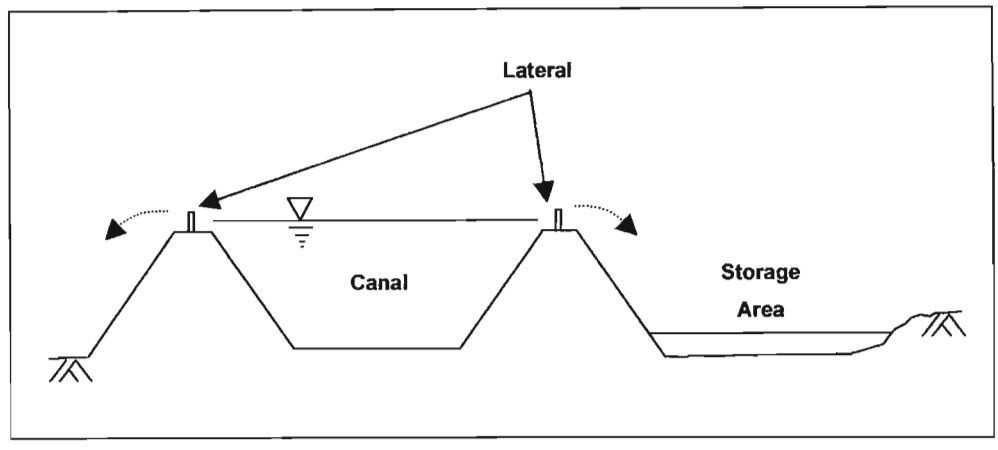

Figure 5.4.2: Canal modelling using Lateral Weirs and Storage Areas

An alternative option is to use the HEC-RAS one-dimensional model, but define the canal walls as 'lateral weirs' and connect these to 'storage areas'. The storage areas represent the low-lying flat land adjacent to the canal into which overspill water discharges. The quantity of water that flows over the lateral weirs depends on the shape and peak of the inflow hydrograph that is routed through the canal (this introduces the 'unsteady flow' component to the model). This inflow hydrograph is taken directly from the catchment runoff model.

The total volume of water that flows over the lateral weirs into the storage areas as well as the actual storage volume available determines the level to which the overspill water rises. This level can thus be defined as the floodline for the particular area.

A plan view of the storage areas that were defined is shown in Figure 5.4.3 Storage areas 1 and 2 are connected to the left bank of the canal and cover the airport runway approach and the Mondi area respectively. The area on the left bank of the canal is split because the SAPREF rail siding is on an embankment, which acts as a dam. A connection has however, been allowed for in the model

so that flow can pass from area 1 to 2 and vice versa through the underpass below the rail siding bridge over the canal.

Storage area 3 is connected to the right bank of the canal and covers the airport and SAPREF areas.

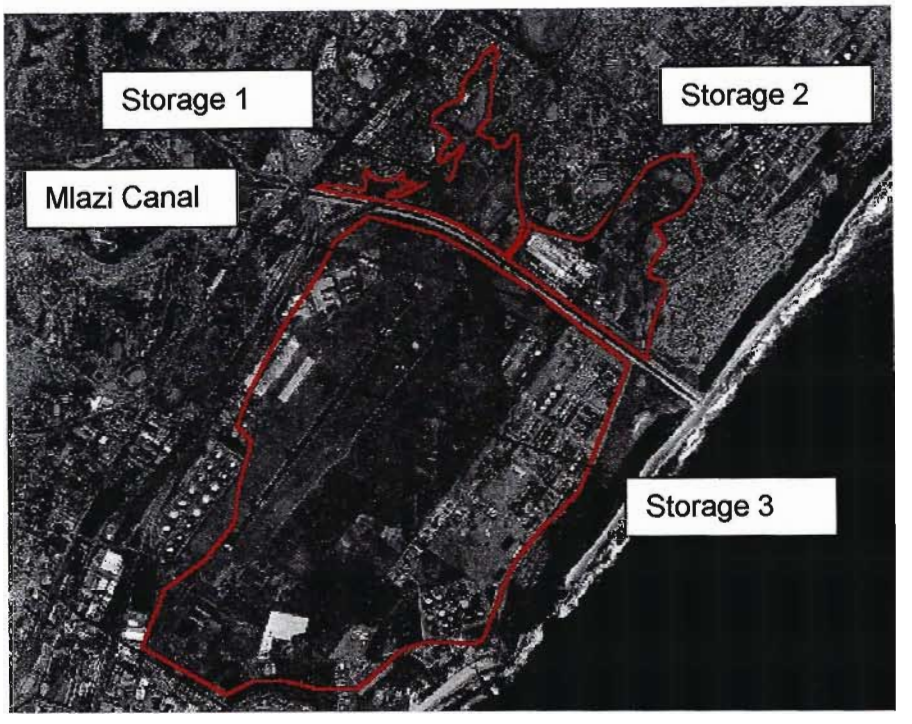

Figure 5.4.3: Storage areas used in Canal modelling

In fact, storage areas 2 and 3 should be allowed to drain to the sea in drains adjacent to the canal through the dunes cutting, as the water level builds up. It was, however, assumed that this outflow from the storage area system is far less than the inflow to the system (i.e. the overflow from the canal), and for our purposes could be ignored. This introduces a slight level of conservatism to the water level estimates in the storage areas.

Off-Storage Data Input

The volume elevation relationship used to define off-storage were obtained through the use of GIS techniques. The desired storages were mapped in ArcView then the surface areas at various elevations where captured for these storages. The volume changes at the selected elevations where computed and entered cumulatively to the storage editor. Below are the volume elevation relationships for the three storages.

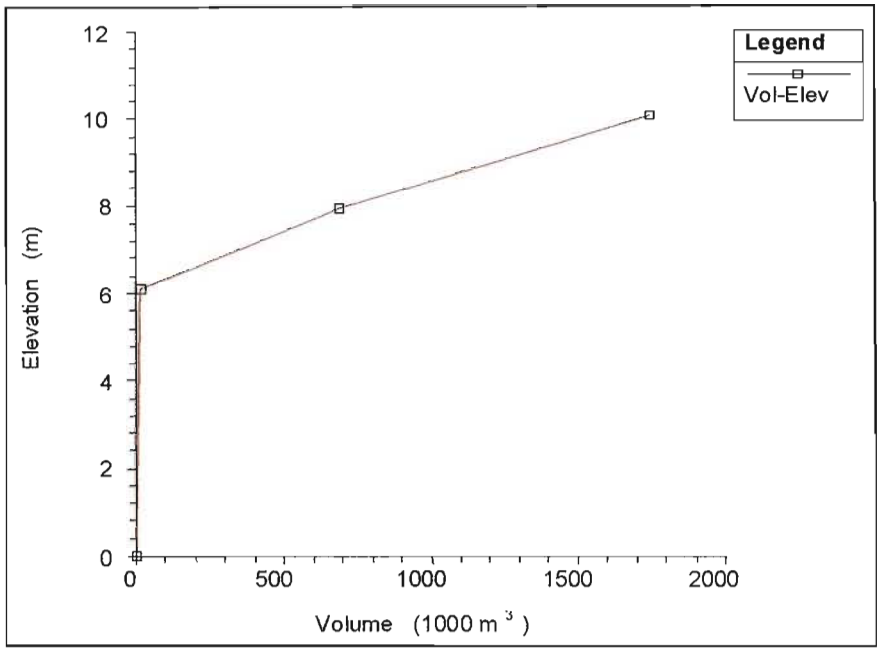

Figure 5.4.4 a: Volume Elevation relationship for Storage 1

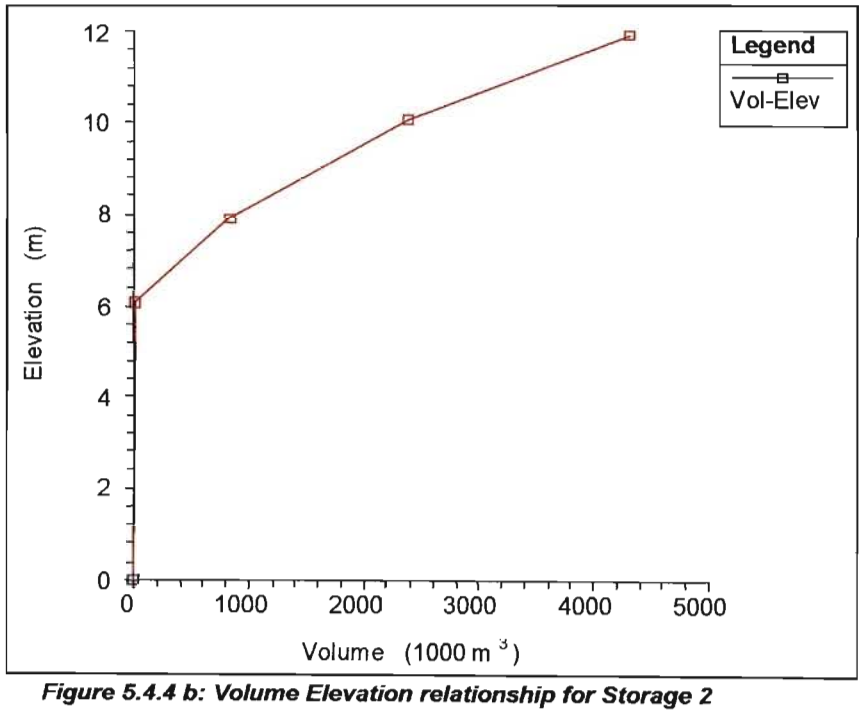

Figure 5.4.4 b: Volume Elevation relationship for Storage 2

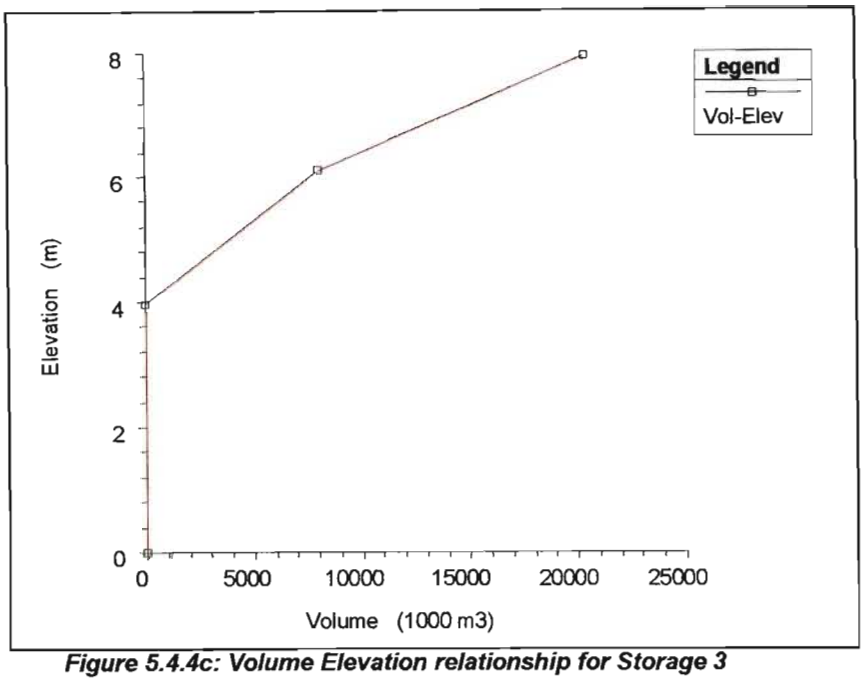

Figure 5.4.4c: Volume Elevation relationship for Storage 3

Lateral Weir Setup

Three Lateral weirs were positioned at the left and right overbanks of the canal. Figure 5.4.5a to 5.4.5c are elevations for the lateral weir connected to the respective storage. The connectivity of these weir to the storage is as stated; the lateral weir in Figure 5.4.4a was connected to the storage 3, the one shown in Figure 5.4.5b was connected to storage 1 and lastly the one in Figure 5.4.5c was connected to storage 2. The mentioned lateral weirs could be subdivided in order to improve the analysis of off-storage flow thereby applying the law of continuity for unsteady flow established by the consideration of the conservation of mass in an infinitesimal space between two canal sections, Chow (1959).

For instance if the canal had to feed laterally with an additional discharge of q' per unit length of the lateral weir, into a storage that was being flooded over then:

$$\frac{\partial Q}{\partial x}+\frac{\partial A}{\partial t}+q^{'}=0$$

where: $\partial Q/\partial x$ = the rate of change of discharge with distance

$\partial A/\partial t$ = the rate of change the elementary water cross section area with time

q' = the supplementary discharge per unit lateral weir.

Chow (1959) states that the continuity equations and dynamic equations for gradually varied unsteady flow derived by Saint-Venant are valid for use in analysis of this kind. However, owing to their complexity, exact integration of the equations is practically impossible therefore for practical applications a solution to these equations is obtainable through the approximate step methods.

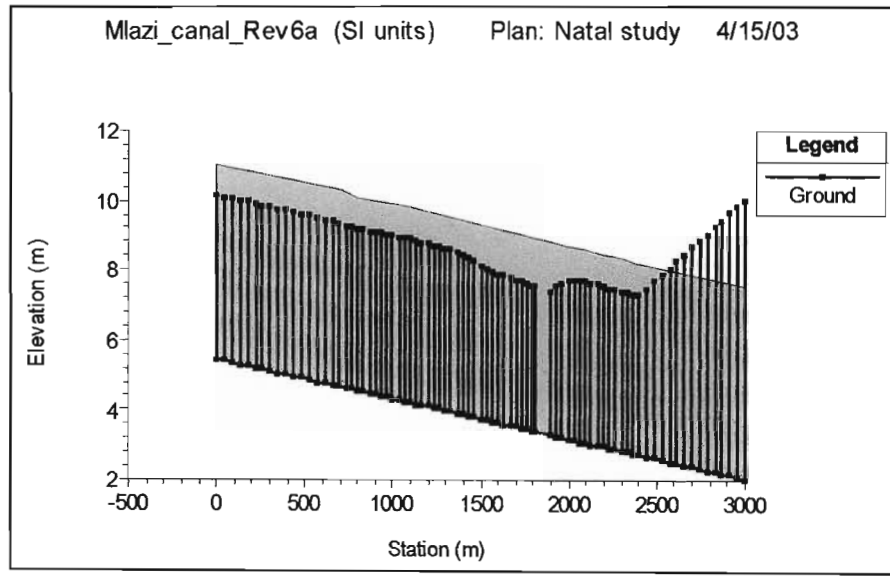

Figure 5.4.5a: Right overbank-Airport SAPREF-Lateral weir at RS3560.

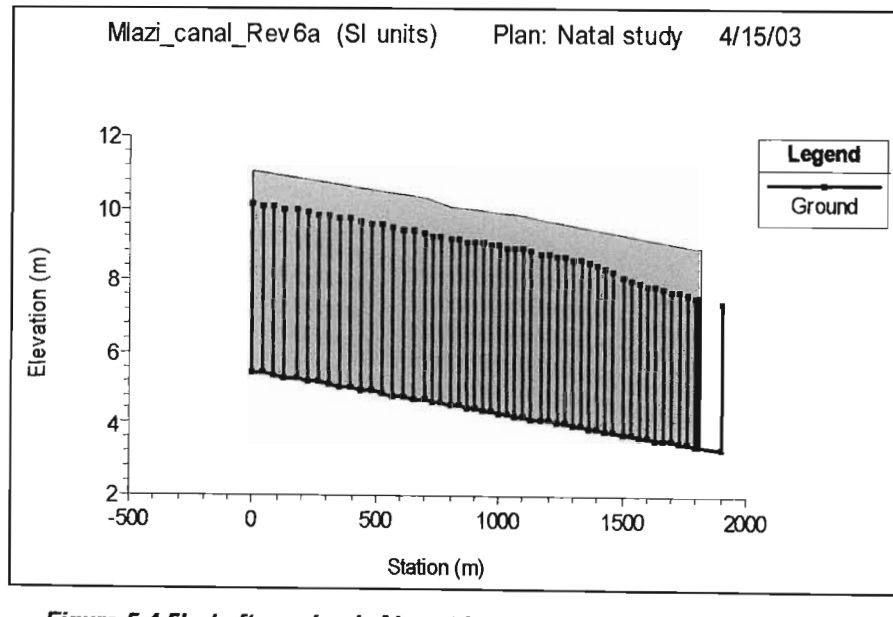

Figure 5.4.5b: Left overbank-Airport Lateral weir at RS3559

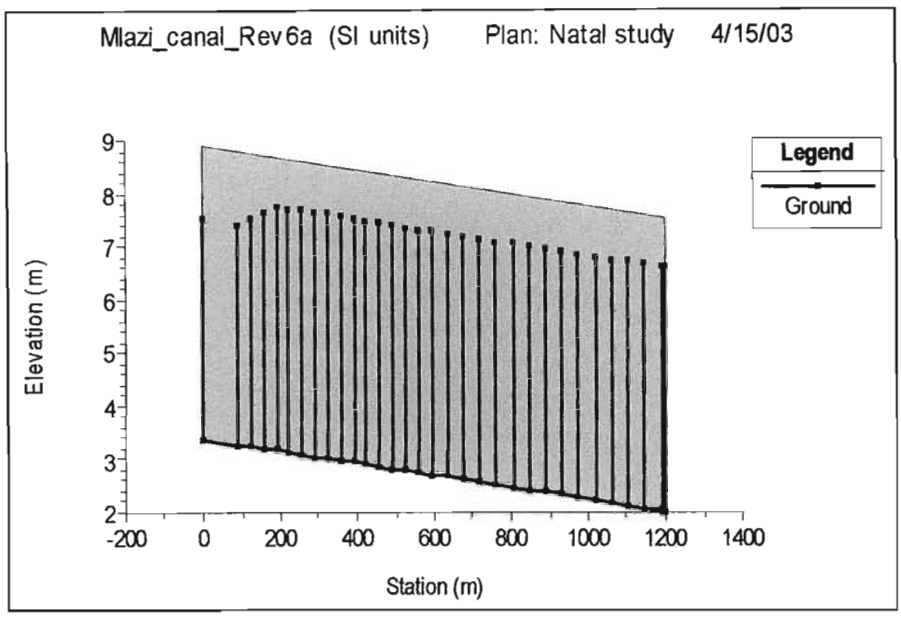

Figure 5.4.5c: Left overbank-Mondi Lateral weir at RS1750

Another hydraulic structure in the form of a weir was put in place as the hydraulic connection between storage 1 and storage two located at the SAPREF Bridge shown in Figure 5.4.5d.

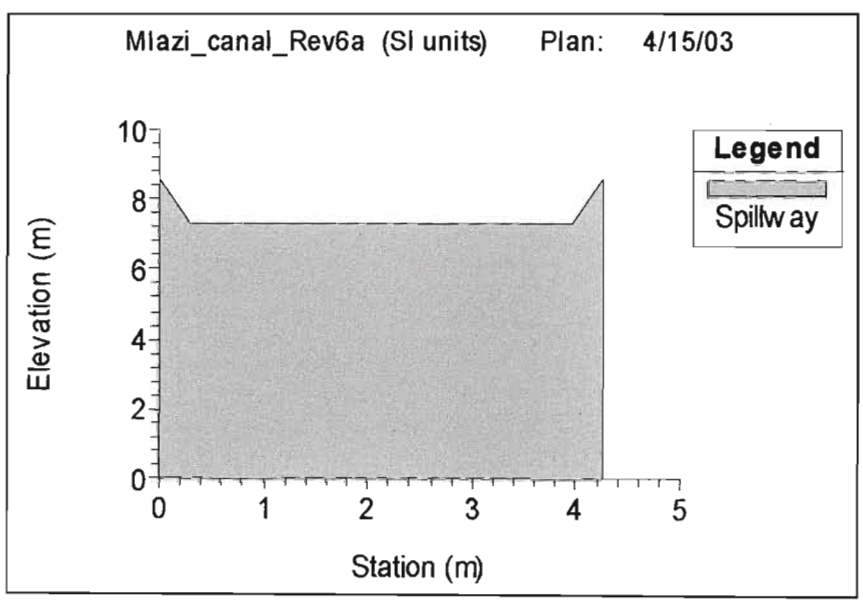

Figure 5.4.5d: SAPREF Bridge Underpass linking the storage 1 to storage 2

Having set up the geometry of the Mlazi canal, the Manning 'n' values for the canal had to be input and this was based on the type of the concrete lining used for the canal. The ranges of values of the Manning 'n' were obtained from Chow

(1959). The effect of the Manning's coefficient on the canal's capacity before overtopping occurs was conducted under sensitivity analysis

HEC-HMS Flow Input

The input hydrographs (Figure 5.4.6) were obtained from the HEC-HMS model. The hydrographs were of a one-hour time series and they represented the total inflow to the canal entrance. As a result they were input at the upstream part of the canal forming the upstream boundary condition and routed through to the downstream part. The downstream boundary condition type used was free overfall.

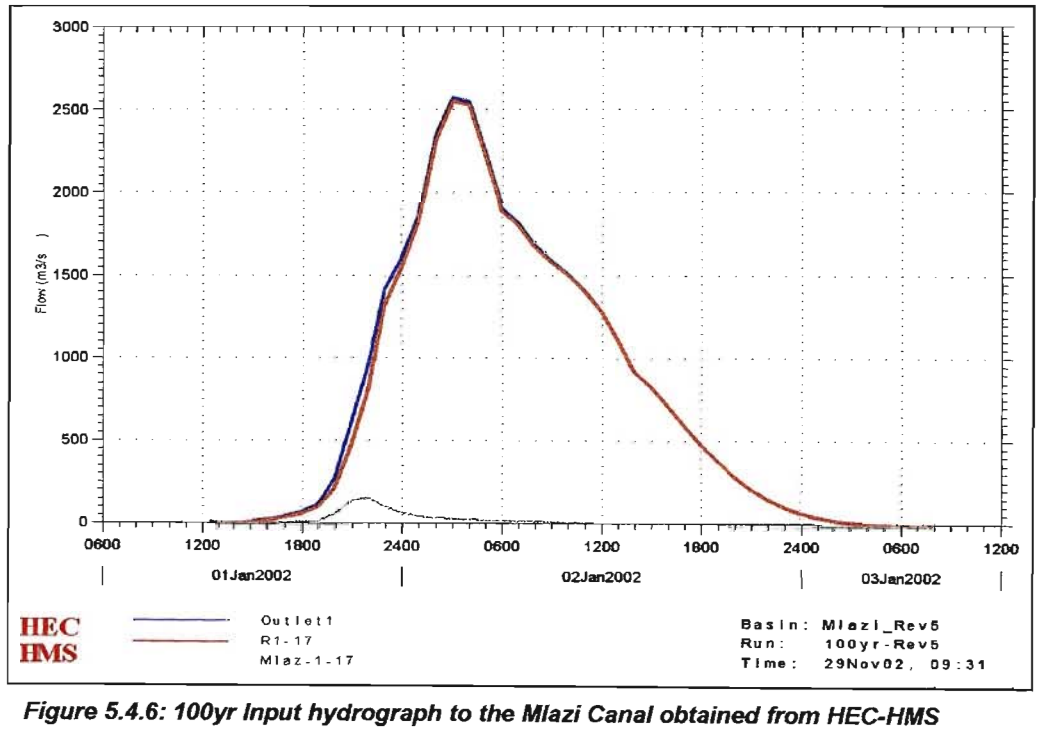

Figure 5.4.6: 100yr Input hydrograph to the Mlazi Canal obtained from HEC-HMS

The computations were carried out under unsteady state. The summary of the results is shown in Table 5.4.1.

5.5 Summary Results

The results from the unsteady flow simulations are shown in Table 5.4.1.

Storage Area Ref.	Description	Return Period	Storage Area Water Level (m MSL)	Volume spilled (m^3)
SA1	Airport approach	20yr	6.10	12 300
		50yr	6.58	191 900
		100yr	9.35	1 400 400
SA2	Mondi	20yr	6.10	12 300
		50yr	6.44	168 300
		100yr	8.13	984 900
SA3	SAPREF	20yr	3.96	1 200
		50yr	4.06	356 300
		100yr	6.31	9 464 100

Table 5.4.1: Floodline results for Canal overbank areas

The results indicate that the nominal capacity of the Canal is approximately equivalent to the flow associated with the 20-year return period flood event (from the above table, the volume of water that spills for this event is small). This means that the risk of overtopping occurring in the next 30 years is 79%.

For the 100-year design event, nearly 12 million cubic meters of water is estimated to spill from the Mlazi Canal. The risk of this widespread inundation occurs within the next 30 years approximately 26% computed by risk the formula:

$$R = 1 - \left(1 - \frac{1}{T}\right)^n$$

where: R = the risk of at least once exceedence of the inundation occurrence during the design life

T = the recurrence interval, and n the expected design life

(Chow et al, 1988).

The flood inundation areas determined from the levels shown in Table 5.4.1 compare closely to those estimated in the DWAF (1988) report.

One option regarding possible flood damage remedial works is to construct bunds around the SAPREF refinery. If this is carried out then there would be a reduction in available storage volume in the right overbank. This has the effect of raising the 100yr-flood level in SA3 by about 0.5m above that indicated in Table 5.4.1.

5.6 Sensitivity Analysis for the HEC-RAS Model

A approach similar to the one carried out for the HEC-HMS model was conducted with regard to the sensitivity analysis of the HEC-RAS model. The relative analysis for Mlazi river model was carried out with the intention of investigating how the water surface elevations in the main channel were being affected by a variation of the following parameters:

- Manning's 'n'
- Off-channel storage
- Steady and unsteady state analysis
- Channel geometry.

The Mlazi concrete canal and its surrounding floodplain were used for the sensitivity analysis. The 100-year design flow was used as the fixed input flow to the upstream part of the canal. The abovementioned parameters were varied independently and computations carried out.

5.6.1 Effect of Manning 'n' on the water surface levels

The selection of Manning' 'n' is an actual means of estimating the resistance to flow (Chow, 1959). The values of 'n' recommended for concrete canal depending on the method of lining range from 0.011 to 0.027. The range of 'n' values chosen for this analysis was from 0.017 to 0.027. The river model was then run under steady state condition and computations were also tried for the unsteady state, but it was later observed that the unsteady state and steady state analyses gave similar results for computations for cases whereby the canal was not over topping. Table 5.6.1 gives the relationship between the Manning 'n' and the computed water surface levels for a particular river station (RS 2900).

Manning'n	Water Surface Elevation (Ws)	%Δn	%ΔWs	Relative Sensitivity
0.015	10.72	13.33	2.71	0.203
0.017	11.01	11.76	3.18	0.270
0.019	11.36	10.53	2.73	0.259
0.021	11.67	9.52	2.66	0.279
0.023	11.98	8.70	2.42	0.278
0.025	12.27	8.00	2.20	0.275
Average				0.26

Table 5.6.1: Manning 'n' relative sensitivity analysis

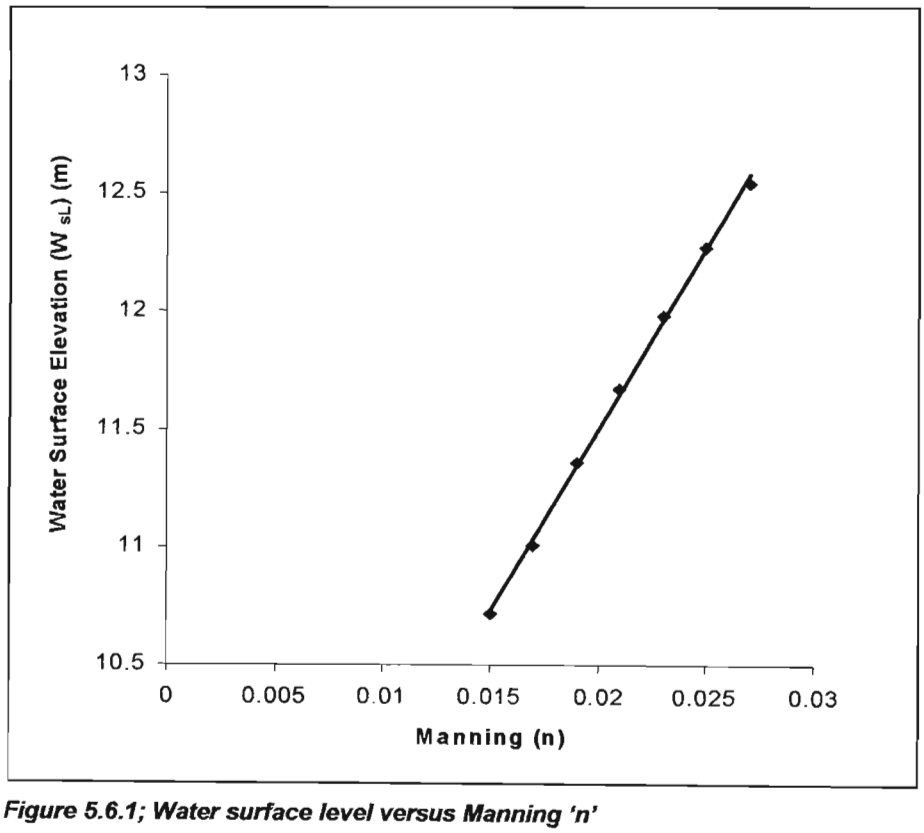

Figure 5.6.1; Water surface level versus Manning 'n'

Figure 5.6.1 shows that the water surface levels increase linearly with the Manning 'n'. The average relative sensitivity is 0.3, which implies that for an increment of 0.002 in the Manning 'n' value, the water surface level increases by a magnitude of 0.3. This is an analytical justification of applying a great effort to the selection of the Manning's coefficient as a measure to reduce uncertainty.

6. FLOOD INUNDATION ASSESSMENT

6.1 General

This chapter identifies those areas within the river system where flooding is problematic. The problems may be related to inundation of properties, overtopping of critical bridges or structures, or erosion damage.

An overview of the general characteristics associated with flooding in the river is given in Section 6.6, whilst in Sections 6.7 to 6.12, specific problem areas are discussed in detail. The process of analysing the hydraulic modelling results in this manner is important because, by understanding the reasons why inundation and damage occurs in certain areas, it is possible to identify which mitigation measures, if any, are suitable. Mitigation measures are only suggested in areas where the effects of flood damage are considered to be more severe.

6.2 Overview of Flood Characteristics

Much of the Mlazi River channel is narrow and well defined, with relatively steep banks. The only wide floodplain areas are in the lower 3km or so, where the river has been canalised. During flood conditions this area is prone to extensive inundation, but elsewhere, flooding generally consists of relatively minor overtopping of banks. Most of the flood related problems are therefore as a result of properties being located too close to the main channel (and thus being vulnerable during high flows).

The hazard rating contours that have been plotted in GIS indicate that along its entire length, the flow velocities and/or depths in the river are high. During floods, therefore, those areas that are affected by the river are subjected to flow conditions, which put human lives and infrastructure at risk.

The high hazard ratings also indicate that the erosion potential during flood conditions is high. Generally, however, the riverbanks are well vegetated, which limits the potential for erosion.

Other than the complex of structures near the entrance to the canal (including the N2, R102 and M4 road bridges, and a rail bridge), there are not many bridge structures across the Mlazi River.

6.3 Mlazi Canal, SAPREF/Merebank East

6.3.1 Description of problem

The Mlazi River is canalised in its lowest reach between South Coast Road and the outlet into the sea. The canal's capacity is about 1200 m^3/s, which is approximately equal to the 20yr return period. Peak floods of this magnitude and higher, therefore, cause inundation of the adjacent Mondi and SAPREF sites.

The extent to which overtopping occurs was investigated through an unsteady flow analysis of the canal as described in Section 5.4. This indicated that overtopping occurs, causing inundation of the surrounding area to depths of up to 3 m for the 100yr design event.

Overtopping also occurs at the canal entrance, causing some inundation of South Coast road and adjacent industries.

The 100yr floodline is indicated in Figure 6.3.1.

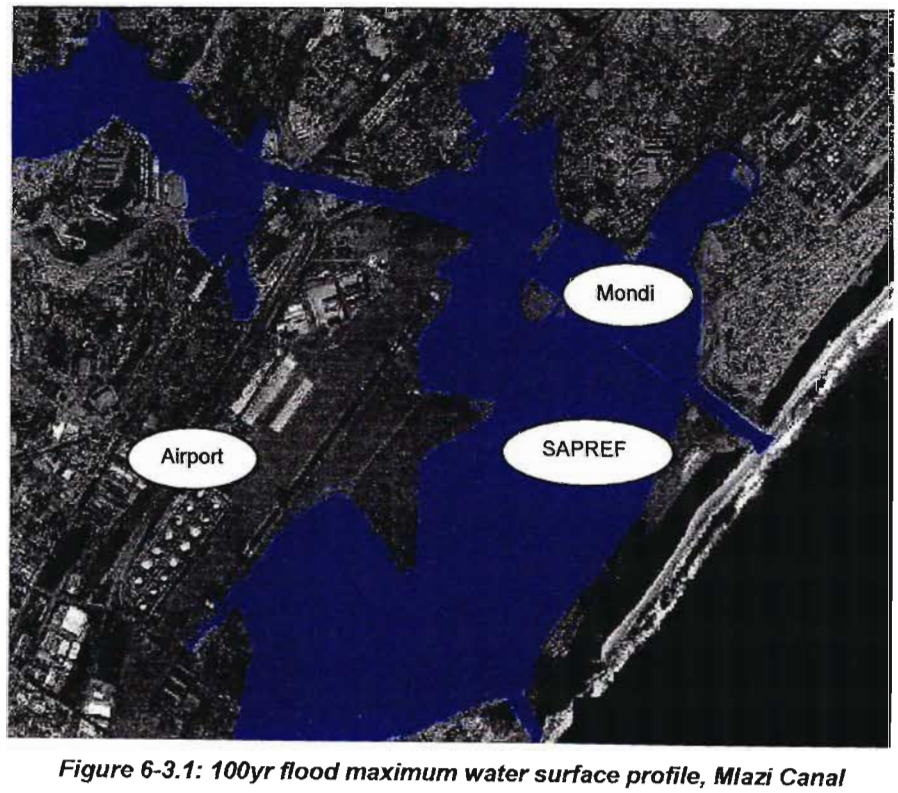

Figure 6-3.1: 100yr flood maximum water surface profile, Mlazi Canal

6.3.2 Possible solutions

Possible solutions that have been proposed in previous reports (including GIBB Africa, 1996):

- increase canal wall height,
- increase canal width,
- flood relief canal,and
- SAPREF flood protection berms.

Of these, the bunding of sensitive areas (such as SAPREF and Mondi) is likely to be the most cost effective and practical solution.

6.3.3 Conclusions and recommendations

The possible solutions to mitigate flood damage due to the Mlazi Canal overtopping have been covered at length in previous reports (particularly relating to the SAPREF site). A decision on the best course of action, if any, can only really be made through the completion of a detailed risk related cost-benefit analysis, due to the very high capital costs associated with remedial works.

6.4 Residential Hostels, Mlazi Glebe

6.4.1 Description of problem

An entire block of the hostels in this area lies within the 100yr flood line. This block together with the structures below it are at risk of being flooded during the higher flood events namely the 50-, and 100yr floods.

There are also several houses in the informal settlement near the hostels that are located within or close to the 100yr flood line. It is evident that there is little difference in the extent to which the 20-, 50- and 100yr floods reach and those houses closest to the river are at risk during moderately high flows in the river.

Figure 6-4.1: 20(cyan)-, 50(purple)-, 100(blue) yr floodlines, Hostels, Umlazi Glebe

6.4.2 Possible solutions

An earth embankment would provide protection to this area up to a point. To prevent inundation by the 100yr event, the berm would need to be up to 3 m in height in some places and about 500 m long.

An alternative option would be to set up an evacuation plan and educate residents on the nature of the flooding risks.

6.4.3 Conclusions and recommendations

The area affected here is not particularly extensive, and as a result, the cost of a flood protection berm may not be fully justified. An effective evacuation plan is likely to be a more appropriate approach to take, and is probably more in line with the approach taken in other areas exposed to similar risks.

6.5 Ndoande Road, Lamontville

6.5.1 Description of problem

Several houses at the end of Ndoande Road, as well as the cemetery are located within, or close to the 100yr flood line. It is evident that there is little difference in the extent to which the 20-, 50- and 100yr floods reach and that those houses closest to the river are at risk during moderately high flows in the river.

Figure 6-5.1: 20(cyan)-, 50(purple)-, 100(blue) yr floodlines, Ndoande Road, Lamontville

6.5.2 Possible solutions

In this instance, structural flood protection measures are not likely to be effective, or particularly appropriate, as only a few houses are affected. A more desirable approach would be to set-up an evacuation plan during periods of flood, and to inform residents of the risk of flooding, or, alternatively, move them to a more suitable area.

6.6 Salvia Road, Birchwood (Situndu Stream)

6.6.1 Description of problem

Several houses along Salvia Road are close to, or within the 100yr floodline. The problem in the Situndu stream is exacerbated by the backwater effect caused by the levels in the Mlazi, and this also results in inundation of the sewage treatment works.

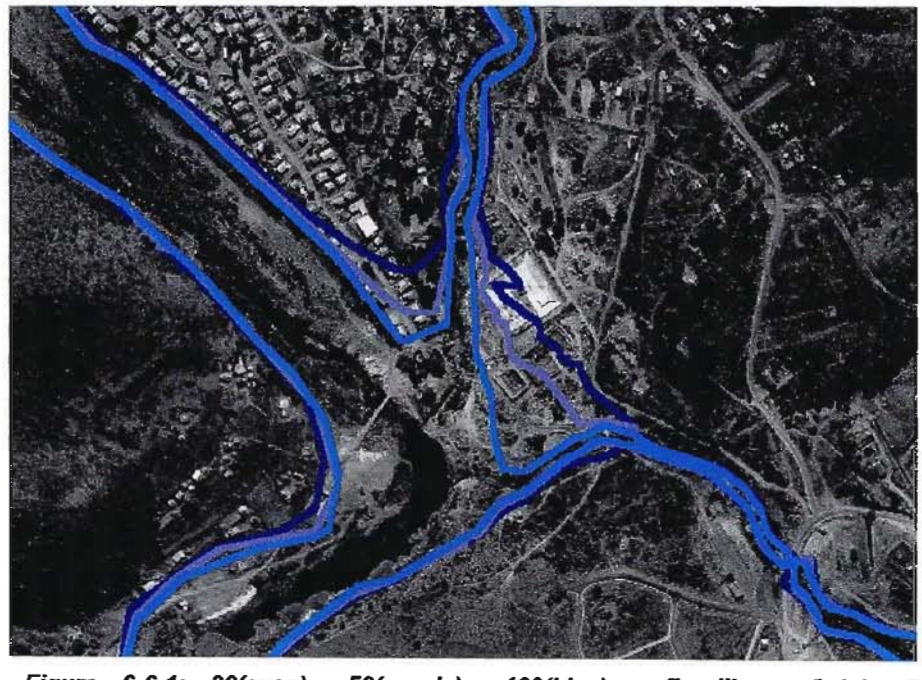

Figure 6-6.1: 20(cyan)-, 50(purple)-, 100(blue) yr-floodlines, Salvia Road, Birchwood

6.6.2 Possible solutions

A flood protection berm could be provided for the sewage treatment works due to the environmental risks that would be posed by inundation there, whilst an evacuation plan is probably appropriate for the nearby residents.

6.7 Coffee Farm (Cutshwayo Stream)

6.7.1 Description of problem

Some encroachment has taken place into the natural drainage path of the Cutshwayo tributary. The properties at risk are limited to a workshop building and one or two houses.

Figure 6-7.1: 20(cyan)-, 50(purple)-, 100(blue) yr floodlines, Coffee Farm (Cutshwayo Stream)

6.7.2 Possible solutions

The fact that a building has been constructed in the drainage channel puts the owner at risk of flooding problems, as well as exacerbating the problem of those around him. In this instance, the preferable option would be to relocate the workshop and formalise the drainage path. The practicalities of this may, however, prove difficult.

6.8 Sterkspruit Road Bridge, Hammersdale (Sterkspruit)

6.8.1 Description of problem

An industrial development and electrical substation located upstream of Sterkspruit road bridge is prone to inundation for floods equivalent to the 20yr return period design event and greater. The power sub-station seems to be located on a natural floodplain of one of the tributaries of the Sterkspruit, although the flooding problems are probably exacerbated by the capacity problem at the road bridge, which can only convey the 19yr return period event without overtopping and causes a backwater effect.

The car park together with some of the structures of the Rainbow Chicken factory is subjected to flooding during moderately high flows in the river. Certain parts of the industries downstream of this bridge are also located either within or close to the 100yr floodline. It is evident that there is little difference in the extent to which the 20-, 50-, and 100yr floods reach and that those portions of the industries closest to the river are at risk during moderately high flows in the river.

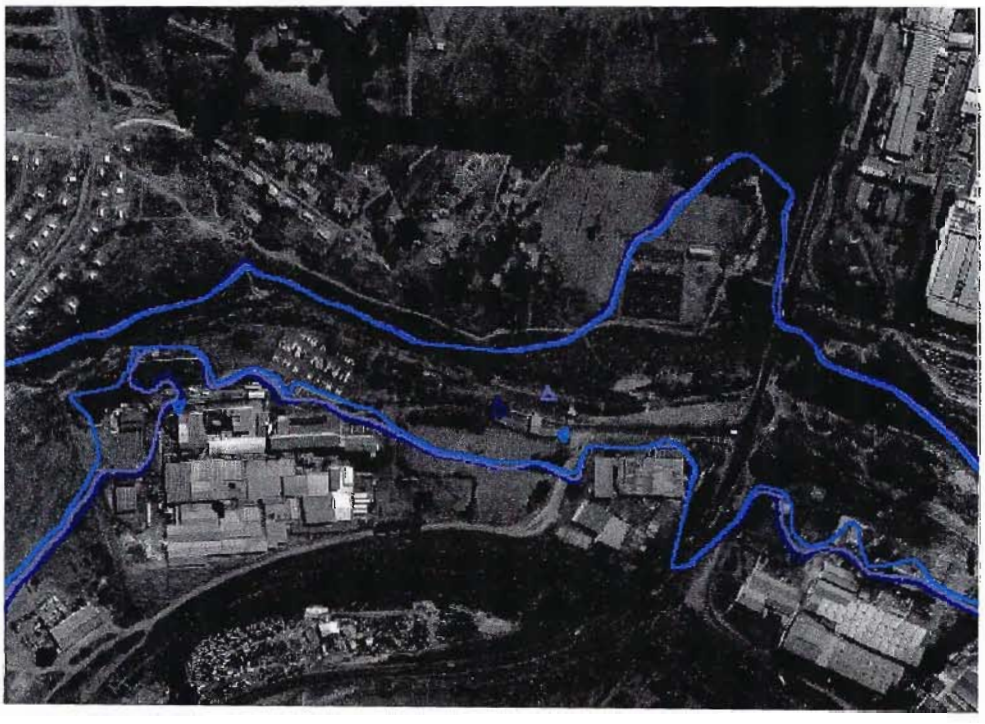

Figure 6-8.1; 20(cyan)-, 50(purple)-, 100(blue) yr floodlines, Sterkspruit Road Bridge, Hammarsdale

6.8.2 Possible solutions

A flood protection berm of 1-2 m height and 200 m long would provide protection to the electrical substation from inundation. Alterations to the road bridge are likely to be prohibitively expensive.

6.8.3 Conclusions and Recommendations

Both areas that are affected here were developed within the natural floodplain of the river and are therefore prone to flooding problems. The Rainbow Chickens car park is not a sensitive area, whilst the electricity substation could be protected by way of an earth embankment.

6.9 Tabulated flood prone areas

A summary of the locations along the river where flood damage can occur and which have been identified in Sections 6.3 to 6.12 is given in Table 6.9.1.

Location	Likelihood of damage	Damage costs	Mitigation Costs	Comment
Mlazi Canal	Medium to High	V. High	V. High	Risk-related detailed cost-benefit analysis required
Hostels, Umlazi	Medium	Low	Medium	Evacuation plan
Houses, Lamontville	Medium	Low	-	Some houses affected
Situndu	Medium	Low	Low	Berm for STW
Coffee Farm	Medium	Low	-	Re-locate
Hammarsdale	High	Medium	Low	Berm for sub-station

Table 6. 9.1: Summary of flood damage areas

The references to low, medium and high under the category of likelihood of occurrence refer to the 20-, 50- and 100yr return period flood events respectively. With respect to costs, the low, medium and high terms are used to give a relative perspective.

6.10 Summary and conclusions

Flood inundation levels have been computed for the Upper Mlazi and Lower Mlazi using one dimensional steady flow analysis. Flood inundation levels for the areas adjacent to the Mlazi Canal have been estimated using a one-dimensional unsteady flow model. The volume of water that overspills from the canal as the design flow hydrograph passes through has been calculated for different return periods. The elevation to which the overspill volume would reach has then been derived by assessing the topography of the receiving low-lying areas.

Conclusions

The fact that the risk of serious flooding of the Mondi and SAPREF areas occurring within the next 30 years is so high (26%) is of concern. Several previous studies have been carried out to assess possible remedial actions, the most recent being by GIBB Africa (1996) for SAPREF. This report recommends that bunds around the SAPREF site would offer the best protection against flood damage. This is still likely to be the best option, as opposed to canal widening or raising. However the introduction of the flood streamflow forecasting in the Mlazi Catchment discussed in chapter 7 is a measure of giving advance warning to the industries within its flood plains. The Mlazi forecasting model described in the next chapter is important bearing in mind the high risk of serious flooding associated with Mlazi catchment.

7. GENERAL DESCRIPTION OF THE MLAZI META MODEL

The model used in real time flood forecasting in the context of the Mlazi Catchment is a linear catchment model. The model consists of a semi-distributed three reservoir cell model applied to each subcatchment and linearly summed to produce the combined catchment output (Pegram and Sinclair, 2002) hereinafter called the Mlazi Meta Model (MMM). This is a conceptual model, which requires parameter adjustments so that it becomes representative of the Mlazi catchment. The validation of this model requires a reliable record of rainfall and historical streamflow data so that an accurate forecast can be performed. However due to the absence of reliable streamguages downstream of Shongweni Dam, together with the poor quality of only daily rainfall data, the implementation of such a system would be difficult. It is these factors which resulted in the introduction of an integrated modelling process that involved the use of design storms together with output time series hydrographs from the HEC-HMS in the set up of the Mlazi Meta Model. The synthetic storms are input into the model and the parameters are calibrated so that the simulated stream flows from the model approximates the output from the calibrated physically based model (HEC-HMS). This approach might seem unreasonable because a model is being validated by another model, but it should be noted that this approach gives a better initial estimate of the parameters than trial and error. The MMM would further be updated using recorded radar data and streamflow data once all structures have been put in place. The confidence in the applicability of the HEC-HMS model is based on the intensive efforts applied in setting it up so that it is representative of the Mlazi catchment. Furthermore the output from the calibrated HEC-HMS model have been compared with other reliable methods of computing peak discharges, discussed in Section 3.6.6.

7.1 The Advantages of using the MMM for real time forecasting

The advantages of using the MMM for real time forecasting as compared to the use of the HEC-HMS model is as follows:

- The HEC-HMS model is subject to human judgement requires laborious, time-consuming work such as feeding information into ACII files by hand. Furthermore the state and characteristics of the catchment is a snap shot based on historical analysis of the system. By contrast the

MMM has few parameters, seven at most (usually three or four) and these are calibrated on some input and output sequences.

- In forecast mode it would be difficult to adjust the parameters of the HEC-HMS model at frequent intervals to match the output with observed flows. This is because the parameter files would have to be altered by hand and it would not be clear how much to alter the parameters such as the SCS curve number and initial abstraction. By contrast, the MMM's few parameters of the model are designed to be optimally adjusted in real time to match the modeled output to the observed flows.
- The philosophy of the MMM is to accomplish the objective of meaningful forecasting, one needs to start with a good estimate of the MMM parameters and this is achieved by calibrating it on the input to and output from the fitted HEC-HMS model to selected flow events.

7.2 The Creation of the Mlazi Meta Model

During the integration process, rainfall data in the form of hyetographs, and streamflow data in the form of hydrographs for historical flood events were used for calibration of the Mlazi HEC-HMS model. Design storms at various recurrence intervals were computed using the appropriate synthetic storm distribution type and the mean 24-hour design rainfall depth. These design storms were input to the HEC-HMS to enable peak discharge flows to be computed. The same design storms will then be input to the MMM (during the validation and testing stage). The MMM created was a conceptual representation of the Mlazi catchment once it was tuned so that the outputs were close to those obtained from the Arcus Gibb model. The fine tuned forecasting model was then to be used together with telemetering flow gauges at the Shongweni Dam to conduct real time forecasts.

7.3 Structure of the Integrated Forecasting System

The general structure of the forecasting system was presented in Figure 1.1.1. The Mlazi Meta Model is represented by the Semi-Distributed Linear Catchment model.

MMM is basically a mathematical conceptual model. It is a linear catchment model that produces flood forecasts in real time. The forecast can be made at time steps, which are of the order of a fraction of the catchment response time (Pegram and Sinclair, 2002). The use of streamflow gauges together with

computed river stages and the associated rating curve to reassess continuously how much water is in the river channel is a vital part of the forecast process. MMM consists of three main components, which are as follows:

a) **Best Spatial Rainfield**: The best spatial rainfield is a result of the combination of the point rain data, radar rainfield and, possibly in the future, satellite rainfields. The joint use of radar and raingauge data aims at the utilisation of the high point accuracy of the latter and the wide spatial coverage of the former. The merged rainfield is input to the rainfield-forecasting model and also to the linear catchment model.

b) **Rainfield Forecasting Model**; In cases where the catchment response time is short (<2hrs), there is an advantage in taking trouble to forecast the rainfall up to one hour ahead in real time. The rainfall forecast is carried out by the use of the String of Beads model (Pegram and Clothier, 2002). The model manipulates the time and space dependence in rainfields in forecast mode. The forecast rainfield is input to the linear catchment model.

c) **Semi-Distributed Linear Catchment Model**; This model consists of semi-distributed cell models which in turn uses a system of three linear reservoirs to conduct rainfall-runoff conversions to compute streamflows for each cell. The response of the arrangement of linear reservoirs is governed by the use of an Auto Regressive Moving Average (ARMA) type equation which is a form of the State-Space equations (Pegram and Sinclair, 2002). The input to the model is the best-observed spatial rainfall field. Functions of the ARMA type are parametrically efficient and are easy to adjust in real time. This means that optimal (Kalman) filtering techniques can be applied to update the state and parameters of the model based on the real flows (also input) available and the current state of the catchment. The outputs from the model are forecasted flows, which are similar to observed flows. The forecasted streamflows are then routed through the river channel model (HEC-RAS) from the Shongweni Dam through the canal to the outlet.

7.4 Application of the Suggested Calibration Procedure for the MMM.

Having studied the catchment and concluded that it meets the specifications for the application of the MMM to flood forecasting, the calibration procedure proposed by Pegram and Sinclair (2002) was conducted as follows:

- **Calibration Data**: Due to the uncertainty and unavailability of historical streamflow data, the procedure of extracting a representative historical streamflow sequence at regular discrete timesteps was replaced by the extraction of a synthetic streamflow sequence. This was conducted for a selected recurrence interval, computed from the HEC-HMS based on the synthetic hyetograph and the physical parameters set up in the HEC-HMS model.
- **Determination of the contributing precipitation inputs**: The synthetic hyetographs input to the HEC-HMS were used as input to the MMM. The computation of these precipitation inputs were discussed in Section 3.5.
- **Fitting MMM model parameters to the HEC-HMS data sets**: The parameter data fitting procedure is shown in Figure 7.2.1. Each of the four subcatchments U60a, U60b and U60c and U60d were treated as individual cells initially. The cell of particular concern was the U60d, which is the cell downstream of the Shongweni dam towards the Mlazi canal entrance.
- **Verification of the Parameter set**: This process required the use of the fitted model configuration and parameter set to produce flow estimates from historical data not used in the determination of the parameters. However due to unavailability of historical data this would be done later as accumulation of radar rainfall and streamflow data become available.

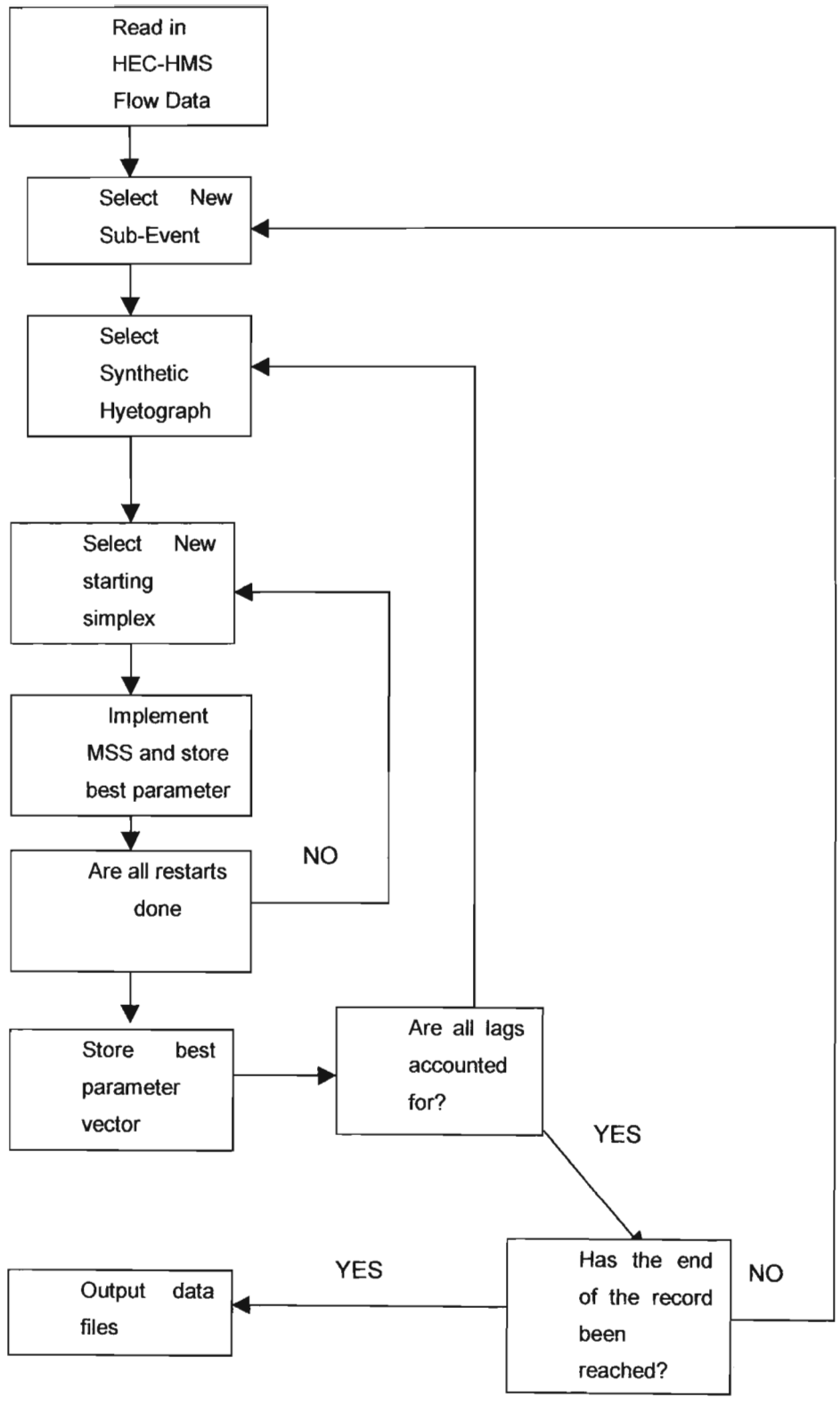

Figure 7.2.1: Flow chart for the parameter fitting procedure (Sinclair, 2002)

Calibration Results of the MMM

The results shown below are from a MMM fitting process carried out by a Phd student at Natal University which involved selecting starting values for the MMM to ensure that the forecasting process starts suitably close to some observed streamflows. The input and output data set used for the parameter tuning was obtained from the HEC-HMS model produced during a desk top study.

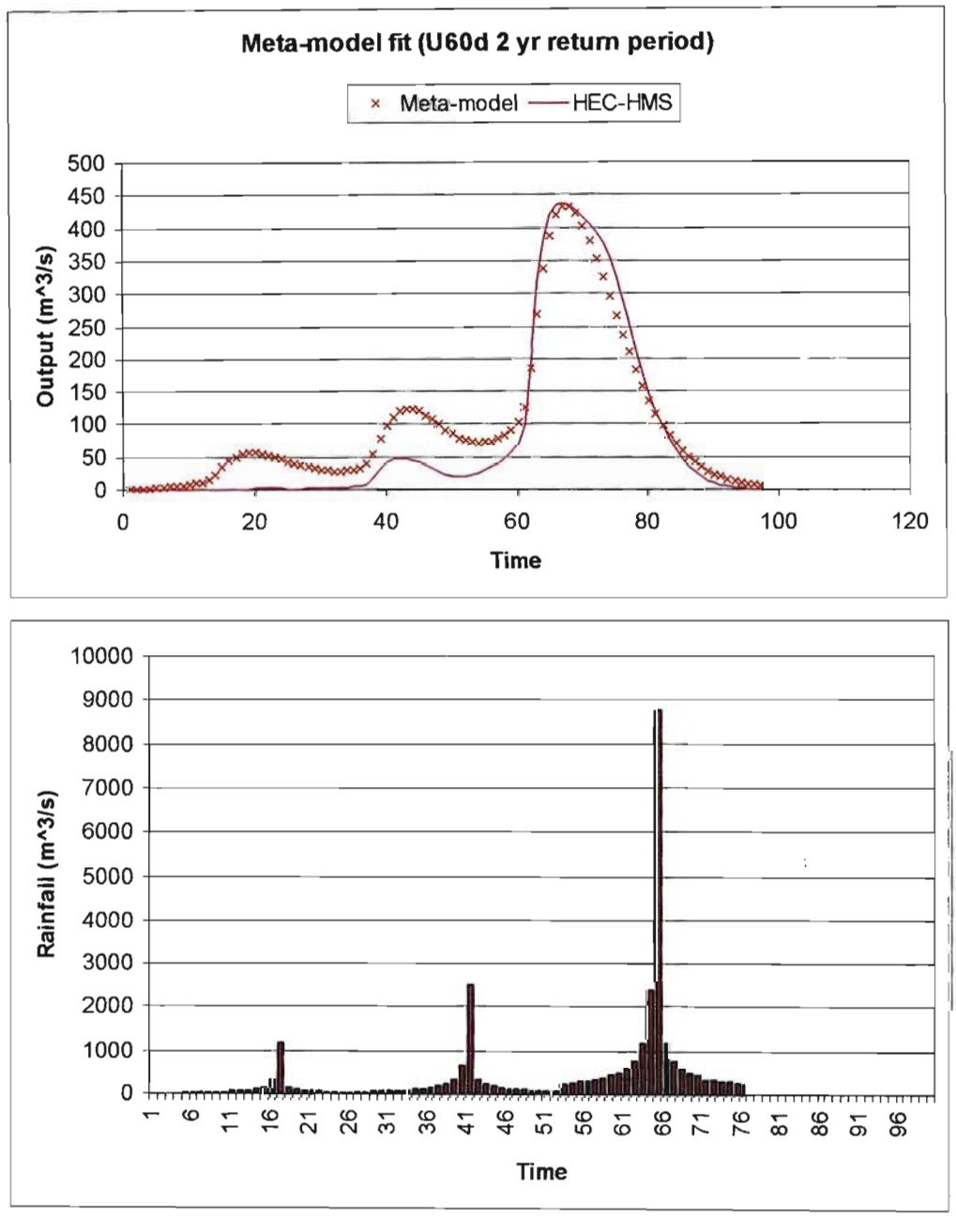

Figure 7.2.2: Flow chart for the parameter fitting procedure

The Meta model fit shown in Figure 7.2.2 is for the downstream outflow to the canal. The 3-Day rainfall design (LMH) was for a 2yr recurrence interval and therefore the output hydrograph was also assumed to be for a 2yr recurrence interval. The rainfall was measured as a volumetric quantity falling over the quaternary area per second resulting in the rainfall units in y-axis being m^3/sec. From the output graph it is observed that a close fit was obtained for the highest peak (due to the third day storm) and the Meta Model produced peak discharge from the first two-day storms which were slightly higher in magnitude than those obtained from the HEC-HMS model.

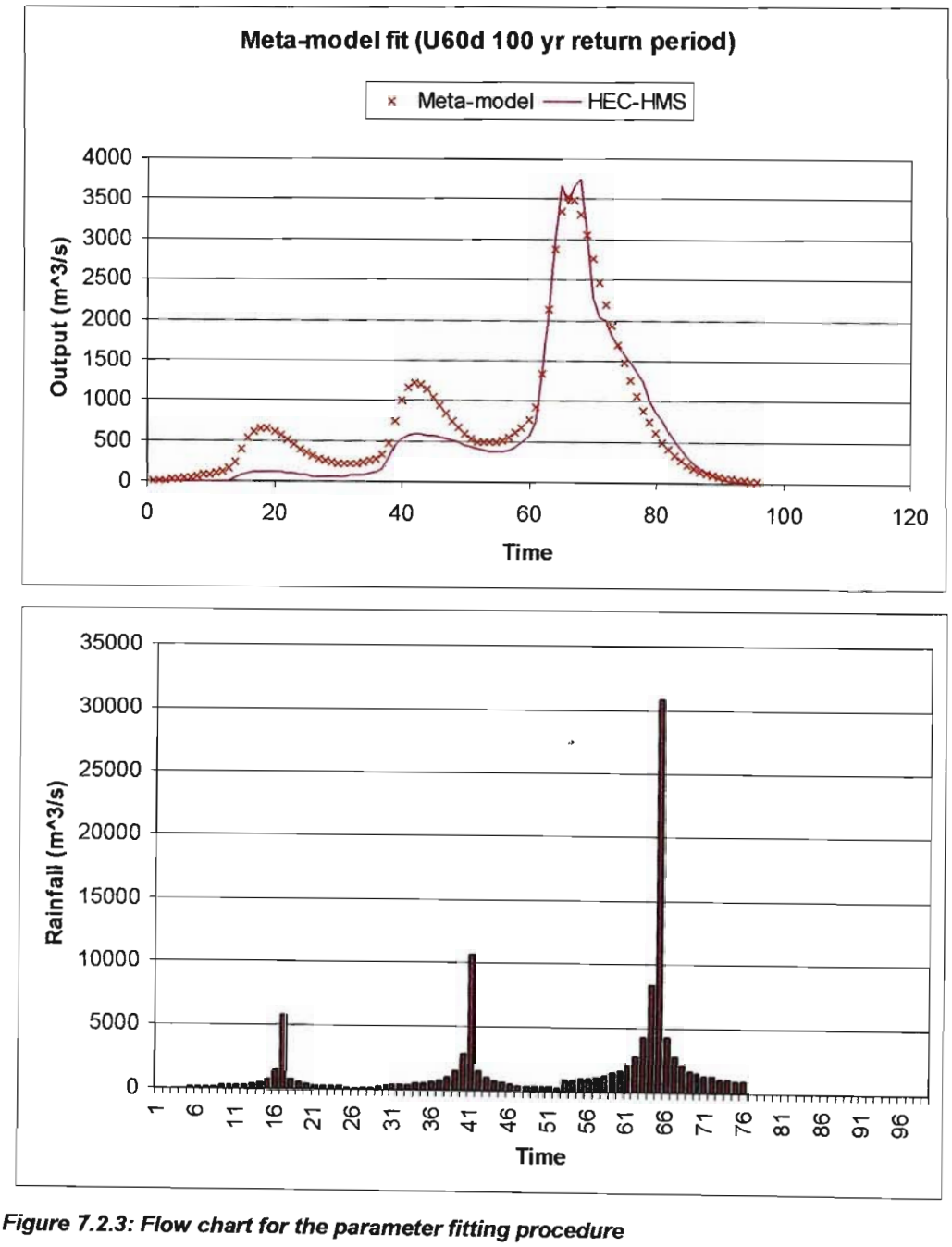

Figure 7.2.3: Flow chart for the parameter fitting procedure

The Meta model fit shown in Figure 7.2.3 is for the downstream outflow to the canal. The 3-Day rainfall design (LMH) was for a 100yr recurrence interval and therefore the output hydrograph was also assumed to be for a 100yr recurrence interval. From the output graph it is observed that a close fit was obtained for the highest peak (due to the third day storm) and the Meta Model produced peak discharges from the first two-day storms which were slightly higher in magnitude than those obtained from the HEC-HMS model.

Shown in Table 7.2.4 and 7.2.5 are parameter values for the above plotted graphs. The values are based on the connectivity of elements in the Mlazi represented by Figure 7.2.3.

Parameter	Value
K_1	4.7
K_2	**17.5***
K_3	7.5
K_4	6.7
K_5	**272.6***
K_6	7.2
K_7	8.1

Table 7.2.4: 2 year Return Period Parameter Values

Parameter	Value
K_1	1.7
K_2	**177.3***
K_3	2.1
K_4	6.3
K_5	**1102.8***
K_6	9.4
K_7	18.2

Table 7.2.5: 100 year Return Period Parameter Values

The parameters are the average residence times of water in the individual storage elements from the point of view of the associated outlet. Thus the larger the k values the smaller the flow through the corresponding exit. A very large value of k indicates that the exit could be closed off to yield a less complicated

model. Thus k_2 and k_5 (in bold and asterisks) could be set to infinity in both models reducing the general number of three tank model to a cascade of 3 tanks as shown by the red arrows in Figure 7.2.5. Once this happens, the inference is that the total residence time in the system (input to outflow) equal $k_1+k_3+k_4$ (in red) reduces from 19.1 hr for the 2yr flood to 10.2hr for the 100yr flood which makes physical sense. Thus the linear model is adaptable to the data. As expected thus the starting values of the parameter of MMM can be set with reasonable confidence and will adapt with the application of the Kalman filter once real time flows are available.

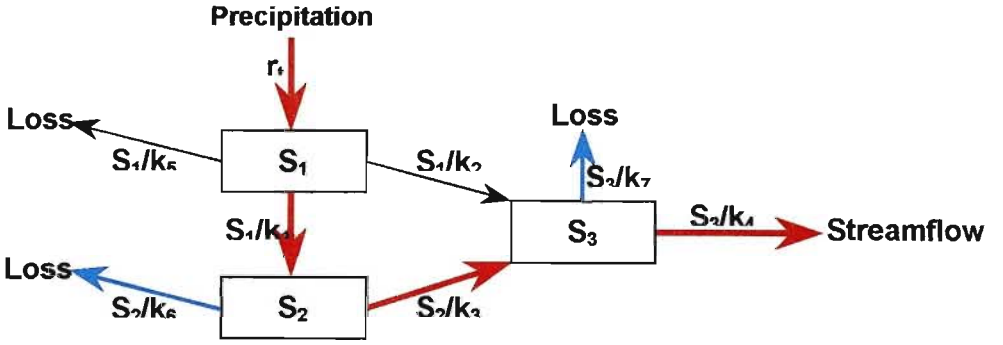

Figure 7.2.4: A general linear 3 reservoir feed forward model with (possible) losses from each reservoir.

The (continuous time) State-Space representation for the arrangement in Figure 7.2.4. is given by the following set of differential equations:

$$\dot{S}_1(t) = -\left(\frac{1}{k_1}+\frac{1}{k_2}+\frac{1}{k_5}\right)S_1(t)+r(t-\tau)$$

$$\dot{S}_2(t) = \frac{1}{k_1}S_1(t)-\left(\frac{1}{k_3}+\frac{1}{k_6}\right)S_2(t)$$

$$\dot{S}_3(t) = \frac{1}{k_2}S_1(t)+\frac{1}{k_3}S_2(t)-\left(\frac{1}{k_4}+\frac{1}{k_7}\right)S_3(t)$$

where: $\dot{S}_i(t)$ = the time derivative of the storage in the i'th reservoir at time t, $S_i(t)$ is the sequence of storage's in the i'th reservoir

k_i's = the response constants for each of the reservoirs and

$r(t-\tau)$ = is the lagged (by τ intervals) sequence of precipitation inputs to the system.

The resulting streamflow *y(t)* is:

$$y(t) = \frac{1}{k_4} S_3(t)$$

7.5 Conclusion and Recommendations

The objective of this study was to apply the linear catchment model for real time flood forecasting to the Mlazi catchment (MMM model) and subsequently produce levels of inundation which were to be displayed at the eThekwini disaster management center.

The Mlazi catchment meets the requirements for application of the real time forecasting model (MMM model) although this was subject to some uncertainty due to unavailability of historical rainfall and streamflow data.

The requirements for application of the model to the Mlazi are:

- A network of telemetering stream gauge. The DWAF representatives at WRC meeting confirmed that a stream gauge station has been set up at the outlet of the Shongweni dam. The location of the stream gauge was confirmed through the HEC-HMS (physical rainfall -runoff model) model to be the strategic point for the location of the real-time forecasting system for early flood warnings for the industrial areas around the Mlazi canal. This would enable online updating of the streamflow estimates since they would require up to date measurements of streamflow.
- There is coverage of the catchment by weather radar. The Mlazi catchment is located Southwest of the Mgeni catchment, which are both covered by the Durban Radar.
- Telemetering rain gauge within the Mlazi Catchment. The eThekwini Municipality and METSYS are installing telemetering raingauges and making their data and the SAWS data available in a single database.

8. SUMMARY, RECOMMENDED SOLUTION AND CONCLUSION

8.1 Summary

The main objective in this study as discussed in chapter 1, was to deliver an operational system that would produce flood forecasting in real time, using real time data and produce levels of inundation for the Mlazi catchment.

The most appropriate approach would have involved the direct use of the real time forecasting model created by Pegram and Sinclair (2002) in the context of the Mlazi catchment. This was to be conducted through the acquisition of historical stream data with correlating radar rainfall data, to calibrate and validate the Mlazi Meta Model (MMM).

However since the study was conducted in an environment where there is uncertainty due to lack of historical data for input calibration and validation purposes, it was necessary to adopt approaches to overcome these difficulties.

The approach to this study was therefore based on integration of modeling techniques intended to address the uncertainty. A strategy was determined to address the difficulties by introducing a physically based model described in Chapter 3. The physically based HEC-HMS model was configured for the Mlazi Catchment. The HEC-HMS was intended to be used for the initial adjustment of the MMM parameters, so that the MMM would be representative of the Mlazi catchment and therefore be suitable for real time flood forecasting once real time data from the Mlazi river was improved and made available. In addition to that, the computed peak discharges were input to the HEC-RAS model used for the delineation of inundation levels.

The HEC-HMS model described in Chapter 3 was set up through the use of sound hydrological principles using GIS technology to capture input data and create the Digital Elevation Model (DEM) of Mlazi. Since the initial parameter estimates for the MMM were based on the HEC-HMS model, it was important that an effort be applied to reduce human error and make sure that the model provided a good representation of the Mlazi catchment.

One shortcoming of the project was the lack of correlating rainfall and streamflow data, even for the calibration of the HEC-HMS model. It was important therefore to ensure that the physical parameters to be used to set up the model were appropriate. A sensitivity analysis conducted for the HEC-HMS model input parameters (based on the SCS curve number method) confirmed that the computed discharges were sensitive to the variation of the SCS curve number. It was therefore apparent that one should get the best estimates of the CN values for each identified subcatchment so as to obtain realistic peak discharges. This was conducted through the overlaying of physical catchment characteristics such as soil type, and landuse in a GIS environment. The overlay process enabled the computation of weighted CN values and the initial abstraction and lag time. The SCS land category was obtained from Schmidt *et al* (1987).

The problem of historical rainfall data was encountered by the use of design synthetic hyetographs based upon the design one day mean rainfall depth and three day mean rainfall depths for various recurrence intervals obtained from Smithers and Schulze (2000). These had to be, distributed using a suitable temporal storm distributions based on the dimensionless SCS Type 2 synthetic storm distribution created by Schmidt and Schulze (1987) and later revised by applying Adamson (1982) distribution which was mainly appropriate for the Durban type of rainfall.

The three-day design storm had six random combinations, which are equi probable temporal distributions because there is negligible correlation between daily amounts of rain in a sequence of wet days. (Zucchium and Adamson, 1984). The scenarios were based on the order in which the magnitude of rainfall depth was selected. LMH represented the order in which the lowest depth L was considered to contribute to the first day of the 3 days followed by the medium M and then the highest H. The worst scenario (LMH) could have been the most favourable to be used for analysis. However it was deduced from the historical flooding of the canal that such a scenario has not really occurred as yet and since the delineation of flood plains was calibrated based on historical flood events, the scenario selected was the MHL.

The synthetic rainfall data was used as input to the HEC-HMS model and also as input to the MMM.

The HEC-HMS model required that a routing method be defined to compute the downstream hydrographs. The most appropriate method selected was the Modified Puls (or storage routing), the method however required storage-flow relationship which were obtained from the HEC-RAS model. This method had an advantage over the other routing methods available such as kinematic wave, Muskingum- Cunge, and lag method in that it could incorporate the backwater effects caused by downstream conditions, such as bridges and culverts. It should be noted that the initial estimates of the storage –flow relationship were obtained from the Mhlatuzana sub-catchment since it has the same physical characteristics as Mlazi Catchment. However these storage – flow relationships were later replaced by the storage - flow relationship computed from the volume storage in the reach calculated by numerical interaction in the HEC-RAS River.

The HEC-HMS model also required input data for baseflow, which was assumed to be zero as it was small in magnitude compared with the flood discharges.

In Section 3.6 the procedure for the calibration process of the HEC-HMS model is described. The calibration process involved adjusting model parameter values (CN, Initial abstraction and Lag time) until modelled peak discharges matched historical observed peak flows. Due to the unavailability of data for the whole catchement, the calibration process was first applied to two selected subcatchments of the Mlazi Catchment, which happened to have reasonable historical streamflow and rainfall data. Five storm events were identified and of these five, only one was used for the calibration (2-4 Feb 1999 storm event) because its rainfall data had a good correlation with the stream-flow data. The calibration procedure was carried out in two phases. The first phase involved the use of the 2-4 Feb storm event which had streamflow data correlating to 3-Day total rainfall depths which had to be "stitched " to the radar distribution for the 2-4 Feb 1999 storm event so as to spatially distribute it over the quaternary catchments.

The peak discharge values obtained after conducting the first phase of the calibration process were compared to those obtained using other methods such as the RMF and rational method. It was at this point that the values were also compared with the other HEC-HMS peak discharges computed from the

previous studies of other catchments within the Durban metropolitan boundary. For instance the Standard Design Formula (SDF) and Durban Corporation formula (DCF) were applied. The later is intended to be replaced by an empirical formula based on the HEC-HMS peak discharges and the catchment size derived to enable an early estimate of the HEC-HMS peak discharges for selected return periods when given the catchment area. The formula is represented in Section 3.6.5 as:

$$Q = C(T)A^{0.42}$$

The formula is applied to compute Q (m^3/sec) for various return periods T. The term C (T) varying for each return period caters for the physical parameters of the catchment of an area A (km^2).

The second phase was the validation process that involved the use of flood frequency analysis of the 20-year peak discharges from the two stream gauge stations (Baynesfield and Mlaas Road). The observed flows were ranked and assigned a probability value computed by use of the Cunnane (1978) plotting position formula quoted by Chow *et al* (1988), further more the reduced variate y_T was computed based on the computed return period. The observed flows were plotted against y_T. The HEC-HMS computed flows were plotted against the variate y_T (which was computed using the selected return periods of the design rainfall depth). The two plots were compared and the HEC-HMS output adjusted to align with the observed through the manipulation of the SCS curve number and the lag time until there was a good match.

Once the HEC-HMS was up and running the HEC-HMS output peak discharges were captured and routed through the HEC-RAS model. In Chapter 4 the Mlazi river model was set up using the HEC-RAS program. The model was used for the determination of the levels of inundation for the Mlazi to be displayed at the disaster management center of the eThekwini Metro municipality using GIS. The HEC-RAS program also required a DEM but of a high resolution since this model was to be used for producing levels of inundation. The hydraulic and assumptions applicable to the Mlazi HEC-RAS model are found in hydraulic textbooks such as Chow (1959), and Henderson (1966) and the HEC-RAS manual (1997). The Mlazi River was split into three components during the modelling process, namely; Upper Mlazi, Lower Mlazi and the Mlazi canalised

section. The assumptions with regard to the analysis were based on the channel characteristics of the three portions. For instance steady state analysis was applied for the Upper and Lower Mlazi where the river is characterised by steep, well-defined channels with supercritical flows. The canalised (concrete lining) reach susceptible to overtopping of the canal resulting in inundation of low-lying areas was modelled under unsteady state condition.

The HEC-RAS program required data input such as the flow data (steady flow/or unsteady flow data) and the geometric data which is a geometric representation of the river system including, Mannings's coefficients and the bridge and culvert structures. An interesting aspect of the study was the fieldwork conducted to capture the Manning's roughness coefficient and structural data. The Manning's coefficient values determined during fieldwork was based on a consensus of a consortium of four field researchers who walked along the Lower Mlazi and the Mlazi canal. They assessed the vegetation cover and streambed condition in terms of bedding and water depth thereby assigned Manning's 'n' values based on roughness coefficients table from Chow (1959). A desk top evaluation of the values was also carried out using the photographs shot on site and comparing them with published guides for selecting Manning's roughness coefficients for natural and flood plains produced by the United States Geological Survey and Water supply (Arcement and Schneider, 2001).

The steady state computation procedure to determine water surfaces from one cross section to the next was carried out by solving the energy equation with an iterative procedure called the standard step method. The computation was carried out as recommended by Chow (1959), i.e. the computation was carried out in an upstream direction for the subcritical flow and in a downstream direction for the supercritical flow.

The Mlazi canal hydrodynamic analysis was discussed in chapter 5. The canal portion of Mlazi was analysed under unsteady state conditions using HEC-RAS program. Off channel storages were introduced to monitor the lateral flow spilling over the canal during over topping. The canal was constructed in the mid 1950's by the Department of Transport, its purpose was to deviate the Mlazi river away from the site of the Botha Airport (Durban Airport). Apart from the airport the Mlazi lagoon attracted industries such as the SAPREF oil refinery (in the early 1960s) and the Mondi paper factory (in the early 1970s). These were

constructed in the south and north of the canal respectively, subsequently each is built below the level of the canal and is therefore susceptible to flooding as evidenced during the 1987 floods.

The purpose of the investigation into the flood of the Mlazi canal was to delineate the inundation levels for the 20-, 50- and 100 year return periods. The methodology as explained in section 5.4 is that which involved a one dimensional unsteady flow analysis whereby input hydrographs of a one-hour time series representing an inflow to the canal were input at the upstream part of the modelled canal. Off-channel storage was introduced to monitor the lateral flow spilling over the canal during overtopping. A typical section of the HEC-RAS model of the canal showed that lateral weirs connected to the storage areas monitored the lateral flow into off channel storages.

It was observed that the quantity of water that flow over the lateral weirs depended on the shape and peak of the flow hydrograph that was being routed through the canal. The total volume of the water that flowed over the lateral weirs into the storage areas as well as the actual storage volume available determined the level to which the overspill water rises. This level thus defined the inundation levels for the floodplain at the canal areas.

The analysis therefore indicated the following:

- The results indicate that the nominal capacity of the canal is approximately 1200m^3/secequivalent to the flow associated with the 20-year return period flood event.
- The risk of overtopping occurring in the next 30 years is 79%.
- For the 100-year design event, nearly 12 million cubic meters of water is spilled from the Mlazi canal.
- The risk of this wide spread inundation occurring within the next 30 years is approximately 26%.
- The sensitivity analysis carried out shows that the inundation levels increase linearly with the Manning's 'n' and that an increment of 0.02 in the Manning's 'n' value results in an increment of 0.3 m on the inundation levels. This observation justifies the need for a selection of a good estimate of the Manning's 'n'.

A flood damage assessment was carried out as discussed in Chapter 6. In the chapter, areas within the Mlazi river system where flooding was problematic were identified and subsequent engineering mitigation measures were suggested. The area where severe flooding would occur is sited on the wide flood plain areas in the lower 3km canalised section of the Mlazi River. The analysis indicates that peak floods of a magnitude equal to a 20-year return period and above, would inundate the Mondi and SAPREF sites located within the floodplain. When overtopping occurs, the surrounding areas are inundated to a depth approximately 3m for the 100-year design event. The South Coast road and adjacent areas are also inundated at the entrance to the canal. The 100-year floodplain for the canalised portion of the Mlazi was shown in Figure 6.3.1.

8.2 Recommended Solutions

Previous reports have included the following solutions:

- Increase canal wall height
- Increase canal width
- Build a flood relief canal
- Provide SAPREF flood protection berms.

Of the above mentioned, the bunding of sensitive areas (such as SAPREF and Mondi) is likely to be the most cost effective and practical solution. However the most cost-effective flood damage mitigation would be the implementation of the Mlazi flood forecasting system at the downstream of the Shongweni dam. This early warning to the industries would assist in alerting the industries and thereby give them time to close down their machines and ensure that employees and the surrounding residents are evacuated from the area before the flood occurs. This would assist to prevent loss of lives and plant damage due to seizure of machines as a failure caused by improper close down.

The Mlazi flood forecasting system was investigated and set up as discussed in Chapter 7. The model used for the real time flood forecasting in the context of Mlazi is a linear model. The model consist of a semi –distributed three reservoir cell model applied to each subcatchment and linearly summed to produce the combined catchment output (Pegram and Sinclair, 2002) hereinafter called the Mlazi Meta Model (MMM). This is a conceptual model, which required parameter adjustments so that it became a representative of the Mlazi

catchment. The validation of this model requires a reliable record of rainfall and historical streamflow data so that an accurate forecast can be conducted. However, due to the absence of reliable streamgauges downstream of Shongweni Dam together with poor time series of only daily rainfall data, the implementation of such a system would be difficult.

It was the lack of suitable observed data which resulted in the introduction of an integration modelling process which involved the use of design storms together with output time series hydrographs from the calibrated physically based model (HEC-HMS). This approach might seem unreasonable because a model is being validated by another model but it should be noted that this approach gives better initial estimate of the parameters than trial and error. The MMM would further be updated using recorded radar data and streamflow data once all structures have been put in place.

The confidence in the applicability of the HEC-HMS model was based on the intensive efforts that were applied in setting it up so that it was a representative of the Mlazi catchment. The HEC-HMS it self could not have been a good model for real time forecasting following its comparison with the MMM. The advantages of using the MMM for real time forecasting as compared to the use of the HEC-HMS model was as follows:

- The HEC-HMS model is subject to human judgement requires detailed work such as feeding information into ACII files by hand. Furthermore the state and characteristics of the catchment is a snap short based on historical analysis of the system. By contrast the MMM has few parameters, seven at most (usually three or four) and these are calibrated on some input and output sequences.
- In forecast mode it would be difficult to adjust the parameters of the HEC-HMS model at frequent intervals to match the output with observed flows. Currently, the parameter files are altered manually which would have to be automated. It would not be evident by how much to alter the parameters such as the SCS curve number and initial abstraction and an optimizing outline would have to be developed. By contrast, the MMM's few parameters of the model are designed to be optimally adjusted in real time to match the modeled output to the observed flows.
- The philosophy of the MMM is to accomplish the objective of meaningful forecasting, which needs to start with a good estimate of the MMM

parameters and this is achieved by calibrating it on the input to and output from the fitted HEC-HMS model to selected flow events.

8.3 Conclusion and Prognosis

The objective of this study was to apply the linear catchment model (the MMM) for real time flood forecasting to the Mlazi catchment and subsequently produce levels of inundation which were to be displayed at the eThekwini disaster management center. This was achieved by the integration of various modelling techniques such as the use of GIS technology, application of the physical based model for flood analysis, the set up of the forecasting model for real time forecasting and the hydraulic modelling process to produce inundation levels.

The Mlazi catchment meets the requirements for application of the real time forecasting model (MMM) although this was subject to some uncertainty due to unavailability of historical rainfall and streamflow data.

The requirements for application of the model to the Mlazi are:

- A telemetering network of stream gauge. The DWAF representatives at WRC meeting confirmed that a stream gauge station has been set up at the outlet of the Shongweni dam. The location of the stream gauge was confirmed through the HEC-HMS (physical rainfall -runoff model) model to be the strategic point for the location of the real-time forecasting system for early flood warnings for the industrial areas around the Mlazi canal. This would enable online updating of the streamflow estimates since they would require up to date measurements of streamflow.
- There is coverage of the catchment by weather radar. The Mlazi catchment is located Southwest of the Mgeni catchment, which are both covered by the Durban Radar.
- Telemetering raingauges within the Mlazi Catchment. The eThekwini Municipality and METSYS are installing telemetering raingauges and making their data and the SAWS data available in one database.

9. REFERENCES

Adamson P.T. (1982). "South African storm rainfall." *Tech. Rep. TR102*, Dept. Water Affair and Forestry, Pretoria, South Africa.

Al-Futaisi A. and Stedinger J.R. (1999). "Hydrologic and Economic Uncertainties and Flood-Risk Project Design." *Journal Water Resources Planning and Management, Vol. 125, No. 6*, ASCE, 314-324.

Alexander W.J.R. (2000). "Standard Flood Design User Manual for Southern Africa." *United Nations Scientific and Technical Committee.* South African Institute of Civil Engineering.

Alexander W.J.R. (1993). "Flood Risk Reduction Measures incorporating Flood Hydrology for Southern Africa." *United Nations Scientific and Technical Committee.* South African Institute of Civil Engineering.

Arcus Gibb (2002). "Mlazi Flood Study." *eThekwini Metropolitan City Council*, South Africa.

Arcement G.T. and Schneider V.R. (2001). "Guide for Selecting Manning's Roughness Coefficient for Natural Channels and Flood Plains." *United States Geological Survey Water Supply.* Atlas.

Arnell N.W. (1989). "Expected Annual Damages and Uncertainties in Flood Frequency Estimation." *J .Water Resources Planning and Management, Vol. 115, No. 1*,ASCE, 94-107.

Bauer S.W. and Midgley D.C. (1974). "A simple procedure for synthesizing direct runoff hydrographs." *Hydrological Research Unit Report 1/74,* Witwatersrand University, Johannesburg.

Beard L.R. (1960). "Probability estimates based on small normal distribution samples." *J Geophys.* Res, 65 2143-2148.

Bradley A.A., Cooper P.J., Potter K.W. and Thomas P. (1996). "Floodplain Mapping Using Continuous Hydrologic and Hydraulic Simulation Models." *J. Hydrologic. Engrg.*, ASCE, 63-68.

Bradley A.A., Potter. K.W, (1992). "Flood frequency analysis of simulated flows." *Water Resource Res.*, 28(9), 2375-2385.

Bell F.C. (1969). "Generalised Rainfall-duration-frequency relationships." Journal of Hydraulic Engineering., 95(HYI), 311-327.

Campbell, Bernstern and Irving (1988). "Report on Umlaas Canal Flooding." Shell and BP S.A. Petroleum Refineries (Pty) Ltd Prospecton, South Africa.

Christiaens K. and Feyen J. (1999). "Sensitivity and Uncertainty Analysis of Complex Distributed Hydrological Models Using Latin Hypercube." *Institute for Land and Water Management*, Belgium.

Chow V.T. (1959). *Open Channel Hydraulics*. MacGraw-Hill Series.

Chow V.T., Maidment D.R. and Mays L.W. (1988). *Applied Hydrology.* McGraw-Hill.

Clothier A.N. and Pegram G.G.S. (2002). "Space-Time modelling of rainfall using the String of Beads Model: Integration of radar and rainfall-gauge data." *WRC Report, No. 1010*, South Africa.

County P. (1990). "Storm Water Management Manual." *Flood Control and Water Conservation District*, Auburn, CA.

Cowan W.L. (1956). "Estimating hydraulic roughness coefficients." *Journal of Agricultural Engineering*, vol.37, no.7. Page 473-475.

CSRA (1994). "*Hydraulics, Hydrology and Ecology. Volume 1 - Guidelines for the Hydraulic Design and Maintenance of River Crossings.*" Committee of State Road Authorities, Pretoria.

De Michele C. and Rosso R. (2001). "Uncertainty Assessment of Regionalised Flood Frequency Estimates." *J. Hydrological Engrg.* ASCE 6(6).

DWAF (1988). "Mlazi Canal." *Report on the Repair of the Flood Damage and Results of the Investigation into an increase of the capacity of the canal. Rep. No.U602/18/CD01.* Dept of Water Affairs South Africa.

GIBB Africa (1996). "Flood Protection of SAPREF Complex from Umlazi Canal." *Report No MC 2546* . Shell and BP South African Petroleum Refineries (Pty) Limited.

Guttien M.J., Ahmad R., Stark J.C. and Souza E. (1999). "Crop Breeding, Genetics and Cytology." *Agriculture Experiment Station*, University of Idoho. Aberdeen Research and Extention Ctr, P.O. Box AA,Aberdeen, USA.

GRASS (1993). "Grass 4.1 user reference manual." *U.S. Army Corps of Engineeers Construction Engineering Research Laboratory.* Champaign, 111.

Hazen A. (1914). Discussion on "Flood Flows." by W.E. *Fulter, Transactions, ASCE,* 77, 628.

Harvey H.D.P. (1998). "Flood Forecasting." http://eis.bris.ac.uk/~cedph/project/node16.html

Henderson F.M. (1966). *"Open Channel Flow."* MacMillan Company.

Hensen A., Kitching J. and McDonald.A. (2001). "GIS Application in Floodline Studies." *GIMS User Conference,* South Africa.

Herschfield D.M. (1961). "Rainfall frequency Atlas of the United States for durations from 30 minutes to 24 hours and return periods from 1 to 10 years." *TP 40. Weather Bureau, US Dept of Commerce*, Washington, DC.

HKS (1986). "Durban Rivers Hydrology." *Report on Durban Rivers Volume 1.* Hill Kaplan Scott and Partners, Durban, South Africa.

HKS (1996). "Flood Characteristics of UMlaas River Study." *Report on Durban Rivers Volume 16.* Hill Kaplan Scott and Partners, Durban, South Africa.

HEC-FDA (1998). "HEC-FDA Flood Damage Reduction Analysis." User Manual, *US ARMY CORPS of Engineers Hydrologic Engineering Center*, USA.

HEC-GeoHMS (2000). "Geospatial Hydrologic Modelling Extention." User Manual. *US ARMY CORPS of Engineers Hydrologic Engineering Center*, USA.

HEC-HMS (2000). "HEC-HMS Hydrology Modelling System." Technical Reference Manual. *US ARMY CORPS of Engineers Hydrologic Engineering Center*, USA.

HEC-RAS (1997). "HEC-RAS River Analysis System." User Guide. *US ARMY CORPS of Engineers Hydrologic Engineering Center*, USA.

Jensen S.K. and Domingue J.O (1988). "Extracting topographic structure from digital elevation data for Geographic Information System Analysis." *J. Photogrammetric Engrg. and Remote Sensing*, S4 (11), 1593 - 1600.

Johnson, E. (1989). "MAPHYD-A digital map-based hydrologic modelling systems." *J. Photogrammetric Engineering and Remote Sensing.*

Koutsoyiannis D., Kozonis D. and Manetas A. (1982). "A Mathematical framework for studying rainfall intensity-duration-frequency relationships." *Journal of Hydrology*, 206, 118-135.

Kovacs Z.P. (1988). "Maximum flood peak discharges in South Africa. An Empirical Approach." *Technical Report TR 105,* Department of Water Affairs, Pretoria, South Africa.

Le Roux J.J. (1994). "Extreme values of rainfall, temperature and wind for selected return periods." *Report WB 36,* Weather Bureau, Pretoria, South Africa.

Levy B. and McCuen R. (1999). "Assessment of storm duration for hydrologic design." *ASCE Journal of Hydrological Engineering*, 4(3), 209-213.

Limerinos J.T. (1970). "Determination of the Manning coefficient from measured bed roughness in natural channels." , *U.S. Geological Survey Water Supply Paper 1898-B.*

Maidment D.R. (1991). "GIS and Hydrologic Modelling." *Proc., 1st Int. Symp./Workshop on GIS and Envir. Modelling*, Boulder, Colorado.

Mancini M. and Rosso. R. (1989). "Using GIS to Access spatial variability of SCS curve number at the basin scale. New Direction for Surface Water Modelling." *IAHS Publ. No. 181,* International Association of Hydrological Sciences.

Menabde M. Seed A. and Pegram G.S.S. (1999). "A Simple Scaling Model for Extreme Rainfall." *Water Resources Research,* (35)1, 335-339.

Midgley D.C., Pitman W.V. and Middleton B.J. (1994). "Water Resources of South Africa 1990." *Volume VI. Drainage Regions U,V,W,X. WRC Rep. No. 298/6.1/94,* Water Research Commission, Pretoria.

Midgley D.C. and Pitman V.W. (1978) "A Depth Duration–Frequency diagram for point rainfall in South Africa." *Hydrological Research Unit, Report No. 2178,* Witwatersrand University, Johannesburg.

Miller J.F., Fredericks R.H. and Tracey, R.J. (1973). "Precipitation – Frequency Atlas of the Western United States." *NOAA Atlas 2,* National Weather Service, Silver Spring, MD.

Ogden F.L. Garbrecht J. DeBarry P.A. and Johnson L.E. (2001). "GIS and Distributed Watershed Models. II: Modules, Interfaces, and Models." *J. Hydrologic. Engrg., Vol.6,* Am. Soc. Civ. Eng., 515-522.

Oliver F. (2001). "Extracting Hydrologic Information from Spatial Data for HMS Modelling." *J. Hydrologic. Engrg.*, Am. Soc. Civ. Eng., 524-530.

Oliver F. and Maidment D.R. (1998). "GIS for hydrologic data development for design of highway drainage facilities." *Transportation Research Record No 1625,* 131-138, Transportation Research Board, Washington, D.C.

Pegram G.G.S. and Sinclair D.S. (2002). "A linear Catchment Model for Real Time Flood Forecasting." *WRC Report No.1005/1/02,* Water Research Commission, Pretoria.

Ponce V.M. (1989). *Engineering Hydrology, Principles and Practice,* Prentice Hall.

Pullen R.A., Wiederhold J.F.A. and Midgley .D.C. (1969). "Storm studies in South Africa, Large area storms: depth-area-duration analysis by digital computer." *Trans. S.A. Soc. Civ. Eng.*

Pearson K. (1902). "On the systematic fitting of curves to observations and measurements." *Biometrika,* 1(3), 265-303.

Pretner A., and WAMM Project Partners (1999). "WAMM-Water Management Model." *3rd DHL Software Conference, 15-1-35050,* Sarmeola di Rubano, Italy.

Schimdt E.J. and Schulze R.E. (1987). "Flood Volume and Peak Discharge from Small Catchments in South Africa Based on the SCS Technique." *Agricultural Catchments Research Unit. Report No. 24,* Dept. of Agricultural Engrg., University of Natal, Pietermaritzburg, South Africa.

Schmidt E.J., Schulze R.E. and Dent M.C. (1987). "Flood Volume and Peak Discharge from Small Catchments in South Africa Based on the SCS Technique: Appendices" *Agricultural Catchments Research Unit. Report No. 26*, Dept. of Agricultural Engrg., University of Natal, Pietermaritzburg, South Africa.

Sherman C.W. (1905). "Maximum rates of rainfall at Boston." *Trans. Am. Soc. Civil Engineering,* LIV, 173-181.

Sherman L.K. (1932). "Streamflow from rainfall by the unit-graph method." *Eng. News Record,* 108, 501-505.

Shipley S.T., Groffman I.A. and Beddoe D.P. (1996). "GIS does weather." *ESRI International Users Conference*, USA. http://www.esri.com/products.html

Sinclair S. (2000). "A linear Catchment Model for Real Time Flood Forecasting." *Unpublished MScEng Thesis,* Civil Engrg., University of Natal, South Africa.

Singh V.P. Asce F. and Woolhiser D.A. (2002). "Mathematical Modelling of Watershed Hydrology." *J. Hydrologic. Engrg.*, ASCE, 7, 270-291.

Smithers J.C. and Schulze R.E. (2000). "Long duration design rainfall in South Africa." *WRC Report No. 811/1/00,* Water Research Commision, Pretoria.

SCS (1971). "Hydrology." *National Engineering Handbook, Section 4*, Soil Conservation Services, USDA, Springfield, VA.

SCS (1986). "Urban Hydrology for Small Watersheds." *Technical Report 55*, Soil Conservation Services, USDA, Springfield, VA.

Stedinger J.R. (1997). "Expected probability and annual damage estimates." *J. Water Resources Planning and Management,* ASCE, 123(2), 125-135.

Stewart Scott (1993). "Shongweni Dam Rehabilitation Preliminary Report on Dam Stability Evaluation and Rehabilitation Proposals." Stewart Scott Consulting Engineers, Sandton, South Africa.

Thomas J. (2001). "GIS in Meteorology." *Geo 5453*. GIS Paper.

Tingsanchali T. (2001). "Application of Combined Tank Model and AR Model in Flood Forecasting." *Water Engineering and Management Program, School of Civil Engineering*, Asian Institute of Technology, Thailand.

USGS (1999). "Stream Gaging and Flood Forecasting." *U.S. Geological Survey Fact Sheet* - 209-95. http://water.usgs.gov/wid/fs-209-95/mason_wager.html

Vieux B.E. (1991). "Geographic Information Systems and non-point source water quality and quantity modelling." *Hydrological Processes*, 5, 101-113.

Wenzel H.G. (1982). "Rainfall for urban stormwater design." In Kibler, D.F. (Ed), *Urban storm Hydrology Water Resource Management*, 7, 35-67, AGU, Washington, D.C.

Zucchini W. and Adamson P.T. (1984). "The Occurrence and Severity of Droughts in South Africa." *WRC Report. No. 91/1*, Water Research Commission, Pretoria, South Africa.

APPENDIX -A

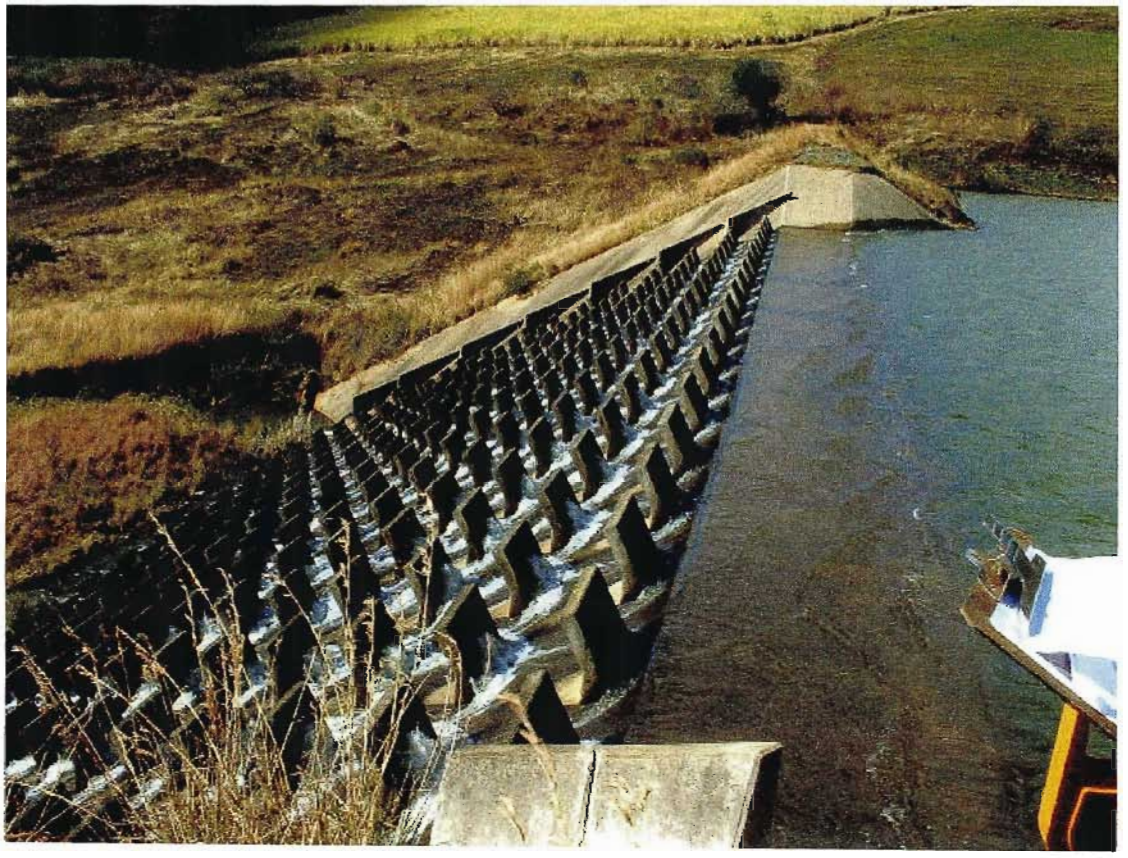

Ref. No		Mlazi-1A-07766
Description		Foot Bridge
Opening Size		446 m^2
Overtopping Capacity (m^3/s)		952
Corresponding Return Period		18
Overtopping depth (m)	20yr flood	0.4
	50yr flood	1.6
	100yr flood	3.3

Backwater Effects:

	Length (m)	Depth (m)
20yr flood	914	0.2
50yr flood	914	0.2
100yr flood	1421	0.3

Mlazi E-Section Foot Bridge

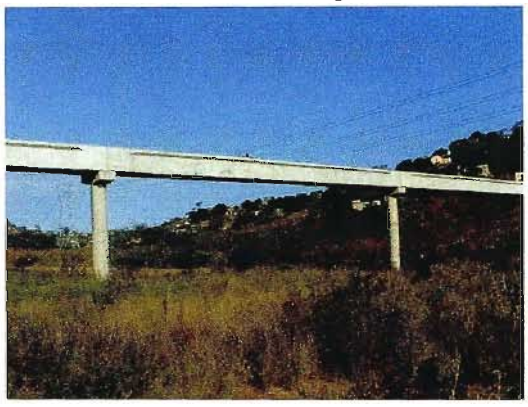

Ref. No.		Mlazi-1A-11477
Description		Foot Bridge
Opening Size		319 m^2
Overtopping Capacity (m^3/s)		895
Corresponding Return Period		16
Overtopping depth (m)	20yr flood	0.8
	50yr flood	2.3
	100yr flood	4.0

Backwater Effects:

	Length (m)	Depth (m)
20yr flood	594	0.4
50yr flood	594	0.3
100yr flood	594	0.2

Havenside Foot Bridge

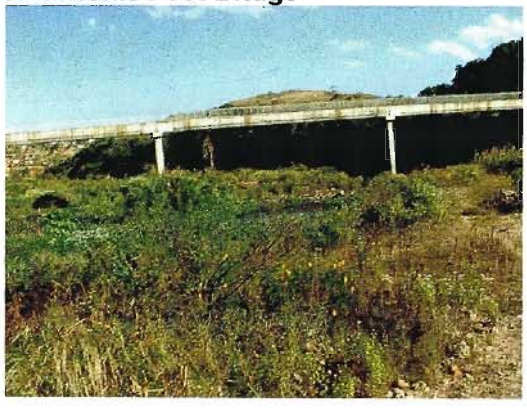

Ref. No.		Mlazi-1A-12090
Description		Foot Bridge
Opening Size		416 m^2
Overtopping Capacity (m^3/s)		1494
Corresponding Return Period		42
Overtopping depth (m)	20yr flood	-
	50yr flood	0.6
	100yr flood	2.6

Backwater Effects:

	Length (m)	Depth (m)
20yr flood	677	0.6
50yr flood	1131	0.8
100yr flood	1592	1.0

Umlazi F-Section Foot Bridge

Ref. No.		Mlazi-1A-15117
Description		Foot and Pipe Bridge
Opening Size		840 m^2
Overtopping Capacity (m^3/s)		3560
Corresponding Return Period		154
Overtopping depth (m)	20yr flood	-
	50yr flood	-
	100yr flood	-

Backwater Effects:

	Length (m)	Depth (m)
20yr flood	-	-
50yr flood	-	-
100yr flood	744	0.9

Umlazi H-Section Bridge

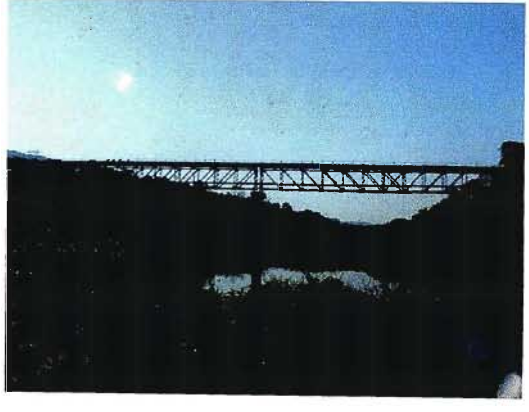

Ref. No.		Mlazi-1A-15879
Description		Foot Bridge
Opening Size		589 m^2
Overtopping Capacity (m^3/s)		2218
Corresponding Return Period		78
Overtopping depth (m)	20yr flood	-
	50yr flood	-
	100yr flood	1.1

Backwater Effects:

	Length (m)	Depth (m)
20yr flood	429	0.1
50yr flood	652	0.7
100yr flood	863	0.8

Umlazi H-Section Foot Bridge

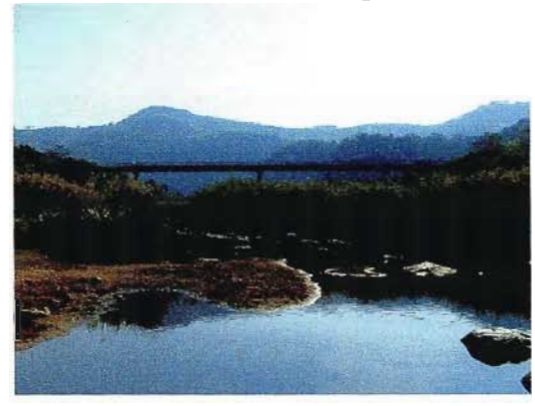

Ref. No.		Mlazi-1A-17283
Description		Foot Bridge
Opening Size		569 m^2
Overtopping Capacity (m^3/s)		2166
Corresponding Return Period		75
Overtopping depth (m)	20yr flood	-
	50yr flood	-
	100yr flood	1.5

Backwater Effects:

	Length (m)	Depth (m)
20yr flood	-	-
50yr flood	476	0.3
100yr flood	692	0.6

Umlazi H-Section Foot Bridge

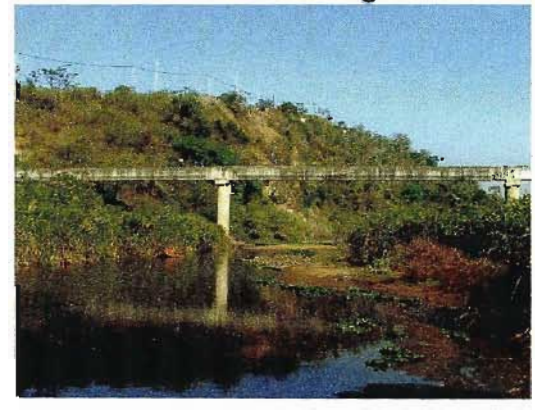

Ref. No.		Mlazi-1A-17976
Description		Foot Bridge
Opening Size		640 m^2
Overtopping Capacity (m^3/s)		2200
Corresponding Return Period		77
Overtopping depth (m)	20yr flood	-
	50yr flood	-
	100yr flood	0.9

Backwater Effects:

	Length (m)	Depth (m)
20yr flood	399	0.3
50yr flood	283	0.6
100yr flood	156	0.9

Umlazi H-Section Foot Bridge

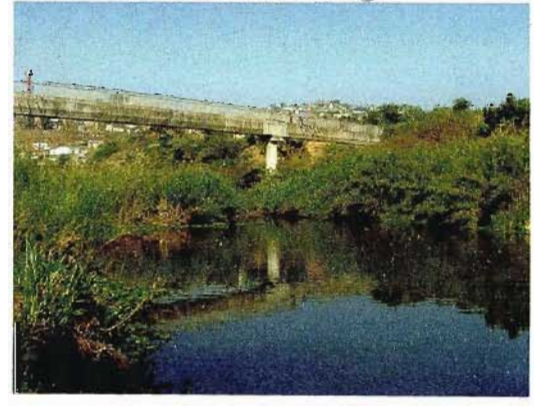

Ref. No.		Mlazi-1A-18844
Description		Foot Bridge
Opening Size		676 m^2
Overtopping Capacity (m^3/s)		2360
Corresponding Return Period		85
Overtopping depth (m)	20yr flood	-
	50yr flood	-
	100yr flood	0.9

Backwater Effects:

	Length (m)	Depth (m)
20yr flood	-	-
50yr flood	-	-
100yr flood	772	0.5

Umlazi J-Section Foot Bridge

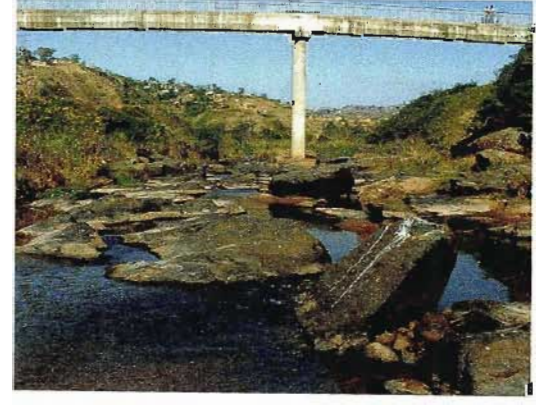

Ref. No.		**Mlazi-1A-19736**
Description		Foot Bridge
Opening Size		658 m^2
Overtopping Capacity (m^3/s)		2200
Corresponding Return Period		77
Overtopping depth (m)	20yr flood	-
	50yr flood	-
	100yr flood	1.1

Backwater Effects:

	Length (m)	Depth (m)
20yr flood	200	0.2
50yr flood	381	0.2
100yr flood	547	0.5

Umlazi J-Section Foot Bridge

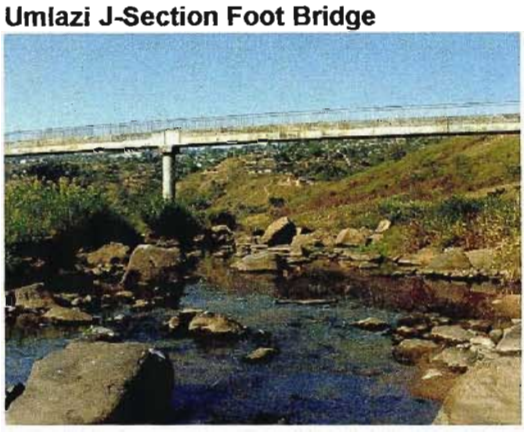

Ref. No.		**Mlazi-1A-20283**
Description		Foot Bridge
Opening Size		342 m^2
Overtopping Capacity (m^3/s)		1970
Corresponding Return Period		65
Overtopping depth (m)	20yr flood	-
	50yr flood	-
	100yr flood	0.2

Backwater Effects:

	Length (m)	Depth (m)
20yr flood	-	-
50yr flood	633	0.6
100yr flood	70	0.2

Umlazi J-Section Foot Bridge

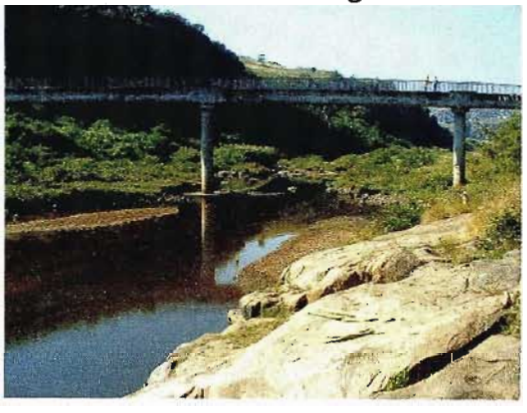

Ref. No.		**Mlazi-1A-22437**
Description		Road Bridge
Opening Size		671 m^2
Overtopping Capacity (m^3/s)		2576
Corresponding Return Period		95
Overtopping depth (m)	20yr flood	-
	50yr flood	-
	100yr flood	0.2

Backwater Effects:

	Length (m)	Depth (m)
20yr flood	190	0.5
50yr flood	190	0.5
100yr flood	200	1.0

Umlazi J-Section Foot Bridge

Ref. No.		**Mlazi-1A-25098**
Description		Foot Bridge
Opening Size		756
Overtopping Capacity (m^3/s)		2576
Corresponding Return Period		80
Overtopping depth (m)	20yr flood	-
	50yr flood	-
	100yr flood	1.2

Backwater Effects:

	Length (m)	Depth (m)
20yr flood	-	-
50yr flood	-	-
100yr flood	978	0.4

Welbedacht Foot Bridge

Ref. No.		Mlazi-1A-29065
Description		Pipe Culvert
Opening Size		0.07m^2
Overtopping Capacity (m^3/s)		40
Corresponding Return Period		< 2
Overtopping depth (m)	20yr flood	5.1
	50yr flood	6.5
	100yr flood	8.3

Backwater Effects:

	Length (m)	Depth (m)
20yr flood	336	0.8
50yr flood	336	0.8
100yr flood	336	0.8

Culvert/Weir at Welbedacht

Ref. No.		Mlazi-1A-31533
Description		Road Bridge
Opening Size		179 m^2
Overtopping Capacity (m^3/s)		490
Corresponding Return Period		5
Overtopping depth (m)	20yr flood	1.3
	50yr flood	2.3
	100yr flood	3.5

Backwater Effects:

	Length (m)	Depth (m)
20yr flood	310	0.6
50yr flood	320	0.6
100yr flood	201	0.6

Welbedacht Bridge

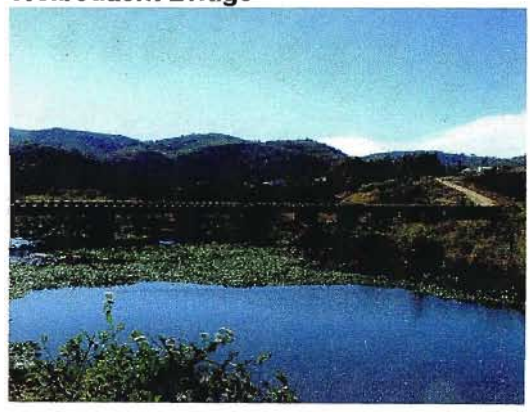

Ref. No.		Mlazi-1A-33457
Description		Road Culvert
Opening Size		6.36 m^2
Overtopping Capacity (m^3/s)		103
Corresponding Return Period		< 2
Overtopping depth (m)	20yr flood	2.6
	50yr flood	3.6
	100yr flood	4.8

Backwater Effects:

	Length (m)	Depth (m)
20yr flood	94	0.2
50yr flood	-	-
100yr flood	-	-

Culvert/Weir at Welbedacht

Ref. No.		Mlazi-1A-38298
Description		Road Culvert
Opening Size		6.43 m^2
Overtopping Capacity (m^3/s)		80
Corresponding Return Period		< 2
Overtopping depth (m)	20yr flood	3.5
	50yr flood	5.0
	100yr flood	6.8

Backwater Effects:

	Length (m)	Depth (m)
20yr flood	103	0.1
50yr flood	-	-
100yr flood	-	-

Culvert/Weir at Welbedacht